Ollscoil na hÉireann, Corcaigh

National University of Ireland, Cork

University College Cork, Ireland
Coláiste na hOllscoile Corcaigh

The impacts of a suite of Nature-based Solutions on hydrology and water quality in an agricultural landscape

Thesis presented by

Darragh Murphy

https://orcid.org/0009-0007-6782-7546

for the degree of

Doctor of Philosophy

University College Cork

School of Biological, Earth and Environmental Sciences

Head of School/Department: Professor Astrid Wingler

Supervisor(s): Dr Simon Harrison, Dr John Weatherill, Dr Mary Bourke (P.I.)

2024

Table of Contents

Declaration

This is to certify that the work I am submitting is my own and has not been submitted for another degree, either at University College Cork or elsewhere. All external references and sources are clearly acknowledged and identified within the contents. I have read and understood the regulations of University College Cork concerning plagiarism and intellectual property.

Signed: 

Darragh Murphy, 03/05/2024

Acknowledgements

Firstly, I must acknowledge the funding support and guidance provided by the EPA (Environmental Protection Agency) and OPW (Office of Public Works) to the SloWaters project. They were always interested and encouraging in this research.

There are many people who have been essential in getting this thesis to where it is. I must give my sincere thanks to Simon Harrison and John Weatherill. This thesis exists because of their unwavering support, guidance and enthusiasm. Many hours were spent at Leades Farm sawing, digging, lifting, talking; and even more hours spent in Simon's office where he devoted his seemingly unlimited energy and passion to educating me and lighting the fire to produce the best work we could. Thanks to Mary Bourke, Mark Wilkinson and Paul Quinn for the many conversations about water and farming and people: their experience and willingness to share was vital to this research. Colin Wolfe provided me with every raw material for environmental research that I could have dreamed of. Colin's optimism and willingness to take risks for the benefit of nature is truly inspiring. Thanks to Tim Sullivan for offering occasional, yet very necessary, support and guidance.

I would like to thank Rossana Henriques for her crucial input and for introducing me to the mind-boggling world of plant physiology. Thank you to Xie Quishi for the tireless and valiant processing of many, many water and soil samples. I don't know how you do it, but I'm very grateful. Thanks to all at the Environmental Research Institute for providing such a great environment for research and researchers. Thanks to Camila Barria Diaz for helping with all those soil samples and thanks to Colin O'Flynn and Pia Laue for getting the research going in those early, lockdown days of the project. To the lovely big gang in the Cooperage that I've gotten to know over the past four and a half years: thanks. It's been a pleasure.

Thanks to my fantastic friends and family for listening to me moan about water for so long. A huge thank you to my parents whose boundless care and support was invaluable: I'll take it with me onwards. Thank you to Claire, Felix and Remi. I'm very lucky.

General Abstract

Across much of the world, rural catchments have been substantially modified by human activity to meet the demand for greater production of a limited number of crops for human and livestock consumption. Much of the expansion of tillage and pasture areas has been at the expense of transitional zones such as wetlands, floodplains and riparian zones, and of hydraulically and geomorphologically complex stream environments which can mediate the flux of water and nutrients through catchments. Modifications to rural catchments to limit over-bank flooding may bring about more severe flooding downstream as flood peaks are conveyed more quickly through straightened channels. In Ireland, as agricultural activity has increased over the past 70 years, the impacts of agriculture on water quality have increased in kind, with a current estimate of 50% of rivers in Ireland being in satisfactory ecological condition. Field surfaces, farm drains and hard-standing areas can harbor high loadings of organic and mineral nutrients and sediment which are mobilized by rainfall to adjacent water ways. In the relative absence natural sites of retention and processing of these water quality pressures, large fluxes may be conveyed downstream during high-flow events, harming aquatic communities and affecting drinking water supplies.

Nature-based Solutions (NbS) are applied in landscapes which have been modified by human activities, with the goals of reinstating and supporting natural processes which mediate and mitigate the flux of pressures such as high stream discharges and agricultural pollution. NbS features may operate passively within landscapes, requiring low initial and ongoing costs and are therefore advocated to complement or replace traditional engineering solutions to anthropogenic pressures. In Ireland, however, empirical data on the potential to of NbS features to mitigate target

pressures is lacking. This is especially true in agricultural catchments where flood peak mitigation and water quality management are affected by complex biological and geo-chemical cycling of nutrients, as well as the cultural and social constraints imposed by modern farming practices.

This thesis investigates the performance of four NbS features reduction of flood peaks discharges and the flux of agricultural water quality pressures on a farm in Ireland. In addition to examination of key biological (sediment retention, nutrient uptake, sward health) and hydrological (peak discharge reduction) effects of NbS features, the success of these features was contingent on bringing no harm to the farming enterprise or channel morphology within the study area. We found that the four studied NbS features - a flood detention basin, a runoff-treatment woodland swale, in-stream boulder weirs and leaky wooden dams – brought about notable improvements to water quality and/or reduced stream discharges during high-flow events. Specifically, this research has demonstrated that the storage of stream water on farm pastures during peak discharge periods may bring about reductions in downstream discharge, and nutrients and sediment concentrations; and that such short-term (12-24hours) inundation of pasture during winter does not impair summer growth of the sward. In-stream features were also shown to reduce stream discharges during high-flow periods but their scouring effects on stream and channel sediments were cause for concern. The study also found that modest, yet scientifically led, modifications to open farm drains may improve water quality and reduce the risk of contamination of downstream water courses. Importantly, however, the effects of all NbS features were strongly influenced by antecedent hydrological conditions, upstream nutrient loading and the stoichiometry of nutrient-enriched water flowing through the features. In summary, NbS features may be utilized for targeted mitigation of anthropogenic and natural issues, but they require careful, context-specific management to ensure they do not cause more harm than good.

Chapter 1: General Introduction

1.1 The Irish agricultural landscape

The geographical position of Ireland along the Atlantic seaboard and proximity to the gulf stream produces an almost year-round mild, wet climate (Hurtado-Uria et al., 2013). Its northern position and mild climate facilitates an extended growing season (Doody et al., 2016). Additionally, the relatively flat topography of interior and eastern areas of the country have promoted the development of fertile soils and numerous water bodies with short reaches, which were historically well-connected to flood plains (Bhattarai and O'Connor, 2004). Extensive areas of Carboniferous limestone bedrock in the midlands, south and west of the country promote strong ground-water recharge and well-drained soils (Misstear et al., 2009).

Despite its advantageous geographical and geological situation, the persistence of wetlands and *marginal* ground across much of the Irish rural landscape limited Ireland's agricultural productivity until recent times. The enactment of the Arterial Drainage Act in 1945 (Government Publications Office, 1945) gave public bodies and landowners greater powers to modify surface and sub-surface flows and increase the extent and value of agricultural land . This was largely conducted through the development of land-drains, the deepening and widening of river channels and activities such as channel straightening and bank levee construction (Bhattarai and O'Connor, 2004). Areas of poorly draining, calcium rich soils of the midlands have been managed to promote widespread beef and dairy farming, while freely draining soils, especially in the south and east of the country can support more intensive dairying and arable agriculture. Combined with enhanced methods of fertilisation and management of livestock breeds and grazing patterns, these drainage practices promote intensive and predictable agricultural activity for much of the year (Doody et al., 2016).

Importantly, the intensification of agricultural output brings about the increase in application and loss of nutrients to adjacent water bodies (Ockenden et al., 2014). In Ireland and elsewhere in the EU, the ambitions for greater agricultural activity are often in conflict with those nations' commitments to environmental regulations such as the Water Framework Directive (Doody et al., 2016; Environmental Protection Agency, 2022; Flávio et al., 2017).

1.2 Hydro-morphology and nutrient processing

Naturally occurring woody debris and variable geomorphology (e.g., boulders, channel slope, riffles, pools) in streams and rivers can have substantial impacts on the flux of water, nutrients and sediment between headwater and downstream areas of catchments (Poff et al., 1997; Wohl and Beckman, 2014). In-stream features impede the flow of water and, as such, can cause localised zones of slow-moving water where nutrients and sediment can deposit and be retained on the upstream side, while promoting scouring high-flow areas just downstream (Grabowski et al., 2019). The storage of large woody debris (LWD) at localised points may range from minutes to decades and these areas may serve as 'hotspots' of ecosystem respiration, supporting the breakdown, biological uptake and transformation of nutrients (Blaen et al., 2018; Oviedo-Vargas et al., 2013). In the presence of permeable gravel beds and hydrostatic pressure differentials between areas upstream and downstream of LWD, surface water is driven through the streambed: a region known as a hyporheic zone (Boulton, 2007). Persistent flow of oxygen- and nutrient-rich surface waters into the hyporheic zone can promote the development of microbial biofilms over interstitial surfaces. The presence of well-mixed gravels can greatly enhance the metabolic turn-over of nutrients in channels, as they offer greater surface area for microbial colonisation, and can provide sufficient contact-time to enable breakdown and transformation of organic matter and nutrients (Fischer et al., 2005; Boulton, 2007; Cunha et al., 2018). Through the production of intermediate compounds in hyporheic zones and in LWD accumulations, nutrients are retained and further utilised within the biofilm matrix, so reducing the flux of nutrients through catchments during high-flow events (Battin et al., 2003; Krause et al., 2014; Blaen et al., 2018). Groundwater-surface-water exchange within the hyporheic zone can also help sustain the metabolism of surface-borne nutrients by creating variable redox conditions within the hyporheic sediments (Hester and Gooseff, 2010; Robertson and Wood, 2010; Romani et al., 2016).

Large woody debris (LWD) in channels can enhance the hydrological connectivity between channels and adjacent riparian areas by establishing localised points of channel over-flow to floodplains. During high-flow events, LWD can induce the back-up of stream water which can overflow onto adjacent floodplains thereby substantially increasing the surface area through which peak flows move through catchments and flattening and extending the discharge hydrograph (Wenzel et al., 2014; Wohl and Beckman, 2014; Keys et al., 2018; Barnes et al., 2023). In this way, floodplains can substantially increase the storage volume of catchments during high flows and may help reduce the risk of flooding in downstream areas (Suttles et al., 2021). Dissolved nutrients, particulate organic matter and sediment may also be delivered to, and stored on, flood plains during high-flow events. Reduction in flow velocities and greater contact with soil and micro-organisms within floodplains can bring about retention and transformation of particulates and dissolved nutrients (Tockner et al., 1999; Noe et al., 2019). In natural floodplains, riparian zones and wetlands, complex biological geochemical conditions may develop over centuries of regular seasonal inundation in which nutrient transformation processing varies over short spatial scales due to differences in soil saturation, soil porosity (hydraulic conductivity) and soil chemistry (Tockner et al., 1999). As water passes through soils, processing of nitrogen, phosphorus and carbon may occur, where local variability in saturation, redox and stoichiometric conditions influence rates of mineralization of organic forms of P, N and C, geochemical binding to ions within the soil (e.g., Fe, Al, Mn, Ca), and immobilization of dissolved inorganic nutrients into organic matter with microbial or autotrophic uptake of mineral nutrients (McClain et al., 2003; Roberts et al., 2012; Stutter et al., 2018).

Throughout the world, catchments have been modified to promote agricultural intensification. Central to this has been the disconnection of water courses from floodplains and riparian zones so that specific soil conditions required for optimal growth of arable and forage crops can be maintained across larger areas and for extended growing seasons (Davidson, 2014). Through the removal of in-stream impediments, drainage of wetlands, and interception of groundwater via subsurface drains, the extent of agriculturally productive land has been dramatically increased in recent centuries (Poff et al., 1997; Flávio et al., 2017; Abbe et al., 2019). Furthermore, widening and straightening of stream channels helps to convey peak flows more quickly downstream without over-topping channel banks (Rogger et al., 2017). These modifications have significant impacts on conveyance of water, nutrients and sediment through agricultural catchments. During high discharge events, flood peaks may reach downstream areas in shorter but higher magnitudes, putting downstream settlements at greater risk of flooding (Pierce et al., 2012; Watson et al., 2016). Higher loadings of organic matter and mineral fertilizers within farmland may be mobilised from terrestrial sources during over-land flow events, and in the absence of nutrient transformation hotspots such as in wetlands, natural floodplains, gravel beds and behind accumulations of LWD, large pulses of nutrients can be delivered to lakes and estuaries where they can induce eutrophication and localised pollution (Blaen et al., 2018; Krause et al., 2014; Raymond et al., 2016).

In countries like Ireland, where pasture-based agriculture is a predominant land-use, large stores of organic matter (e.g., silage, slurry, manure) and organic and inorganic fertilizers, are present at diffuse scales (e.g., the surfaces of fields; Doody et al., 2012; Mancuso et al., 2021) and as localised deposits (e.g., surfaces of yards, trackways and hardstanding areas; Edwards et al., 2008; Edwards and Hooda, 2008; Fenton et al., 2022). Mobilisation of nutrients from these source areas tends to occur during rainfall events when over-land flow establishes connections to adjacent water courses (Moloney et al., 2020; Fenton et al., 2022). Increases in stream discharge may mobilise sediment and nutrients within streambeds and channel banks, transporting them to receiving waters downstream (Jarvie et al., 2012). Additionally, dissolved nutrients like nitrate, ammonium, soluble reactive phosphorus (SRP) and dissolved organic carbon (DOC) applied to the land as mineral and organic fertilizers can infiltrate subsurface tile drains or groundwater aquifers when application of fertilizer exceeds uptake potential of soil microbial communities and crops (Jordan et al., 2005; Vero et al., 2019; Moloney et al., 2020).

In Ireland, agriculture accounts for approximately 67% of the land cover and is implicated as the industry which has the highest contribution to impaired water quality (DAFM (Department of Agriculture, 2017; Environmental Protection Agency, 2022). Under EU legislation such as the Water Framework Directive (CEC, 2000), the Floods Directive (European Union, 2007) and the Habitats Directive (Council

Directive 92/43/EEC, 1992), Ireland, as a member state of the EU, is obliged to limit the deterioration of water quality and mitigate the risks of flooding imposed by high flow events and anthropogenic modifications to stream hydro-morphology.

Given the extent of modification to the hydrological and ecological nature of agricultural catchments, substantial investment of money and expertise may be required to mitigate the flood risk and reduction in water quality resulting from these modifications. To meet the objectives of flood risk mitigation and water quality and habitat restoration, the Water Framework Directive (CEC, 2000) advocates the use of Nature-based Solutions (NbS, e.g. Sustainable Urban Drainage Systems, Tree-planting; Wild et al., 2000), in addition to more traditional, hard-engineering (e.g. dams and urban flood defence barriers) and best management practices (e.g. restrictions to the spreading of organic and mineral fertilisers to farmland). The European Council defines NbS as "*solutions that are inspired and supported by nature, which are cost-effective, simultaneously provide environmental, social and economic benefits and help build resilience; such solutions bring more, and more diverse, nature and natural features and processes into cities, landscapes and seascapes, through locally adapted, resource-efficient and systemic interventions"* (EC, 2015; Wild et al., 2020). Additionally, by being inspired by natural processes and derived from natural materials, NbS features are generally considered to bring about multiple benefits in being able to attenuate coincidental or linked environmental pressures (Collier and Bourke, 2020; Short et al., 2019). For example, features which help to impede the slow of water through catchments may have potential both as flood-mitigation structures and structures which mediate the flux of sediment and nutrients. Effective NbS features (in terms of function and cost/benefit) are those which are designed with a comprehensive understanding of the natural processes which they set out to restore (Keesstra et al., 2018). Appropriate implementation of NbS features may be guided by the “right practice, right place” approach in which NbS appropriately designed features are positioned within the landscape at locations where they have the greatest effect on a specific pressure (Kröger et al., 2013).

The recently ratified Nature Restoration Law outlines specific goals to combat biodiversity loss and ecological degradation, and contains provisions to enforce EU member states to meet nature restoration obligations (Stoffers et al. 2024). While the Nature Restoration Law sets out to restore natural ecosystems for their own sake, NbS features typically are developed to enhance or manage natural processes for the benefit of society, e.g. flood management through catchment-scale tree planting (Grabowski, 2019). Research into the functioning and long-term effects of NbS features on natural systems is likely, however, to enable countries to more effectively put measures in place that will meet the obligations of the Nature Restoration Law (Waylen et al., 2024).

Many empirical and modelling studies have been conducted in recent years to illustrate the effectiveness of various NbS features in mitigating floods and water quality issues (e.g., Black et al., 2021; Levine et al., 2021; Quinn et al., 2022; Robotham et al., 2022). Evidence is lacking, however, on whether NbS features may confer quantifiable multiple benefits, or can operate on a scale by which natural events, such as floods, are mitigated to the extent that society has benefited from their presence (Heneghan et al., 2021; van Leeuwen et al., 2024). Questions also exist around the compatibility of effective NbS features (i.e. those which bring about a quantifiable benefit) and the continuing agricultural use of farmland which hosts NbS features (Liu et al., 2018). This thesis investigated the potential of four NbS features installed within a working farm to attenuate flood peaks and improve water quality over an extended time period and range of flows.

The following section describes the key sources, constituents and the transformation and attenuation processes of agricultural runoff, as well as the impacts of runoff pollution on aquatic environments. These processes are discussed in the context of the specific hydrological conditions which mediate the transport and mitigation of water quality parameters.

1.3 Flux, processing and impacts of water and nutrients

1.3.1 Sediment and POM

Although natural component of the sediment load that moves through stream systems, fine suspended solids tend to be emitted in high concentrations from farmland, especially during rainfall events from exposed surfaces and soils e.g. tractor tramways, unvegetated fields after harvesting, farm trackways and hard-standing areas (Deasy et al., 2009; Ockenden et al., 2014; Moloney et al., 2020). Agricultural particulate organic matter (POM) in the forms of animal waste (faecal matter) and, silage and vegetation may also be delivered to streams from farm fields, trackways and hardstanding areas. The breakdown of POM by detritivores and micro-organisms can cause the release of highly labile organic and mineral forms of phosphorus, nitrogen, and carbon. These nutrients can stimulate rapid growth of autotrophic and heterotrophic micro-organisms in surface waters, and potentially induce eutrophication, oxygen depletion and the build-up of toxic by-products.

In agricultural catchments, the combination of sources of high loadings of sediment and OM (e.g. exposed soils, trackways, channel-banks) and the relative absence of areas where particulates may be detained (e.g. LWD accumulations, floodplains) can cause high loads of organic and mineral particulate matter to be deposited when flow velocities are low enough for sedimentation to occur, such as in shallow low-order streams, lakes and estuaries (Magette et al., 2007; Stutter et al., 2008; Vero et al., 2019). The deposition of POM and fine solids on gravel beds can lead to the clogging, or colmation, of streambeds (Brunke, 1999; Moloney et al., 2020). Colmation can reduce the flow of oxygen and nutrient rich surface- and ground-waters through the streambed, inhibit hyporheic exchange, and limit the survival of in-faunal macro-invertebrates (Brunke, 1999; Brunke and Gonser, 1997), especially those with a low threshold for oxygen deprivation such taxa from the orders Plecoptera, Trichoptera and Ephemeroptera (EPT). The combination of physical blocking of streambed interstices and the effects of OM breakdown on dissolved oxygen concentrations in pore-waters can have negative effects on stream biota. Being important prey species for young salmonids and riverine birds such as dippers, damage to macro-invertebrate communities by fine sediments has obvious knock-on effects through the freshwater community (Friberg et al., 2010). Where particulate organic matter and sediment are deposited in quantities such that they can form deep anoxic sediments, the highly reducing conditions below the surface can lead to mineralization of OM and form methane and iron sulphides which can be toxic to aquatic live and contribute to the greenhouse effect when outgassing to the atmosphere occurs (Sweka and Hartman, 2001; Søvik et al., 2006; Carballeira et al., 2017; Weatherill et al., 2019).

1.3.2 Phosphorus

Phosphorus is an essential component of organic molecules and is limiting in natural streams. To promote growth of crops and pasture species, phosphorus is applied to farmland within mineral and organic fertilisers. In soils and stream sediments, it is bound to particles and exists in complexes with metals such as magnesium and potassium at pH greater than 7, and with calcium ions at pH less than 7 (Roberts et al., 2017; Fenton et al., 2022). Organic run-off from farmland can induce high loadings of phosphorus to streams and drive eutrophication (Jordan et al., 2012). In streambeds, phosphorus may be mobilised via sediment transport during high flows and be deposited in slow-flowing reaches and lakes downstream (Fig. 1). Soluble phosphorus may desorb from sediments under low oxygen conditions, and induce substantial algal growth (Jordan et al., 2012; Shore et al., 2016). As phosphorus does not have a gaseous phase, the flux of phosphorus through agricultural catchments is affected by a complex suite of factors such as spatial and temporal variability in rainfall, stream discharge and the presence of areas where phosphorus may be physically trapped or adsorbed to streambed and soil substrates (Withers and Jarvie, 2008).

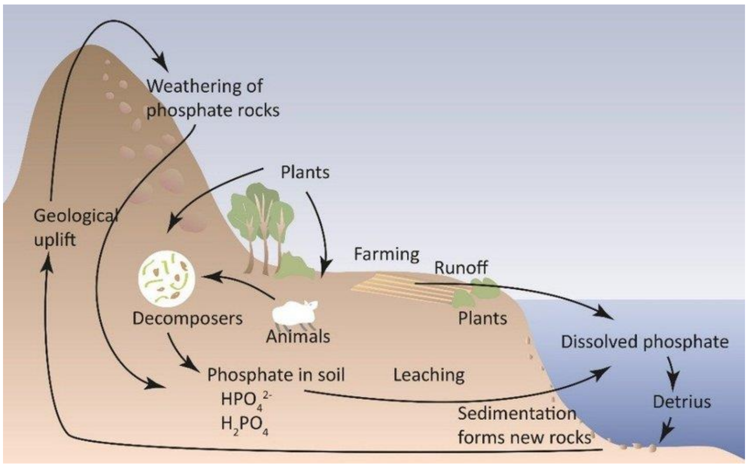

Figure 1 Schematic of the phosphorus cycle. From Lappalainen et al. 2016

1.3.3 Nitrogen

Nitrogen is an essential component in primary production. Changes in fluxes of N to freshwater systems, or changes in its stoichiometry with other nutrients (e.g. carbon, phosphorus, silica) can bring about dramatic changes in primary production, and in turn community composition, oxygen levels and freshwater acidity (Durand et al., 2011).

In agricultural catchments, substantial nitrogen delivery to surface and groundwaters may occur via diffuse flow through soil porewater and groundwater, or via points sources from pipes and drains (e.g. from domestic and agricultural waste; Birgand et al., 2007; Durand et al., 2011). The chemical form of nitrogen present in the system is affected by a complex suite of factors including pH, temperature, substrate for microbial communities and the relative abundance of nutrients involved in microbial transformations of N such as carbon and phosphorus (Durand et al., 2011). In aerated zones such as the soil surface, reduced forms of nitrogen such as nitrite and ammonium, or DON from animal and human waste inputs, are quickly oxidized to form nitrate (Dodds et al., 2004; Durand et al., 2011; Fig. 2). Nitrogen as nitrate is the predominant form, therefore, in sub-surface soils and streambeds, where it moves downwards into deeper groundwaters (Durand et al., 2011). In agricultural catchments where N loadings are high, groundwater contamination with nitrate can be significant (Hiscock et al., 2003; Rajta et al., 2020; Rivett et al., 2008).

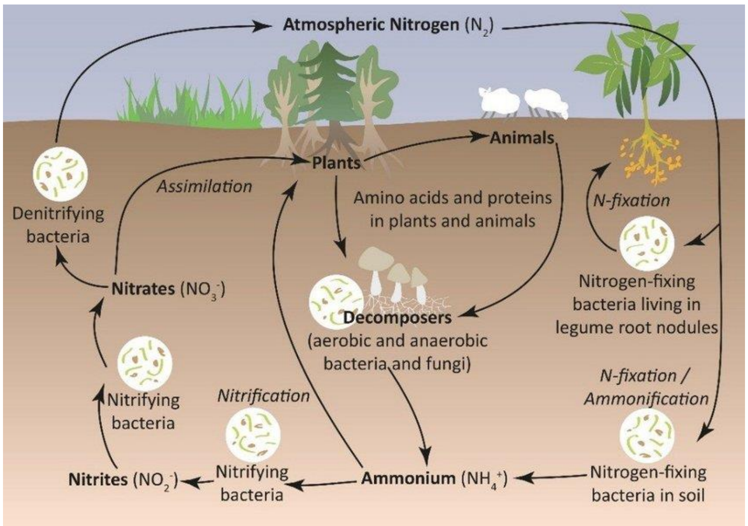

Figure 2 Schematic of the terrestrial nitrogen cycle in terrestrial systems. From Lappalainen et al. 2016.

Much scrutiny is applied to nitrate loading in agricultural catchments, partly because it is the dominant form of nitrogen in groundwater and in higher order streams which are more important as drinking water sources for towns and cities (Lloyd et al., 2019; Parris, 2011). In low-order streams, the delivery of ON and subsequent conversion to ammonium and ammonia can have substantial, yet localised consequences to stream health and aquatic life (Hooda et al., 2000; Friberg et al., 2010). Under aerobic conditions, large loadings of ammonium may be mineralised from OM during OM breakdown by heterotrophic micro-organisms (Harrison et al., 2019; Stutter et al., 2018). Ammonium is readily assimilated by micro-organisms and plants and may be utilized directly as a source of energy via reduction to nitrate. Ammonium pollution therefore induces rapid stimulation of growth of autotrophic and heterotrophic organisms in receiving waters, with substantial knock-on effects to community composition, dissolved oxygen concentrations, and toxic by-products of algal blooms (Friberg et al., 2010; Martí et al., 2020). As free un-ionised ammonia, which may also be produced through mineralization of OM, it is toxic to aquatic life (Guthrie et al., 2018).

Removal of N from freshwaters occurs via a number of bio-geochemical processes. Denitrification, the reduction of nitrate to N_2 gas, permanently removes N as it is passed to the atmosphere, and is considered the dominant mode of N removal from soils and freshwaters (Burgin and Hamilton, 2007). Denitrifying organisms utilise nitrate as an electron donor in the respiration of organic matter in the absence of dissolved oxygen (DO). Nitrate is also attenuated through assimilatory uptake i.e. nitrate is converted to biomass. In dissimilatory nitrate reduction to ammonium (DNRA), nitrate is reduced to yield electrons for further oxidation of compounds such as Fe^{2+}. The ammonium yielded by DNRA is readily available for assimilation into plant and microbial biomass (Burgin and Hamilton, 2007; Durand et al., 2011; Kelso et al., 1997). Ammonium can also be nitrified back to nitrate. Indeed denitrification, DNRA and nitrification may occur simultaneously within bacterial biofilms, with the rate of reaction in a given direction being continuously altered by local differences in availability of oxygen, DOC, pH, substrate surface area for microbial colonisation, temperature and presence of toxins (Durand et al., 2011; Fischer et al., 2005).

Plant uptake and immobilization of bio-available forms such as nitrate, ammonium and nitrite temporarily attenuate nitrogen from soils and freshwaters to form organic nitrogen. Organic nitrogen is released back into the environment following die-back and decay of tissues (Ranalli and Macalady, 2010) unless it is permanently transported out of the environment e.g. in the tissues of animals. Nitrogen can be stored as nitrate in groundwater aquifers for periods of decades to years. In agricultural catchments where there can be excessive fertilizer application, groundwater contamination with nitrate can be high. In this way, groundwater aquifers can deliver N from the land to streams at upwelling zones with a lag of years to decades in between (Durand et al., 2011), posing substantial challenges to those attempting to reduce freshwater N concentrations.

1.4 Nature-based Solutions to promote natural processes and reduce impacts on society

Offline and in-stream features can benefit water quality and attenuate peak flows to mitigate downstream flood risk. Offline features such as flood detention basins simulate the role that natural flood plains have in being able to accommodate and store water from stream channels during peak flow periods, or help to retain overland flow so that in-stream peak discharges can be reduced and flood peak durations extended (Lockwood et al., 2022; Quinn et al., 2022). Flood detention basins can be constructed with relatively simple hydrological engineering principles to help detain and release waters during and after peak flow events. From a water quality perspective, these features may also promote the deposition and retention of particulate organic matter and sediment, reducing the efflux of particulates from terrestrial sources to surface waters during rainfall or peak flow events (Robotham et al., 2022). There is evidence that offline flood detention features can also facilitate the nutrient uptake, transformation and attenuation processes of natural floodplains by providing surface area and extended hydraulic retention time at the interface between the flood water and soil within the detention basin, such that dissolved nutrients are be geochemically or biologically retained and attenuated on land (Fiener et al., 2005). There is also evidence, however, that flood detention basins may be a net source of nutrients and sediment, especially when they are installed on farmland where the presence of exposed soils which are rich in OM is mobilised by overlaying waters (Jones et al., 2015). As a result of previous decades agricultural land-use, the potential for flood detention basins on farmland to both attenuate flood peaks and promote the re-establishment the geo-chemical and biological functions of natural floodplains and wetlands may be a substantial challenge (Noe et al., 2019).

If effectively designed and cited within the landscape, a single NbS feature may confer multiple benefits and therefore occupy less space or require less investment (Keesstra et al., 2018; Short et al., 2019). While it is desirable to install NbS features which confer multiple benefits, NbS features which more effectively attenuate a narrower range of pressures may be more cost-effective approach (Kröger et al., 2013). The role of NbS in mediating nutrient turnover in terrestrial and riparian zones has been investigated via the development of constructed wetlands, bio-swales and riparian buffers. These features can be constructed to support a range of nutrient uptake and transformation processes to maximise the attenuation of agricultural runoff. Swales and constructed wetlands are designed to retain nutrient-enriched water within substrates which can provide appropriate surface area for microbial biofilm development, geochemical conditions and redox gradients to mediate aerobic (e.g., OM mineralisation and nitrification) and anaerobic nutrient transformation processes (e.g., denitrification). While constructed wetlands and swales may be effective in sequestering and attenuating certain water quality parameters (Shaw Yu et al., 2001; Vymazal, 2007; Zhang et al., 2008), the composition of agricultural runoff is such that the conditions which promote the attenuation of a given component may be the same conditions which promote the production of another (Kröger et al., 2013). For example, the addition of DOC to riparian zones has been shown to enhance denitrification rates in waters with a high nitrate burden (Stutter et al., 2009). Riparian soils tend to be rich in organic matter and DOC, supplied by leaves of trees at the soil surface and DOC exudates from tree roots (Jaynes and Isenhart, 2014). Anaerobic conditions in the waterlogged soil and availability of carbon can promote denitrification but may also promote the release of SRP from soils (Stutter et al., 2018a, 2009). Additionally, riparian buffer zones and constructed wetlands are typically situated downslope of fields where they can intercept organic and mineral runoff from fields and trackways. The DOC supplied by organically rich agricultural runoff may promote denitrification within wetlands and riparian soils, but agricultural runoff will also contain high loadings of organic N, ammonium/ammonia, and organic and mineral forms of P. The risks imposed by high nitrate loadings to surface waters must be carefully weighed against those imposed by efflux of other water quality parameters (Stutter et al., 2018). Runoff from field and trackway surfaces in dairy farms is also likely to contain high loads of faecal pathogens such as *Escherichia coli*, which may persist for extended periods within the anaerobic environments of constructed wetlands (Romani et al., 2016; VanKempen-Fryling and Camper, 2017). The potential incompatibility between flood-mitigation and water quality management has already been highlighted. Given the complexity, and potential incompatibility, of nutrient-transformation processes, the risk of 'pollution swapping' should also be carefully considered when designing NbS features for water quality management (Kröger et al., 2013; Stutter et al., 2019). To address incompatibilities among NbS features, a 'treatment-train' approach has been advocated in which NbS features are installed in a sequence whereby appropriate conditions are established in each feature for effective attenuation of the effluent of each feature by the next one in the treatment train (Ekka et al., 2021; Herzog et al., 2019). This approach may be an effective in dealing with the complex and variable nature of agricultural runoff composition and attenuation processes and facilitate the attenuation of water quality and flood pressures within a confined set of NbS features. Importantly, however, effectiveness is inherently contingent on all features being designed, constructed and managed appropriately, which may be a substantial task for individual land-owners and require substantial land-take which may preclude profitable agricultural land-use (O'Rourke, E.; Finn, 2020; Suttles et al., 2021). The issue of appropriate levels of management required to achieve effective mitigation of water quality or quantity problems may be a substantial barrier to the uptake of NbS, generally. Moreover, the long-term and seasonal variation in the performance of detention basins for peak flow mitigation and water quality management remains poorly explored (Penning et al. 2023).

In-stream NbS features such as leaky dams and low-head boulder weirs are installed to replicate the role that naturally-occurring LWD and other in-stream geomorphic features have on the flux of water and water quality parameters through the catchment (Grabowski et al., 2019). Leaky dams are a commonly-applied form of NbS in agricultural catchments as they can be installed at relatively low cost by small groups of trained individuals. They are typically constructed of timber boards or logs positioned within the channels perpendicular to the direction of flow and secured to each bank to prevent them from being forced downstream during high flows (Yorkshire Dales Rivers Trust, 2018). They are designed to intercept high flows by causing water to back up within the channel when water levels rise above a threshold, below which a 'freeboard' zone permits the unimpeded flow of water and the upstream/downstream movement of fish. During high-flows, leaky dams may attenuate flood peaks by increasing channel roughness, so increasing the degree of in-channel storage or by forcing backed-up water to spill onto banksides, helping to hydraulically connect channels to riparian floodplains and offline storage areas such as flood detention basins (van Leeuwen et al., 2024; Yorkshire Dales Rivers Trust, 2018). Through the installation of leaky dams throughout anthropogenically altered catchments, they may help to restore natural woody debris and sediment transport processes, and over time become increasingly effective at impeding high flows as natural debris accumulates at each leaky dam. Numerous modelling-based studies suggest that leaky dams can be effective in attenuating flood peaks (Black et al., 2021; Hankin et al., 2020; Wenzel et al., 2014), although empirical evidence on their efficacy in mitigating damaging floods, however, is rare (van Leeuwen et al., 2024)

The impounding of water behind channel-spanning natural and human-made features inherently results in localised regions of slow-moving water upstream and fast-moving water on the downstream side. The sediment and woody debris that can be deposited and collect on the upstream side may provide adequate substrate for colonisation of macroinvertebrates and micro-organisms which can break down and transform organic material and dissolved nutrients (Blaen et al., 2018). Channel spanning features may help to establish sufficient pressure gradients between the streambed surface and the hyporheic zone beneath the feature (Magliozzi et al., 2018). Low-head boulder weirs have been installed in streams and rivers which had been modified for anthropogenic land-uses in order to re-establish processes of hyporheic exchange and associated nutrient transformations (Rana et al., 2017; Liu et al., 2022). In the presence of gravel beds with sufficient hydraulic conductivity, these features can bring about substantial attenuation of dissolved organic and inorganic pollutants (Herzog et al., 2016; 2023).

It must be noted that an inherent consequence of the retention of water by discrete in-stream or offline features is the establishment of hydraulic gradients and pressure differentials between upstream and downstream sides of a given feature. The more effective a feature is at storing water, the larger this differential will be and the greater the hydraulic pressure exerted on the feature (Muhawenimana et al., 2021). The risks of scour and erosion of streambeds and banks, and the collapse of in-stream NbS features like leaky dams and offline features like flood detention basins must be acutely considered prior to construction, and the features must be sited and designed so that the consequences of failure are minimised. Likewise, features which may store and facilitate the treatment of agricultural runoff must not themselves become point sources for pollution, for example, during periods of overland flow when material in swales and wetlands may be mobilised to adjacent surface waters.

1.5 Thesis aims and knowledge gaps

This thesis explores the implementation of four NbS features to address water quality and flood peak management at the farm-scale. It is the first empirical study of the functioning and impacts of these features in Ireland. This thesis set out to explore:

1. The effects of farm-scale NbS features on downstream flood peaks
2. The effects of farm-scale NbS features on water quality
3. The impact of offline storage of water during flood peak events on grass pastures and soil health
4. The effectiveness of NbS features on flood peaks and water quality under naturally variable seasonal conditions of flow discharge, nutrient loading and temperature
5. The feasibility of farm scale NbS features in bringing about meaningful flood peak and water quality management from the perspective of feature construction, maintenance and monitoring.

It was with these considerations that we could be confident that, should the features bring about the desired benefits to flood management or water quality, they could be adopted by the wider community.

Chapter 2 details the impacts of an offline flood detention basin on flood peak attenuation and water quality over successive high-flow events between 2021 and 2023. The flood detention basin was constructed on a pasture field accommodating a herd of up to 50 heifers and calves. Stream water was diverted to the detention basin during flood peaks and slowly drained back to the channel in its wake.

Chapter 3 describes the effects of repeated inundations of the flood detention basin on sward health and productivity over a 13-month period between June 2022 and July 2023. The potential for the flood detention basin to attenuate high-flows and water quality parameters without disrupting farm activities or enterprise was a key marker of the success of NbS features in the study.

Chapter 4 illustrates the role of in-stream features in mediating the flux and transformation of water and dissolved nutrients through the channel under low- and high-flow conditions. Two features were constructed along a contiguous section of the stream that flows through the study site. The upstream feature was a series of low-head boulder weirs which were examined for their capacity to promote transient storage and nutrient uptake within and at the surface of streambeds upstream of each weir under low to moderate flows. Downstream of the boulder weirs, a series of leaky dams were constructed so that during low flows, stream-water would flow beneath the transverse logs of the leaky dams but would become partially impounded by the leaky dams at higher flows. The potential for the leaky dams to attenuate flood peaks was examined over a range of high-flow events before and after leaky dam installation.

Chapter 5 presents results on dissolved nutrient transformations along a woodland swale feature. The swale was designed to promote the processing of agricultural runoff from adjacent fields and trackways by maximizing the surface area of the swale in contact with the air and the soil, and by fitting ‘check dams’ at regular intervals to help retain water within the swale and maximise the degree of contact between contaminated water and the soil surface of the swale.

Chapter 6 presents a discussion of the results outlined in the previous chapters, and the possible implications of the research on the application of NbS at the farm scale for management of flood risk and water quality in agricultural catchments. It will explore challenges facing the adoption of the NbS approach and how NbS features may be best applied to bring about the greatest benefit to the environment and communities.

Chapter 2:

The hydrological and water quality performance of an agricultural flood detention basin

Abstract

The role of Nature-based Solutions (NbS) for flood and water quality management has been explored across many projects over the past recent decades, but there exist significant barriers to more widespread adoption. While studies have illustrated some benefits, the effectiveness of NbS features for flood attenuation and water quality improvement has been shown to vary among flood events and may change as the features age. Studies illustrating the effectiveness of NbS in Ireland in particular are lacking and, given the severity of water quality issues in agricultural catchments, there is a pressing need for empirical evidence on any benefits they may provide. We report here the impacts on peak flow attenuation and water quality parameters of a flood detention basin constructed on a farm in the south of Ireland. The detention basin consisted of a raised earthen bund constructed within a field bordering a first order tributary, which temporarily stored floodwaters leaving the stream via a constructed sluice. Data from flood events over two years showed marked flood peak attenuation by the detention basin, except under conditions of prolonged rainfall. The detention basin brought about significant attenuation of suspended solids and nitrate, but acted as a source of soluble reactive and particulate phosphorus. The detention basin did not impair any day-to-day workings of the farm and has yielded important insights into how similar features may be adopted across agricultural catchments.

2.1 Introduction

Throughout history, fluvial flooding has been an important factor in determining the distribution and extent of human settlement. Over-bank flooding occurs when the hydrological conveyance capacity of a river channel for a given water flow rate is exceeded (Abbe et al., 2019; Short et al., 2019). Over the past 200 years in industrialised nations, substantial changes have been made to the hydrological characteristics of many catchments to facilitate the expansion and intensification of agricultural activities (Poff et al., 1997; Robotham et al., 2022). These changes have included extensive land drainage and the widening, straightening and deepening of stream channels to enhance conveyance of peak flows through catchments and away from agricultural fields, so leading to the disconnection of streams and rivers from their natural floodplains (Poff et al., 1997; Janes et al., 2017; Rogger et al., 2017). The cumulative impacts of these hydrological flow path modifications within catchment headwaters inevitably increase flood risk lower in the catchment from both seasonal and extreme hydrological events. Additionally, the development of hydraulically smooth and deeply incised land drains may contribute to increased flood risk downstream as shorter and more severe flood peaks move down through the catchment (Pierce et al., 2012; Dadson et al., 2017). While these changes have facilitated important increases in agricultural production and economic expansion, they have coincided with, and possibly contributed to, greater risks to society from large-scale flood events (Dadson et al., 2017; Rogger et al., 2017). As the extent and economic value of urban settlements have increased, so too have the costs involved in repairing damage caused by floods (Dadson et al., 2017; Cooper et al., 2021). Extreme hydrological scenarios (e.g., floods and droughts), are predicted to become more severe in the future and to have greater societal impacts due to climate change (Smith et al., 2019; Keesstra et al., 2021), hence, there is an urgent need for integrated and practical hydrological interventions for improved flood risk management in agricultural catchments.

As well as affecting the hydrology of catchments, agricultural intensification has contributed to altering the flux of dissolved and particulate pollutants to receiving waters. In Ireland, agriculture has been implicated as the greatest driver of impaired water quality nationwide (Environmental Protection Agency, 2022). Agriculture accounts for an estimated 67% of total landcover in Ireland (Department of Agriculture, Food and the Marine, 2017) and studies have shown that intense and localised impacts from nutrients on water bodies can result from the mobilisation of mineral and organic fertilisers from fields, farm trackways and farmyards during rainfall events and during periods when water tables are close to the surface and connecting with surface drainage (Edwards et al., 2012; Harrison et al., 2019; Fenton et al., 2021). Increases in flashiness and peak flow velocities of watercourses in agricultural catchments may also contribute to higher loadings of nutrients and fine sediment being delivered to areas lower in the catchment during high-flow events (Jordan et al., 2012). Compaction of soils by livestock and machinery can reduce infiltration of rainwater and exposes bare soils to more erosive overland flows during rainfall events: increasing suspended sediment fluxes downstream (Deasy et al., 2009; Rogger et al., 2017).

Throughout the European Union (EU), implementation of the Water Framework Directive (Directive 2000/60/EC; (CEC, 2000) has neccesitated a holistic manangement approach to protect and restore water quality and ecosystem function at river basin scale across across Europe. Within this framework, the EU Floods Directive (2007/60/EC) was introduced to mitigate the risk posed by flooding on human health and the environment (Crawford et al., 2022) and promotes the inclusion of nature-based solutions (NbSs) in flooding and water quality interventions (Collier and Bourke, 2020; Heneghan et al., 2021). NbSs feature ‘soft’ engineering solutions which tend to be inspired by, and include the use of, natural processes and materials, and as such, may bring about additional co-benefits to river corridors such as habitat restoration, carbon sequestration, biodiversity enhancement, bank stability as well as water quality benefits (Cole et al., 2020; Heneghan et al., 2021; Robotham et al., 2022). NbS for flood management aims to reduce flood risk to society (living in downstream settlements) by reducing and extending flood peaks through temporary storage of flood water throughout a catchment, and through increasing flowpath length and rugosity (Lane, 2017; Quinn et al., 2022). This may be achieved through hydromorphological alterations to the land to reduce flow rates to channels (e.g. woodland and hedgerow planting); increasing stream channel length and roughness (e.g. channel re-meandering, installation of large woody debris); and through re-connection of streams to floodplains for ‘offline’ storage opportunties (Lane, 2017; Black et al., 2021; Cooper et al., 2021; Janes et al., 2017). While imposing the greatest negative impact on water quality, agricultural catchments, by their scale within the landscape, may also serve as important locations for both natural flood management and for water quality (Heneghan et al., 2021).

Flood detention basins are a form of NbS which may attenuate flood peaks through partial diversion of stream waters to out-of-bank detention areas during peak flows, followed by post-event release after the main flood peak has abated (Acreman et al., 2003; Brasil et al., 2021; Lane, 2017). These features are typically sited on historic floodplains and use local soils to create linear features (bunds) which temporarily store ponded water behind them and have been demonstrated to reduce peak discharge and flashiness (Fiener et al., 2005; Kail and Hering, 2005; Nicholson et al., 2012; Lockwood, 2022). Much less is known, however of the water quality co-benefits of detention basins (Barber, 2013; Ludwig et al., 2016; Robotham et al., 2022). Temporary storage of turbid flood waters may facilitate settlement of suspended solids and associated retention of adsorbed pollutants such as phosphorus and pesticides (Robotham et al., 2022). Detention basins can increase the residence time of nutrient-laden water at pivotal catchment locations and increased contact time with biologically active terrestrial soils may facilitate nutrient uptake and transformation by soil microbial communities, where attenuation process such as nitrification, denitrification and metabolism of organic matter may be favoured (Revsbech et al., 2005; Quinn et al., 2013; Robotham et al., 2022).

This study investigated, for the first time in Ireland, the potential of detention basins in headwater agricultural catchments as an implementation of NbS for the dual benefit of attenuation of flood peaks and improvement of water quality in downstream surface water. Specifically, we designed and constructed an flood detention basin, consisting of an earthen bund in an agricultural field, retaining over-bank floodwaters from a first order stream draining a 1 km^2 catchment in SW Ireland. During spate flows, stream water was partially directed to the detention basin through a constructed sluice in the stream bank and flowed over the field before being retained behind the bund. Water left the detention basin via drainage pipes within the bund. Stream water levels were monitored upstream and downstream of the bund to record the impact of the detention basin on stream discharge over a series of spate events over the course of 24 months. Dissolved and particulate substances, including suspended sediment, plant nutrients and dissolved organic carbon, were also quantified before and after water had entered and left the detention basin, during the spates, so as to quantify the potential impact of the detention basin on water quality.

2.2 Materials and methods

2.2.1 Study area characteristics

The study site was located within the upper Lee Valley in Co. Cork, Ireland (51°56'09 N 8°52'59W; 150.07 – 146.47m above sea level). As part of a wider project, NbS features were developed along a c. 1km section of an unnamed first order stream which is a tributary of the Glashagarriff River which joins the Inniscarra Reservoir of on the River Lee approximately 7 km southeast of the study site (Fig. 1). The soil upstream of the study site consists primarily of fine loamy soil over sandstone bedrock (Teagasc, 2023). The stream rises approximately 2km north of the study site. The catchment is comprised of approximately 80% agricultural grassland, with the remaining land dominated by heathland and conifer plantations, with some broadleaf plantations within the farm itself (Environmental Protection Agency, 2018). The area receives an average annual rainfall of 1305 mm (2000 – 2022; (met.ie, 2023). At the study site, the stream drains a catchment area of 1 km^2 (Government of Ireland and Tailte Eire, 2023), as calculated by area within the upstream watershed of the stream that flows through the study site.

In Spring 2020, an earthen bund of length c. 60m was constructed at the downslope edge of 1hectare pasture field, for the retention of floodwaters during high-flow events in the detention basin (Fig. 2a-d). The bund was formed from local top-soil which had been recently collected by the local council during drain maintenance. The soil was laid in an L-shaped mound, with sides approximately 20 m × 60 m. The bund was shaped and compacted by a backhoe loader so that it was 2 m above the field level at its highest; 2 m wide at the top and 4 m wide at the base (Fig. 2a, c). The bund was compacted and fenced off until it was fully vegetated (a period of about 3 months). The bund suffered only minor erosion due to trampling of livestock, but it remained largely intact in the 4 years following construction despite continual grazing by livestock and flood waters ponding against it during inundation events. A concrete-reinforced sluice was constructed in the detention basin inlet within which wooden boards could be fitted horizontally. The sluice was constructed using concrete blocks and shuttering to form an erosion-resistant and smooth surface. The structure was fitted with iron brackets in which wooden boards could be fitted to allow the level at which the stream water entered the detention basin to be adjusted *(*Fig. 2b*).* A porous stone weir of height c.0.5 m was constructed from boulders and stones found allow the stream channel. The weir spanned the channel at an angle of c. 45° from the to help direct high flows through the sluice at the detention basin inlet (Fig. 2a). Stream water was delivered to the detention basin via the sluice and travelled along the overland flow-path for 80 m at a mean gradient of 4% where it was impounded against an earthen bund at the base of the field (Fig. 2c). Two 15 cm diameter plastic pipes were installed within the bund, to allow floodwaters to be temporarily retained within the detention basin to drain back slowly into the stream channel after the flood peak had passed (Fig. 2d).

The field on which the detention basin was constructed was selected on the basis of its sloping profile, which facilitated the formation of a ponding zone, and due to the presence of the stream channel running along its northern and eastern perimeter which could be easily diverted to the field and re-directed to the channel below the detention basin bund. The field had some sub-surface drainage which had been installed in recent decades. During bund construction, efforts were made to seal this drain from the field surface in the ponding zone through laying and compacting grass-sod over the line of the drain and further laying topsoil and bund material above this.

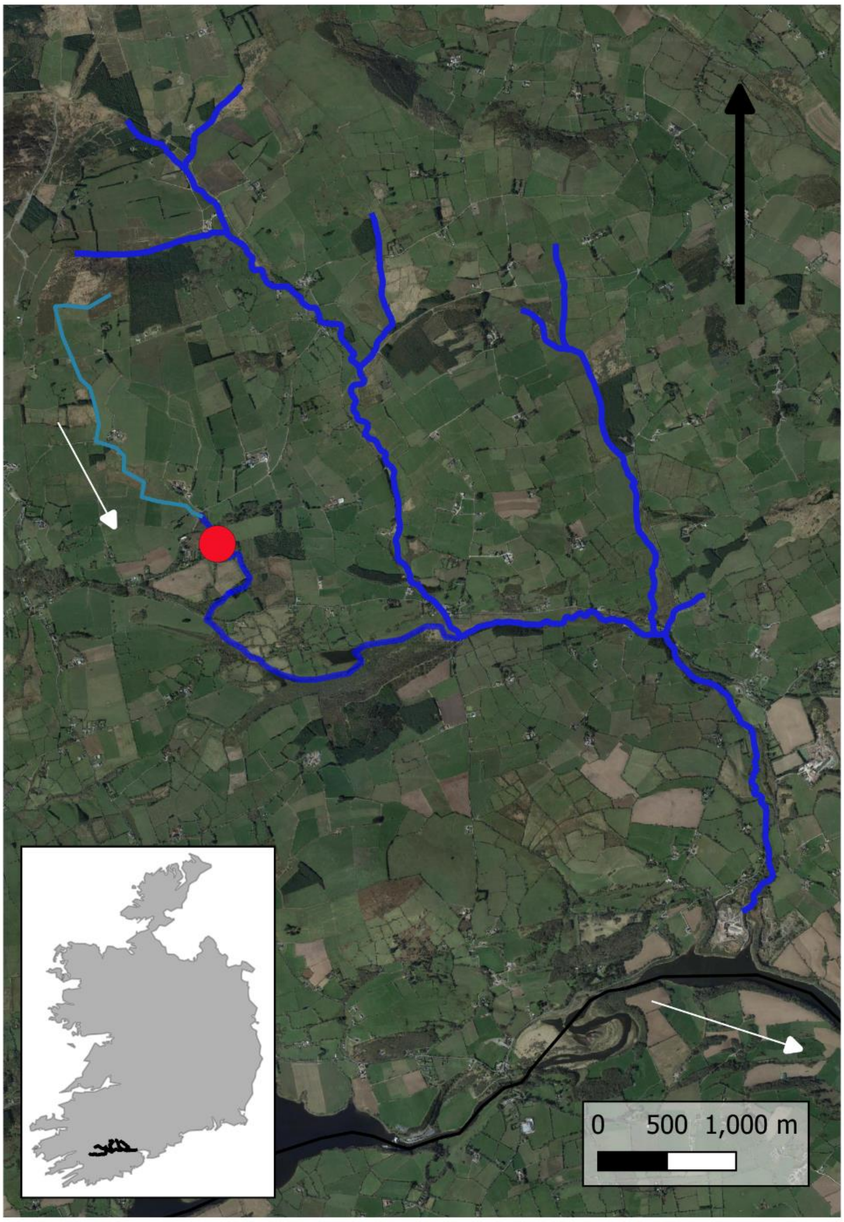

Figure 1 Map of Glashagarriff sub-catchment (main: blue line) within the River Lee catchment (Inset; black line) in the south of Ireland. The study site (main: red marker) is along the route of a first order stream which feeds into the Glashagarriff catchment (main: light blue line). The Glashagarriff flow southwards before meeting the River Lee (Black Line). White arrows indicate direction of flow of streams. Black arrow indicates north. Source: Fieldmap contributors and GIS user Community

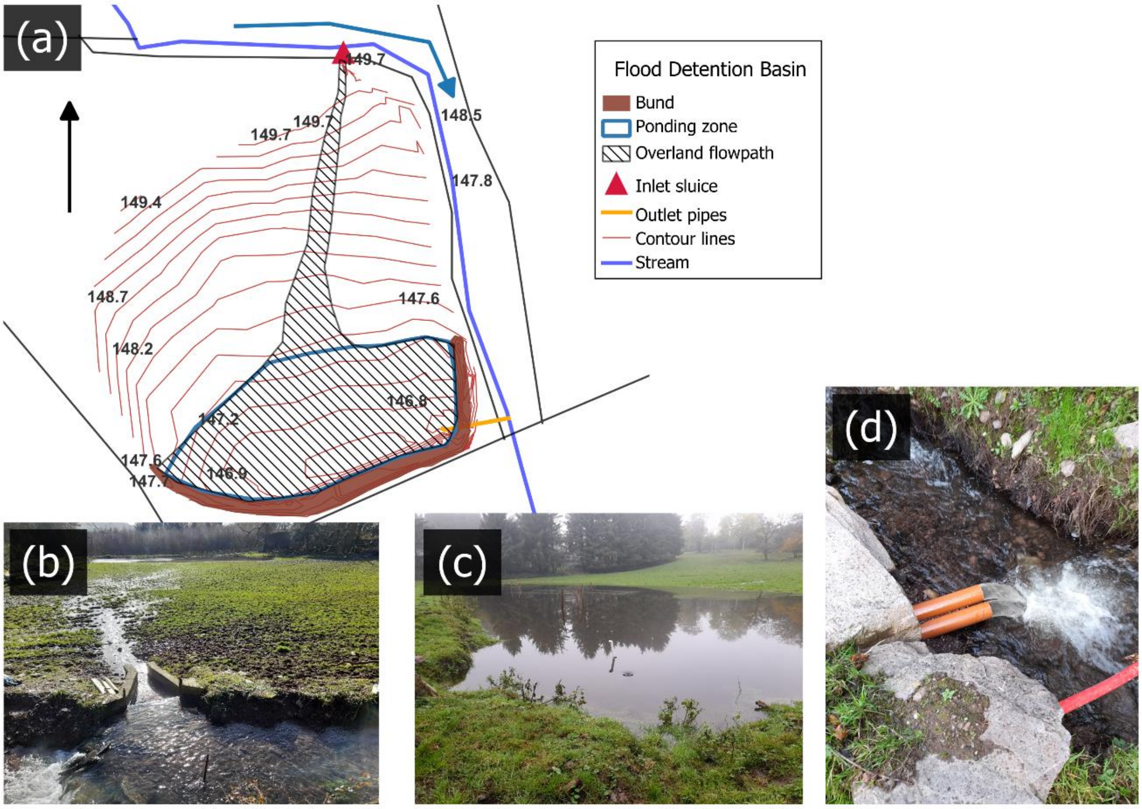

Figure 2a-d shows the study site flood detention basin. 2a shows detention basin schematic with first order stream (Leades stream; blue arrow) flowing from north to south along the northern and eastern side of the detention basin. Red contour lines denote elevation above sea level. Panels 2b-d show detention basin features functioning during an inundation event: (b) high flows being partially directed from channel through sluice of detention basin inlet to detention basin ponding zone via overland flow path; (c) ponding zone of detention basin; (d) detention basin outlet pipes draining detention basin back to stream channel.

2.2.2 Detention basin storage volume estimation

In July 2021, a topographic survey was conducted using ground telemetry of 180 spatial data points (easting, northing, elevation above sea-level) collected from the detention basin and the stream area upstream and downstream of the detention basin. These data were accurate to 1 cm altitude and used to produce a volume-estimation curve for ponding depths from 0-1.5 m at the topographic minimum of the detention basin (the detention basin water level recorder location; 146.54 mASL) using the QGIS Volume Calculation Tool (REDCatch Volume Calculation Tool 0.4; QGIS version 3.24.3-Tisler, Boston, MA, USA). A second order polynomial equation was derived for the curve in Excel (Fig. 3; Equation 1) to estimate volume storage volume along the water level time series data. This equation was then applied to time series depth data at the detention basin WLR for estimation of detention basin volume (m^3) during flood events.

$$V = ah^b \qquad \text{(Equation 1)}$$

V = Volume (m^3); a and b = coefficients, h = pond stage (m)

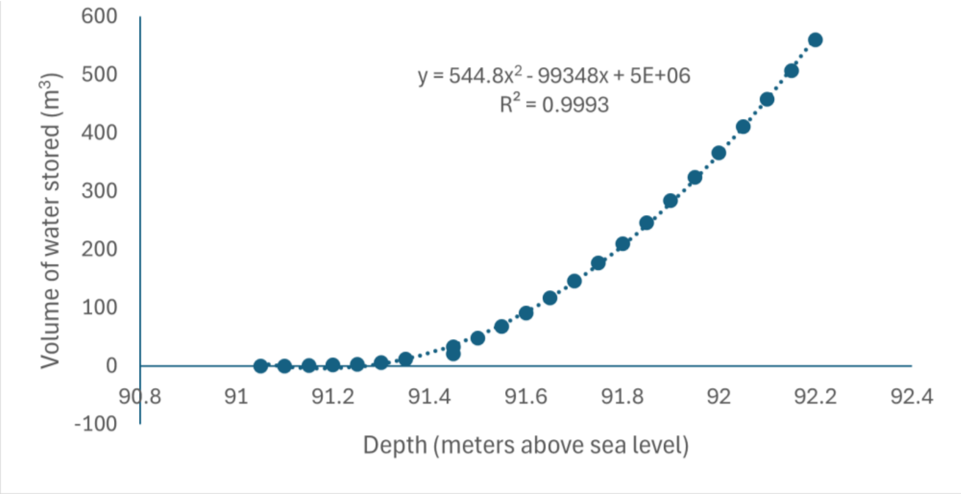

Figure 3 The line derived from the relationship between Depth of water stored at the topographic minimum of the detention basin (x-axis; meters above sea level) and the volume stored in the detention basin (y-axis; m^3) as estimated from topographic data from the detention basin. The equation of the line and the R^2 value for fit of the data to the model.

2.2.3 Rainfall and hydrological measurements

A tipping bucket rain gauge (SBS500 Tipping Bucket Rain Gauge, Campbell Scientific, Canada) was installed c. 500m upstream of the detention basin in August 2020. Data were collected from 24 August 2020 to 30 November 2020. Due to technical issues, only inconsistent rainfall data collection occurred between November 2020 and September 2021. A consistent dataset is available from 27 September 2021 to 8 November 2021, and 7 January 2022 to 19 April 2023. Where there are gaps in the rainfall data collected from the site, rainfall data was acquired from the Irish Meteorological Service at the closest meteorological station to the site (Carrigadrohid station 3604; 51°53'49.8"N 8°51'49".7W; Elevation: 65m: (met.ie, 2023) located c.4.5 km south of the site. A conversion factor was derived through comparison of publicly available regional rainfall data (met.ie, 2023); and contemporary data from the study site rain gauge (See Appendix 1A, Supplementary Methods, Fig. S1A3). This factor was used to derive an estimate for local rainfall from the met.ie data during periods when local data were missing. An estimated

2510 mm of precipitation fell at the study site over the study period: 1283.4 mm fell in 2021 (Carrigadrohid weather station: (met.ie, 2023; and 1226 mm in 2022 (study site rain gauge). This is close to the mean annual rainfall of 1305 mm for the region (2000-2022; (met.ie, 2023).

Water level recorders (WLRs; *In-Situ Inc. Rugged TROLL® 100*, *USA*) were deployed in stilling wells at the topographic minimum of the detention basin, within the stream channel 5m upstream of the detention basin inlet and 5m downstream of the detention basin and recorded barometric pressure at 5-minute intervals. A Barometric Pressure Recorder (BPR; *In-Situ Inc. Rugged BaroTROLL®*, *USA*) was deployed about 200m south of the detention basin to measure atmospheric pressure at the same time as the WLRs and estimate water level from absolute pressure data from the WLRs (Trill et al., 2022).

Stream flow velocity was measured using a Valeport Electromagnetic Flow Meter (Model 801; Flat Type 0801001, UK). Between November 2020 and April 2023, flow velocity and cross-sectional measurements were made across a range of flows (baseflow to high-flow) between November 2020 and November 2022 to establish a stage-discharge relationship and develop a rating curve for each WLR location using Equation 2, below (Acreman et al., 2003; Nicholson et al., 2020). See Appendix 1A for discharge data and rating curves.

$$Q = ch^d \qquad \text{(Equation 2)}$$

Where Q = stream discharge (m s^{-1}), c and d = coefficients and h = stream stage (m).

Dilution gauging using a conservative tracer solution (NaCl) was performed within the channel to provide comparative measure of discharge (Piper et al., 2017). Q derived from dilution gauging showed agreement with rating curves derived by equation 2 within c.0.002 $m^3 s^{-1}$ (R^2 = 0.3761; correlation coefficient = 0.613, n = 6).

2.2.4 Hydrological Analysis

Estimation of flood peak discharge attenuation was illustrated through comparing peak discharges upstream and downstream of the detention basin during inundation events (Nicholson et al., 2020) the net increase in volume of water within the detention basin (Lockwood et al., 2022) and the difference in area under curve values for the upstream and downstream hydrographs during the detention basin filling period (Quinn et al., 2013) The area under the curves (AUC) for discharge hydrographs of the WLR locations upstream and downstream of the detention basin were calculated for filling periods during inundation events - i.e. the start of detention basin volume increasing until reaching the maximum volume for the event. The difference between the upstream and downstream AUC values was taken as the volume of water that was diverted to the detention basin during the filling period (Quinn et al., 2013). Flood events were categorised as single or multi-peak events and according to whether there was standing water present in the detention basin prior to a given flood peak. Single-peak events and the initial inundation of the detention basin of a multi-peak event were grouped together. Inundations occurring within an extended event after the initial filling event were categorised as multi-peak events (Lockwood et al., 2022).

Flood attenuation was also assessed through estimation of the extension of the flood peak resulting from storage in the detention basin. It was assumed that the detention basin conferred flood peak attenuation through increasing flow path-length and channel rugosity as long as water captured during the flood peak was retained by the detention basin (Nicholson et al., 2012). The flood peak extension period was thus taken as the entire time water was stored in the detention basin minus the period during which water entered the detention basin at the sluice inlet - i.e. the period when upstream discharge exceeded the take-off threshold. The calculation was possible for inundation events for which the detention basin started and returned to an inundation volume of 0m^3 after individual flood peaks i.e. single-peak events. The flood peak recurrence interval was measured based on the maximum mean daily discharges for each month between December 2021 and October 2023 and fitting the ranked values to a Gumbel distribution (Gulap and Gitika, 2019).

2.2.5 Water quality sampling and analysis

2.2.5.1 Sampling protocol

Surface water sampling at the detention basin during flood events consisted of grab samples in sterile 1L bottles and in-situ measurements of Electrical Conductivity (EC) and dissolved oxygen (DO) using a portable meter (WTW ProfiLine Cond 3110, Xylem Analytics, Germany; Oxygen and temperature: OxyGuard® Handy Polaris Hv. 3.15, EU, (https://www.oxyguard.dk, 2020). In-situ and grab sampling on all occasions was conducted at the detention basin inlet. Sample bottles were stored in a cool-bag and frozen at -80°C with 6 hours of collection. On all but one occasion (event of 30-31 Dec 2021) samples were obtained from the outlet of the detention basin base pipe. On the event of 30-31 Dec 2021 high water levels in the channel at the detention basin outlet caused the outlet pipes to be submerged within the main channel for an extended period. On this occasion, the ‘outlet’ sample was acquired from the water column of the detention basin pond zone as near as possible to the outlet pipes: the sample bottle was secured to a pole and extended into the water column to prevent trampling and mobilisation of sediment during acquisition. To help identify locations within the detention basin where changes in water quality may be occurring, additional sites were also sampled during certain flood events (Kianpoor Kalkhajeh et al., 2019) (7th Oct 2021, 9th Mar 2022, 26th Oct 2022, 23rd Nov 2022).

When possible, three surface water samples were collected simultaneously from both the detention basin inlet and detention basin outlet during detention basin inundation events. Single surface water samples only were collected from the detention basin inlet and detention basin outlet on 26th October 2022 and 23rd November 2022. SEC and DO measurements were made in-situ during sampling events. Due to technical issues with the hand-meters, measurements during all events were not possible. On the sampling event of 9th mar 2022, water quality data were collected various sites within the detention basin, to aid in identifying locations of parameter concentration changes at a finer scale. Samples were taken at 15 m intervals along the flow path from the detention basin inlet to the detention basin outlet, as well as from the surface and bottom of the deepest are of the detention basin.

2.2.5.2 Laboratory water quality analysis

Composite water samples were collected in sterile 1L HDPE bottles from the water column. Bottles were stored in a cooler (4ºC) and frozen at -80°C within 6 hours of collection. Samples were analysed for Nitrate (NO_3^- - N), Ammonium (NH_4^+- N), Soluble Reactive Phosphorus (SRP), Total Phosphorus (TP), Dissolved Organic Carbon (DOC) and Chloride. For determination of NH_4^+, samples were filtered through 0.45 µm PVDF membrane filter and analysed by automated salicylate method using the Lachat Quikchem 8000 FIA (Zellweger Analytics, Inc. Milwaukee. USA. Method Code: QuikChem Method 10-107-06-3-D) (Method Detection Limit (MDL) = 0.002, Relative Standard Deviation (RSD) = 12%). Determination of SRP was done through automated ascorbic acid method using the Lachat Quikchem 8000

FIA (Zellweger Analytics, Inc. (Milwaukee. USA. Method Code: QuikChem Method 10-115-01-1-B) (MDL = 0.001 mg P L^{-1}; RSD = 5%), following filtration through 0.45µm PVDF membrane filter. NO_3^- was analysed by automated FIA colorimetric method following filtration through 0.45µm PVDF membrane filter and reduction of nitrate to nitrite through copperised cadmium column (Method Code: 10-107-04-1-C) (MDL = 0.007 mg N L^{-1}; RSD = 3%). To determine TP, unfiltered samples were digested in an autoclave at 121°C with ammonium persulphate and sulphuric acid. The digested samples were analysed using manual Murphy & Riley(Murphy and Riley, 1962) Method (Molybdate – Ascorbic Acid method) (MDL = 0.001 mg P L^{-1}; %RSD = 5). Chloride was determined via the ferricyanide method following filtration through a <0.45µm PVDF membrane filter (MDL = 0.034; RSD = 1%). For DOC determination, samples were filtered through <0.45µm GF/C filter paper then measured by high-temperature combustion method using TOC-VCPH/CPN (SHIMADZU) (MDL = 0.12; RSD = 2.22%). For measurement of suspended solids (SS), a known volume sample water was passed through <0.45µm GF/C filter paper of known mass. Filter paper was dried at 104°C for two hours, then re-weighed. For quality assurance, all methods were carried out in a commercial laboratory in accordance with Irish Environmental Protection Agency National Laboratory Proficiency Scheme, since 2010.

2.3 Data analysis

All statistical analysis was performed in RStudio v2023.03.0.386 (RStudio Team, Boston, MA, USA, 2023) using the R programming language. Mean, maximum and minimum values of water quality parameters were derived for each sampling event. Changes in water quality parameter mean values between the detention basin Inlet and detention basin outlet were calculated as percentage change between upstream to downstream sample sites to give percentage Removal Efficiency (%RE; Robotham et al., 2022). Pooled analyses of concentration changes between the detention basin inlet and detention basin outlet between March 2021 and November 2022 was done using mixed effect linear models with flood event as a random effect using the R package “lme4”. Tests on model fit were performed through inspection of normality plots produced using the R package “DHARMa.” The null hypothesis being tested was that overland flow of flood water through the detention basin would not affect concentrations of sampled water quality parameters. Models with an adequate model fit and with a significance level of $p < 0.05$ were deemed sufficient to allow rejection of the null hypothesis. Linear models and ANOVAs were performed to test whether the presence or absence of standing water affected the above flood attenuation parameters. Under the null hypothesis, the presence or absence of standing water did not affect the attenuation potential of the detention basin ($p > 0.05$).

2.4 Results and discussion

2.4.1 Volumetric attenuation by the detention basin during peak flows.

The detention basin was effective in attenuating peak flows in the first order tributary throughout the study period, by both reducing the downstream peak discharge through volumetric storage behind the bund, and by extending the duration of peak flows beyond the recession period of flood peaks. The potential for the detention basin to affect downstream flows was first demonstrated during the manual test inundations conducted in March, May and October 2021 (Fig. 3). The inundation of the detention basin in March 2021 (Fig. 3a) occurred under winter baseflow conditions, as opposed to during a flood peak (Q c. 0.04 $m^3 s^{-1}$), while the subsequent two, in May and October, were associated with flood peaks (Fig. 3b and

3c). Differences between the discharge hydrographs for the upstream and downstream locations on these dates reflect the reduction in downstream discharge due to diversion of waters to the detention basin (Fig 3 dashed lines); followed by sudden increases in downstream discharge when water was manually released from the detention basin by lowering the outlet pipes to the base of the detention basin (Fig. 3 solid lines). Further information on manual inundations and management of detention basin inlet and detention basin outlet structures is given in Appendix 1A. The boards that closed the sluice were removed for the experimental inundations in March and May 2021, leading to the sharp changes in downstream discharge (Fig. 3a, b). During the October 2021 event, however, the boards were removed, prior to flooding, in anticipation of a peak flow event. Fig. 3c, therefore illustrates a more gradual change difference between upstream and downstream discharges. The sluice was closed prior to the second peak during the October 2021 event, and no substantial difference between upstream and downstream discharges was observed. On the basis of these manual inundations, an appropriate take-off discharge could be set at the sluice that would allow the detention basin to begin filling during the latter portion of a flood peak (e.g. $Q > 0.07$ m^3 s^{-1}). The outlet pipes were arranged so that they slowly, drained stored water back to the channel. In this way, flood peaks during rainfall events led to ‘automatic' inundation of the detention basin. While the rate of flow into the detention basin exceeded the rate of flow out of the detention basin via the outlet pipes, the stage and volume of water in the detention basin increased, i.e. the detention basin attenuated peak discharge (Quinn et al., 2013).

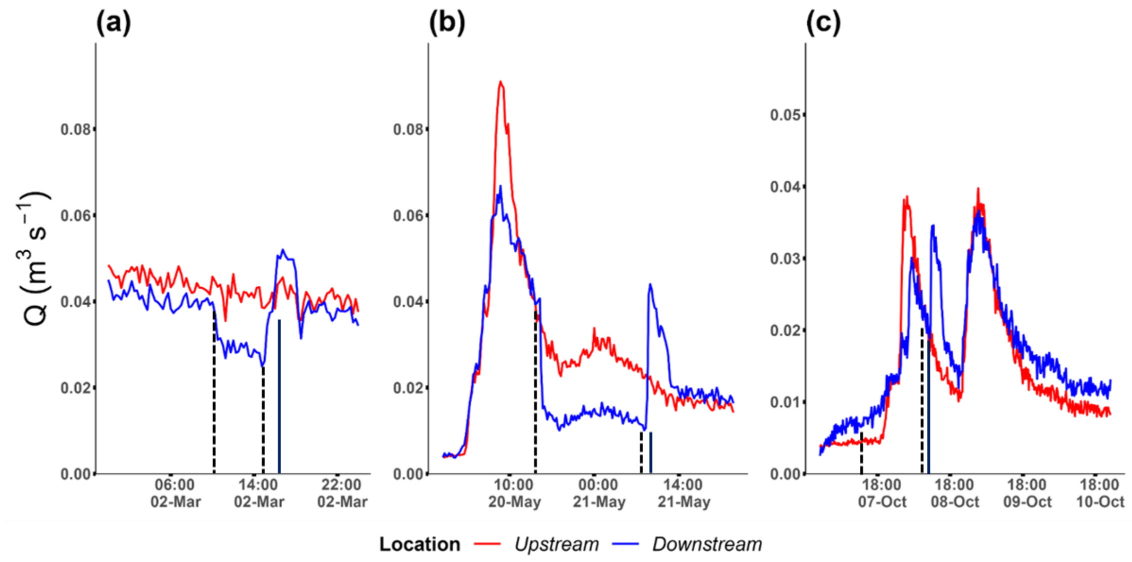

Figure 4 Manual test inundations of the detention basin in March, May and October 2021 (a-c, respectively). Dashed lines indicate removal or replacement of the boards of the sluice at the detention basin inlet to allow water into the detention basin, or stop take-off. Solid lines indicate the time that outlet pipes were lowered to allow the stored water to drain back to the stream.

During the automatic peak take-off period (Stream take-off Q > 0.07 $m^3 s^{-1}$ (1 Nov 2021 – 26 Oct 2022); Q > 0.1 $m^3 s^{-1}$ (26 Oct 2022 – 17 Mar 2023), the detention basin was inundated during 13 high-flow events (Fig. 5). Of these, eight were considered single-peak events (Fig. 5a-h), and five were considered multi-peak events - i.e. the detention basin captured water from the stream before it had fully emptied water from previous flood peaks (Fig. 5i-m). As for the 'test' floodings (Fig. 4), flood peak attenuation was illustrated by the increase in the volume of water stored within the detention basin during the rising limb of flood peaks (Fig 5; black line), and concurrent differences between the hydrograph curves for upstream and downstream of the detention basin (Fig. 5; Red and blue lines respectively). The plots for both single peak and multi-peak events in Fig. 5 consistently indicate flood peak attenuation with downstream peaks less sharp and lower than upstream flood peaks. The upstream and downstream discharges hydrographs also tend to show different discharges while the bund retains water, providing further indication that the observed change in the shapes of downstream hydrographs resulted from water attenuation within the detention basin.

With a maximum storage volume of 245m^3, the detention basin reached an average maximum storage volume of 186.68 m^3 over all events (Standard error 14.67m^3, 76% Table 1). The mean net increase in detention basin volume (i.e., the volume of water directed from the stream to the detention basin during a given flood peak resulting in an increase in water level within the detention basin ponding zone), was 146.36m^3. When accounting for the presence of standing water present in the detention basin during flood peaks, the mean detention basin net volume was 115.197 m^3 (SE 46.84m^3, Table 1). Importantly, the presence of standing water within the detention basin did not have a statistically significant effect on net volume increase during inundation events (ANOVA, $p > 0.05$; Table 1).

Table 1 Detention basin flood peak attenuation summary data for 13 automatic inundation events during peak flows between 7th December 2021 and 17th January 2023 (Single peak events: n = 8; multi-peak events: n = 5). Means and standard error (SE) values for hydrological parameters, as well means for events when the detention basin was empty prior to inundation or had standing water ("DB Inundated"). Columns 2-4 show the difference in peak discharge and time between peaks between upstream and downstream WLR locations; columns 5 and 6 show the difference in areas under curves of upstream and downstream hydrographs during the filling period of the detention basin; columns 7-9 show the metrics on the volume of water stored in the detention basin as registered by the WLR within the detention basin. See table S3 for hydrological parameter data for each event.

	In-stream peak Q difference (m^3 s^{-1})	In-stream peak reduction (%)	Peak delay (mins)	AUC Difference (m^3)	AUC % difference	DB net volume increase (m^3)	Max DB volume (m^3)	Max % DB inundated
All events	0.063	37.84	78.95	820.51	33.48	146.36	186.68	76.2
All events SE	0.008	2.35	31.12	122.27	2.7	16.84	14.69	6
DB empty	0.067	39.247	96.25	889.45	33.55	164.541	166.081	67.79
DB inundated	0.057	35.425	49.286	702.34	33.36	115.197	221.989	90.61

Table 2 Flood peak attenuation through flood peak extension summary data for single peak events. Filing period indicates duration of the detention basin (DB) filling from minimum to maximum volume during a given inundation event (Peak date within a single or initial filling of a multi-peak event). The peak extension time is calculated as the entire detention basin inundation duration minus the Take-off period, where the discharge upstream of the detention basin exceeded the take-off discharge.

Event Period	Peak Date	Filling period	Take-off period	DB inundation duration	Peak extension time
7th-8th Dec 2021	7th Dec 2021	4 hr 15 mins	6 hrs 30 mins	33 hrs	26 hrs 30 mins
30th Dec 2021 – 1st Jan 2022	30th Dec 2021	13 hr 30 mins	34 hrs	57 hrs 30mins	23 hrs 30 mins
9th – 12th March 2022	9th Mar 2022	10 hrs 15 mins	24 hrs	34 hrs	10 hrs
6th Sept 2022	6th Sept 2022	5 hrs 30 mins	1 hr	8 hrs	7 hrs
10th – 13th Sept 2022	11th Sept 2022	4 hrs 45 mins	5 hrs	40 hrs 30 mins	35 hrs 30 mins
30th Oct – 1st Nov 2022	31st Oct 2022	3 hrs 15 mins	20 hrs	45 hrs 30 mins	25 hrs 30 mins
6th – 9th Nov 2022	7th Nov 2022	6 hrs 45 mins	22 hrs	35 hrs	7 hrs
23rd – 24th Dec 2022	24th Dec 2022	4 hrs	3 hrs 30 mins	43 hrs	39 hrs 30 mins
	Mean	6hrs 23mins	14 hrs 30 mins	37 hrs	21 hrs 50 mins
	Standard Error	1hr 15mins	4hrs 15mins	5hrs	4hrs 30mins

Attenuation as estimated through comparison of the area under curve (AUC) of hydrographs upstream and downstream of the detention basin during the filling phase of the detention basin resembled data on the net detention basin volume increase, but AUC differences were higher than net detention basin volume increases (ΔV) in all cases (Appendix 1B, Table S1B2). AUC calculations indicate that the overall mean difference in AUC was 820.51m^3 representing a 33.48% decrease in stream volume downstream of the detention basin, i.e. 33.48% of the upstream flow was directed to the detention basin during the filling period of the detention basin (Table 1). Discrepancies between the ΔV and the AUC values may be attributed to (1) flood water diverted to the detention basin not reaching the pond area but instead being retained on the surface of, or within, the field soil upslope of the detention basin (Jones et al., 2015), and/or (2) water within the detention basin being lost to subsurface drains (Fiener et al., 2005; Levine et al., 2021), (3) water being lost from the detention basin through sub-surface drains. Water balance analysis of upstream and downstream AUCs for whole flood peaks (i.e. the beginning to end of a single flood peak) revealed that an average of 44% of the water diverted from the stream was not accounted for at the downstream logger, with the remaining 56% of the water diverted from the channel by-passing the downstream water level recorder/gauging point. i.e. water was lost through sub-surface drainage and re-entered the channel downstream of the downstream gauging point (Appendix 1B, Table S1B7). The volume of water stored in the bund accounts for an average of 15% (min 1%, max 34%) of the water diverted from the stream. The loss of water through sub-surface drains would have, nonetheless contributed to flood peak mitigation by increasing the path length taken by water diverted from the channel.

When accounting for the filling phase of the detention basin only, the mean AUC difference when the detention basin was empty prior to filling was 889.45m^3 and was 702.34m^3 on average when standing water was present (Table 1). This difference was not statistically significant (ANOVA, F = 0.531*, df* = 17, p > 0.05), but gives some indication of the greater attenuation potential of the detention basin when higher volumetric capacity was available in the detention basin following drier antecedent conditions.

The mean difference in peak discharges upstream and downstream of the detention basin was 0.063 m^3 s^{-1}, representing a peak reduction of 37.84% (Table 1). The difference was slightly higher when the detention basin was empty (0.067 m^3 s^{-1}) relative to when there was standing water (0.057 m^3 s^{-1}), but these differences were not statistically significant (p >0.05). The percentage attenuation of peak Q did not differ significantly between events when the detention basin was empty or inundated (p > 0.05) which indicates that despite the presence of water stored by the bund prior to the onsite of flood peaks within multi-peak events, considerable attenuation may still be occurring within the field without contributing to large changes in the volume as estimated from changes in water level at the topographic minimum. During inundation events, water was observed to sit on the soil surface within natural depressions and within hoof-prints of livestock upslope of the ponding area. This storage of water would not have contributed to changes in the water level (and therefore estimated volume) of the ponded water, but was attenuated by the detention basin, nonetheless. The degree of difference between peak discharges upstream and downstream of the detention basin (peak attenuation) was found to increase linearly with increasing discharge upstream of the detention basin (Estimate: 0.558, se = 0.05, t = 12.929, p <0.001; Fig. 6). This indicates that while a greater proportion of stream water was directed into the detention basin during larger events, the detention basin effectiveness remained constant. The detention basin appeared to have a variable effect on the onset of the downstream flood peak (Peak delay: Table 1; mean = 79mins after upstream flood peak), but the effect was not statistically significant (ANOVA, $p > 0.5$).

Extended rainfall events, such as those in February and October 2022 (Fig. 5i, k) led to sustained high baseflow between flood peaks which limited release of water from the detention basin between flood peaks, leading reduced volumetric capacity in the detention basin. During the February 2022 multi-peak event, the detention basin reached capacity following initial flood peaks. The upstream and downstream curves illustrate the difference in upstream and downstream discharges during the initial filling. During the flood peaks following 21st February, less difference is observed between upstream and downstream curves as the detention basin is at capacity and is having a reduced effect on downstream discharge. A similar situation occurred during the multi-peak event in October 2022 (Fig. 5k), except that differences between upstream and downstream discharge are apparent even when the detention basin volume has reached its maximum. This may be a result of the detention basin overtopping around 22nd October 2022, and again from the 25th October before the sluice level was raised on 27th October, after which stream water was diverted to the detention basin at discharges > $0.1 m^3 s^{-1}$. While the detention basin bund was over topping, much of the outflowing water by-passed the gauging point downstream of the detention basin, giving the illusion of attenuation. This was the only event during the ‘automatic’ detention basin operating period when the detention basin was observed to overtop.

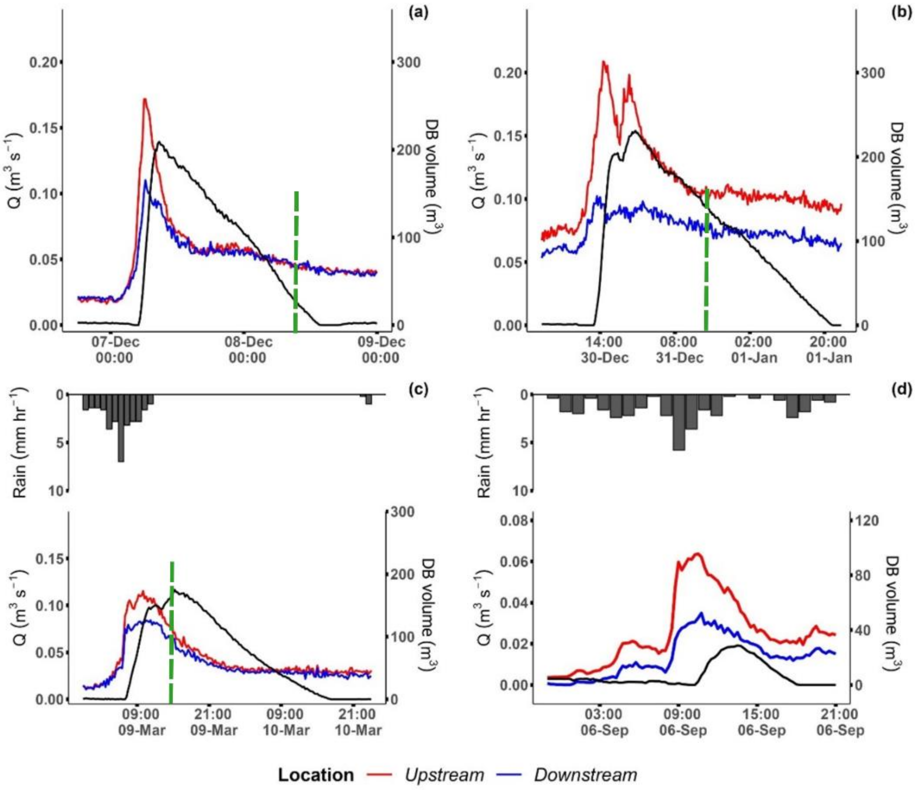

Figure 5a-d Upstream (red) and downstream (blue) hydrographs showing stream discharge ($m^3 s^{-1}$; left y-axis) during single-peak automatic detention basin inundation events between 7th and 8th December 2021 (4a), 30th December 2021 and 1st January 2022 (4b), 9th and 10th March 2022 (4c) and on 6th September 2022 (4d). Solid black line shows the volume of water stored within the detention basin for the same period (m^3; right y-axis). Local hourly rainfall accumalation values ($mm\ hr^{--1}$; onsite rain gauge) were available for the events between March and September 2022 and are denoted with grey bars above respective hydrographs. Dashed green lines indicate the time of water quality sampling where relevant: 8/12/2021: 13:45; 31/12/2021: 16:45; 9/3/2022: 13:00

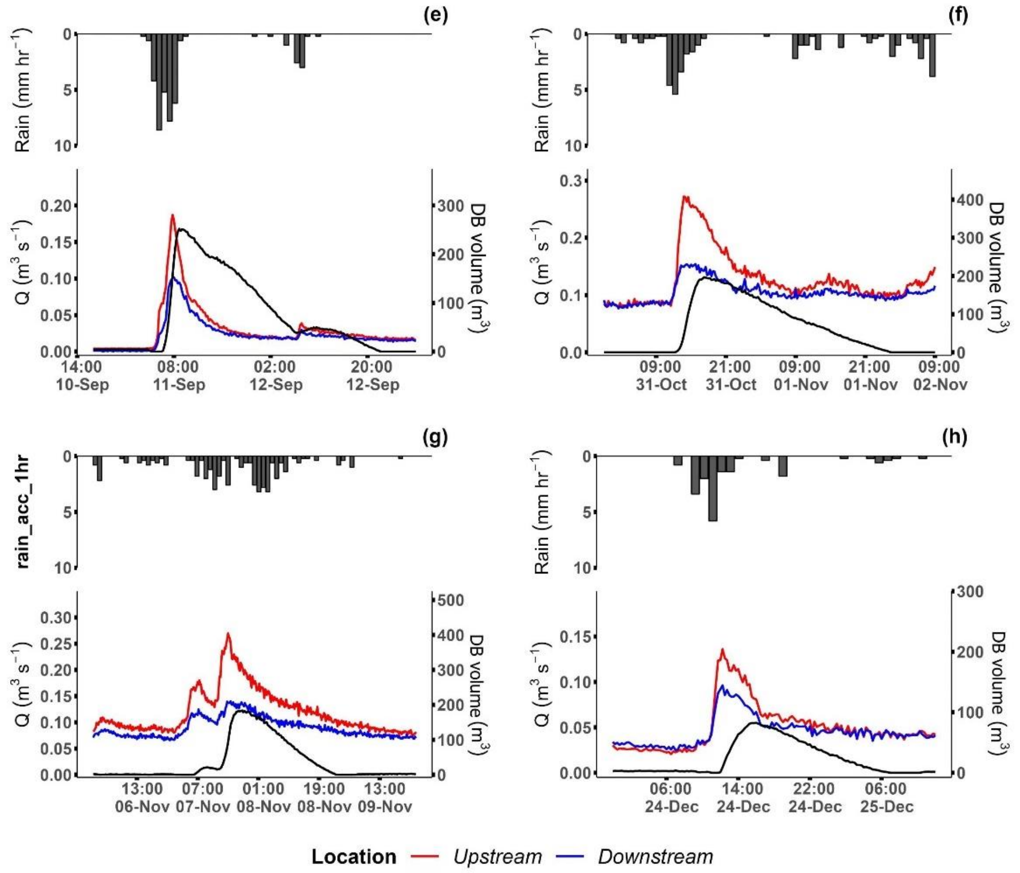

Figure 5e-h Upstream (red) and downstream (blue) hydrographs showing stream discharge (m^3 s^{-1}; left y-axis) during single-peak automatic detention basin inundation events between 10th and 12th September 2022 (4e), 31st October and 2nd November 2022 (4f), 6th and 9th November 2022 (4g), and 24th to 25th December 2022 (4h). Solid black line shows the estimated volume of water stored within the detention basin for the same period (m^3; right y-axis). Local hourly rainfall accumalation values (mm hr^{-1}; onsite rain gauge) are denoted with grey bars above respective hydrographs.

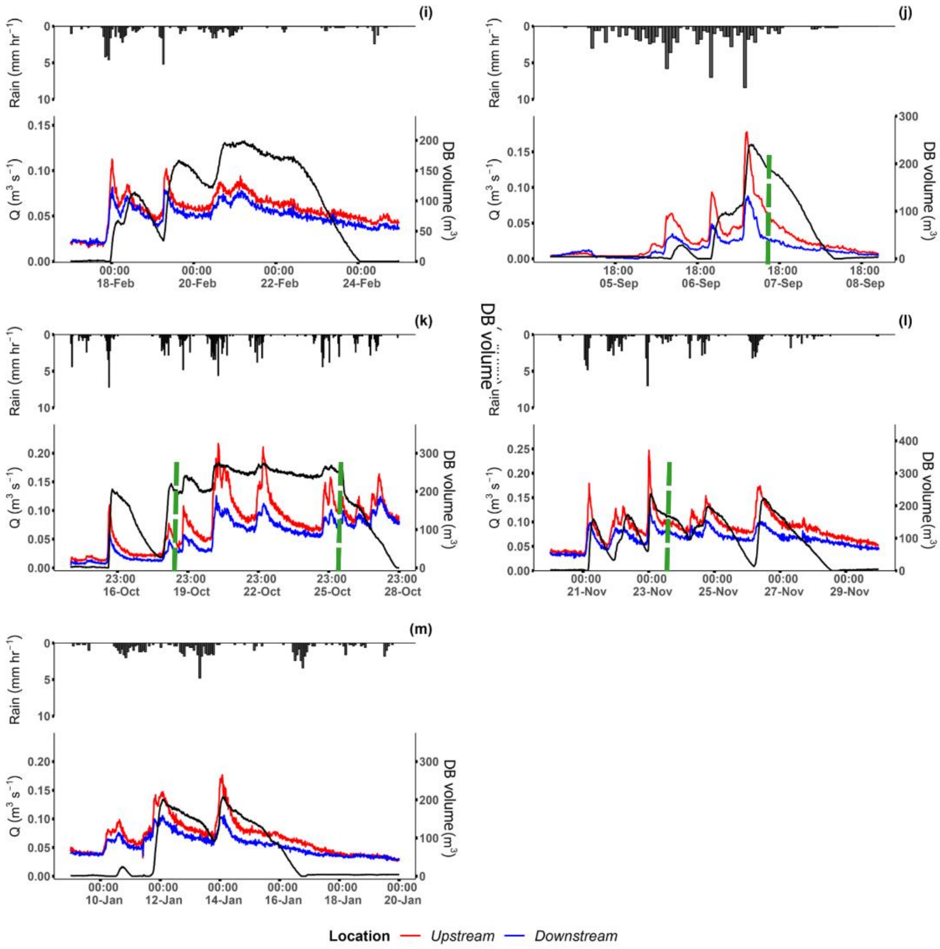

Figure 5i-m Upstream (red) and downstream (blue) hydrographs showing stream discharge (m^3s^{-1}; left y-axis) during multi-peak detention basin inundation events between 18h and 24th February 2022 (4i), 5th and 8th September 2022 (4j), 16th and 28th October 2022 (4k), 21st and 29th November 2022 (4l) and 10th to 17th January 2023. Solid black line shows the estimated volume of water stored within the detention basin for the same period (m^3; right y-axis). Local hourly rain-fall accumalation values mm hr^{-1}; onsite rain gauge) are denoted with grey bars above respective hydrographs. The take-off level at the sluice was raised on 27th October 2022 due to the bund overtopping. Dashed green lines indicate the time of water quality sampling where relevant: 7/9/2022: 13:00; 19/10/2022: 11:15; 26/10/2022: 14:00; 23/11/2022: 11:00

Approximately 67 mm of rain fell during the February 2022 event, leading to the detention basin being inundated for 6 days. 80 mm of rain fell over a comparable period during the September 2022 multi-peak event (Fig. 5j), but this led to the detention basin being inundated for a maximum of only 36 hours and emptying substantially between flood peaks (Fig. 5c, Appendix 1B, Table S1B2, Table S1B3).

The September 2022 multi-peak event followed a period of about 6 weeks of warm, dry weather. The channel bed was dry in several places prior to this rain event and the field soil and vegetation of the detention basin was dry. In the February 2022 event, however, high channel discharge (Q >0.02 m^3 s^{-1}) preceded the rain event starting on 18th February. Antecedent conditions have been highlighted as an important factor determining the performance of NbS for flood mitigation by numerous authors in modelling studies (Pattison et al., 2014; Metcalfe et al., 2017a) and empirical studies (Black et al., 2021; Lockwood et al., 2022). In a study examining the seasonal variation in biogeochemical and hydrological processes in a detention basin, Jones et al. (2015) observed that water levels within a detention basin rose more quickly when soils were saturated than during drier summer inundation events. In the current study, sustained high flows and consecutive flood peaks over a relatively short period in October 2022 led to the detention basin overflowing on 27th October 2022, at which point the take-off level was raised to allow filling at Q = 0.1 m^3 s^{-1}. Thereafter, the detention basin showed improved functioning in terms of emptying between flood peaks and providing additional storage during the large multi-peak events in November 2022 and January 2023 (Fig. 5l-m). Notably, the November 2022 multi-peak event (Fig. 5l) had a flood peak with the study's highest estimated recurrence interval of 2.7 years, while the October 2022 multi-peak events (Fig. 5i) had flood peaks of only 1.1-year recurrence. The detention basin did not overflow in November 2022 but did overflow in October 2022, indicating peak discharge may not be the only factor that determines the effectiveness of the detention basin in mitigating floods. Instead, its effectiveness may be affected by complex interplay among rainfall volume and duration, peak flow discharges and inter-peak discharges, and the take-off level of the detention basin.

Several authors have indicated that an essential aspect of flood storage features is that they must not fill up within the rising limb of a flood peak (Lane, 2017; Quinn et al., 2022). In all 13 automatic inundation events, the detention basin reached a maximum volume after the time of peak flow upstream of the detention basin (mean time between upstream peak and detention basin peak volume: 3hrs 36mins (SE: 43mins; max.: 7hrs 45mins; min.: 30mins; Appendix 1B, Table S1B3). This interval was lower when there was already ponding in the detention basin from previous inundations (30mins on 19th Oct 2022 and 45mins on 25th Oct 2022), but there was no significant effect of the presence of standing water across the whole study (ANOVA, $p > 0.05$).

In all single-peak events, the detention basin was inundated for considerably longer than water was entering the detention basin (mean extension time of 21hrs 50mins, 2.5 times longer than the take-off period; Table 2), thereby extending the flood peak. An important aspect of flood attenuation is flood peak elongation through offline storage beyond the in-stream flood peak period (Lane, 2017). This potential, of course, varies over the course of the inundation. Inflow discharge exceeds outflow discharge until the detention basin is full. While the detention basin is at its maximum volume, inflow discharge equals outflow discharge. As the detention basin volume decreases, outflow rate is initially high, but reduces as the pressure on the outlet pipes lessens with decreasing head of water above the pipes. The optimal volumetric attenuation period is from the start of take-off to the moment of maximum detention basin volume, but attenuation does occur beyond that.

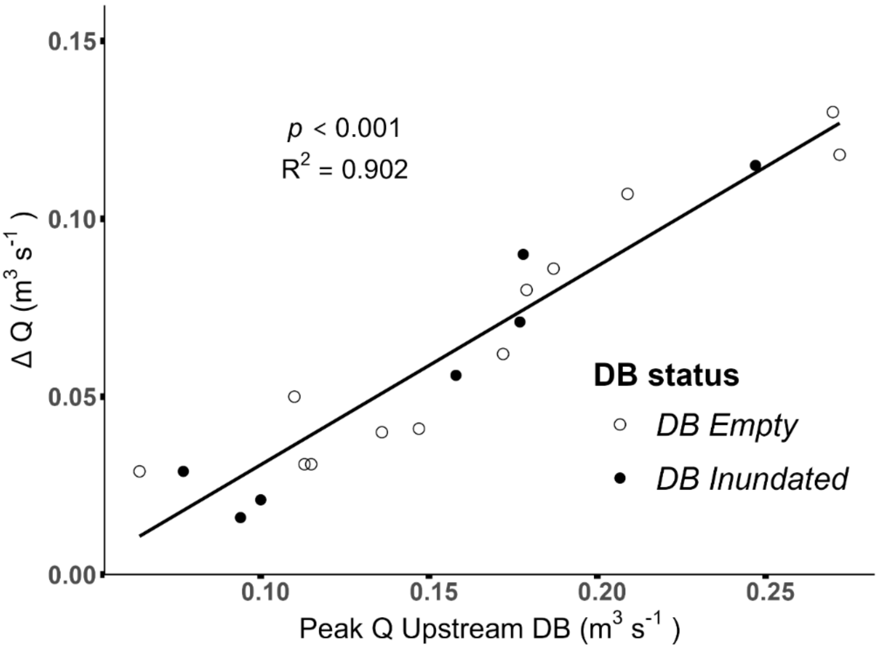

Figure 6 Relationship between peak discharge upstream of the detention basin (DB) ($m^3 s^{-1}$; x-axis) and peak discharge difference (ΔQ $m^3 s^{-1}$) between upstream and downstream locations (y-axis). Significant relationship identified in general linear model analysis illustrated with black line and in-figure p and R^2 statistics (GLM, df = 17, t = 12.929). DB status (Empty vs. inundated at time of stream take-off) had no statistically significant effect on attenuation potential of DB at different upstream discharges ($p > 0.05$).

Diverting flows from stream channels to offline floodplains also has the effect of increasing the path length and overall roughness of the flow path (Pattison and Lane, 2012). This is particularly true in the case of stream channels in agricultural catchments, which tend to have been deepened, straightened and cleared of impediments such as boulders. These amendments reduce the risk of over-bank flooding and allow formation of straight field margins which facilitate movement of large farm machinery (O'Connell et al., 2007). These engineered channels are inherently smoother than natural channels and endow flashy stream hydrology, which makes them prone to eroding high loads of SS and dissolved nutrients during peak flows (Poff et al., 1997; Robotham et al., 2021). While the increase in path length and roughness through flood-plain reconnection is an important aspect of flood peak attenuation, it is more difficult to quantify than flood peak discharge reduction (Nicholson et al., 2012). Nonetheless, the detention basin effectively stored water during and beyond flood peaks and emptied after flood peaks without inducing high downstream peak discharges while emptying. The detention basin extended flood peaks through offline storage and through extending the duration of flood peaks. Fig. 7 illustrates the consistent effect that the detention basin had on reducing downstream discharges during flood peaks throughout the study period. The figure also gives good indication of the hydrologically 'flashy' nature of the stream at the study site in that flood peaks tend to occur almost instantaneously with peak rainfall. Through reducing and extending peak flows, the detention basin may have had a pronounced, but localised, effect on the flashiness of the catchment. Fig. 7 also demonstrates the effect that manipulation of the sluice had on the detention basin's potential for attenuating flows during multi-peak events in October 2022 (Fig. 5k). The multi-peak events that followed the raising of the take-off level in November 2022 and January 2023 had some of the highest peak discharges of the study (Table 1; Fig. 5l-m), but the detention basin displayed good attenuation of these peaks without leading to the bund overtopping.

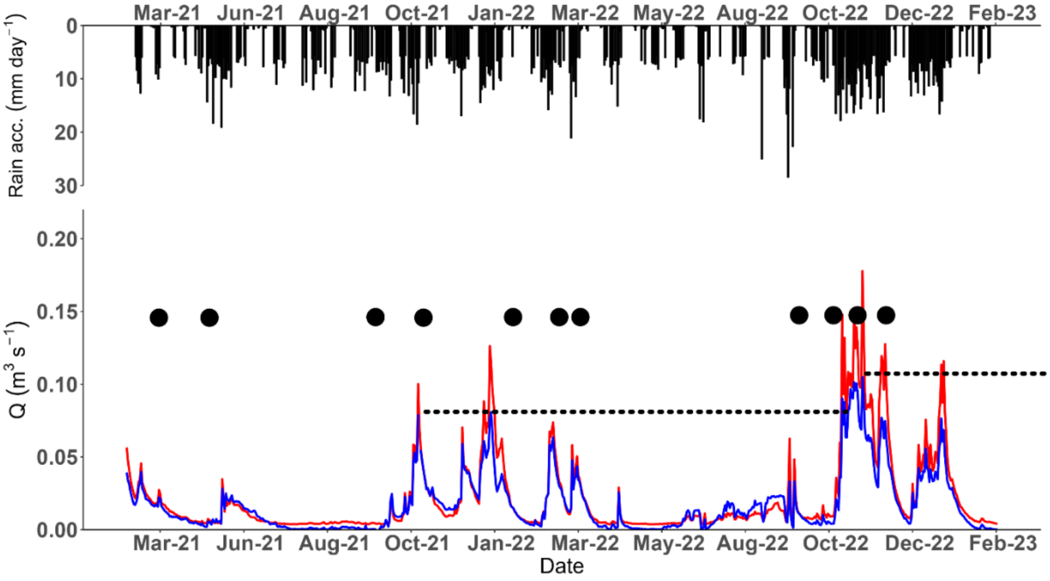

Figure 7 Study site daily rainfall accumulations (mm day^{-1}; top) and daily mean discharge (Q m^3 s^{-1}) immediately upstream (red line) and downstream (blue line) of the flood detention basin (DB; bottom) from Jan 2021 to Feb 2023. Rainfall is estimated from combining local data from tipping-bucket rain gauge and nearest weather station (Carrigadrohid). Black dots indicate DB inundation events. Initial three inundation events occurred through manual removal of sluice boards (Mar – Oct 2021). Dashed horizontal lines indicate take-off discharge during the automatic phase of the study: Nov 2021 to Oct 2022: Take-off discharge of 0.07m^3 s^{-1}; Oct 2022 to Jan 2023: Take-off discharge of 0.1m^3 s^{-1}.

2.4.2 Water quality changes in the detention basin

Between March 2021 and November 2022, water quality data were collected during 11 inundation events at the detention basin (Fig. 8, 9; Appendix 1B, Table S1B4). Overall, the effect of detention basin flooding on reduction of water quality parameters was greatest overall for suspended sediment and nitrate concentrations. The detention basin showed substantial attenuation of suspended solids over many sampling events, although there was considerable variation (Fig. 8a). Percentage removal efficiency (%RE) ((Carstensen et al., 2020; of suspended solids (SS) within the detention basin ranged from -67.3% to 80% (Fig. 8a). Overall, the detention basin attenuated SS by an average of 5.4% in each event (Table 3). Linear mixed-effects models on the pooled dataset revealed significant attenuation of concentrations of SS (p = 0.008; Table 3, Fig. 9a). %RE of nitrate ranged from to -9.2% to 48.7% (Fig 8b; Table 3) and mixed-effect models revealed significant attenuation over the entire study (Table 3; Fig. 9b; p < 0.001). Levine et al. (2021) found that retention of storm-generated runoff on floodplains resulted in substantial decreases in losses of SS, TP and total nitrogen. The results of the current study differ from that of Levine et al. (2021), however, in that the detention basin acted as a source of both soluble reactive phosphorus (SRP; Fig. 8d; Table 3) and total phosphorus (TP; Fig. 8e; Table 3). %RE of SRP ranged from -358.3% to -6% with a mean of -95% (Fig. 8d, Table 3). %RE of TP ranged from -306.98% to 20.9% with a mean of -83.3% (Fig. 8 Table 3). Mixed effect models showed that the detention basin outlet SRP and TP concentrations were significantly higher than inlet concentrations (SRP: p < 0.001; TP: p < 0.001; Table 3). Much of the attenuation of P in the study by Levine et al. (2021) was attributed to soil infiltration. The soil of the detention basin in the current study was compacted by livestock and had a clay pan beneath c.12cm of topsoil across much of the ponding zone. It is likely that soil infiltration in the current study was relatively limited, as were attenuation processes dependent on soil infiltration, such as the binding of phosphorus from flood waters to soil particles within the soil profile.

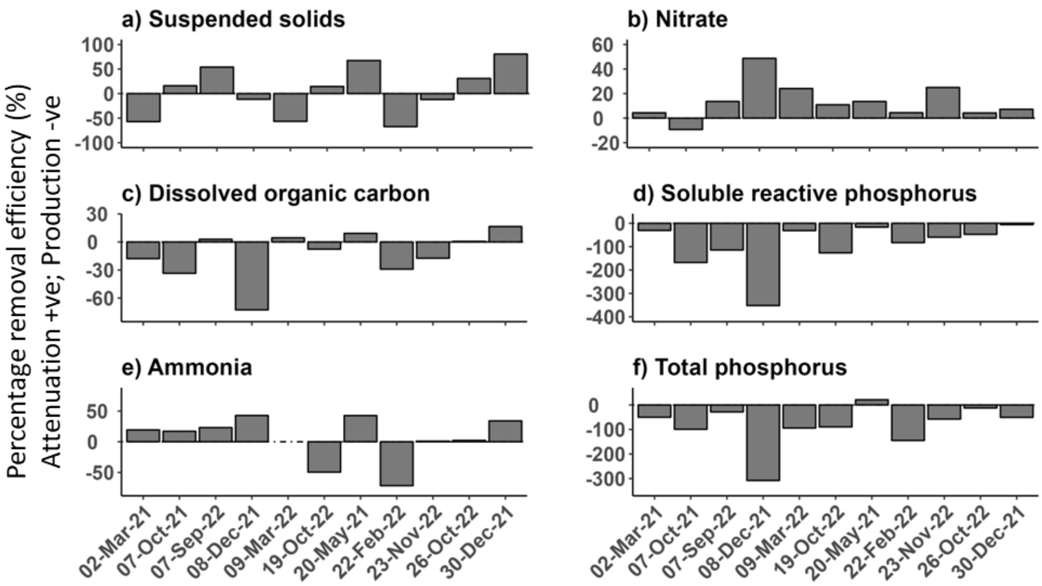

Figure 8 Percentage removal efficiency (%RE) of water quality parameters (a-f) based on mean changes in concentration between the DB inlet and DB outlet; only single samples were collected on 9th March 2022 and 26th October 2022.

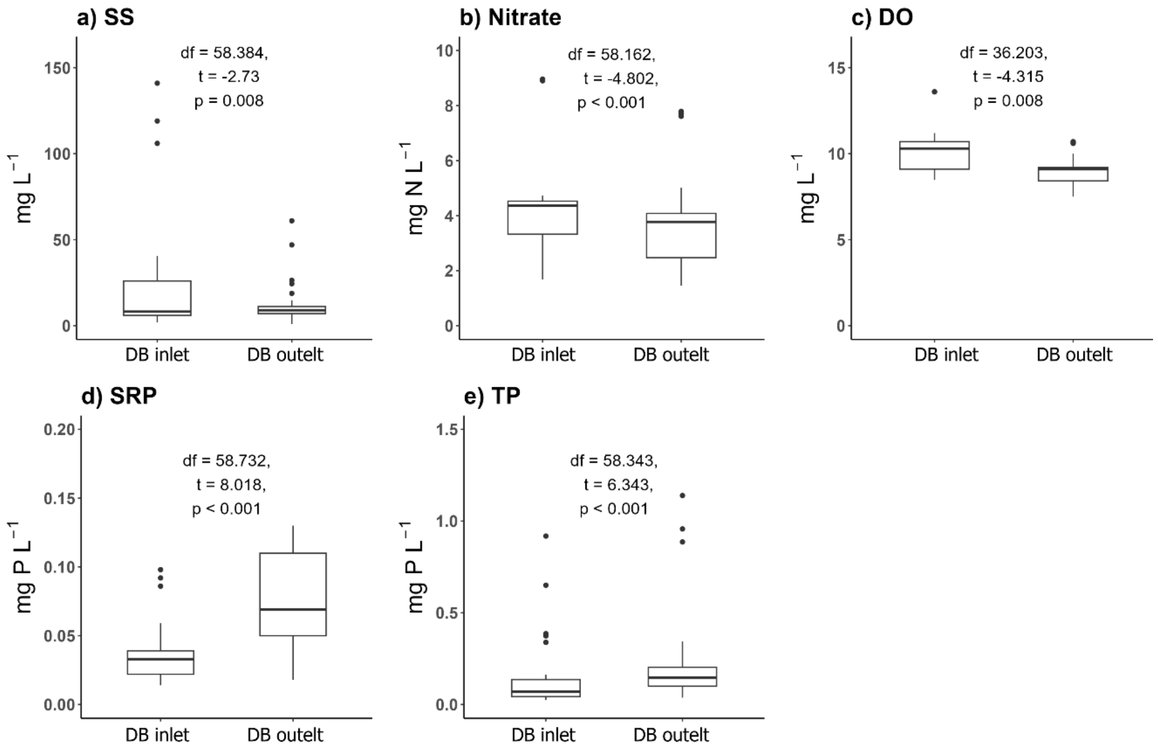

Figure 9 Pooled water quality data shown in boxplots for parameters whose concentrations (y axis; mg L $^{-1}$) were found to have statistically significant differences (p <0.05) between the DB inlet and DB outlet (x-axis). Relevant statistics from mixed effect linear models on 11 sampling events between Mar 2021 and Nov 2022 are shown within plots 8a-e.

The event on 30th Dec 2021 had both the highest concentration of suspended solids at the detention basin inlet, and the greatest degree of SS attenuation by the detention basin (Fig 8/a; Table 3). Substantial removal of SS was observed by Clarke (2013) when retention bunds captured runoff during a rain event which led to overland flow over bare soil. Similar to the current study, Clarke (2013) also found that retention bunds failed to attenuate dissolved nutrients (SRP, dissolved nitrogen) and led to an increase in dissolved nutrients during some events. Several studies have reported that SS attenuation was correlated with TP attenuation, a function of the adsorption of particulate phosphorus to fine soil particles (Barber and Quinn, 2012; Clarke, 2013; Noe et al., 2019). The fact that there was attenuation of SS and production of TP during this event indicates that the soil within detention basin was already saturated for phosphorus prior to the event. Despite the detention basin physically slowing and trapping SS, TP may have also been washed from the surface of the field. In the current study, dissolved oxygen (DO) concentrations were found to be significantly lower at the detention basin outlet ($p < 0.001$; Table 3, Fig. 9c), which may have promoted the desorption of SRP from the soil surface beneath the ponded water, and attenuation of nitrate through denitrification. Similar results were shown by Jones et al. (2015) in which a manually-connected floodplain attenuated nitrate but acted as a source of TP, with variable effects on the flux of DOC and ammonium. In their study, as in the current study, this re-connected flood plain had been used for agriculture, which the authors implicated in leading to mobilisation of legacy nutrients in the soil and recommended care in choosing agricultural land for flood attenuation. Noe et al., (2019) found that natural floodplains showed greater nutrient attenuation than restored floodplains, i.e. agricultural land which was reconnected to adjacent streams during high flows via breaches in levees. In addition to the role that legacy nutrients may play in the processes that occur in agricultural soils, natural reaches and floodplains are inherently more complex than anthropogenically altered ones. This added complexity has been suggested to have an important role in the biological and hydrological functioning of natural floodplains, and therefore in their capacity to attenuate water quality pressures (Friberg, 2014; Newcomer Johnson et al., 2016; Noe et al., 2019).

The other sampled water quality parameters did not show any significant trend over the course of the study (Table 3, Fig. 9), and %RE varied considerably within the detention basin during certain events (e.g. DOC production and ammonia attenuation on 8th December 2022 Fig. 8). Changes to DOC concentrations ranged from -72.6% to 16.5% with a mean of -13.1%. Ammonium %RE ranged from -167.3% to 42.86%, with a mean of -9.62% . Chloride %RE ranged from -19.9% to 13% with a mean of -0.22% (Fig. 8; Table 3).

In addition to the temporal variability in the direction and degree of change of water quality parameters in the detention basin, there was some evidence for spatial variability in water quality within the detention basin. Water quality sampling along the course of water flowing from the detention basin inlet to the detention basin outlet during the flood event of 9th March 2022 indicated that the processes of attenuation and production tended to happen mainly within the ponding zone (Fig. 10; Appendix 1B, Table S1B6). For most water quality parameters, minor increases were observed along the overland flow-path (Fig. 2a), but more pronounced changes in DO, ammonia, TP and SS were observed at the base of the detention basin (Fig. 10). Notably, despite changes in concentrations of water quality parameters within the detention basin, there was little change in concentrations within the channel downstream of the detention basin due to dilution of was from the detention basin (Fig. 10, red line).

Additional evidence for the water at the base of the detention basin being the main site of water quality changes comes from sampling during the event on 8th December 2022 which occurred at the tail-end of the event, when much of the water that had been stored in the detention basin had already drained back to the channel. This event showed the highest %RE of nitrate (%RE 48.73%; Fig. 8b, Appendix 1B, Table S1B4, S1B5) and the highest increase in concentrations of SRP (mean RE 0.86 mg P/ L^{-1}; %RE 358.33%; Appendix 1B, Table S1B4, S1B5; Fig. 8d).

The sampling of residual ponded water at the site where greatest microbial activity would have occurred (i.e. the soil surface) may have revealed a key location for nitrate transformation and SRP production in the detention basin. It also indicates that the timing at which water sampling is conducted over the course of a flood event affects changes in water quality that occur within the detention basin. Processes such as denitrification may become more prominent as ponding-time progresses and bottom waters become increasingly anoxic (Burgin and Hamilton, 2008; Robotham et al. 2021). The flux of nutrients and sediment is also understood to vary over the course of a given flood peak (Dalzell et al. 2005; Robotham et al. 2021). It is likely therefore that variability in the time of sampling across the various flood peaks affected not only the %RE of nutrients and suspended solids, but the upstream concentrations of these parameters. Nonetheless, the tendency for nitrate concentrations to decrease in tandem with increases in phosphorus concentrations in the detention basin suggests that the conditions that may help attenuate nitrate from stream waters may be the same conditions which promote the release of phosphorus (Duan et al., 2016; Bernard-Jannin et al., 2017). The processes which contributed to the observed reduction in nitrate concentration are unclear, but it is possible that denitrification was occurring at the soil surface where oxygen concentrations were lower. In a parallel study to the one discussed here, the soil organic carbon content was shown to be particularly high within in the detention basin (mean of 719.3 mg C kg $^{-1}$) and DOC concentrations in water at the detention basin outlet were 8.51 mg L^{-1} (Table 3). Substantial denitrification was observed in similar studies by Jones et al. (2015) and Forshay and Stanley (2005). In their studies, high carbon availability, reduced oxygen concentration under flood waters and short residence times (< 12 hours), all of which are comparable to the current study, were implicated in contributing to the observed denitrification. Further investigation into chemical transformations occurring at the soil-ponded water interface are warranted to better understand the potential of detention basins for nitrate attenuation.

Table 3 Results from analysis on water quality sampling from detention basin (DB) inlet and DB outlet over 11 sampling events between 2nd Mar 2021 and 23rd Nov 2022. Mean concentration data were calculated directly from water quality concentrations for all sampling events and were used to calculate Removal Efficiency concentration (Mean RE) and percentage RE. Results from mixed effect models use comparisons of DB inlet and DB outlet concentrations in Mixed effect models accounting for variance between sampling events. Water quality parameters whose concentrations changed significantly ($p < 0.05$) between the DB Take-off and DB Outlet are denoted with an asterisk.

Water quality parameter	Mean concentration data from DB inlet and DB outlet						Results from mixed effect models				
	Mean DB inlet conc. (mg L^{-1}); (SD)	Mean DB outlet conc. (mg L^{-1}); (SD)	Mean RE (mg L^{-1}); (2.5% CI, 97.5% CI)	Mean RE (%)	Max. RE (%)	Min. RE (%)	Model conc. Change	Std. error	df	t-value	p-value
Ammonia	0.09 (0.08)	0.09 (0.09)	0.004 (-0.01, 0.03)	9.62	167.31	-42.86	0.95	0.1	58.36	-0.52	0.602
Chloride	19.98 (5.69)	19.96 (5.56)	-0.016 (-1.2, 0.69)	0.22	19.95	-12.95	1	0.01	58.08	0.25	0.801
DOC	7.88 (3.9)	8.51 (3.9)	0.627 (-2.06, 0.44)	13.12	72.63	-16.52	0.69	0.4	58.34	1.73	0.088
Nitrate *	4.14 (1.8)	3.57 (1.64)	-0.567 (0.24, 0.95)	-13.37	9.23	-48.75	-0.86	0.03	58.16	-4.8	<0.00*
SRP *	0.04 (0.02)	0.07 (0.03)	0.030 (-0.04, -0.02)	94.13	352.06	5.8	1.85	0.08	58.73	8.02	<0.00*
Suspended Solids *	19.55 (24.21)	11.72 (10.81)	-7.835 (-0.52, 22.6)	-5.35	67.31	-80.61	-0.71	0.13	58.38	-2.73	0.008*
Total P *	0.12 (0.14)	0.19 (0.21)	0.071 (-0.15, 0.01)	83.03	307.75	-21.14	1.7	0.08	58.34	6.34	<0.00*
Dissolved Oxygen*	9.85 (1.05)	9.06 (0.87)	-0.788	-7.5	0	-24.42	-0.85	0.2	36.2	-4.32	0.008*

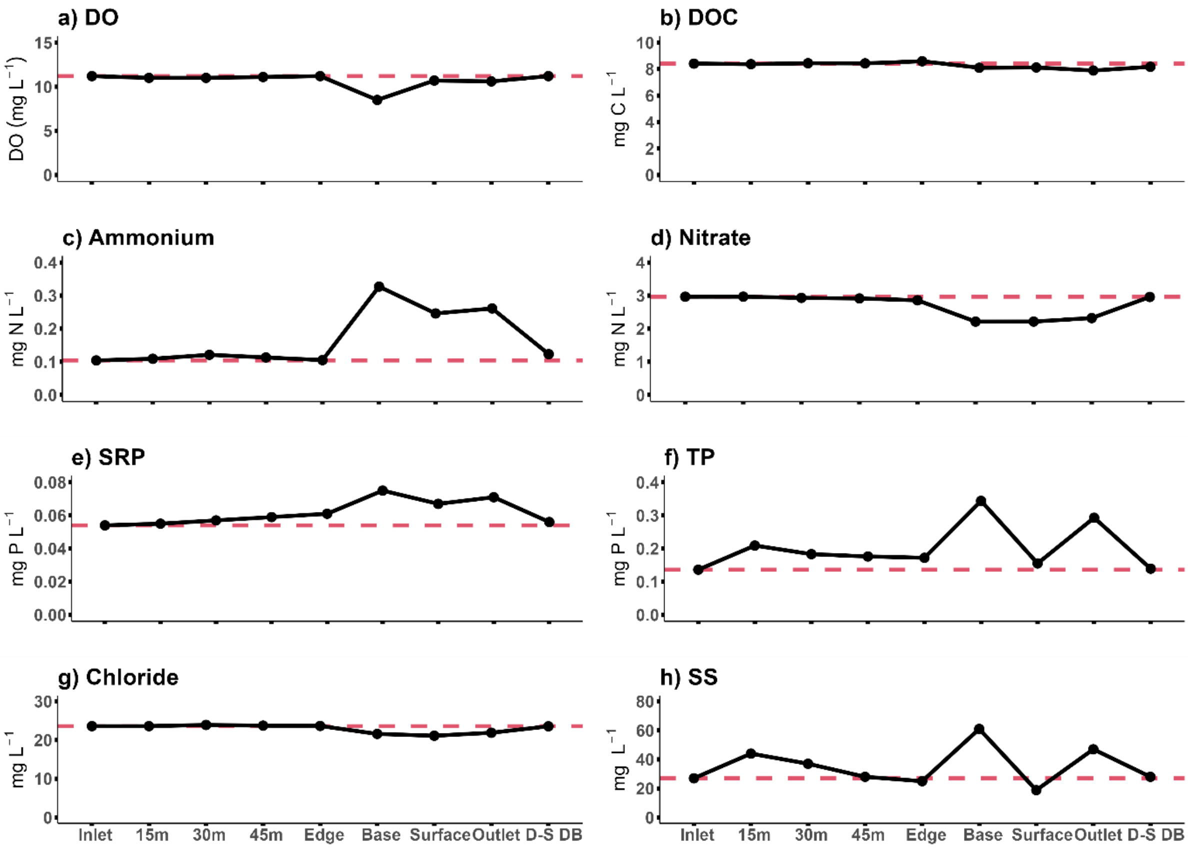

Figure 103 Water quality parameter data from flow path of water in the DB during 9th March 2022 inundation event. Concentrations of dissolved oxygen (DO mg L^{-1}), DO saturation, ammonia, nitrate, soluble reactive phosphorus (SRP), total phosphorus (TP), chloride and suspended solids (SS) were measured from locations, within the pond zone. From most upstream to downstream (L-R) DB inlet; 15 m downslope of DB inlet, 30 m downslope of DB inlet, 45 m downslope of DB inlet, the ponding zone edge (1 m wide zone where water slows as the overland flow-path meets the ponding zone); the pond base (bottom 10 cm of ponding water); surface (top 5 cm of ponding water); the outlet of the DB outlet pipe draining the base of the DB; D-S DB within the stream downstream of the DB. Dashed red line shows concentration at DB inlet.

2.4.3 Benefits and limitations of offline storage

The detention basin was effective at attenuating flood peaks when rainfall events were below a threshold of rainfall accumulation but was not tested under flood peaks of >3-year recurrence interval. The detention basin was not overwhelmed by the largest discharges observed over the study period, nor by the rainfall events with highest hourly rainfall intensity. The detention basin functioning was, however, reduced under prolonged rainfall. Extended rainfall events such as those that lead to high peak and inter-peak discharges in February (Fig. 5i) and October 2022 (Fig. 5k) may be more representative of the events which would present a flood risk to homes and business, than those shorter or isolated flood peaks which the detention basin was able to accommodate. Storm events that lead to social or economic harm are relatively infrequent (> 2-year recurrence; Gordon et al., 2004; O'Sullivan et al., 2012) and exhibit high peak and inter-peak flows. What, then, is the role of offline retention of short-lived minor peaks, or spates? The floods which cause harm to society, through flooding homes and businesses, may be beyond the potential of the detention basin in the current study to attenuate. In studies which have designed detention basins to fill under higher peak flows, these flows can be either too infrequent for rigorous testing of the effectiveness of the detention basin (e.g. Lockwood et al., 2022), or bring such high flows that the detention basin is overwhelmed (e.g. Levine et al., 2021). In the cases of these studies by Lockwood et al. (2022) and Levine et al. (2021), it was necessary for the authors to model the effects that the detention basins would have had on peak flows under more optimal flow or storage conditions. Many more studies have modelled the impact of detention basins on higher flows, or across larger spatial scales (Pearson, 2016; Collentine and Futter, 2018), but empirical evidence for the impact of detention basins on large, infrequent and potentially damaging floods is still relatively untested.

The detention basin in the current study had some impacts on water quality, but the scale and direction of these effects varied among events. The take-off threshold of the detention basin was set to allow frequent inundation and observation of changes in water quality. In catchments with impaired water quality throughout the year, delivery of polluted waters to offline treatment zones during common spate flows may be more useful than relying on rarer and larger peak events for water quality mitigation. From an ecological perspective, is it better allow short flood peaks, or spates, to move through the channel without overtopping banks, so that the natural regime of sediment erosion, transport and deposition is maintained? These spate flows are an important feature of the natural flow regime in that they clear fine sediments from gravel beds, deliver nutrients, woody debris and gravels to lower parts of the catchment (Poff et al., 1997; Dalzell et al., 2005; Enders et al., 2009). In agricultural catchments, excessive sediment and nutrient loadings can lead to colmation of streambeds and eutrophication in lakes and estuaries (Weigelhofer et al., 2018a). The detention basin may have a role in mitigating these regular pulses of nutrients and sediment, so they do not accumulate in areas where their effects are more pronounced and/or more difficult to remediate e.g. lakes and estuaries.

It is also important to consider that local conditions at the detention basin are likely to have a strong effect on the direction and scale of changes to water quality parameter concentrations. In the current study, the detention basin may have aided in nitrate attenuation, but the concurrent production of P is unlikely to be a desirable outcome. In catchments where phosphorus loss is of high concern, the use of detention basins to attenuate phosphorus should be restricted to sites where local soils have greater settling and phosphorus-binding potential (Kløve, 2000; Jordan et al., 2005; Clarke, 2013).

Another important consideration is the coincidence of increased flood risk with periods when water quality pressures in agricultural streams are most acute. (Lewis et al., 2013) found that exports of SS, TP and total dissolved phosphorus from fields to watercourses in rural catchment in Ireland were greatest during the wet winter months, and wet periods outside of winter. They also found that winter slurry application was strongly associated with P and SS runoff. Flood mitigation using detention basins may be more important during winter, when peak flows are more frequent, but this period of greater hydrological risk is likely to coincide with the period when capacity for the land to attenuate water or additional applications of nutrients will be lowest. The mobilisation of solids (TSS) and dissolved nutrients (SRP, ammonia) has been shown to be enhanced while soils are saturated (Dunne et al., 2005; Lewis et al., 2013). In a study by Grimaldi et al. (2012), saturated soils around the root zones of hedgerows in agricultural fields during winter were suggested to enhance denitrification. Conversely, in a study into the effectiveness of in-stream ponds to attenuate sediment and nitrate, Robotham et al. (2021) found that denitrification rates were lowest during winter. While the current study identified differences in the detention basin's potential to attenuate certain water quality parameters, there may be an inherent conflict in utilising a flood mitigation measure as a water quality management measure.

If a detention basin is designed to capture large, infrequent floods, attenuation may only occur if many detention basins throughout the catchment are set up to function in a carefully coordinated manner, for example, through the use of Real-Time Control Systems (RTCs; Brasil et al., 2021). RTCs have been utilised in urban flood defence and sewerage control systems in which storage volume in detention structures may be adjusted in response to weather forecasts. Multiple structures may be adjusted from a centralised control location, but the construction, maintenance and co-ordination of such structures may a significant task, and one which may not be applicable in rural areas. Distributed rural flood mitigation structures would have to be sited and calibrated to prevent them all filling and emptying at the same time: a scenario which could be hazardous in multi-peak events as a result of tributary synchronisation and/or piggy-backing (Metcalfe et al., 2017b; Black et al., 2021; Brasil et al., 2021; Lockwood et al., 2022). As catchment scale increases, so too does the difficulty in predicting the effects of land management on floods (Rogger et al., 2017). Adding to the difficulty in coordinating multiple detention basins throughout a catchment for the mitigation of large floods would be the fact that they would be out of use for years at a time. Without proper financial support it is unlikely that landowners would maintain detention basin take-off and release structures continually for years when they are not in use.

2.5 Conclusions

This study examined the impact of an in-field flood retention measure on both flood peak mitigation and water quality management. The feature functioned during storm events to attenuate peak flows, but the extent of peak attenuation was influenced by flood peak frequency, inter-peak stream discharges and peak discharge. The detention basin was found to attenuate suspended solids and nitrate over nine flood events, but it acted as a source of SRP and TP. Additionally, the scale and direction of changes in water quality parameter concentrations within the detention basin was found to vary between floods and may have been variable within a given flood peak. Rural areas of catchments may play an important role in mitigating flood surges and certainly have an impact on water quality within the wider catchment. Findings in the current study indicate that, while providing some hydrological and water quality benefits, NbS for flooding and water quality management in these areas should be implemented with care so that appreciable benefits can be realised.

2.6 Appendix 1A: Supplementary Methods

2.6.1 Manual DB inundation events

Manual inundations of the flood detention basin (DB) were performed on 2nd Mar 2021, 20-21st May 2021 and 7-8th Oct 2021 to assess effects of the DB hydrographs upstream and downstream of the DB, and the effects on storage of waters in the DB on water quality parameters concentrations. Flood peak attenuation through inundation of the DB was contingent on the diversion of water from the channel during the appropriate period during the rising-limb of the flood peak. If water was allowed into the DB too early, it would reach capacity before the in-stream flood peak had arrived (Nicholson et al., 2012; Wilkinson et al., 2019). The flood attenuation potential of the DB was also contingent on the rates of inflow to and outflow from the DB: acute monitoring of water levels upstream and downstream of the DB and within the DB was conducted during these manual inundations of the DB. This information was then linked to time-series water-level data from the WLRs after events to examine the effects of the manual adjustments to the DB and DB outlet pipes on in-stream water levels.

During three manual inundations of the DB in on 2nd Mar 2021, 20-21st May 2021 and 7-8th Oct 2021 the sluice boards were removed to allow water into the DB and the outlet pipes were kept in an upright position to allow the DB to fill until reaching the pipe openings, but would quickly drain once that level was reached. On 3 March 2021, the sluice at DB Inlet was opened at 10:15 and closed at 15:15. While stream water entered the DB the outlet pipes were kept in an upright position allowing the DB to fil. Outlet pipes were lowered into the bunded water at 16:00 to release water back to the channel (Fig 4a). Three surface water samples were collected from the

DB inlet and from the DB Outlet for analysis of inlet and outlet concentrations of water quality parameters.

The sluice was opened on 20 May 2021 to capture the flood peak following a rain event on 19-20 May. Fig. 4b illustrates the substantial effect that opening of the sluice had on discharge downstream of the DB. Surface water samples were collected from the DB inlet at 16:10 (5-min prior to opening the DB sluice) on 20 May and from the DB Outlet at 10:00 on 21 May (5-min after lowering the DB outlet pipes). During this event, the high flows caused the DB to be overwhelmed overnight on 20-21st May. Once water quality sampling was completed, the sluice was closed and the outlet pipes were brought down to ground-level to allow swift draining of the DB. Following this event, a 10cm portion of the top of the outlet pipes was removed so that water would drain via the pipes at a lower level, and prevent overwhelming lower parts of the bund.

The final manual flooding of the DB occurred on 8 Oct 2021 (Fig. 4c). The sluice was opened at 14:00 on 7 Oct 2021 in anticipation of a rain event forecasted for overnight 7-8 Oct 2021. Stream water-level increased over-night and the DB received water until the sluice was closed and the DB outlet pipes lowered at 12:40 on 8 Oct 2021. As water levels dropped on 8 Oct 2021, measurement of the water height on the sluice were made to help determine the appropriate level at which to set the "*take-off water level"* for automatic functioning of the sluice for future events. The sluice was closed on 8th Oct 2021 ahead of another forecasted storm surge. The hydrograph for the following event shows the discharges upstream and downstream of the DB to be aligned i.e. no attenuation of flow. This event aided in illustrating the effectiveness of the DB in attenuating flows and the water level at which take-off of the rising limb of the flood should occur. Thus, the event provided valuable information to allow successive flood events to be directed to the DB “automatically” i.e. over a pre-determined stream discharge. During each of the trial inundations the outlet pipes at the bund were manually raised or lowered into the pond for control of the release of stored water from the DB. The water level at the sluice over the course of the flood event (i.e. during the rising and declining limbs of the flood peak) was monitored so that the stream level for the critical period of the flood-peak could be determined and the take-off level of the sluice at the DB Inlet could be determined.

On 1 November 2021, the stream level at which water over-topped the sluice and entered the field was set at a stream level of c0.3m (discharge of c. 0.075 $m^3 s^{-1}$) at a stream gauging point 3m upstream of the DB inlet. Winter baseflow was found to be c0.15m with a discharge of c. 0.038 $m^3 s^{-1}$. A take-off level at twice baseflow was found to be sufficient to capture water during the rising limb of the flood peak but still provide sufficient storage up to and beyond the flood peak. The DB outlet pipes were augmented to allow water to slowly drain from the DB: One pipe was secured in a vertical position so that water stored by the bund would drain once the level reached 0.8m above the topographic minimum. The second pipe was perforated and laid horizontally on the ground to allow slow and constant drainage of water from the DB (Fig. S3). The DB thereafter received diverted stream water, via the sluice during high flows until 17 March 2023 when the sluice was closed. Summary data of rainfall and inundation periods is given for all inundation events in Table 2.

Figure S1B1Top: DB outlet pipes in lowered position to allow fast draining stored water from the DB. Bottom: Outlet pipes amended 1st Nov 2021. Left pipe was capped and perforated along its length to allow slow, constant drainage of stored water; right pipe is secured in upright position to allow fast draining of water once the DB reaches a maximum depth of 0.85m above the topographic minimum

Table S1A1 Data from flow discharge gauging sessions at the water level locations upstream and downstream of the flood detention basin between 2020 and 2022. Discharge was derived from the sum of stream velocities per unit wetted area at 10 – 20cm intervals. Total wetted area and mean velocities for each sampling event are shown in columns 6 and 7.

Location	Date	Stream width (m)	Depth (m)	Discharge Q (L s^{-1})	Wetted area (m^2)	Mean velocity (m s^{-1})
Upstream of flood detention basin	16-Dec-2020	1.8	0.15	0.06	0.25	0.43
	6-May-2021	1.2	0.06	0.01	0.06	0.19
	21-May-2021	1.8	0.11	0.01	0.06	0.35
	8-Jul-2021	0.9	0.07	0.00	0.03	0.19
	7-Oct-2021	1.1	0.07	0.00	0.05	0.18
	27-Oct-2021	1.8	0.15	0.04	0.20	0.37
	7-Jan-2022	1.4	0.16	0.05	0.17	0.52
	22-Feb-2022	1.4	0.16	0.05	0.19	0.51
	17-Apr-2022	1.4	0.16	0.04	0.17	0.46
	26-Oct-2022	2	0.20	0.10	0.33	0.45
	1-Nov-2022	2	0.22	0.12	0.38	0.52
Downstream of flood detention basin	16-Dec-2020	2.2	0.19	0.07	0.29	0.47
	11-May-2021	1.1	0.09	0.00	0.07	0.14
	21-May-2021	2	0.16	0.04	0.33	0.36
	8-Jul-2021	0.8	0.09	0.00	0.13	0.14
	21-Sept-2021	0.8	0.07	0.00	0.04	0.08
	7-Oct-2021	1	0.11	0.00	0.06	0.12
	27-Oct-2021	1.8	0.16	0.05	0.20	0.40
	7-Jan-2022	2	0.15	0.06	0.26	0.44
	22-Feb-2022	2	0.16	0.06	0.26	0.49
	17-Apr-2022	2	0.16	0.05	0.21	0.45
	8-Sept-2022	1.8	0.11	0.01	0.11	0.24
	1-Nov-2022	2.4	0.21	0.13	0.38	0.53

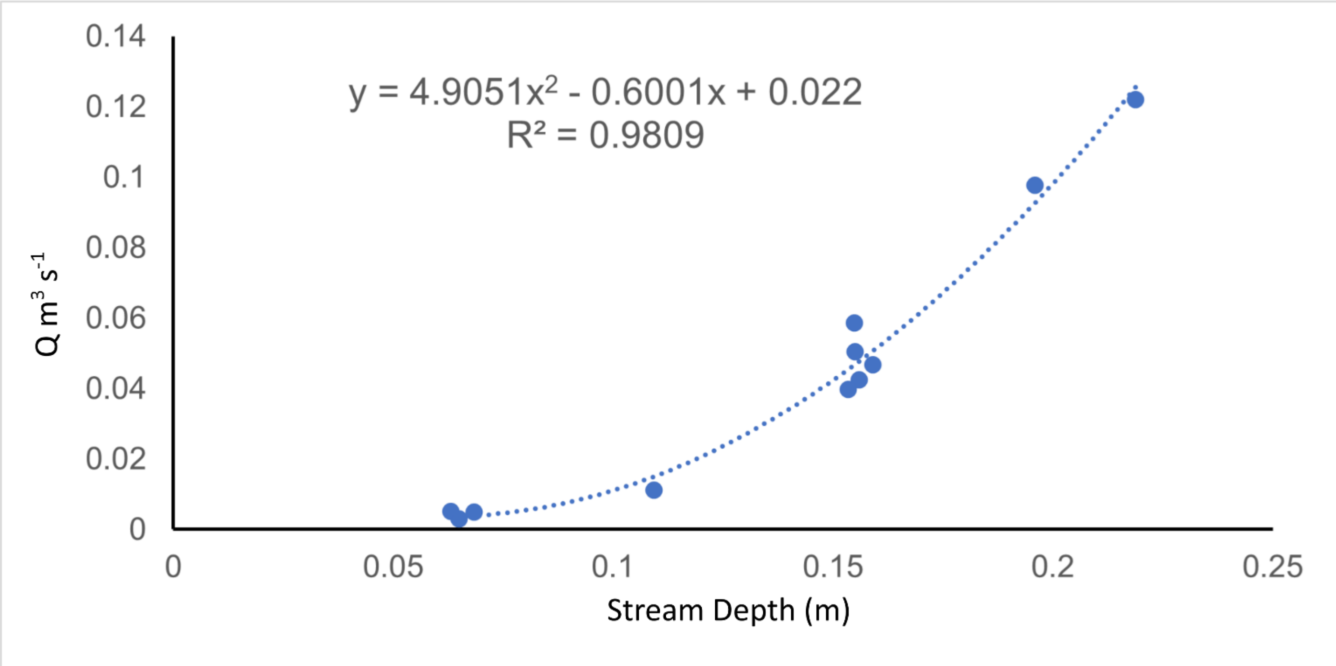

Figure S1A1 Rating curve for water level recorder location upstream of the flood detention basin. Line of best fit ($y = 4.9x^2 – 0.6x + 0.2$) is derived from stream water level data (x axis) and concurrent discharge (y-axis) using flow-velocity gauging, to produce discharge estimates (y-axis; Q (m^3s^{-1}) for the range of stream depth (x-axis, m) as recorded by the water level recorder.

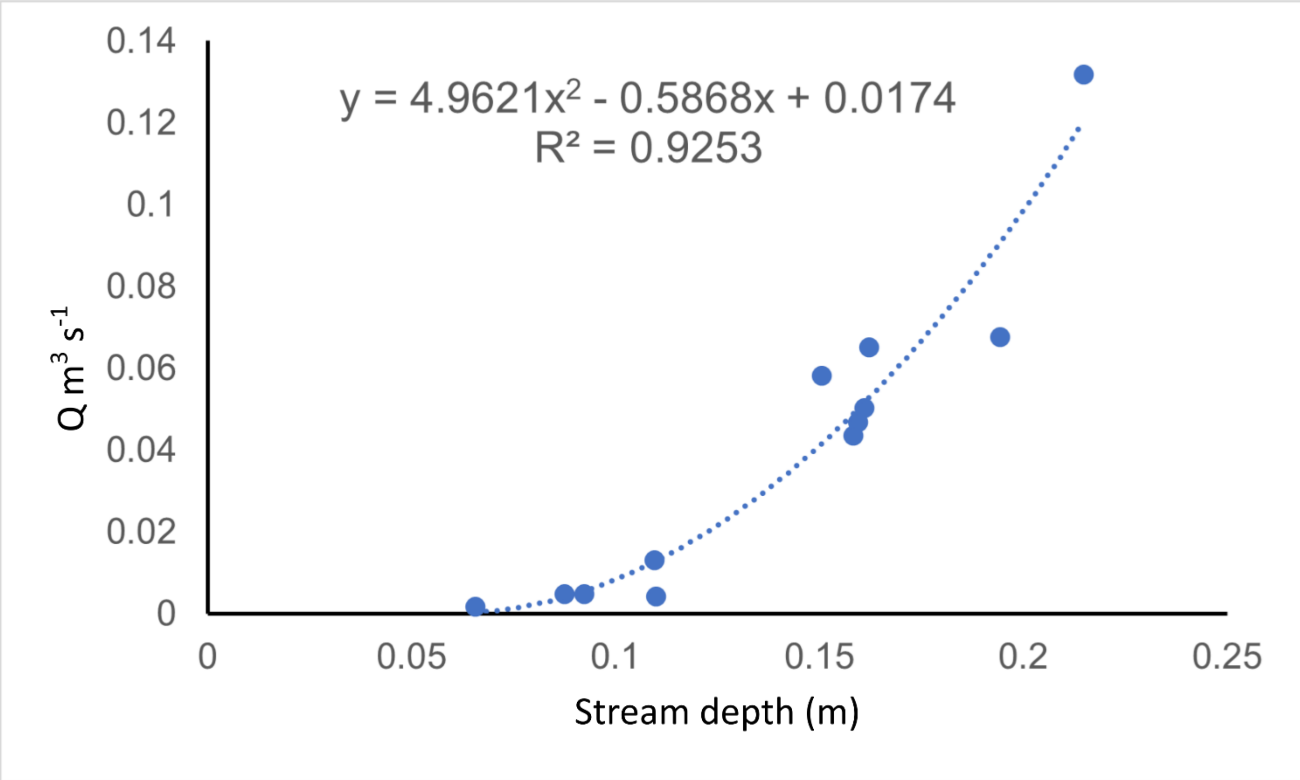

Figure S1A2 Rating curve for water level recorder location upstream of the flood detention basin. Line of best fit ($y = 4.96x^2 – 0.6x + 0.02$) is derived from stream water level data (x axis) and concurrent discharge (y-axis) using flow-velocity gauging, to produce discharge estimates (y-axis; Q (m^3s^{-1}) for the range of stream depth (x-axis, m) as recorded by the water level recorder.

Rainfall estimation

During certain periods, rainfall data was not recorded by the on-site tipping bucket rain gauge at the site. An estimate of rainfall at the study site was calculated by regressing the daily rainfall accumulation from the study site and from data from the nearest available Met Eireann rainfall monitoring site at Carrigadrohid, c. 4.8 km to the south of the study site. A conversion factor could then be derived using the model estimates from the regression (following comparison of normality plots of various models, e.g. log-transformed rainfall data, 2^{nd} order polynomials etc. For periods when rainfall data were missing from the study site, the publicly available Met Eireann data were converted using the derived equation to provide a contemporary estimate of the rainfall at the study site (Fig S1A3).

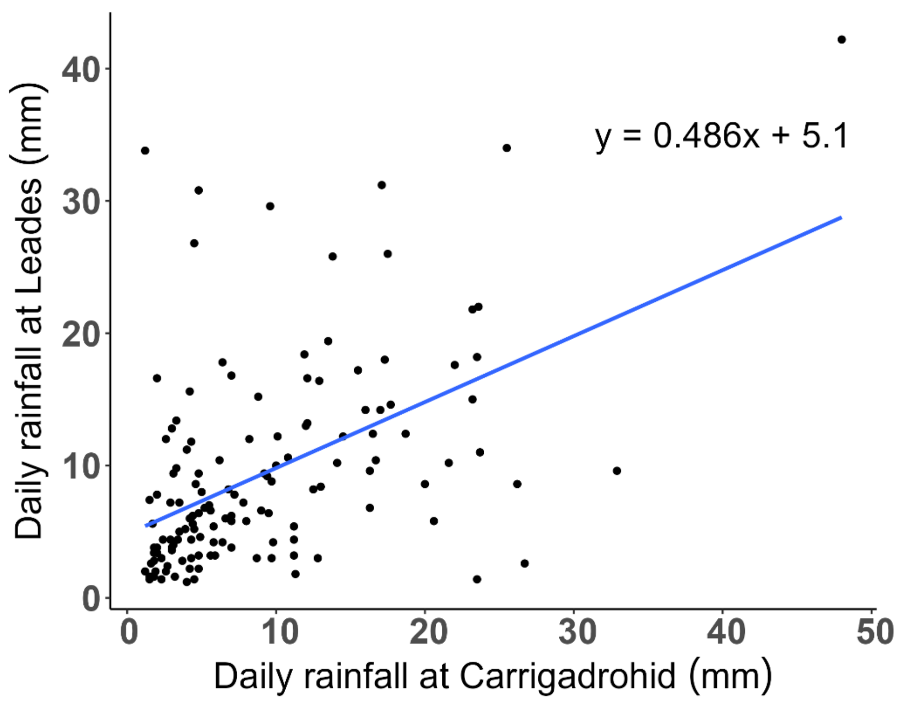

*Figure S1A3 Plot of daily rainfall at Leades Farm study site (y – axis) and at the Carrigadrohid Met Eireann weather station 8 km to the south of the study site (x – axis). The equation of the line based on linear regression between the two locations' datasets is shown within the plot. This was used to estimate daily rainfall at Leades (**y**) during periods when data were only available from the Met Eireann weather station at Carrigadrohid (x).*

2.7 Appendix 1B: Supplementary Results

Table S1B1 Flood detention basin (DB) rainfall and inundation summary Mar 2021 - Dec 2022. Hourly rainfall data were not available until the 18th – 23rd Feb 2021 event. Rainfall data prior to that are from the Leades Estimate. Sluice was manually operated on initial three events, but was set to allow take-off from stream to detention basin at discharge Q = 0.07 m^3 s^{-1} between 7 Dec 2021 and 28 Oct 2022, after which take-off was at Q = 0.1m^3 s^{-1} .

Dates of DB inundation	Full event rainfall (filling to emptying of DB; mm)	Peak rainfall (mm/hr)	Peak Rain time	Flood Duration (Days)	Flood peaks	Inter-flood period (Days)
2 Mar 2021	N/A	N/A	N/A	1	Single	90
20-21 May 2021	62	N/A	N/A	1	Single	79
7 - 8 Oct 2021	61	N/A	N/A	1	Single	139
7 - 9 Dec 2021	62	N/A	N/A	1	Single	60
30 Dec 2021 - 1 Jan 2022	69	N/A	N/A	2	Single	22
18 - 23 Feb 2022	67	5.2	19 Feb 2022 06:00	5	Multiple	48
9 - 12 Mar 2022	32	7	09 Mar 2022 06:00	1	Single	14
7 -12 Sept 2022	80.8	8.4	07 Sep 2022 08:00	1	Multiple	181
11 - 13 Sept 2022	41	8.6	11 Sep 2022 05:00	2	Single	1
16- 28 Oct 2022	159	7.2	18:00 16th Oct 2022	11	Multiple	34
30 Oct - 1 Nov 2022	41.2	5.4	31 Oct 2022 12:00	2	Single	1
6 - 9 Nov 2022	44	3.2	07 Nov 2022 13:00	3	Single	5
21- 27 Nov 2022	25.2	7	22 Nov 2022 23:00	6	Multiple	20
24 - 25 Dec 2022	19	5.8	24 Dec 2022 11:00	1	Single	26
12– 16 Jan 2023	71.4	4.8	14 Jan 2023 02:00	4	Multiple	18

Mean	59	6		2		44
Max	159	9		11		139
Min	19	3		1		1

Table S1B2 Flood detention basin (DB) flood peak attenuation summary data for Single and Multiple flood peak events between 7th December 2021 and 17th January 2023. DB Status refers to whether the DB was retained 'Standing water' from previous flood peaks within a multi-peak event, or whether the DB was empty prior to a flood peak in a single peak event, or the first peak in a multi-peak event. Means and standard error of the mean for full dataset of each parameter are shown below table, as well means for events when the DB was empty prior to inundation or had standing water. Take-off discharge between 7th December 2021 and 28th October 2022 was 0.7 $m^3 s^{-1}$ and was 0.1 $m^3 s^{-1}$ between 29th October 2022 and 17th March 2022.

Event period	Peak date	Event type	DB status	In-stream peak Q difference	In-stream percentage peak reduction	Peak delay	AUC Difference	AUC % difference	DB net vol increase	DB Vol	% DB inundated
7 - 9 Dec 2021	7 Dec 2021	Single	Empty	0.062	35.9	150 mins	969.91	11.39	209.05	209.05	85.33
30 Dec 2021 - 1 Jan 2022	30 Dec 2021	Single	Empty	0.107	51	555 mins	1079.65	49.53	230.67	230.9	94.24
18 - 23 Feb 2022	18 Feb 2022	Multiple	Empty	0.031	27.41	15 mins	351.02	23.44	67.58	67.58	27.58
	19 Feb 2022	Multiple	Standing water	0.021	21	- 60 mins	405.71	16.98	130.24	166.45	67.94
	20 Feb 2022	Multiple	Standing water	0.016	17.1	105 mins	319.98	16.18	77.85	198.85	81.16
9 - 12 Mar 2022	9 Mar 2022	Single	Empty	0.031	27.1	240 mins	619.41	21.48	174.6	174.95	71.41
6 Sep 2022	6 Sep 2022	Single	Empty	0.029	45.21	15 mins	462.05	44.64	28.76	28.76	11.74
6 - 9 Sept 2022	7 Sep 2022	Multiple	Standing water	0.09	50.5	60 mins	824.73	46.08	238.64	238.64	97.4
11 - 13 Sept 2022	11 Sep 2022	Single	Empty	0.086	45.7	- 15 mins	621.77	41.34	252.11	252.11	102.9
16- 28 Oct 2022	16 Oct 2022	Multiple	Empty	0.05	45.04	0 mins	562.95	44.37	205.91	205.91	84.04
	19 Oct 2022	Multiple	Standing water	0.029	37	120 mins	390.24	43.03	43	240	97.96
	25 Oct 2022	Multiple	Standing water	0.056	35.7	-15 mins	1477.56	33.03	27.66	267.66	109.25
30 Oct - 1 Nov 2022	31 Oct 2022	Single	Empty	0.118	43.38	120 mins	1661.35	37.92	196.9	196.9	80.37
6 - 9 Nov 2022	7 Nov 2022	Single	Empty	0.13	48.09	45 mins	2384.19	43.07	167.19	183.79	75.02
21- 27 Nov 2022	21 Nov 2022	Multiple	Empty	0.08	44.83	45 mins	610.02	33.59	159.54	159.54	65.12
	22 Nov 2022	Multiple	Standing water	0.115	46.56	60 mins	586.18	45.39	176.57	237.17	96.8
24 - 25 Dec 2022	24 Dec 2022	Single	Empty	0.04	29.18	0 mins	369.43	26.19	82.58	82.58	33.7
12– 16 Jan 2023	12 Jan 2023	Multiple	Empty	0.041	28.12	- 15 mins	981.65	25.66	199.6	200.9	82
	13 Jan 2023	Multiple	Standing water	0.071	40.11	75 mins	911.96	32.83	112.42	205.15	83.74
		Overall Mean		0.063	37.84	79 mins	820.51	33.48	146.36	186.68	76.20
		Standard Error		0.008	2.35	31 mins	122.27	2.70	16.84	14.69	6.00
		Mean Empty		0.067	39.247	96 mins	889.45	33.55	164.54	166.08	67.79
		Mean Standing Water		0.057	35.425	49 mins	702.34	33.36	115.20	221.99	90.61

Table S1B3 Times of instream flood peaks upstream of DB and times of peak volumes in the DB. Instream – DB peak difference time was calculated to indicate whether take-off and outlet discharges prescribed by the sluice and DB outlet pipes, respectively, were appropriately calibrated (Lockwood et al., 2022c)

Date of DB inundation	Event type	DB status	Date of peak Q upstream of DB	Time of peak Q upstream of DB	DB peak volume time	Instream – DB peak difference time
7 - 9 Dec 2021	Single	Empty	7th Dec 2021	06:15	08:45	02:30
30 Dec 2021 - 1 Jan 2022	Single	Empty	30th Dec	14:45	22:30	07:45
18 - 23 Feb 2022	Multiple	Empty	18th Feb	00:15	13:00	12:45
	Multiple	Standing water	19th Feb	08:00	17:00	09:00
	Multiple	Standing water	21st Feb	03:15	05:30	02:15
9 - 12 Mar 2022	Single	Empty	9th Mar 2022	10:00	15:15	05:15
6 - 9 Sept 2022	Single	Empty	6th Sept	11:30	14:30	03:00
	Multiple	Standing water	7th Sept	09:30	10:45	01:15
10th – 13th Sept 2022	Single	Empty	11th Sept 2022	08:45	10:00	01:15
16- 28 Oct 2022	Multiple	Empty	16th Oct	16:00	18:45	02:45
	Multiple	Standing water	19th Oct	04:15	06:15	02:00
	Multiple	Standing water	26th Oct	01:45	02:30	00:45
30 Oct - 1 Nov 2022	Single	Empty	31st Oct	13:45	17:15	03:30
6 - 9 Nov 2022	Single	Empty	7th Nov 2022	16:00	20:15	04:15
21- 27 Nov 2022	Multiple	Empty	21st Nov	04:45	08:00	03:15
	Multiple	Standing water	23rd Nov	00:15	01:45	01:30
24 - 25 Dec 2022	Single	Empty	24th Dec	12:15	16:00	03:45
12– 16 Jan 2023	Multiple	Empty	12th Jan	02:15	02:45	00:30
	Multiple	Standing water	14th Jan 2023	02:00	03:15	01:15

Mean time difference	3hrs 36mins
Standard error	43mins

Table S1B4a Inlet, outlet and concentration reduction data for sampled water quality parameters in 11 inundation events between 2-Mar-21 and 23-Nov-23. Mean concentrations of water quality parameters at DB inlet and DB outlet; mean reductions in concentrations and upper (2.5%) and lower (97.5%) confidence intervals are given for each event. Confidence intervals were not calculated for dissolved oxygen concentrations or for any samples taken on 9th Mar 2022 and 26th Oct 2022 as single samples were taken at inlet and outlet on these occasions. Statutory limits: a refers to Freshwater Fish Directive [78/659/EEC]; b EU Surface Water Regulations [1989]

Flood Event	DO (mg/L) (>9mg/L)			SS (mg/L) (</25mg/L salmonids)					Ammonia (mg N/L)					Nitrate (mg N/L)				
	Statutory limit a >9mg/L			Statutory limit a <25mg/L					Statutory limit a <1mg N/L					Statutory limit b <11mg N/L				
	Inlet conc. (mg/L)	Outlet conc. (mg/l)	Mean change (mg/L)	Inlet conc. (mg/L)	Outlet conc. (mg/l)	Mean change (mg/L)	Lower CI	Upper CI	Inlet conc. (mg/L)	Outlet conc. (mg/l)	Mean change (mg/L)	2.5% Conf Int	97.5 Conf Int	Inlet conc. (mg/L)	Outlet conc. (mg/l)	Mean change (mg/L)	2.5% Conf Int	97.5 Conf Int
2 Mar 2021	N/A	N/A	N/A	2.33	3.67	-1.33	-9.48	6.81	0.04	0.03	0.01	0.01	0.01	3.73	3.57	0.16	0.02	0.31
20 May 2021	8.48	8.34	-0.14	34.37	11.20	23.17	15.75	30.58	0.07	0.04	0.03	0.03	0.04	1.69	1.46	0.23	0.21	0.25
7 Oct 2021	N/A	N/A	N/A	10.72	9.00	1.72	-2.91	6.34	0.04	0.04	0.01	-0.02	0.04	3.74	4.09	-0.35	-1.08	0.39
8 Dec 2021	N/A	N/A	N/A	6.07	6.77	-0.70	-2.00	0.60	0.06	0.03	0.02	0.02	0.03	4.73	2.42	2.31	2.17	2.44
30 Dec 2021	10.32	7.8	2.52	85.46	16.58	68.89	4.94	132.83	0.12	0.08	0.04	-0.04	0.13	3.96	3.68	0.29	-0.25	0.82
22 Feb 2022	10.7	10	0.7	6.93	11.60	-4.67	-10.65	1.32	0.05	0.08	-0.03	-0.06	-0.01	4.54	4.34	0.20	-1.26	1.67
9 Mar 2022	11.2	9.933	1.267	27.00	42.27	-15.27	n = 1	n = 1	0.10	0.28	-0.17	n = 1	n = 1	2.97	2.25	0.72	n = 1	n = 1
7 Sep 2022	9.3	9.2	0.1	22.83	10.50	12.33	4.27	20.40	0.32	0.24	0.07	0.07	0.08	8.93	7.71	1.22	1.14	1.29
19 Oct 2022	9.1	9.1	0	5.50	4.70	0.80	0.20	1.40	0.05	0.07	-0.03	-0.03	-0.02	4.44	3.96	0.49	0.40	0.57
26 Oct 2022	N/A	N/A	N/A	6.80	4.70	2.10	n = 1	n = 1	0.04	0.04	0.00	n = 1	n = 1	3.50	3.35	0.15	n = 1	n = 1
23 Nov 2022	N/A	N/A	N/A	7.05	7.90	-0.85	-4.84	3.14	0.05	0.05	0.00	-0.01	0.01	3.32	2.49	0.83	0.80	0.86

Table S1B4b Inlet, outlet and concentration reduction data for sampled water quality parameters in 11 inundation events between 2-Mar-21 and 23-Nov-22. Mean concentrations of water quality parameters at DB inlet and DB outlet; mean reductions in concentrations and upper (2.5%) and lower (97.5%) confidence intervals are given for each event. Confidence intervals were not calculated for dissolved oxygen concentrations or for any samples taken on 9th Mar 2022 and 26th Oct 2022 as single samples were taken at inlet and outlet on these occasions: data for these events are denoted with 'n=1'. Statutory limits: c Drinking Water Directive [98/83/EC]

Flood Event	SRP (mg P/L)					TP (mg P/L)					DOC (mg C/L)					Chloride (mg/L)				
	Statutory limit c < 0.025mg P/L																			
	Inlet conc. (mg/L)	Outlet conc. (mg/l)	Mean change (mg/L)	2.5% Conf Int	97.5 Conf Int	Inlet conc. (mg/L)	Outlet conc. (mg/l)	Mean change (mg/L)	2.5% Conf Int	97.5 Conf Int	Inlet conc. (mg/L)	Outlet conc. (mg/l)	Mean change (mg/L)	2.5% Conf Int	97.5 Conf Int	Inlet conc. (mg/L)	Outlet conc. (mg/l)	Mean change (mg/L)	2.5% Conf Int	97.5 Conf Int
2 Mar 2021	0.02	0.02	-0.01	-0.01	0.00	0.03	0.04	-0.01	-0.02	-0.01	2.25	2.65	-0.40	-0.85	0.05	14.90	14.89	0.01	-0.70	0.72
20 May 2021	0.04	0.04	-0.01	-0.01	0.00	0.13	0.11	0.03	0.02	0.03	11.86	10.76	1.09	0.82	1.37	12.07	12.13	-0.06	-0.14	0.03
7 Oct 2021	0.03	0.08	-0.05	-0.06	-0.04	0.07	0.15	-0.07	-0.11	-0.04	11.28	15.06	-3.78	-7.45	-0.10	20.02	20.36	-0.34	-1.92	1.24
8 Dec 2021	0.02	0.11	-0.09	-0.09	-0.08	0.04	0.18	-0.13	-0.14	-0.13	4.79	8.26	-3.48	-5.05	-1.91	20.02	24.01	-3.99	-5.22	-2.77
30 Dec 2021	0.07	0.07	0.00	-0.06	0.05	0.53	0.80	-0.27	-0.86	0.32	8.16	6.82	1.35	-2.25	4.95	18.62	18.31	0.31	-0.78	1.41
22 Feb 2022	0.02	0.03	-0.01	-0.02	-0.01	0.03	0.07	-0.04	-0.05	-0.04	3.20	4.13	-0.93	-1.23	-0.63	18.13	19.84	-1.71	-1.95	-1.47
9 Mar 2022	0.05	0.07	-0.02	n = 1	n = 1	0.14	0.26	-0.13	n = 1	n = 1	8.41	8.04	0.37	n = 1	n = 1	23.60	21.53	2.07	n = 1	n = 1
7 Sep 2022	0.06	0.13	-0.07	-0.07	-0.06	0.16	0.20	-0.05	-0.05	-0.04	15.09	14.65	0.44	0.12	0.76	34.42	33.20	1.22	-1.31	3.75
19 Oct 2022	0.03	0.07	-0.04	-0.04	-0.04	0.06	0.12	-0.06	-0.07	-0.04	9.18	9.89	-0.71	-1.44	0.02	20.89	20.50	0.40	0.18	0.61
26 Oct 2022	0.04	0.06	-0.02	n = 1	n = 1	0.08	0.09	-0.01	n = 1	n = 1	7.27	7.22	0.05	n = 1	n = 1	19.84	19.80	0.04	n = 1	n = 1
23 Nov 2022	0.04	0.06	-0.02	-0.03	-0.01	0.07	0.10	-0.04	-0.07	-0.01	5.21	6.11	-0.91	-1.25	-0.56	17.24	15.01	2.23	1.74	2.73

*Table S1B5 Percentage change (**Δ** %) for all water quality parameters in 11 sampled flood events. Negative values denote decrease in mean concentrations between the DB inlet and DB outlet. Samples taken during manually-operated flooding of the DB: 2nd Mar 2021 – 26 Oct 2022; samples were taken under automatic take-off to the DB (1st Nov 2021 – 26th Oct 2022 Q > 0.075 m^3sec^{-1}; 26th Oct 2022 – 23rd Nov 2022 Q > 0.1 m^3sec^{-1})*

Flood Event	DO %	SS (%)	Ammonia (%)	Nitrate (%)	SRP (%)	TP (%)	DOC (%)	Chloride (%)
2 Mar 2021	N/A	-20	1.09	-4.37	52	17.8	17.8	-0.07
20 May 2021	-1.65	-67.41	0.65	-13.59	16.67	319.05	-9.22	0.47
7 Oct 2021	N/A	-16.02	0.47	9.22	170	90.24	33.49	1.7
8 Dec 2021	N/A	11.54	0.83	-48.74	358.33	39.09	72.63	19.95
30 Dec 2021	-24.42	-80.6	0.75	-7.24	6.06	761.43	-16.52	-1.68
22 Feb 2022	-6.54	67.32	0.4	-4.45	81.25	100	29.04	9.43
9 Mar 2022	-11.31	56.54	0.25	-24.15	31.48	191.55	-4.44	-8.76
7 Sep 2022	-1.08	-54.01	3.01	-13.61	113.56	126.19	-2.9	-3.54
19 Oct 2022	0	-14.55	1.06	-10.94	125.81	90	7.7	-1.9
26 Oct 2022	N/A	-30.88	0.94	-4.23	47.37	142.86	-0.69	-0.2
23 Nov 2022	N/A	12.06	0.61	-25	58.33	114.04	17.39	-12.95
n	44	70	70	70	70	70	70	70
Mean	-7.5	-12.37	0.91	-13.37	96.44	181.11	13.12	0.22
Min	-24.42	-80.6	0.25	-48.74	6.06	17.8	-16.52	-12.95
Max	0	67.32	3.01	9.22	358.33	761.43	72.63	19.95

Table S1B6 Water quality parameter data from DB spatial sampling during inundation event on 9-Mar-2022. 1L samples were collected from the indicated sampling locations during the inundation event, as well as in-situ measurements of temperature and dissolved oxygen (% and concentration mg L^{-1})

Sample location	Temperature (°C)	DO (%)	DO (mg L^{-1})	Ammonia (mg N L^{-1})	SRP (mg P L^{-1})	TP (mg P L^{-1})	Nitrate (mg N L^{-1})	SS (mg L^{-1})	DOC (mg C L^{-1})	Chloride (mg L^{-1})
DB Inlet	7.7	96	11.2	0.104	0.054	0.136	2.965	27	8.41	23.6
15m after inlet	7.6	95	11.1	0.113	0.059	0.176	2.913	28	8.43	23.73
30m after inlet	7.8	95	11	0.121	0.057	0.183	2.93	37	8.44	23.91
45m after inlet	7.9	95	11	0.109	0.055	0.209	2.967	44	8.37	23.6
Ponded zone edge	7.6	96	11.2	0.105	0.061	0.172	2.857	25	8.59	23.65
Ponded zone bottom	7	72	8.5	0.327	0.075	0.344	2.213	61	8.1	21.59
Ponded zone surface	7.5	91	10.7	0.246	0.067	0.155	2.214	18.8	8.12	21.12
DB outlet pipe	7.7	92	10.6	0.261	0.071	0.293	2.32	47	7.89	21.89
Channel d-s of DB	7.7	96	11.2	0.123	0.056	0.139	2.958	28	8.17	23.56

Table S1B7 Table showing areas under hydrograph curves (AUC) for all single peak events upstream of the detention basin (U/S AUC), downstream of the detention basin (D/S AUC), the difference between upstream and downstream, and the percentage (%) difference. AUC values are derived from entire curve above the take-off threshold (4th Dec 2021 – 26th Oct 2022: take-off Q = 0.075 m^3s^{-1}; 30th Oct 2022 – 31ST Jan 2023: take-off Q = 0.1 m^3s^{-1}). Detention basin peak volume and the percentage of this volume that can account for the U/S – D/S AUC difference are shown in columns 6 and 7 respectively. Mean values for each column are shown below the main table.

Date	U/S AUC (m^3)	D/S AUC (m^3)	AUC difference U/S – D/S (m^3)	% Difference	Detention basin peak volume (m^3)	Difference in detention basin (%)
04/12/2021	2796.91	1572.31	1224.6	43.78	209.05	20.58
30/12/2021	40447.46	10523.11	29924.34	73.98	230.9	0.78
07/03/2022	2752.06	1525.21	1226.85	44.58	174.95	16.63
06/09/2022	2036.6	1095.24	941.36	46.22	238.64	33.96
10/09/2022	2071.98	998.37	1073.62	51.82	252.11	30.69
31/10/2022	30903.98	21385.12	9518.86	30.8	196.9	2.11
07/11/2022	26903.12	11661.79	15241.33	56.65	183.79	1.22
24/12/2022	8349.49	7715.2	634.29	7.6	82.58	14.97
Mean	14532.7	7059.54	7473.16	44.43	196.115	15.12

Chapter 3:

The impacts of inundations during flood peak periods on pasture sward biomass and health

Abstract

Many agricultural catchments throughout the world have been dramatically altered to facilitate greater productivity and agricultural intensification. Hydro-morphological modifications have reduced the occurrence of over-bank flooding during high-flow periods and saturation of soils from overland flow and groundwater. While these modifications are associated with marked increases in agricultural productivity, especially over the past 60 years, reduction in the extent of floodplains in the upper catchment may cause more severe flooding downstream. ‘Natural’ or ‘soft-engineered’ flood management features like flood detention basins have been advocated in agricultural catchments for the mitigation of downstream flood peaks, but the effects of such short-term (approx. 24 hours) inundation of farmland on pasture health remain relatively unexplored. In this study, we analysed the monthly growth and sward quality of grassland within a flood detention basin constructed on a mixed beef/arable farm in southern Ireland, over a 12-month period. The flood detention basin acted to reduce downstream peak discharges in a headwater stream flowing through the farm during 15 inundation events between July 2022 and July 2023. During the late autumn and winter of 2022, the growth and health of the sward in the ponding zone of the detention basin was somewhat reduced compared to the unflooded sward of the same field. There was little difference however in growth or health of the sward between the ponding and non-ponding zones of the field during spring and summer months, with some indication of greater growth in the ponding-zone during the peak growth period between April and June. Our results show that short-term (12-24 hours) inundation of agricultural grassland to alleviate downstream flooding does not impair sward growth in spring and summer, but that extended inundation during the growing season may impose greater stress on plants.

3.1 Introduction

Until relatively recently, seasonal flooding has been an inherent component of agricultural activities across much of the world and has been tolerated, and sometimes exploited, to improve agricultural productivity (Cook et al., 2003; Ma et al., 2020; Seliger and Zeiringer, 2018). Since the industrial revolution and consequent increases in urbanisation and demand for agricultural products, more of the natural landscape has been augmented to enhance agricultural productivity. Much of this has been achieved through permanent reclamation of land by draining wetlands, adjusting the path of streams, altering channel and bank-morphology to enhance conveyance of water and limit over-bank flooding, and through the formation of open and sub-surface drains to intercept ground water below the root zone of crops (Jaynes and Isenhart, 2014; Poff et al., 1997; Rogger et al., 2017). Wetland loss has facilitated urban and agricultural expansion for many centuries but the rate of loss accelerated in the 18th century before peaking in the mid-20th century, to the extent that Davidson (2014) estimated that up to 70% of world's wetlands have been lost in the 20th century.

In contemporary intensively-managed agricultural landscapes, the perceived risk of flood damage to crops and grassland drives landowners to protect fields from over-bank flooding in all but the most extreme high-flow events (Brown et al., 2018). This may diminish the flood alleviation ecosystem services of catchments with evidence that channelisation has led to more severe flood peaks and negatively affected important habitats for aquatic life (Burek et al., 2012; Poff et al., 1997). Additionally, the social and financial cost of flooding of downstream urban settlements has increased markedly over recent decades (Ellis et al., 2021). The EU Floods Directive (Directive 2007/60/EC); and associated national programmes such as the River Basin Management Plans impose requirements on local and national bodies to enhance flood mitigation across catchments and advocates the inclusion of Nature-based solutions such as Natural Flood Management (NFM) (Department of Housing Local Government and Heritage, 2022; Doody et al., 2012; Heneghan et al., 2021). Utilising farmland to host NFM features has been advocated (Quinn et al., 2022; Robotham et al., 2022). In Ireland, agricultural land occupies an estimated 67% of the landscape (DAFM (Department of Agriculture, Food and the Marine, 2017). The careful placement of NFM features, such as flood detention basins, riparian buffer zones and cross-contour woodland buffer strips, throughout rural catchments, NFM features may provide substantial hydrological storage and mitigate flood risk to downstream urban settlements (Cooper et al., 2021; Joyce et al., 2016). These features can reduce peak discharges in channels by intercepting overland flow across a large area such that stream channels receive water from rainfall events over a longer period (Quinn et al., 2013). Furthermore, NFM features on land may also promote resilience of crops during periods of drought through enhancing soil water availability (Keesstra et al., 2018). It is predicted that climate change will alter grassland hydrology, especially through increased frequency of drought and extreme flood events (Joyce et al., 2016; Morris and Brewin, 2014; Fenton et al., 2021). It is vital, therefore, that the effects of extreme climatic events on crop production are well understood so that appropriate steps may be taken to maintain food security (Moreno et al., 2023).

In studies investigating the effects of flooding on commercial vegetable, arable and agricultural grassland, flooding has been shown to impair biomass production, reduce photosynthetic efficiency and consequentially increase in metabolism of carbohydrates in plant tissues (Barickman et al., 2019; Son and Oh, 2015; Striker and Colmer, 2017; Todorova et al., 2022; Wang et al., 2020). Both drought and inundation have been shown to reduce plant health by reducing relative water-dry mass content, as plants experience both scenarios as a ‘physiological drought’ due to oxygen deficiency (Barickman et al., 2019; Jung et al., 2009; Wang et al., 2008).

In tissues of plants, chlorophyll content reflects plant photosynthetic activity and efficiency, and overall plant health (Lichtenthaler and Buschmann, 2001). While Chl *a* and Chl *b* are both important light-harvesting pigments, Chl *a* is more directly involved in the splitting of water to yield electrons and the production of ATP in the photosynthetic reaction centres of Photosystem II (PSII). Chl *b* is present only in the pigment antenna complexes of PSI and PSII where it is bound to light-harvesting complex proteins (LHCs) for the transfer of energy to Chl *a* in the reaction centres (Dalal and Tripathy, 2018; Todorova et al., 2022). Chl *a,* therefore, is central to energy production through photosynthesis, while Chl *b* improves the efficiency of Chl *a* activity (Ebrahimiyan et al., 2013; Lichtenthaler and Buschmann, 2001). Water stress on plants through waterlogging or submergence can lead to reduction in oxygen uptake in the rhizosphere and exchange of oxygen and carbon dioxide via the leaves (Pan et al., 2021). In the absence of adequate gaseous exchange, excess light absorption by LHCs can lead to production of reactive oxygen species (ROS) such has hydrogen peroxide, which can damage proteins within plant cells (Dalal and Tripathy, 2018). To mitigate build-up of ROS, plants may reduce Chl *b* production and consequently reduce production and activity of LHCs. Changes in the overall chlorophyll content (Tot Chl) can therefore can yield useful information on the degree of stress being imposed on a plant, while changes in Chl *a*, Chl *b* and the Chl *a*/*b* ratio can reveal how various sites within the photosynthetic apparatus are responding to that stress (Lichtenthaler and Buschmann, 2001).

The composition of inorganic and organic nutrients in the soil is another important determinant of plant productivity and can provide insight into how plants respond to drought and flood stress. For example, relative compositions of organic and inorganic nitrogen in the soil can indicate the level of stress imposed on plants by flooding and drought, as conditions which favour plant biomass production will have higher organic:inorganic nitrogen levels (Walworth, 2013; Lehmann et al., 2020), and the stoichiometric balance of carbon, nitrogen and phosphorus is an important determinant of nutrient cycling within soils (Heuck et al., 2015; Kuypers et al., 2018; Stutter et al., 2018).

Our understanding of the impacts of flooding on crop productivity is largely derived from studies conducted in laboratory or greenhouse conditions in which cultivars are subjected to a narrow set of stressors, often for prolonged periods (> 2 weeks; e.g. (Gattringer et al., 2018; Kitanović et al., 2023; McFarlane et al., 2003; Moreno et al., 2023). The effects of short-term (12-24 hours), flood peak storage on important agricultural grassland species such as ryegrasses, various legumes and plantains (e.g., *Plantago lanceolata*) are largely untested (Beloni et al., 2017; Striker and Colmer, 2017; Van Eck et al., 2006; Wang et al., 2020). Given the potential benefits of NFM on farmland for flood peak mitigation and drought resilience, it is important that the effects of inundation during flood peaks to plant and soil health are assessed.

To test the impact of short-term flooding on grassland productivity, we constructed a field-scale flood detention basin, receiving over-bank floodwater from a first order stream, on farmland in Co. Cork, SW Ireland. The aim of the detention basin was to mitigate peak flows in the stream by diverting flood waters from the stream channel to an adjacent agricultural grassland field behind an earthen bund, before slowly releasing stored water back to the channel. Sward health within flooded and unflooded parts of the field was assessed as fresh and dry biomass, chlorophyll content and sward diversity and monitored over a 13-month portion of this 24-month inundation experiment to examine the impact of these short-term inundation events.

3.2 Methods

3.2.1 Catchment and study site

The study site was located within a mixed-use farm within the Glashagarriff sub-catchment of the River Lee, SW Ireland. A first-order tributary of the river flows through the farm (Fig. 1). As part of a parallel study, a flood detention basin was constructed within a field on the farm to investigate the hydrological impacts of directing overbank floodwaters from the channel to the field. During these inundation events, water flowing into the field from the stream was stored in a shallow depression behind a raised earthen bund within the field for a few hours beyond the flood peak (Fig. 2). The field, therefore, consisted of an overland flow-path to a flooded part of the field (the '*ponding zone')* and a portion of the field away from the detention basin that was not flooded (the '*non-ponding zone')* (Fig. 2), which allowed comparison of the effects flooding on mixed sward productivity and health over an extended period of intermittent flooding (July 2022 – July 2023). The field was grazed between the months of March and November each year by a herd of approximately 45 calves and suckler cows. The field was not subject to regular artificial fertilisation or reseeding in the 10 years preceding the study.

To exclude livestock grazing as a factor driving grass sward dynamics during the experiment, 1.5 m high livestock-proof enclosures (approx. 0.5 m^2 in surface area) were constructed using wooden stakes and three layers of sheep fencing within the field, three in the ponding zone and three in the non-ponding zone (Fig. 2). During inundation events, the vegetation enclosures in the ponding zone were submerged by floodwaters to a maximum depth of approx 0.6 m. Within each enclosure, four 0.1 vm X 0.1m sub-plots were sampled monthly for collection of vegetation data (Fig. 2c). The grass enclosures were positioned within the field where they represented typical vegetation growth and grazing potential, while being at similar elevations, aspect and soil type. During flood events, the depth at each grass enclosure was measured by extrapolating from depth data from a water level recorder (*In-Situ Inc. Rugged TROLL® 100*, *USA*) positioned at the topographic minimum of the field and from 180 ground telemetry topographic data points collected from the field.

The soil within the stream catchment consists primarily of fine loamy soil over sandstone bedrock (Teagasc, 2023). Catchment land use is predominantly (80% of land surface area) improved or semi-natural grassland, with the remaining land consisting largely of conifer plantation and peat-soil heathland and rough grazing in the higher elevation part of the catchment (Environmental Protection Agency, 2018). The catchment receives an average annual rainfall of 1305 mm per year (2000 – 2022; (met.ie, 2023). The study site itself may be classified as semi-natural grassland GS1 (Fossitt, 2000) based on vegetation types, and on grazing and fertilizing regimes.

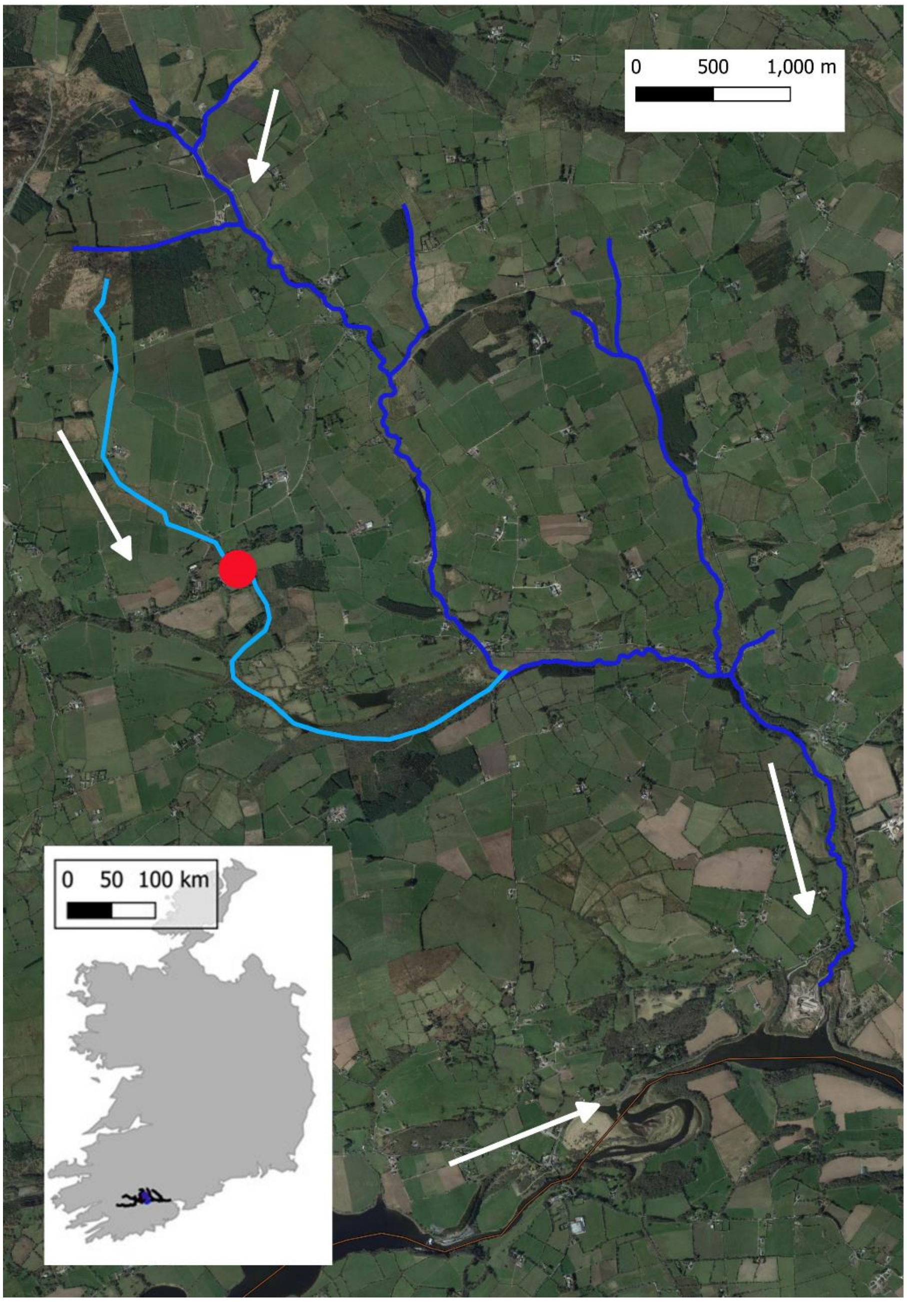

Figure 1 River Lee catchment (Black line) in the south of Ireland (inset) with the Glashagarriff sub-catchment highlighted in blue. The study site at Leades House (red marker) is along the route of a minor stream which feeds into the Glashagarriff catchment (light blue line, main figure)

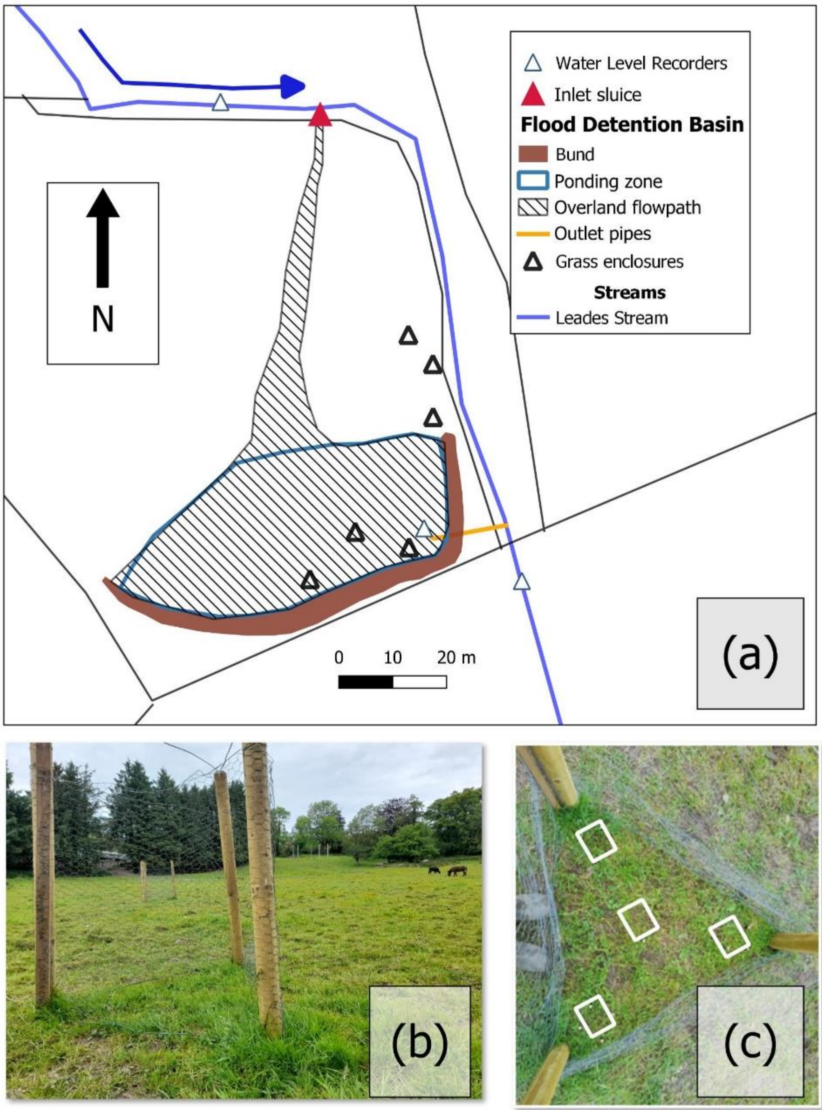

Figure 2 Schematic of the flood detention basin and associated legend (a). Blue line indicates direction of direction of flow of Leades Stream (the stream through Leades Farm); grey lines indicate field boundaries. Stream water is directed from the channel to the detention basin during high flows during high-flow events, then flows along the overland flow path to the ponding zone; Triangles indicate grass enclosures within and outside the ponding zone (b) photograph of grass enclosures at field on Leades Farm; (c) photograph looking into grass enclosure with super-imposed squares indicating 10 x 10cm sub-plots from which grass samples were taken.

3.2.2 Data collection and analysis

3.2.2.1 Grass sampling and weighing

Data were collected in the middle of each month from the sub-plots in the ponding and non-ponding zones. On sampling events, all fresh plant material from each sub-plot was cut at 5 cm above the ground to mimic recommended grazing levels for livestock to prevent damage to the meristem and promote optimal ongoing grass growth (Ganche et al., 2015). Each fresh sample was immediately put in a paper bag and weighed within 8 hours of being harvested. 200 mg (+/- 2 mg) sub-samples were taken from each fresh sample for chlorophyll analysis, and refrigerated over-night. The remainder was dried in an oven (Thermo Scientific™ Heratherm™ Advanced Protocol Ovens, 230VAC 60Hz) to constant weight at 50°C for four days after which each sample was re-weighed to assess dry weight and relative water content (Ebrahimiyan et al., 2013; Son and Oh, 2015).

3.2.2.2 Chlorophyll analysis

Chlorophyll extraction on the 200 mg fresh plant material sub-samples was performed using the method outlined in Son and Oh (2015). Briefly, each 200 mg sample was removed from cold-storage on the day after harvesting and was frozen with 5-10 ml of liquid nitrogen and ground in a mortar with a pestle until a fine powder was obtained, which was then mixed with 5 ml of 80% (v/v) acetone. Samples could not be immediately frozen upon harvesting due to time restrictions imposed by distance from the site to the laboratory facilities. 1.5 ml of this extract was pipetted into two Eppendorf tubes for each sub-sample and spun at 900Xg for five minutes in a centrifuge. The absorbance of samples was read at 663nm and 645nm in a spectrophotometer (Shimadzu, UV-160A) for assessment of absorbance of chlorophyll *a* (Chl *a*), and chlorophyll *b* (Chl *b*) respectively. Total chlorophyll (Tot Chl), Chl *a* and Chl *b* content were measured using Equation 1 below:

$$\textit{Total Chl content } [\mu g\ mL^{-1}\ 200\ mg^{-1}] = (20.3 \times A_{645}) + (7.22 \times A_{663})$$

$$\textit{Chl a content } [\mu g\ mL^{-1}\ 200\ mg^{-1}] = (12.72 \times A_{663}) - (2.58 \times A_{645})$$

Chl b content $[\mu g\ mL^{-1}\ 200\ mg^{-1}] = (22.88 \times A_{645}) - (5.50 \times A_{663})$

(Equation 1)

Where A_{663} and A_{645} are absorbance of each Chl *a* and Chl *b* sample, respectively. Values obtained for Tot Chl, Chl *a* and Chl *b* in equation 1 were multiplied by 5 to present Chl content (µg Chl 200 mg^{-1}) from equation 1 as µg Chl g^{-1}. The chlorophyll per sample plot area *(µg Chl* g^{-1} *0.01* m^2*)* could then be estimated using equation 2

Chlorophyll per sample area = Fresh sample weight (g) X Chl_x *content*

(Equation 2)

Where '*Fresh sample weight'* is the weight of fresh grass from the original sub-plot sample (grams); *Chl content* refers to µg Chl g^{-1}; *x* is the chlorophyll parameter of interest (i.e., Total Chl, Chl *a* or Chl *b*). Monthly Total Chl, Chl *a* and Chl *b* content, fresh mass, dry mass and relative water content were estimated for each sub-plot. Relative water content (RWC) was calculated using Equation 3 (Ebrahimiyan et al., 2013):

RWC = 1 – (oven dried mass (g)/ fresh mass (g))

(Equation 3)

3.2.2.3 Sward diversity

The vegetation diversity within enclosures was assessed during sampling events from April – July 2023. Identification of grassland species was done to species or family level, depending on the group. Relative abundance (%) and percentage in flower for each group was estimated within each enclosure. Species diversity indices (Shannon-Weiner and Simpon's indices; Hauer and Lamberti, 2017) in the ponding and non-ponding zones were estimated from relative abundance values.

3.2.2.4 Soil sampling and analysis

In June 2021 and 2022, and September 2022, soil core samples were collected from six locations from each of the treatment zones (ponding zone, non-ponding zone) of the detention basin, as well as the overland flow-path from the sluice to the ponding zone (Fig. 2), for analysis of concentrations of soil nutrients. Samples were collected from the middle area of each 20x20m square of a grid mapped out in QGIS. Cores were collected using a hand-auger and measured c.12 x 5cm (length x width). Samples were stored at -80°C prior to laboratory analysis. Once thawed, samples were homogenised, dried at 55°C until reaching stable mass (c. 24hrs) then sieved to 2 mm. Soil samples were analysed for concentrations of (Morgan's P (mg P/kg), TP (mg P/kg), Available ammonia (mg N/kg), Available TON (mg N/kg), Total Kjeldahl Nitrogen (mg N/kg)). Soil organic matter (SOM) was estimated through loss on ignition (LOI) at 550°C in a muffle furnace for 2hours for 5g sub-samples from each sample (Ball, 1964; Regan et al., 2010). 2 mg soil samples were extracted in 1M potassium chloride solution (74.55 g KCl/L deionised water), then centrifuged at 5000 rpm for 10mins. The supernatant was filtered through a 0.45µm membrane syringe filter and Ammonia and TON content were estimated using Lachat Quik-Chem 8000 FIA. Morgan’s P was estimated through extracting soil samples with 60 ml 1M potassium chloride solution (74.55 g KCl/L Deionised Water), centrifuging and testing the filtered supernatant for Morgan’s P via the FIA method (Murphy and Riley, 1962). 1g soil samples were digested in 1Kjeltab and 6 ml 95% sulphuric acid. The digested samples were filtered through GF/C filter paper and diluted to 250 ml with deionised water. Total Kjeldahl nitrogen was measured as ammonia using Lachat Quik-Chem 8000 FIA. Total phosphorus was measured by manual colorimetric method (Murphy and Riley, 1962). Results were compared with those of identical analysis of a certified reference material BCR®-129.

3.2.3 Data analysis

Data handling and analysis were performed in RStudio v2023.03.0.386 (RStudio Team, Boston, MA, USA, 2023). Repeated measures analysis on the treatment effect on monthly biomass production (fresh weight, dry weight), relative water content and chlorophyll content (Total chlorophyll, Chlorophyll *a*, Chlorphyll *b*, Chlorophyll *a*/*b* ratio) was performed using mixed effect linear models with sub-plot ID nested in enclosure included as a random effect using the R package "lme4" and the "lmerTest" package to provide *p* and t values for the models. Tests on model fit were performed through inspection of normality plots produced by the R package "DHARMa." Temporal autocorrelation of mixed effect models was tested on model residuals using the *acf*-function from lme4. Differences between treatments were calculated for fresh weight (FW), dry weight (DW), RWC, Chl *a*/*b* ratio and chlorophyll (Tot Chl, Chl *a*, Chl *b*) content of fresh plant material (µg Chl g^{-1}) and chlorophyll per unit area (µg Chl g^{-1} 0.01 m^2). Additionally, results were analysed separately for the winter period while cattle were housed in sheds (November 2022 – March 2023, inclusive) and the 's*ummer'* growing season during which livestock grazed on the study site (July 2022 – October 2022, April 2023 – July 2023), to illustrate the relative impact of flooding on grassland during the summer growing period, compared to the winter 'fallow' period. Results were also analysed form the whole period of the experiment (July 2022 – July 2023).

Area under the curve (AUC) analysis was performed to provide further illustration of differences between the ponding and non-ponding zones over the whole study and during winter (November – March) and summer (April - October) (see Laughlin et al., 2007). AUC was calculated as the integral of the sum of monthly mean parameter values (FW, DW, RWC, chlorophyll) for each treatment for the whole study, winter and summer. The mean AUC mass differences and mean AUC percentage differences between the treatments were calculated for winter, summer and the overall study-period. Mean percentage difference was calculated using equation 4:

$$\text{Mean \% difference} = \frac{(A-B)}{\bar{C}} \times 100$$

(Equation 4)

Where *A* is the parameter value in the ponding zone, *B* is the parameter value in the non-ponding zone and $\bar{C}$ is the mean of *A* and *B.*

While there were an equal number of sub-plots per enclosure and three enclosures in each treatment (ponding and non-ponding zones; Fig. 2), sampling from all sub-plots was not possible on all sampling occasions due to instances of disturbance to enclosures by livestock and due to partial inundation of enclosures. Sampling occurred outside of flood events as much as possible but residual water remained during some sampling events. For this reason, AUC analyses on monthly mean values for plant material weight and chlorophyll were based on total values per 0.01 m^2 subplot divided by the total number of sub-plots sampled in each treatment during each sampling event.

Vegetation metrics were compared between ponding and non-ponding zones using mixed-effect linear models, which included enclosure identity as a random effect to account for repeated measurements and variance between enclosures within ponding/non-ponding treatments.

3.3 Results

3.3.1 Biomass production

Over the study period of July 2022 – July 2023 the ponding zone of the flood detention basin was inundated with flood water for a total of 56 days (22 days during winter (November - March) and 34 days during summer (Apil - October)). Diversion of stream water to the detention basin led to inundation of the ponding zone under a maximum of 1m of water. There was some ponding of water in the flood detention basin between February and March 2023 (maximum depth 0.2m) which was derived from overland flow from the fields upslope of the detention basin, as opposed to water being delivered from the stream. FW and DW of vegetation was weakly significantly ($p < 0.1$) lower (FW 60.74%, DW 139%) during the winter period in the ponding zone; Table 1; Fig. 3, 4). FW and DW were however higher in the ponding zone during summer months (1.26% and 3.87% respectively, Table 1), with a substantial boost in biomass apparent in the ponding zone between May and July 2023 (Fig. 3, 4). The difference between the treatment zones during summer months, however, was not significant ($p > 0.05$, Table 1). RWC in winter was significantly lower in the ponding zone than the dry zone (23.29%, $p = 0.002$, Table 1, Fig. 5). RWC of the sward in the ponding and non-ponding zones was similar during summer months (July to October 2022 and from April to July 2023; Fig. 5). There was no significant difference in RWC between the treatment zones during summer months (1.19%, $p > 0.05$; Table 1).

*Table 1 Summary data on fresh and dry weight, relative water content (RWC) total chlorophyll (Tot Chl) content per gram fresh weight and per m^2 and the Chl a/b ratio per gram fresh weight for sampled plant material. Area under curve (AUC) differences between Ponding and Non-ponding zones in winter, summer and the whole study are presented as mean differences per month for the given period and percentage difference ((Ponding - non-ponding)/mean weight * 100). Positive AUC values indicate ponding zone values are higher than non-ponding zone values. Summary data from mixed effect linear models comparing data between Ponding and Non-ponding zone plant material weight show in columns 5 – 7.*

	Period	AUC		df	t-value	p-value
		Difference between treatments per month	Percentage difference between treatments			
Fresh weight per unit area (kg ha^{-1} $month^{-1}$)	Summer	90	1.26	3.9	-1.16	0.312
	Winter	-790	-60.74	4.03	2.57	0.062.
	All months	320	8.25	3.94	-0.52	0.63
Dry weight per unit area (kg ha^{-1} $month^{-1}$)	Summer	110	6.6	3.87	-1.55	0.198
	Winter	-730	-139.28	4.17	2.64	0.055.
	All months	110	13.69	3.97	-0.98	0.384
Relative water content	Summer	-0.01	-1.19	3.88	0.05	0.966
	Winter	-0.13	-23.29	3.88	7.1	0.002**
	All months	-0.05	-7.39	3.92	3.81	0.02*
µg Tot Chl $gram^{-1}$	Summer	-8.49	-2.67	18.8	1.17	0.243
	Winter	-42.9	-27.85	3.9	5.31	0.0065*
	All Months	-21.45	-11.32	3.92	5.64	0.0052*
µg Tot Chl m^{-2}	Summer	-25.19	-1.56	3.91	-0.96	0.391
	Winter	-228.37	-90.42	4.02	3.38	0.028*
	All Months	36.25	4.53	3.94	-0.2	0.854
Chl a/b (µg Chl a/b $gram^{-1}$)	Summer	0.02	3.48	4	-0.8	0.469
	Winter	0.77	56.65	3.85	-7.19	0.0023**
	All Months	0.41	30.85	21.48	-5.13	< 0.001***

There was poor model fit of the residuals in the mixed effect linear models during the winter period and large differences in the variance of data between the treatments. This is likely to have resulted from natural seasonal growth reduction during winter and consequent zero-values, as well as from a reduction of sample size in the ponding zone due to partial inundation. During winter there was evidence of greater variance in biomass within the ponding zone than the non-ponding which also would have reduced model fit.

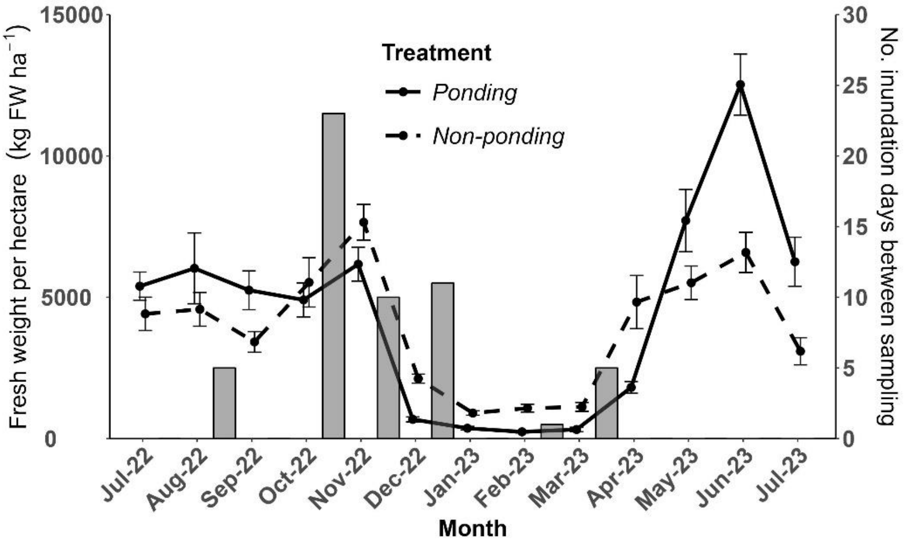

Figure 3 Fresh weight (FW) kg per hectare for ponding and non-ponding zones of the detention basin (unbroken and dashed lines, respectively; left y-axis) and number of inundation days between sampling events (grey bars; right y-axis) plotted along the sampling period from July 2022 to July 2023. Points of FW denote monthly mean values and error bars denote standard error for each treatment.

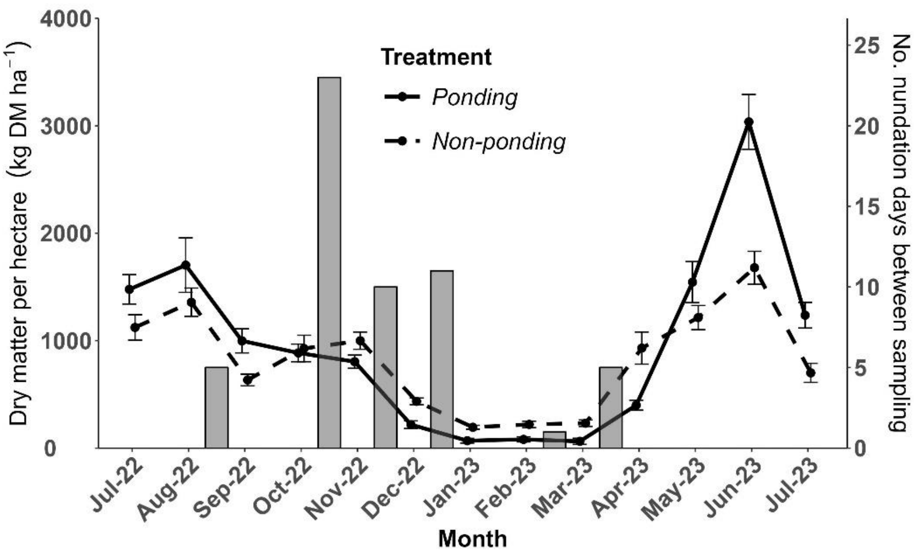

Figure 4 Dry matter (DM) kg per hectare for ponding and non-ponding zones of the detention basin (unbroken and dashed lines, respectively; left y-axis) and number of inundation days between

sampling events (grey bars; right y-axis) plotted along the sampling period from July 2022 to July 2023. Points of DW denote monthly mean values and error bars denote standard error for each treatment.

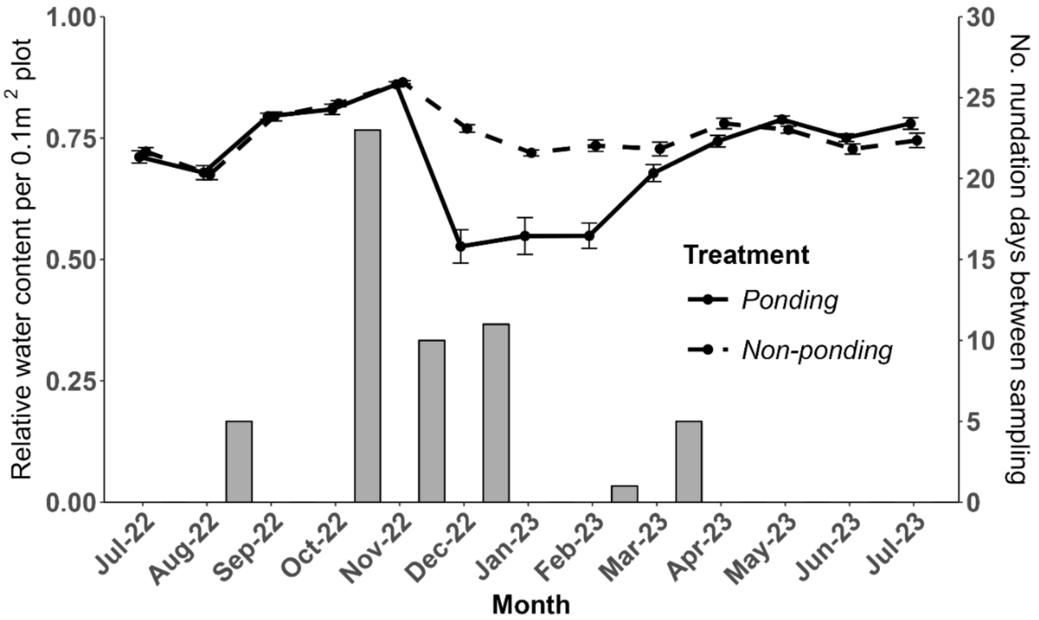

Figure 5 Relative water content (RWC) of sward sample for ponding and non-ponding zones of the detention basin (unbroken and dashed lines, respectively; left y-axis)samples based on comparison of sub-plot mass before and after drying over the sampling period (Jul 2022 – Jul 2023). Error bars indicate standard error around mean RWC. Grey bars denote number of days the ponding area was inundated between monthly sampling events.

3.3.2 Chlorophyll

Tot Chl content per gram was significantly lower in the ponding zone than the non-ponding zone during winter (27.85%, p = 0.0065; Table 1; Fig. 6a), while the summer Tot Chl content did not differ significantly between the treatment zones (2.67%, $p >$ .05, Table 3). Such was the effect of reduced Tot Chl content in winter, Tot Chl content across the whole study period was lower in the ponding zone than the non-ponding zone (11.32%, p = 0.0052, Table 1). When the FW per unit area of samples was accounted for, Tot Chl per unit area was weakly significantly lower in the ponding zone than the non-ponding zone during winter (27.85%, p = 0.028, Table 1), but was not significantly different in summer or over the whole study period ($p > 0.05$, Table 1).

While Tot Chl content per gram was similar in the ponding and non-ponding zones between May and July 2023 (Fig. 6a), the greater biomass production in the ponding zone between May and July 2023 (Fig. 3, 4), resulted in the Tot Chl per unit area being higher during this period in the ponding zone than in the non-ponding zone (Fig. 6b).

Flooding during winter appeared to have a stronger effect on the Chl *a*/*b* ratio than on Tot Chl content per gram. The Chl *a*/*b* ratio in fresh plant material was significantly lower in the ponding zone during winter (56.65%, $p = 0.0023$; Table 1, Fig.7) as Chl *b* production was reduced more by winter flooding that Chl *a* production (Fig. 8a-b). During summer there was no significant difference in Chl *a*/*b* ratio between the ponding and non-ponding zones (3.48%, $p > 0.05$, Table 1, Fig. 7). There was relatively consistent production of Chl *a* in the ponding and non-ponding zones across the study period, with a minor drop in Chl *a* production during winter (Fig. 8a). Chl *b* content per gram was much more variable in both treatment zones throughout the year but reduced more substantially in the ponding zone in winter (Fig. 8b). Chl *a,* Chl *b* and Chl *a*/*b* content per gram recovered during spring of 2023 such that there was no observed difference in summer of 2023 (Fig. 7, 8a-b).

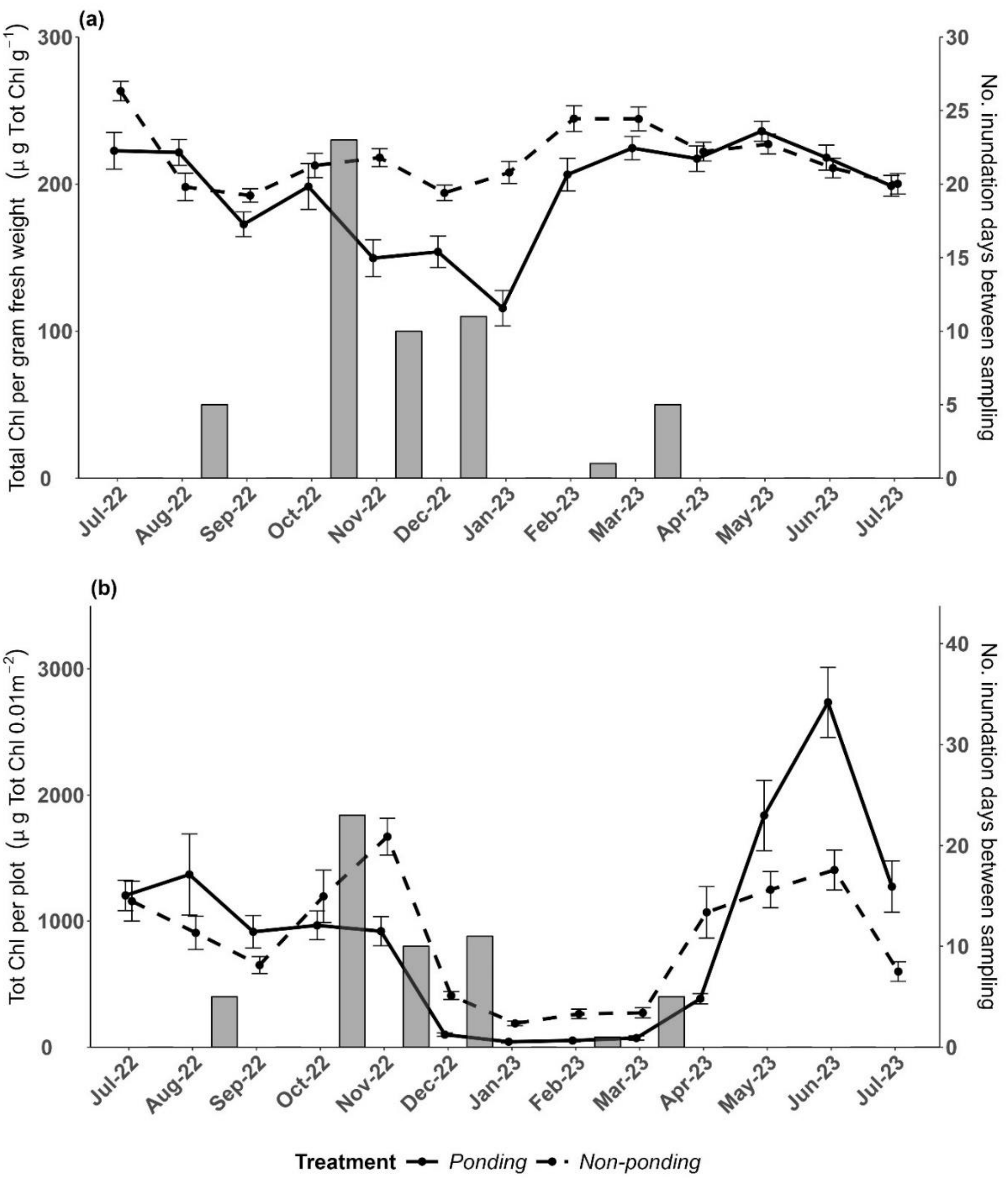

Figure 6a-b Monthly values for µg Total chlorophyll (Tot Chl) per gram fresh plant material (a) and per unit area (b) for the Ponding and Non-ponding zone treatments (unbroken and dashed lines, respectively; left y-axis) over the sampling period (x-axis). Points denote mean Tot Chl and error bars denote standard error around the mean. Grey bars denote the number of days the ponding zone was inundated between vegetation sampling events (right y-axis)

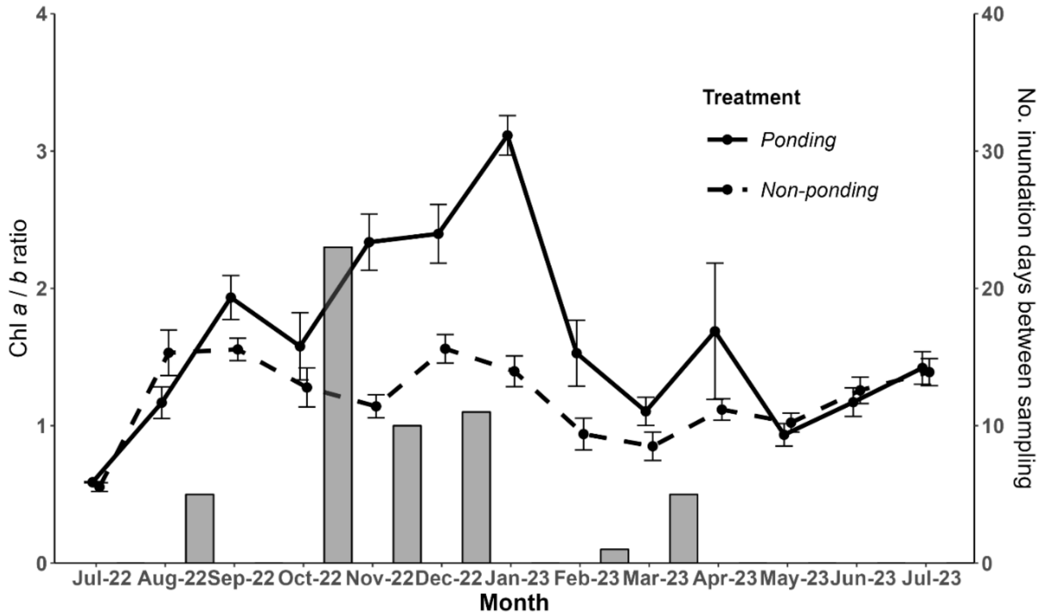

Figure 7 Monthly mean values for Chlorophyll a/b (Chl a/b) ratios per from fresh weight in the Ponding and Non-ponding zone treatments (unbroken and dashed lines, respectively; left y-axis) over the sampling period (x-axis). Points denote mean monthly values and bars are standard error around the mean. Grey bars denote the number of days the ponding zone was inundated between vegetation sampling events (right y-axis)

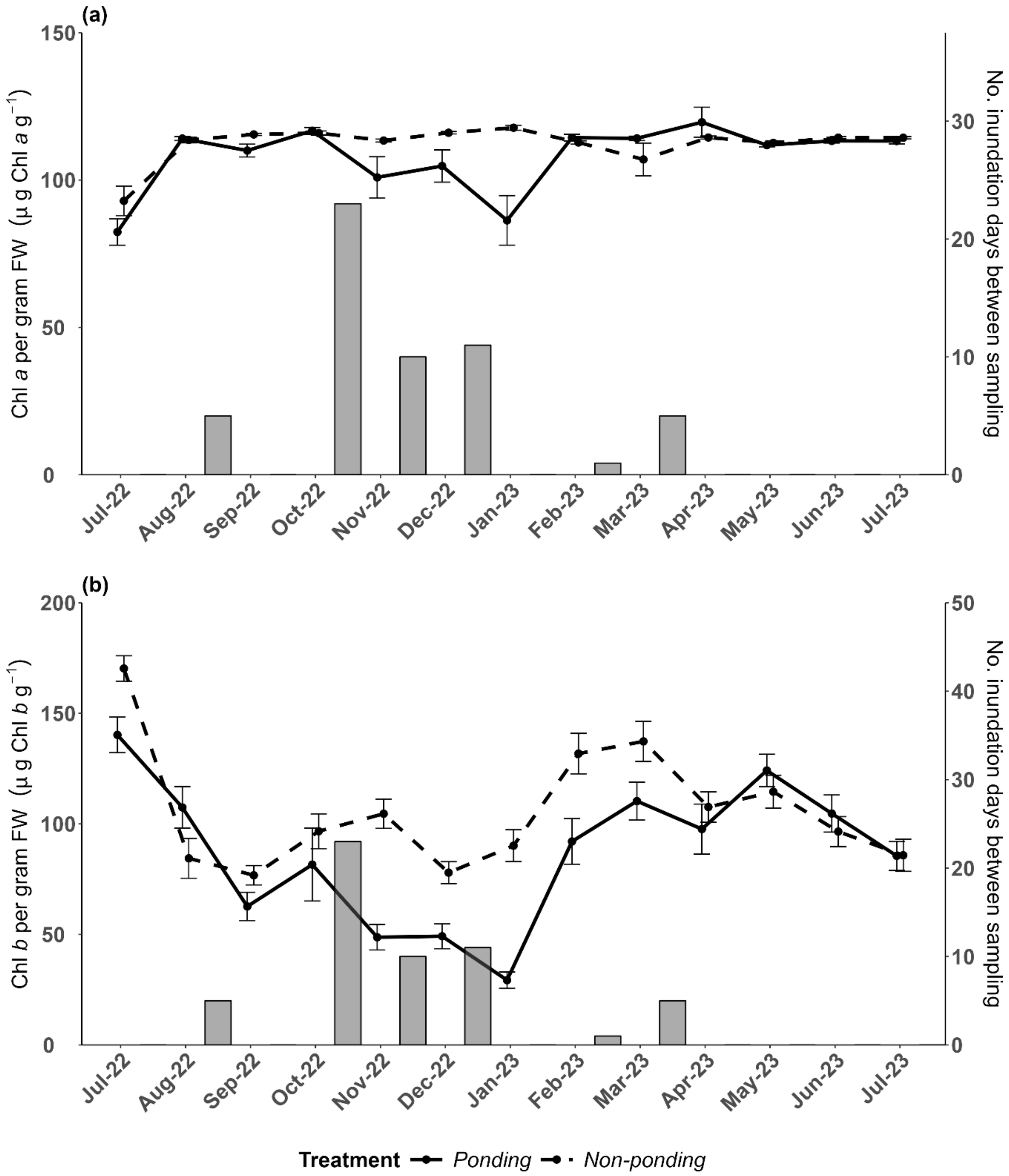

Figure 8 Chl a and Chl b per gram content in FW over the study period ((a) and (b), respectively). Monthly mean values are shown for Chl a and Chl b per gram FW in in the Ponding and Non-ponding zone treatments (unbroken and dashed lines, respectively; left y-axis) over the sampling period (x-axis). Points denote mean monthly values and bars are standard error around the mean. Grey bars denote the number of days the ponding zone was inundated between vegetation sampling events (right y-axis)

3.3.3 Sward diversity

14 plant species were identified during sampling during the flowering period between April and July 2023 (Table 2). Samples were collected during this period to facilitate species identification. Mean Shannon diversity for the Dry and Ponding zones between April and July 2023 inclusive were 4.63 and 3.708; Simpson's diversity indices were 0.47 and 0.45 respectively. No significant differences were identified (ANOVA; $p > 0.05$).

Table 2 Species identified in during sampling of the detention basin between April and July 2023. Shown are plant groups found in the Ponding and Non-ponding zones of the detention basin, and relative abundance for the two zones, averaged over the four sampling occasions.

Ponding Zone			Non-ponding Zone		
Common name	Scientific name	Mean relative abundance (%)	Common name	Scientific name	Mean relative abundance (%)
Grasses	Poaceae	51	Grasses	Poaceae	54
Clover	*Trifolium repens*	40	Clover	*Trifolium repens*	16
Creeping buttercup	*Ranunculus repens*	26	Creeping buttercup	*Ranunculus repens*	13
Cuckoo flower	*Cardamine pratensis*	8	Dock	*Rumex hydrolopathum*	6
Dandelion	*Taraxacum vulgaria*	8	Cleaver	*Galium aparine*	5
Cleaver	*Galium aparine*	5	Cuckoo flower	*Cardamine pratensis*	5
Dock	*Rumex hydrolopathum*	5	Dandelion	*Taraxacum vulgaria*	5
Nettle	*Urtica dioica*	5	Mushrooms	*Hygrocybe* spp.	5
Plantain	*Plantago lanceolata*	5	Plantain	*Plantago lanceolata*	5
			Speedwell	*Veronica persica*	5

3.3.4 Soil chemistry

Morgan's P concentrations in soil samples from across the study site were high under national standards with a mean of 47.1 mg P kg^{-1} (Table 3) (Vero et al., 2022), but concentrations of other nutrients were not elevated (Teagasc, 2017). No statistically significant differences in concentrations of soil chemistry parameters (organic carbon, Morgan's P, total phosphorus (TP), Total available ammonia, total organic nitrogen (TON) and total Kjeldahl nitrogen) were identified between 2021 and 2022 across the whole dataset (Table 3, Fig. 9). When treatment zones were included (non-ponding zone, ponding zone), concentrations of morgan's P in the ponding zone were shown to be significantly higher than in the non-ponding zone ($p = 0.01$, Table 4, Fig. 9), but there were no detectable differences between 2021 and 2022. No other soil chemistry parameters showed evidence of a treatment effect ($p > 0.05$, Table 3).

A prolonged period of warm dry weather occurred between June and early September of 2022 followed by a significant rainfall event which resulted in inundation of the detention basin between 7th and 12th September 2022. Soil samples in September were obtained on 14th September, after all flood waters had receded. This was done to help gain perspective of the short-term changes in soil chemistry which may have resulted from the inundation. No significant effect of drought or flooding was identified.

Table 3 Mean concentrations of soil nutrients (mg kg^{-1}) collected from the Ponding and Non-ponding zones of the detention basin in summers of 2021 (n = 6 per treatment zone), 2022 (n = 12 per treatment zone) and averaged across sampling events (All; n = 18 per treatment zone). Mean difference in concentration and mean percentage differences are shown in columns 5 and 6. Significant difference between zones is denoted by an asterisk (*).

Nutrient	Year	Non-ponding zone	Ponding zone	Difference	Mean percentage difference
Morgan's P (mg P kg^{-1})	2021	46.25	57.98	-11.73	-0.23
	2022	40.62	64.07	-23.45	-0.45
	All	42.49	62.45	-19.96*	-0.38*
	Mean	47.1			
Total P (mg P kg^{-1})	2021	1180.83	1145.75	35.08	0.03
	2022	1143.67	1261.18	-117.51	-0.10
	All	1156.06	1230.4	-74.34	-0.06
	Mean	1197.31			
Ammonia (mg N kg^{-1})	2021	65.07	59.12	5.95	0.10
	2022	63.33	82.9	-19.57	-0.27
	All	63.91	76.56	-12.65	-0.18
	Mean	68.21			
Available TON (mg N kg^{-1})	2021	4.53	3	1.53	0.41
	2022	3.44	2.53	0.91	0.30
	All	3.81	2.65	1.16	0.36
	Mean	3.84			
Total Kjeldahl N (mg N kg^{-1})	2021	4743.83	3848	895.83	0.21
	2022	4676.33	4834.55	-158.22	-0.03
	All	4698.83	4571.47	127.36	0.03
	Mean	4675.36			
Organic Matter %	2021	16.28	16.84	-0.56	-0.034
	2022	13.74	13.67	0.07	0.005
	All	14.59	14.52	0.07	0.005
	Mean	14.56			

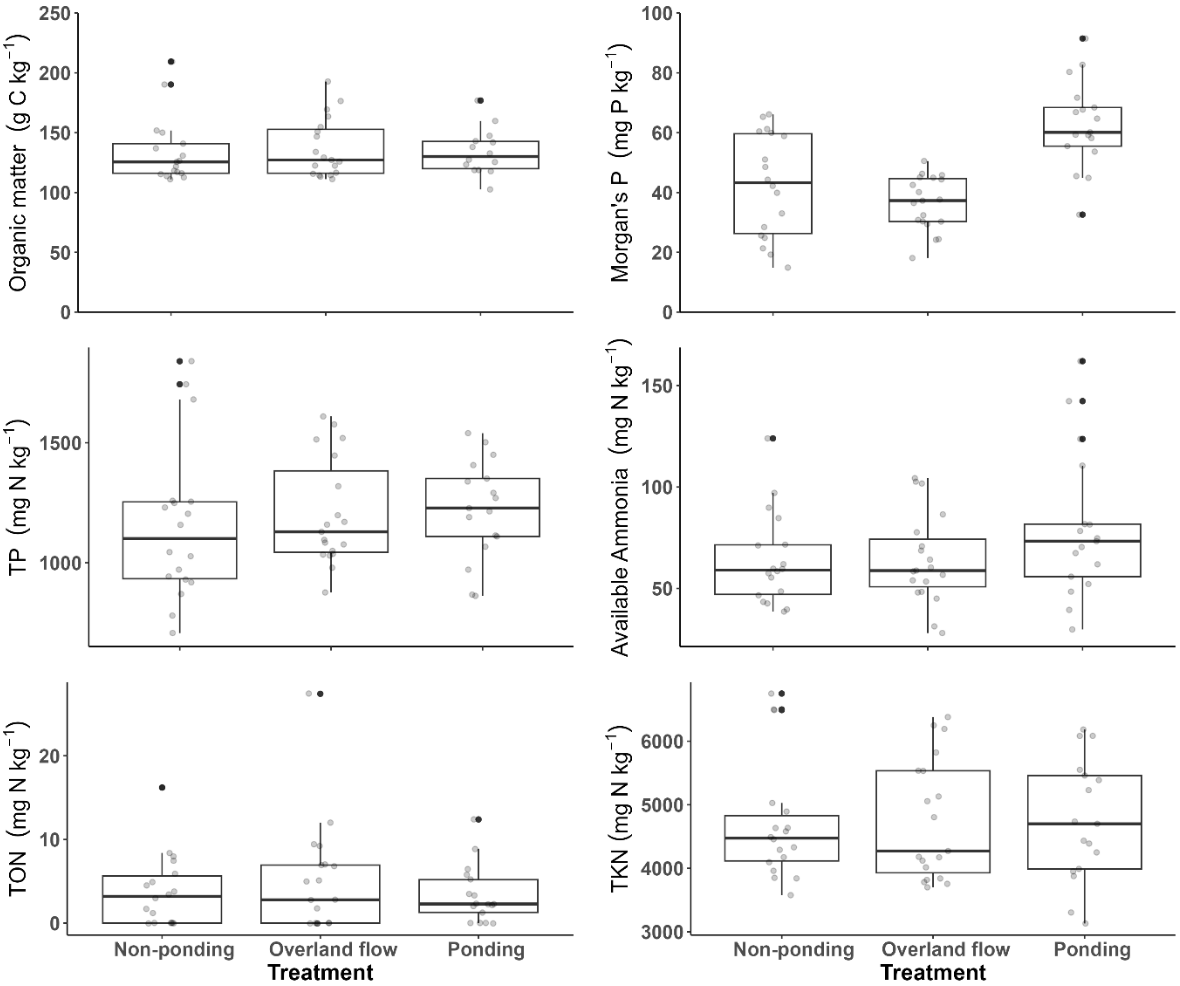

Figure 9 Soil chemistry results samples in 2021 and 2022 from the treatments in the DB (non-ponding zone, overland flowpath and ponding zone). Studied parameters were organic matter, Morgan's P, total phosphorus (TP), Total available ammonia, total organic nitrogen (TON) and total Kjeldahl nitrogen. Morgan's P was significantly higher in the ponding zone than the non-ponding zone (p < 0.05), but there was no significant difference between 2021 and 2022, or in any other soil chemistry parameters.

3.4 Discussion

Analysis of sward biomass, relative water content and chlorophyll content from this study suggest that winter flooding during peak flow periods imposes modest stress on plants. Although flooding negatively affected the biomass production in plants in the ponding zone during winter, the results were not statistically significant (*p* =

0.062). Plant health, as evidenced by chlorophyll content and RWC was significantly reduced during winter, but both biomass production (FW and DW) and plant health (RWC and Chlorophyll content) recovered across the site by spring of 2023. In fact, there was higher biomass in the ponding zone during the summer of 2023 with no evidence of impaired quality. Cattle were taken off the field at the end of October 2022 until March 2023 and were housed in sheds during this period. By the time they returned to the pasture, sward productivity was increasing across the site before peaking in the ponding zone in June 2023.

3.4.1 Physiological effects of flooding on plants

In the current study, the month-on-month rate of biomass production between September to November 2022 reduced more in the ponding zone than in the non-ponding zone. During the winter, however, the rate of biomass production plateaued in both zones, but was lower in the ponding zone. This indicates that the degree stress imposed by inundation during the final months of the summer of 2022 was greater than that experienced by plants during winter flooding. There was also an indication that the RWC of leaves in the ponding zone was reduced during this period. This has been suggested to be an adaptive response to both drought and flood stress in plants, in which plants increase the dry mass production relative to water storage to limit loss of water and solutes from plant tissues (Barickman et al., 2019; Oram et al., 2021; Wang et al., 2008). Despite the evidence of stress in plants in the ponding zone from flooding at the end of the summer of 2022, biomass (FW and DW) and chlorophyll production in the ponding and non-ponding zones largely followed seasonal decline trajectories, with smaller differences in biomass and chlorophyll production observed between November 2022 and March 2022.

There is a large body of evidence that indicates grassland species have higher tolerance to winter flooding than at other times of the year. Van Eck et al. (2005) showed that survival of grassland species under winter floods was greater than under summer flood conditions, which was partially attributed to lower carbohydrate metabolism under lower temperatures during winter flooding. Van Eck et al. (2006) showed that zonation of grassland species along a valley slope was more strongly influenced by summer flooding than winter flooding, with species of lowest tolerance to summer inundation growing at elevations furthest from the river. This zonation was also attributed to greater stress imposed on plants during summer floods. The higher growth demands on plants during summer may limit their tolerance to summer floods, with those most tolerant to summer floods being plants which possessed the ability to utilise stored carbohydrates while inundated, with concurrent reduction in photosynthetic activity (Liu and Jiang, 2015; Wang et al., 2020). Such changes in DW and Tot Chl were observed in plants in the ponding zone of the current study. Importantly however, despite frequent inundation of the ponding zone, plant growth persisted across the site throughout the winter, suggesting that all plant species present possessed some tolerance to the inundation imposed by the experiment. Additionally, the vigorous growth of vegetation in the ponding zone that was observed between April and July 2023 suggests that plants remained viable throughout the period of most intense flooding and were able respond to the improved growth conditions in the spring (Brotherton and Joyce, 2015; Wang et al., 2017).

Plants can induce alterations to the photosynthetic apparatus in response to inundation stress (Dalal and Tripathy, 2018; Lichtenthaler and Buschmann, 2001). For example, down-regulation of the antenna complex of PSII, which is the main site of Chl *b*, can reduce the activity of light-harvesting complexes (LHCs) and thus limit the build-up of ROS (Dalal and Tripathy, 2018). In the current study, the reduction of photosynthetic activity of plants in the ponding zone is indicated primarily by the large reduction in Chl *b* content (Fig. 7, 8b). During winter, the greater increase in Chl *a*/*b* ratios in the ponding zone than in the non-ponding zone indicates flooding led to greater repression of activity in the antenna complexes of PSII than the reaction centres of PSII and PSI where Chl *a* is involved in processes essential for plant metabolism, such as water-splitting reactions and production of ATP (Dalal and Tripathy, 2018; Spundova et al., 2003; Todorova et al., 2022). It is likely therefore that relatively consistent Chl *a* production during the main flood period maintained essential metabolic processes within the plants of the ponding zone, although with reduced efficiency due to reduction in Chl *b* activity (Dalal and Tripathy, 2018). Changes to specific components of the photosynthetic apparatus of plants has been seen as an adaptive response to stress in which plants maintain certain photosynthetic processes (e.g., Chl *a a*ctivity) while reducing those which may exacerbate the stress (e.g., limiting ROS production through downregulation of Chl *b*) (Ebrahimiyan et al., 2013; Lichtenthaler and Buschmann, 2001; Olorunwa et al., 2022; Spundova et al., 2003).

Studies have revealed that tolerance to inundation can vary strongly among plant species, depending on their ability to induce morphological changes, such as the development of aerenchyma to aid in internal gas transport and discharge of CO_2 and toxins (Banach et al., 2009; Pan et al., 2021), increase in leaf extension rate and increase root porosity (Insausti et al., 2001; Moreno et al., 2023). Plant species in the current study such as *Plantago lanceolata*, *Alopecurus pratensis, Agrostis stolonifera* and *Trifolium repens* (Table 4) are known to be important forage plants for livestock

(Andrews et al., 2007; Martin et al., 2018; Oram et al., 2021; Van Eck et al., 2006). Across Europe, the inclusion of multi-species swards in farm pastures is of growing interest due to benefits for biodiversity and reduced requirements for mineral fertilizers in the presence of nitrogen-fixing species (e.g., *T. repens*; Jaramillo et al., 2021; Baker et al., 2023). Van Eck et al. (2006) observed strong tolerance to winter flooding in *P. lanceolata*, *A. pratensis* and *Rumex* spp. which was attributed to rapid colonisation after winter floods, slow utilisation of stored carbohydrates, and strong shoot elongation responses to submergence, respectively. Oram et al. (2021) showed that conservative carbohydrate utilisation in grasses such as *A. stolonifera* and *A. pratensis* was linked to stronger tolerance to inundation. The persistence of these species across the study site in this study is further evidence for the viability of flood detention basins on farmland for flood peak mitigation. It was beyond the scope of the current study to quantify morphological changes in plant species in response to inundation but based on the observed tolerance to and recovery from inundation in the study, further research under similar field conditions is warranted.

In addition to reducing gaseous transfer and increasing the build-up of oxidative species in plant tissues, flooding has also been shown to impair photosynthesis due to fine solids deposited on leaf surfaces reducing light penetration to plant photosynthetic tissues (Vervuren et al., 2003; Lowe et al., 2010;). In the current study, fine sediments deposited on the surfaces of leaves and leaf damage were evident on plants in the ponding zone following certain inundation events, but it was not possible to directly account for the effect that sediment had on plant health. Lowe et al. (2017) noted that despite the reported negative effects that sediment may have under laboratory conditions, these may be offset by the delivery of nutrients and O_2 to plants under flowing water in natural flood conditions. Puijalon et al. (2007)

observed that inundating plants with nutrient-rich flowing water benefited plant growth, relative to plants submerged under nutrient-poor, slow-moving water. In the current study, flood events led to delivery of substantial loadings of suspended sediment and nutrients such as phosphorus, dissolved organic carbon (DOC) and nitrogen (Chapter 2) The detention basin was shown to attenuate suspended solids and nitrate during flood events, indicating possible enrichment of the surface soil in the ponding zone. Soil chemistry analysis from soil samples collected in the Summer of 2021 (after two inundations) and 2022 (after 10 inundation events), did not indicate higher organic or inorganic nitrogen concentrations in the soil, but elevated concentrations of plant-available P were observed in the ponding zone in 2021 and 2022. The presence of higher concentrations of soil phosphorus in the ponding zone may have resulted from delivery of nutrients via overland flow to the lower part of the field in previous decades. It is possible that the higher soil P or nutrients in the flood water contributed to the boost in biomass observed in the ponding zone in the spring and summer of 2023 (Beltman et al., 2007; Sommer et al., 2023). Morgan's-P concentrations in both the ponding and non-ponding and non-ponding zones were high in 2021 and 2022 (Morgans' P > 8 mg/kg, Soil index 4; Teagasc, 2017). It is unlikely therefore that plants in the ponding or non-ponding zone were P-limited. Increased inputs of other nutrients such as N and DOC would have been more likely to improve growth (Dodds et al., 2004; Graeber et al., 2021). Daly (2005) observed that high soil-P was positively correlated with soluble reactive phosphorus in overland flow samples from the same farm pastures. The soil high P-index of the detention basin of the current may help to explain the increase soluble reactive phosphorus concentrations in waters leaving the detention basin during flood events.

We recommend that further investigations are conducted to elucidate relationships between plant nutrition and natural flooding during peak flows.

3.4.2 Flooding duration and plant stress

Flooding has been shown to induce substantial negative effects on pasture crops in both controlled greenhouse pot-experiments and in field studies. In a pot experiment by McFarlane et al. (2003) waterlogging for 14 to 21 days was shown to cause a reduction in root and shoot biomass, and inhibition of photosynthesis by 30-50% after 28 days of waterlogging. Gattringer et al. (2018) subjected seedlings of meadow plants in pots to inundation of various depths for periods of two or four weeks and observed that increasing duration and depth of inundation negatively affected total biomass, root mass fraction and plant height. Prolonged flooding of farmland in Somerset, England during spring of 2012 damaged pasture crops and drainage systems: bringing about substantial reduction in farm productivity and income (Morris and Brewin, 2014). While negative effects of inundation were observed in the current study, the duration of inundation during the various high-flow events was typically much shorter (mean = 2 days; Chapter 2) than those observed in the studies mentioned above, and most studies on the topic. In a study by Kitanović et al. (2023), species of tufted grass subjected to inundation of various durations showed high tolerance to inundation during winter, which they also attributed to reduced metabolic requirements in plants during winter. They found that plants subjected to 1-15 days of inundation tended to reach similar heights and biomass, with plants exhibiting increasing stress and reduced survival when subjected to longer periods of inundation (15-32 days). The mean peak flow period in their study area during winter was reported to range from 2-14 days. The stronger stress responses exhibited by plants that were inundated for more than 15 days (e.g.

reduction in biomass growth and plant height), may indicate tolerance to typical local winter flood conditions, but reduced survival under exceptional, prolonged inundation. This is further evidence of the tolerance of plants to natural winter flood conditions.

While the inundation of the detention basin in the current study was artificial in the sense that flow into and out of the detention basin was facilitated via bespoke adjustable inflow and outflow structures, it occurred predominantly during winter and only during natural flood peaks. Grass enclosures in the ponding zone were inundated to a maximum depth of 0.6m for approx. 10 hours per event, and at least partially inundated for a mean of 2 days per event as flood water receded. Much of the insight into the effects of inundation on plant survival is derived from laboratory-based experiments which subject plants to much longer inundation periods than occurred in the current study. The responses of farmland vegetation to more *natural* inundation, therefore, are likely to diverge in numerous ways from those described in the wider literature. Important forage species such as Perennial ryegrass (*Lolium perenne L.*) are commonly subjected to waterlogging during winter, and, given their economic importance, understanding their responses to natural flooding is essential (McFarlane et al., 2003).

To mitigate the physiological stresses of flooding, plants which are inundated may respond with strategies known as Low Oxygen Quiescence Syndrome (LOQS) or Low Oxygen Escape Syndrome (LOES), in response to shorter or longer inundation durations, respectively. Under the LOQS condition, plants may exhibit reduced metabolic activity and growth during the period of inundation and return to normal growth when waters recede. Under LOES, plants may alter their morphology while inundated, for example by extending petioles so that photosynthetic tissues may emerge above floodwaters. The latter strategy may increase the vertical height of submerged plants without leading to an increase in overall biomass (Colmer and Voesenek, 2009, Striker and Colmer, 2017). Waterlogging, i.e. the condition of excess water in the root zone, can bring about changes to plant root morphology: mainly via the production of aerenchyma and formation of large adventitious roots systems which can better cope with anaerobic conditions in the soil that arise from waterlogging (Colmer and Voesenek, 2009). In the current study it was not feasible to evaluate what changes seen above-ground plant material compared to the root zone could be ascribed to inundation, saturation or a combination of the two. One reason for this is that it was necessary to take repeated monthly samples of grass from the same sub-plots within the enclosures. Examination of changes to root morphology would have required the digging up of the plants, thus preventing study of regrowth of individual plants over successive months. Due to time constraints, neither was it possible to examine above ground changes in plant morphology in response to flooding but further research should aim to identify the specific responses of important forage crops to natural short-term inundation.

Improved growth in the ponding zone during summer may have been related to greater soil moisture within the ponding zone resulting from the delivery of water during flood events. High temperature and potential evapotranspiration during the period from April – July 2023 may have imposed stress on plants within the study site (met.ie, 2023). NFM features such as the one examined in this study have been advocated to combat hydrological extremes of flooding and drought (Collentine and Futter, 2018; Keesstra et al., 2018) and it is possible that the detention basin had the combined effects of mitigating flood peaks and maintaining high soil moisture during periods of high evapotranspiration rates. Plant health metrics such as RWC and Chl *a*/*b* ratios did not indicate plants in the non-ponding zone were under stress during this, but it is possible that higher soil moisture in the ponding-zone contributed to the observed boost in biomass production during this period. It should be noted that direct assessment of soil moisture was not possible during this study, and that further research should be conducted to help explain the observed increases in summer sward growth in the detention basin.

Another relevant aspect to consider is that stress exposure early in plant life history may have promoted tolerance to subsequent stress. This could be explained as a ‘priming’ mechanism leading to the accumulation of signalling proteins which can be upregulated when further stress is imposed, conferring a competitive advantage to individuals faced with seasonal stresses such as drought or inundation (Walter et al., 2011; Tanou et al., 2012). Wang et al. (2017) found that plants exposed to drought or flooding stress had better tolerance to subsequent exposure to flooding or drought, irrespective of which of those stressors they had been previously exposed to. In the current study, plants in the ponding zone were exposed to flooding in winter of 2021/22 and this could have improved their tolerance to inundation during the winter off 2022/23. Additionally, the improved growth of the grass in the flood zone between April and July 2023 relative to the sward in the non-ponding zone may have resulted from greater tolerance to water-deficit stress during this period, having been subject to flooding in the previous months. High temperature and potential evapotranspiration during the period from April – July 2023 may have imposed stress on plants within the study site, but plants in the ponding zone were potentially more tolerant to this due to *priming* from earlier hydrological stress.

Given the flood peak mitigation that was observed at the study site (mean of 40% peak discharge attenuation; Chapter 2) utilising farm pastures to capture winter flood peaks may be a viable flood mitigation measure. Providing additional storage within catchments may be more important for the attenuation of winter floods than at other times of the year as high water-tables and saturated terrestrial soils in winter reduce available storage volume for flood peaks (Acreman and Holden, 2013; Lockwood et al., 2022c; Roberts et al., 2023). Much of agricultural land is out of production in winter and, as this study has shown, can provide valuable additional storage for flood peaks, without displacing livestock or inducing lasting harm to crops.

3.5 Conclusions

This study found that winter flooding of a grassland field, as part of a ‘nature-based’ flood alleviation scheme, had no negative effect on sward productivity during the summer growing season. There was a greater decline in productivity and sward photosynthetic proficiency in the ponding zone than the non-ponding zone during winter, but this was followed by enhanced production of biomass in the ponding zone when the growing season resumed, to the extent that above-ground biomass per unit area of forage was higher overall in the ponding zone than the non-ponding zone in both summers of 2022 and 2023. Further research into the response of plants to short term inundations under field conditions is recommended so that hydrological extremes in rural catchments can be mitigated, while ensuring that agricultural productivity is maintained.

This study presents a novel but robust methodology for investigating the effects of short-term inundation by stream water on forage plant biomass and photosynthetic activity. The experimental set-up of plant enclosures within an operating farm facilitated long-term data collection of experimental and seasonal environmental data.

Chapter 4:

The impacts of two forms of channel-spanning features on hydraulic storage and nutrient processing under low and high-discharge conditions in a modified agricultural channel.

Abstract

Low-order streams in many rural catchments have been dramatically modified to promote agricultural ever greater productivity and intensification. Stream channels in these catchments are often modified to allow rapid drainage of agricultural land and to reduce the risk of over-bank flows, which may reduce localised flood risk but increase the risk and severity of flooding downstream. Additionally, high loadings of dissolved and particulate organic matter, mineral fertiliser and fine sediment may be conveyed through these catchments from terrestrial agricultural sources such as fields, farmyards and trackways throughout the year. Nature-based solutions (NbS) have been advocated in catchments that have been affected by agricultural activities to help restore the natural hydrological and ecosystem function that have been deleteriously impacted by human activities. This study investigated the role of in-stream NbS features targeting transient storage at both low and high stream flows for the first time. Low-head boulder weirs are applied to increase in-stream hydrological residence times favouring nutrient and sediment retention whereas ‘leaky dams’ are employed to target flood peak reduction. Contrary to expectations, boulder weirs appeared to reduce transient storage during low flows but may have helped to retard flow velocities during higher flows. Peak flow discharges tended to be reduced in the presence of leaky dams. Both the boulder weirs and leaky dams led to streambed scour. The more substantial erosion of streambeds and channel banks around leaky dams is a cause for concern and may negate any benefits they may have on flood peak attenuation.

4.1 Introduction

River and stream catchments have been highly modified by humans to facilitate urbanisation and agricultural intensification in recent decades. The linearisation and deepening of channels in agricultural catchments has enabled the formation of straight field boundaries and trackways and promotes the draining of surface waters from fields (Riley et al., 2018; Rogger et al., 2017). Modification of channels in agricultural areas also involves the removal of instream physical roughness elements such as riffles, gravel bars, boulders and large woody debris (LWD), to reduce hydrological residence times and enhance conveyance of water through channels and limit the risk of over-bank flooding (Poff et al., 1997; Wohl and Beckman, 2014). As a result, peak flows may be conveyed more quickly through straightened and smoothened channels, leading to shorter and higher magnitude flood peaks downstream (Abbe et al., 2019; Dadson et al., 2017; Wohl and Beckman, 2014). These modifications have also impaired the capacity for streambeds to retain sediment and particulate organic matter (POM), and may limit the processing of nutrients at the streambed surface and beneath the streambed surface in the hyporheic zone (Fischer et al., 2005; Graeber et al., 2012; Weigelhofer et al., 2012).

Agriculture is a major contributor to impaired water quality in Ireland and throughout Europe (Environmental Protection Agency, 2022) due to the input of excess nutrients (nitrogen, carbon and phosphorus) and sediment loads from both point and diffuse sources, where low-order streams are particularly vulnerable (Edwards and Hooda, 2008; Harrison et al., 2019). Channel modifications to enhance water conveyance and reduce hydrological residence times can lead to the reduction of natural attenuation processes which serve to mitigate in-stream pollutant loads. Under European Union directives such as the Habitats Directive (Council Directive 92/43/EEC, 1992) Water Framework Directive (CEC, 2000) and the Floods Directive (European Union, 2007) EU member states are required to limit the deterioration of water quality and to mitigate the risks of flooding imposed by natural high-flow events and modifications to stream hydro-morphology. In addition to advocating traditional best management practices and engineering solutions, these legislative frameworks encourage the use of Nature-based Solutions (NbS). NbS are active management measures that seek to use natural hydrological, geophysical or biological processes to mitigate problems of anthropogenic origin (Collier and Bourke, 2020). In the context of catchment management, NbS are implemented to temporarily store floodwater within or without a channel, and allow it to be released more slowly, as streamflow or by infiltration into groundwater, so reducing downstream flood risk, and promoting retention of particulate matter, and nutrient uptake and transformation by stream biota (Heneghan et al., 2021; Lane, 2017; Robotham et al., 2022).

Channel-spanning NbS features such as low-head boulder weirs and 'leaky dams' may promote the retention and biological transformation of sediment and nutrients in agricultural catchments by increasing hydraulic retention times (HRT) and the extent of nutrient attenuation zones on streambeds and in the hyporheic zone (Hester and Doyle, 2008; Hester and Gooseff, 2010). Microbial communities within the hyporheic zone form complex biofilms within the interstices of sediments and gravels (Romani et al., 2016) in which nutrient biotransformation may be favoured (Weatherill et al., 2019). Efforts to enhance the nutrient-processing potential of modified streams may be contingent on adequate characterisation and rehabilitation of key areas of nutrient uptake within and between stream sections (Blaen et al., 2018; Hall et al., 2002). The application of conservative tracer solutions to stream channels can illustrate the hydraulic flow paths and the extent of hydraulic storage in stream channels (Herzog et al., 2018; Mendoza-Lera et al., 2019), while biologically-active tracers may describe nutrient uptake rates by microbial communities within the hyporheic zone and at streambed surfaces (Covino et al., 2010; Hall et al., 2002; Liu et al., 2022). In-stream impediments to flow such as boulder weirs can augment hyporheic exchange flows through the hyporheic zone by increasing the vertical hydraulic gradient in streambeds in the area immediately upstream (Hester and Doyle, 2008). Transient storage occurs where there is a reduction in flow velocity in certain parts of the channel, e.g. within the hyporheic zone, and through hydrological exchange with sediment pore water where water and solute velocities are significantly reduced with respect to average flow (Bencala and Walters, 1983; Harvey and Bencala, 1993). Measuring transient storage in streams can give valuable information about the influence of stream morphology on solute residence times and associated biological and geochemical transformation. Transient storage in the hyporheic zone and on the streambed surface is thought to be an important control on in-stream nutrient processing and attenuation (Gooseff et al., 2004; Herzog et al., 2023; Zarnetske et al., 2011b). To this end, boulder weirs may help to increase both the extent and the duration of contact between dissolved nutrients and microbial biofilms, maximising the potential for uptake and transformation of nutrients (Battin et al., 2003; Brunke and Gonser, 1997; Cunha et al., 2018). By forming upstream backwater zones of slow-moving water, boulder weirs may also enhance transient storage and nutrient transformations at the surface of streambeds (Rana et al., 2017).

The artificial reinstatement of natural channel-spanning large woody debris (LWD), in the form of ‘leaky dams’ has been widely advocated to impede high-flows and reduce peak discharges (Lane, 2017; Metcalfe et al., 2017a). Such measures are designed to mimic the role that natural in-stream woody debris may have on storing water within channels and helping to divert high-flows from channels onto adjacent floodplains (Abbe et al., 2019; Barnes et al., 2023). By increasing channel roughness, leaky dams may also help to delay the onset of downstream flood peaks

(Black et al., 2021; Wenzel et al., 2014). Although modelling and flume studies, and controlled flooding experiments in the field have highlighted the potential of leaky dams to provide a degree of local flood attenuation, their operation during naturally-occurring flood events is less certain, owing to variation in flood peak hydrographs and impaired performance during multi-peak events (van Leeuwen et al., 2024). By impeding high-flows however, leaky dams will inevitably increase the risks of bank and stream-bed erosion, potentially leading to slippage of leaky dams and blockage of downstream structures (Grabowski et al., 2019). There continues to be debate around the ideal design of leaky dams for flood peak mitigation and on their performance over longer temporal scales (Grabowski et al., 2019; Muhawenimana et al., 2021).

Whilst the reintroduction of in-stream geomorphic features in heavily modified streams and rivers is of increasing interest in NbS applications, empirical evidence on their efficacy to mitigate water quality problems and reduce peak flows is lacking, especially over multiple peak flow events (Black et al., 2021; van Leeuwen et al., 2024). This study sought to investigate the potential benefits of two types of low-cost in-stream measures, low-head boulder weirs and leaky dams to promote transient storage at low and high flows in a semi-natural first order stream channel draining an agriculture-dominated catchment. We hypothesize that in-stream, low-head boulder weirs promote downwelling of surface water into the streambed thereby increasing low flow transient storage and pollutant retention, whereas woody debris dams increase transient storage under peak flow conditions. Pre- and post-intervention conservative (i.e. solutes which do not take part in biological processes) and non-conservative (i.e. dissolved nutrients available to biotic uptake/metabolism) tracer applications were conducted to quantify the effects of low-head boulder weirs hydraulic retention times and potential pollutant retention. The impacts of leaky dams on high flows were quantified through comparison of pre- and post-intervention peak discharge hydrographs.

4.2 Methods

4.2.1 Study area

The study site was located within a single farm landholding within the catchment of River Lee, SW Ireland (51°56'09 N 8°52'59W; 150.07 – 146.47m above sea level). The soil upstream of the study site consists primarily of fine loamy soil over sandstone bedrock (Teagasc, 2023). The catchment is comprised of approximately 80% agricultural grassland, with the remaining land dominated by heathland and conifer plantations, with some broadleaf plantations within the farm itself (Environmental Protection Agency, 2018). The area receives an average annual rainfall of 1305 mm (2000 – 2022; met.ie, 2023). At the study site, the stream drains a catchment area of 1 km^2 (Government of Ireland and Tailte Eire, 2023), as calculated by area within the upstream watershed of the stream that flows through the study site.

A 300 m section of an unnamed first order tributary stream was chosen for the installation of a selection of NbS features to test their hydrological and water quality effects. The stream flows through the farm and into the impounded River Lee, approximately 7 km downstream of the study site (Fig. 1). Within the study site, the stream channel has been modified from its natural course over the past approx. 200 years to facilitate the formation of linear field boundaries and trackways, and to enhance drainage of fields. The channel is artificially straightened and deepened, such that there is little overbank flooding during peak flows. In-stream NbS measures were installed in two separate stream sections. Boulder weirs were installed along the upstream section for the study of their effects on transient storage, uptake of dissolved nutrients and retention of suspended solids during low flows (Fig. 1). This boulder weir section was 65 m in length, with a mean channel width of 1.5 m and a mean gradient of 1.1%. The downstream leaky dam section was 120 m in length, a mean width of 2.5 m and a mean gradient of 1.7%. Four structures were installed in each section (Fig. 1).

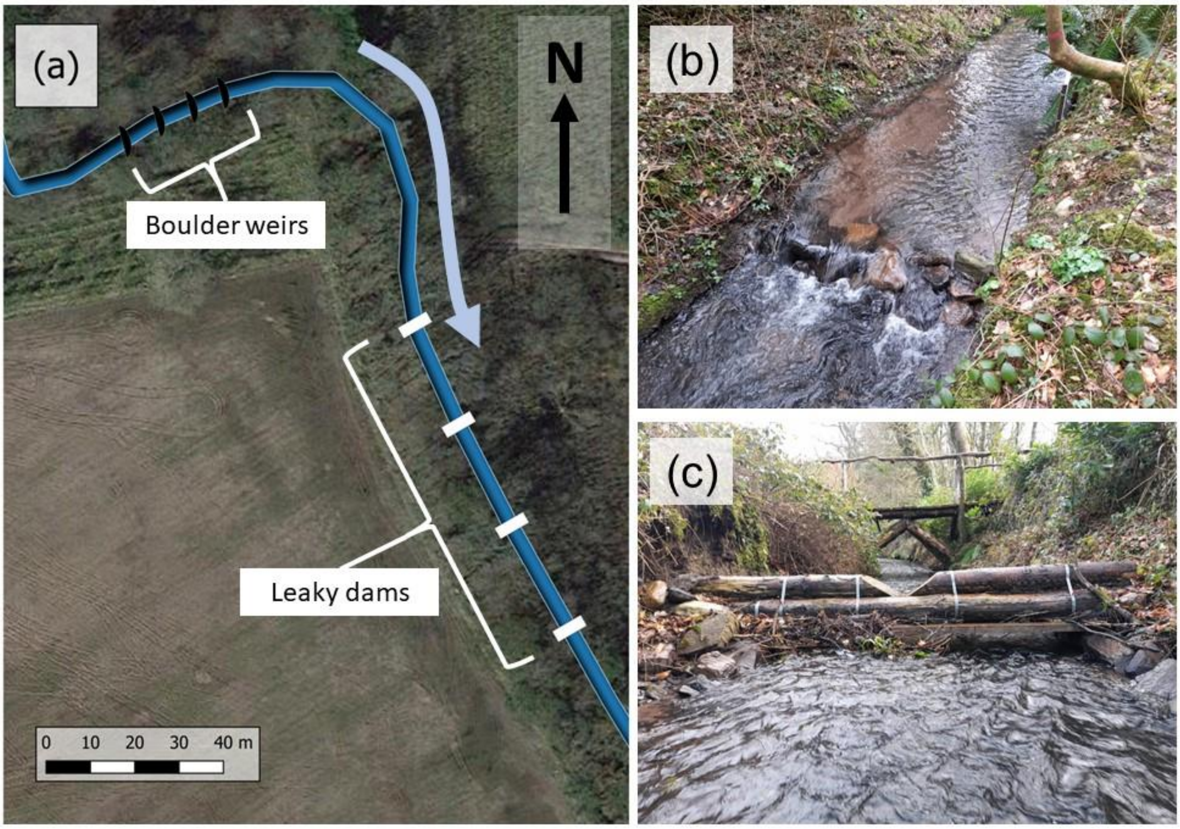

Figure 1 (a) The study reach with boulder weirs indicated by black bars and leaky dams c. 60m downstream indicated by white bars. Blue arrow denotes direction of stream flow. (b) shows a low-head boulder weir viewed from downstream. Note: sediment deposit at upstream left bank due to the formation of an upstream low-flow backwater zone; also fast flowing water is apparent downstream of the weir; (c) shows the most upstream leaky dam during low-flow conditions, viewed from upstream. Not vegetation partially occluding freeboard at left side of leaky dam.

4.2.2 Low-flow features: Low-head weirs

4.2.2.1 Boulder weir construction

In December 2021 low-head boulder weirs were constructed on the streambed from locally occurring boulders (width > 300 mm; Fig. 1b). Weirs spanned the channel, and each reached a height of approx..

0.4m above the stream bed and were slightly lower in the middle to reduced risk of scour at the stream banks (Fig. 1b). The boulder weirs were placed 15m apart and caused water levels to be increased on the upstream side to a distance of approx. 2m. Boulder weirs were installed far enough apart such that a given boulder weir did not cause water to back up as far as the next most upstream weir. This allowed the weirs to function independently but with the aim that they would have a cumulative effect on transient storage, suspended solids retention and nutrient uptake (Rana et al., 2017).

4.2.2.2 In-stream tracer applications

Conservative tracer tests were conducted over the 65m study section using the pulse addition method (Tank et al., 2008) in which a one litre 2.4 molar NaCl solution was introduced as an instantaneous pulse (2-3s in duration) at an ‘injection point’ 12m upstream of an electrical conductivity (EC) logger (CTD-Diver DI272, Van Essen Instruments B.V., Netherlands) laid on the stream bed. A distance of 12m was deemed sufficient to ensure sufficient mixing of the tracer with the stream water before the tracer reached the EC logger (Mason et al., 2012; Tank et al., 2008). A second EC logger was placed at the downstream location and the two were programmed to measure stream EC at a co-ordinated 2-second interval. As the tracer plume passed through the stream, the EC loggers recorded the breakthrough curve (BTC; Fig. 2) of elevated electrical conductivity of the stream. A hand-held conductivity logger (WTW Conductivity portable meter, ProfiLine 3110, Germany) was used to identify the time of upstream and downstream BTCs (beginning, peak and end). The end of the BTC (t_{99}) was taken as the time at which the stream conductivity returned to background conductivity (+/- 0.002 mS cm^{-1}; Fig. 2) (Gooseff et al., 2007; Schmadel et al., 2016).

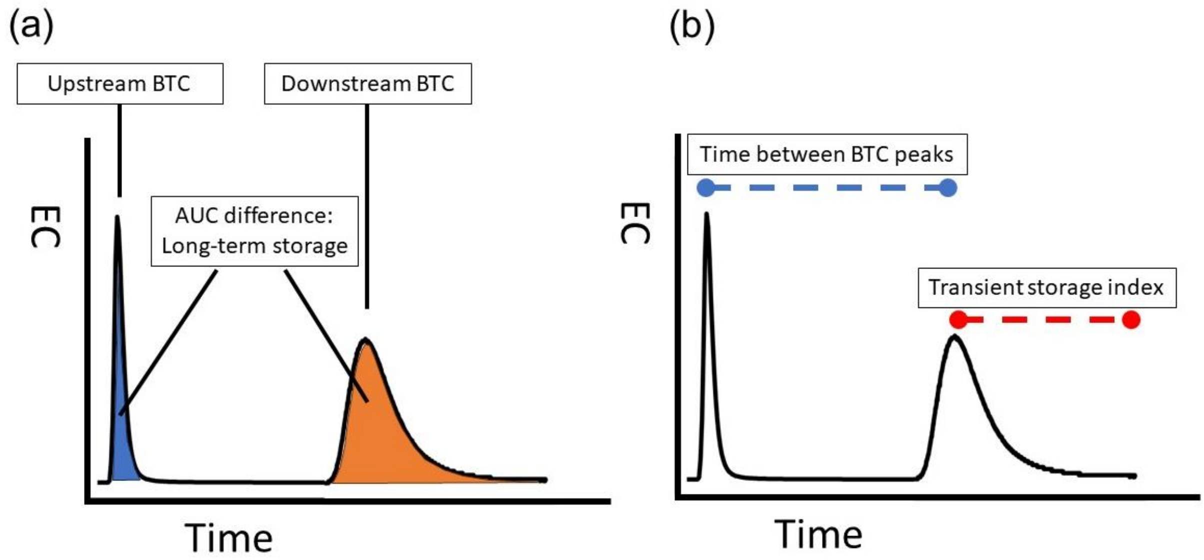

Figure 24 Breakthough curves (BTCs) of electrical conductivity (EC) at upstream and downstream locations along boulder weir stretch of the study site. Fig. 2a indicates methods for calculation of long-term storage of stream solutes as the difference in area under curve (AUC) between upstream and downstream BTCs. Fig. 2b indicates time between upstream and downstream BTC peaks, which is used to calculate modal stream velocity; The transient storage index is calculated as the time from the peak of to the end of the downstream BTC, taking the end as the time at which electrical conductivity returned to within 0.002mS cm^{-1} of baseline electrical conductivity. Distance between point upstream and downstream EC sampling points was 65m.

4.2.2.3 Hydraulic retention analysis

The effects of low-head boulder weirs on hydraulic retention within the section was assessed through comparison of tracer breakthrough curves (BTCs) from conservative tracer tests before and after the addition of the boulder weirs (Fig. 2; Mason et al., 2012; Tank et al., 2008). Analysis on BTCs can describe the potential for streams to store and transform stream solutes and nutrients (Covino et al., 2010). From BTCs produced in conservative tracer tests conducted before (August – December 2021) and after boulder weir installation (January 2022 – September 2022; Appendix 2B, Supplementary Results), three metrics were used to quantify the effects of boulder weirs on hydraulic retention within the reach, (1) long-term in-stream storage, (2) time between BTC peaks and (3) the Transient Storage Index. Long-term in-stream storage, i.e. retention of solutes in the streambed beyond the detection limit of downstream BTCs (*t99*), was quantified through comparison of pre- and post-weir installation changes in BTC area under curve values (g NaCl L^{-1} s^{-1}) between upstream and downstream monitoring points (Fig. 2a; Covino et al., 2010; Gooseff et al., 2007; Mason et al., 2012). A decrease in area under curve (AUC) between upstream and downstream monitoring points may be attributed to loss of tracer to the streambed surface or hyporheic zone, and was quantified using Equation 1 (Cunha et al., 2018; Schmadel et al., 2016; Ward et al., 2013):

1. $$Long - term\ storage = AUC_{us} - AUC_{ds}$$

Equation 1

Where AUC_{us} is area under the curve for the upstream logger and AUC_{ds} area under the curve for the downstream logger. BTC data were corrected for upstream and downstream background electrical conductivity (Cunha et al., 2018). (2) The effects of boulder weirs on transient storage were estimated from hydrologic residence time distribution metrics from BTC data (Mason et al., 2012). These metrics included “time between peaks” (TBP; Fig. 2b; Equation 2) of upstream and downstream BTCs, and a “transient storage index” (TSI; Fig. 2b; Equation 3) for downstream BTCs.

$$TBP = t_{peakDS} - t_{peakus}$$

Equation 2

Where time between peak (TBP) was taken as the time difference between BTC peaks at the upstream (t_{peakUS}) and downstream (t_{peakDS}) locations (Fig. 2b). From TBP, the modal velocity of the tracer over the 65m stretch could be calculated by dividing the distance stretch by TBP (Mason et al., 2012). The inverse modal velocity was also calculated by dividing TBP by 65m to give an estimate of modal residence time of tracer per meter, after Mason et al. (2012).

The transient storage index (TSI; Mason et al., 2012) was calculated using Equation 3 as the time difference between the time of the downstream BTC peak (t_{peak}) and the time of the detection limit of the downstream BTC (t_{99}).

$$TSI = t_{99} - t_{peak}$$

Equation 3

Reactive (slurry) tracer tests were conducted by the simultaneous addition of conservative (2.4 molar NaCl solution) and biologically reactive tracer (i.e. containing dissolved nutrients) at the upstream injection point (Blaen et al., 2018; Weigelhofer et al., 2018b). The effect of boulder weirs on nutrient uptake (e.g., assimilation and transformation) was quantified through measuring percentage changes in AUC values between upstream and downstream BTCs (Fig. 2a) and comparing percentage recovery of soluble nutrients (dissolved organic carbon; ammonium, soluble reactive phosphorus), as well as suspended solids (SS) for pre- and post-intervention tracer tests (Cunha et al., 2018). Percentage change in upstream to downstream AUC values was measured to account for variability in the composition of reactive tracer solutions among tracer test events (Cunha et al., 2018). Reactive tracers consisted of a 1L mixture of stream water and fresh farmyard slurry/silage effluent in a 3:1 v/v ratio applied in a single slug along with 2.4 molar NaCl solution conservative tracer. Surface water samples were collected from the stream in sterile 1L polyethylene bottles prior to tracer additions at the upstream and downstream locations of the boulder weir stretch to provide baseline water quality data. After the conservative and reactive tracers were added upstream, a surface water sample was collected at the time of the upstream BTC peak. Upstream BTCs were too short in duration for multiple samples to be collected over the curve, so the beginning and end of the BTC was assessed from the BTC produced by the upstream EC-logger (Fig. 2 location "A"). 12-15 surface water samples were collected from the downstream location over the course of the downstream BTC. Samples were collected at 15-30 second intervals while conductivity readings on the hand-held in-situ conductivity logger changed more quickly. Intervals between samples were larger after the BTC peak (Cunha et al., 2018). A final surface water sample was collected when the stream conductivity returned to the baseline. Surface water samples were analysed for concentrations of (dissolved organic carbon, ammonium, soluble reactive phosphorus) and suspended solids. Areas under curves from the start to end of the upstream and downstream BTCs for each water quality parameter were quantified, yielding total concentrations of each water quality parameter at upstream and downstream locations (Cunha et al., 2020; Graeber et al., 2012; Weigelhofer et al., 2018b).

Electrical conductivity values and concentrations of dissolved nutrients and suspended solids were corrected against background levels prior to all analyses by subtracting the baseline values from BTC tracer data. The concentration of NaCl contributing to the observed electrical conductivity (EC) of in the BTC data was estimated using equation 4:

$$[NaCl]\ (g\ L^{-1}) = EC * 0.3656$$

Equation 4

Where *EC* is electrical conductivity (mS cm^{-1}) and 0.3656 the conversion factor was calculated by deriving the slope of the line of conductivity following additions of known quantities of NaCl to deionised water in laboratory conditions (Cunha et al., 2018; Tank et al., 2008). Stream discharge (Q) was calculated using the dilution gauging method (after Kilpatrick and Cobb, 1985; Equation 5),

$$Q = \frac{M}{\int_{t_1}^{t_{99}} C(t)dt}$$

Equation 5

in which Q is the stream discharge (L s^{-1}) and M is the tracer mass (NaCl g), and C is the estimated NaCl concentration at time *t* between the beginning and end of the breakthrough curve (t_1 to t_{99}) (Kilpatrick and Cobb, 1985; Mason et al., 2012; Schmadel et al., 2016).

Between August 2021 and September 2022, 16 conservative (n = 7 pre-weir installation; n = 9 post-weir installation) and 5 'reactive' (e.g., NaCl-normalised slurry) (3 prior to weir installation; 2 post-weir installation) tracer tests were conducted on the study reach during baseflow conditions (mean discharge Q = 2 - 140L s^{-1}). No tracer tests were conducted during the 3-week period following boulder weir construction, so the integrity of the boulder weirs under a range of flows could be tested, to allow disturbed sediments to be rinsed from the reach prior to repeating tracer tests (Rana et al., 2017), and to promote development of microbial biofilms ('priming') in hyporheic zone beneath the boulder weirs (Ward et al., 2017).

4.2.2.4 Water quality laboratory analysis

Water samples were collected in sterile 1L plastic bottles from the water column. Bottles were stored in a cool-bag and frozen at -80°C within 6 hours of collection. Samples were analysed for ammonium (NH_4^+- N), soluble reactive phosphorus (SRP; PO_4 - P), dissolved organic carbon (DOC-C), chloride and suspended solids (SS). Methods are described in table 1.

Table 1 Methods for determination of concentration of dissolved nutrients (ammonium, NH_4^+- N; soluble reactive phosphorus, SRP; dissolved organic carbon, DOC) and chloride from surface water samples collected during biologically-reactive tracer tests

Parameter	Method	Method Detection Limit (mg L^{-1})	Relative standard deviation RSD %	Reference
NH_4^+- N	Samples filtered through 0.45µm PVDF membrane filter and analysed by automated salicylate method using the Lachat Quikchem 8000 FIA	0.002	12	Zellweger Analytics, Inc. Milwaukee. USA. Method Code: QuikChem Method 10-107-06-3-D
SRP-P	Determined by automated ascorbic acid method using the Lachat Quikchem 8000 FIA following filtration through 0.45µm PVDF membrane filter.	0.001	5	Zellweger Analytics, Inc. Milwaukee. USA. Method Code: QuikChem Method 10-115-01-1-B
DOC-C	Samples were filtered through GF/C filter paper, then measured by high-temperature combustion method using TOC-VCPH/CPN	0.12	2.22	SHIMADZU
Chloride	Samples were filtered through 0.45µm PVDF membrane filter. Chloride was analysed by ferricyanide method	0.19	7.53	

For measurement of suspended solids, sample water was passed through GF/C filter paper of known mass. Filter paper was dried at 104°C for two hours, then re-weighed. On some sampling occasions electrical conductivity, temperature and dissolved oxygen (concentration and percentage) were measured in-situ using hand-held meters (Electrical conductivity and temperature: WTW ProfiLine Cond 3110, Xylem Analytics, Germany; Oxygen and temperature: OxyGuard® Handy Polaris Hv. 3.15, EU, www.oxyguard.dk). All laboratory analyses were carried out by the Aquatic Services Unit, Environmental Research Institute, University College Cork.

4.2.3 High-flow features: Leaky dams

In July 2021, water level recorders water level recorders (WLRs; *In-Situ Inc. Rugged TROLL® 100*, *USA*) were installed at the upstream and downstream ends of the leaky dams section (Fig. 1a). WLRs recorded water level at 5-minute intervals until November 2023. Following WLR installation, stream discharge gauging was conducted across a range of flows (Peak Q = 125 L s^{-1} – 562 L s^{-1}) at the WLR locations upstream and downstream of the leaky dam section (Fig. 1a). From the discharge measurements flow rating curves were developed to allow discharge estimation from the stream stage time-series data for each WLR location using Equation 6, below (Acreman et al., 2003; Nicholson et al., 2020).

$$Q = ch^d \qquad \text{(Equation 6)}$$

Where Q = stream discharge (m s^{-1}), c and d = coefficients and h = stream stage (m). For further details on discharge and rating curve data and coefficients see Appendix 2A.

Four leaky dams were installed along the section at 25 +/- 5m intervals in May 2022. These were designed to interact with peak flows only (Q > 75 L s^{-1}), with flows below

75 L s^{-1} flowing beneath each leaky dam (Fig 1a, c). The leaky dams were constructed from pine logs which spanned the channel in a pyramidal form and were tethered to a strong frame of timber and pine logs which were braced to each channel bank. These bankside logs were pinned to the streambed and laden with boulders to provide scour protection for the channel banks. The bracing of the transverse logs to the longitudinal logs ensured that the leaky dam was a rigid structure that would move as one if dislodged, reducing the risk of individual logs being washed downstream and posing risk to pipe crossings and culverts. Above the discharge of 75 L s $^{-1}$ flow was partially impeded by each leaky dam as water was forced to back up into the channel until flowing over the leaky dam (Fig. 1c). High-flow events were selected from the time-series data and discharges were calculated to allow comparison of high-flow hydrographs during pre-leaky dam installation high-flow events and those in the presence of leaky dams.

Effectiveness of leaky dams at attenuating peak flows was measured using three widely used metrics: (a) Peak discharge attenuation; (b) peak discharge velocity reduction; and (c) 'peakiness' (i.e. the effect of leaky dams on the shape of flood peaks). These values were compared for flood events before and after leaky dam installation (van Leeuwen et al., 2024).

Peak discharge attenuation (ΔQ_{peak}) was calculated using Equation 7:

$$\Delta Q_{peak} = Q_{peakDS-\, Q_{peak}US}$$

Equation 7

Where Q_{peakDS} is the peak discharge of a given flood peak hydrograph at the downstream WLR location and Q_{peakUS} is the peak discharge upstream of the leaky dams, for the same flood peak. The treatment effect of leaky dams was calculated as the absolute difference (L s^{-1}) and as the percentage difference between upstream and downstream gauging stations (van Leeuwen et al., 2024).

Peak discharge velocity has been utilised as in important metric for quantifying the impact of leaky dams on peak flow rates (Thomas and Nisbet, 2012; Wenzel et al., 2014). Peak discharge velocity was calculated as the time-difference between upstream (T_{peakUS}) and downstream flood peak discharges divided by the distance between upstream and downstream points (110m) for a given flood peak (T_{peakDS}; Equation 8):

$$Peak\ velocity = \frac{T_{peakDS} - T_{peakUS}}{110}$$

Equation 8

The effect that LDs had on the shape of the hydrograph peakiness was calculated using Equation 9 (Wenzel et al., 2014):

$$P = \frac{Q_{peakDS}}{t_{75}}$$

Equation 9

Where *peakiness* (*P*) is the shape of the hydrograph as a function of the peak discharge at the downstream WLR (Q_{peakDS}) and t_{75}: the time during which discharge exceeded the minimum discharge threshold of interaction with a leaky dam (Q ≥ 75 L s^{-1}). Wenzel et al., (2014) observed that leaky dams reduced the period of peak flow discharge with higher flow volumes being reallocated to lower discharges for longer periods. In the current study lower values of P were taken to show leaky dams caused flattening of flood peaks by causing peak flows to for persist longer but with lower peak Q (Wenzel et al., 2014).

Lastly, the natural accumulation of woody debris (leaves, twigs and small branches transported downstream) trapped at the face of the leaky dam, and changes to streambed and bank morphology at leaky dams were monitored visually over the 18 months following leaky dam installation. Accumulation of such woody debris can occlude the leaky dam, effectively turning it into a solid dam, greatly increasing both the hydraulic force on the leaky dam structure itself and the force on the stream bed and stream banks, and so increasing the risk of downstream displacement, or even collapse of the leaky dam (Hankin et al. 2020).

4.2.4 Data analysis

Values were derived for the described metrics for the boulder weir and leaky dam studies for each tracer test or high-flow event, respectively. The treatment effect (pre-installation vs. post-installation) was calculated using analysis of variance (ANOVA) from the dplyr package in the free statistical software R Studio (R Core Team, 2023). Regression analysis was performed to identify effects of discharge (explanatory variable) on conservative tracer BTC metrics (dependent variables: long-term storage, TSI, modal velocity and inverse modal velocity) including status (pre-weir installation or in presence of weirs) as a fixed effect.

In the leaky dam study, the treatment effect of leaky dams was also assessed through analysis on the effect upstream peak discharge (explanatory variable) on the change in peak discharge between upstream and downstream locations (dependent variable) with leaky dam status (flood peaks pre-installation vs. flood peaks in presence of leaky dams) as an additional explanatory variable, using general linear models from the dplyr package in the free statistical software R Studio (R Core Team, 2023). All models were checked for normality by visual inspection of Residual and Q-Q plots of model fit produced by the autoplot function in the ggplot2 package (Wickham, 2016).

4.3 Results

4.3.1 Low head weirs

4.3.1.1 Conservative tracers

The low-head weirs led to a reduction in conservative solute retention within the experiment section. Long-term storage (i.e. solute transient storage beyond the BTC detection limit t_{99} measured as the difference between upstream and downstream AUCs) was significantly lower in the presence of weirs (Table 2). There also was an indication that the tailing effect on the passage of conservative tracer was reduced in the presence of the boulder weirs as the TSI score was decreased by 69% following weir installation, but this effect was not significant (Table 2). Long-term storage and TSI also had lower standard error values during tracer tests in the presence of weirs (Table 2). Modal velocity (i.e. the velocity of the BTC peak along the study section) was significantly lower in the presence of weirs. Standard error values of each metric of long-term storage, TSI and modal velocity were all lower following weir installation (Table 2).

Table 2 Mean pre-installation (n = 7) and post-weir installation (n = 9) and standard error values (in parentheses) for solute storage metrics from conservative tracer studies (column 2, 3) as well as mean and percentage differences (columns 4, 5) between pre-installation and weir tracer studies. Columns 6-8 show summary statistics from ANOVA tables. F-values are on 1 and 14 degrees of freedom. See Appendix 2B for metrics derived for each sampling event.

Metric	Pre-installation	Weirs	Difference	% Difference	ANOVA		
					Mean square	$f_{(1, 14)}$	*p*-value
Long-term storage (g NaCl L^{-1})	4.28 (0.67)	-1.97 (0.62)	6.25	143.03	153.9	5.66	0.0321
Transient storage index (s)	185.47 (19)	55.69 (3.26)	129.78	69.97	115488	3.27	0.0819
Modal velocity (m s^{-1})	2.17 (0.25)	0.677 (0.05)	1.49	68.66	8.8	6.38	0.0242

As can been seen in Fig. 3, each of the derived metrics were strongly affected by stream discharge. There was a significant effect of boulder weirs on the interaction between discharge and long-term storage (Fig. 3a, Table 3). Fig. 3a shows that under low flows, conservative tracer tended to be lost between the upstream and downstream sampling points prior to weir installation, but in the presence of weirs, downstream concentrations of conservative tracer are higher (larger AUC values downstream give negative long-term storage values). Fig. 3b indicates that at low flows, TSI was higher prior to weir installation, but this effect was not significant (Table 3, Fig. 3b). Fig. 3c shows that as stream discharge increases flow velocities increased more during pre-weir installation conservative tracer tests than following weir installation, and this effect was significantly different between pre-installation and post-weir installation conservative tracer tests (Table 3). The inverse modal velocity i.e. residence time per meter, indicates that at low discharges there was higher residence time in pre-weir installation tracer tests, but at higher discharges residence time was slightly higher after weir installation, but the overall interaction between inverse modal velocity, discharge and weir status was not significant.

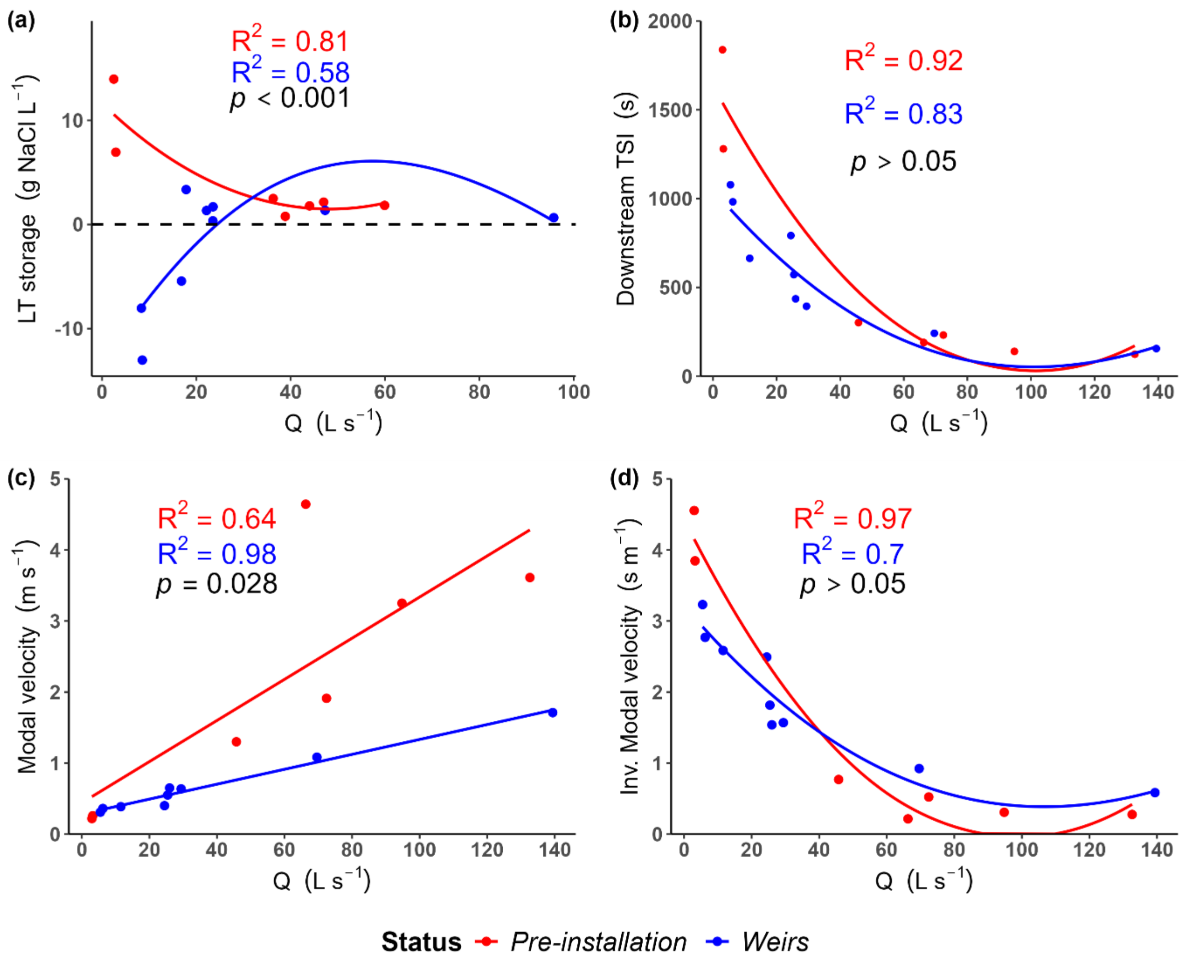

Figure 3 Pre- and post-weir installation (red and blue lines resp.) solute transient storage metrics from conservative tracer breakthrough curves as a function of stream discharge (x-axis; Q L s^{-1}). Fig. 3a shows calculated long-term (LT) storage of NaCl tracer (g L^{-1}) derived from differences between upstream and downstream areas under curves of breakthrough curves (BTCs); positive values denote decrease in upstream-downstream electrical conductivity (i.e. retention of solute tracer), negative values denote increase in stream conductivity along the study sectin. Fig. 3b shows Downstream BTC transient storage index (TSI) as a function of Q (L s^{-1}). Fig. 3c shows modal stream velocity (m s^{-1}) as a function of Q (L s^{-1}). Fig. 3d shows the inverse modal velocity i.e. residence time of solute per meter, as a function of discharge. Regression lines for each group are shown in plots along with R^2 values for the Pre-installation (red) and post weir installation (blue) and the p-value ascribed to significance of difference between groups in regression analysis. Downstream conservative tracer curves can be found in Supplementary Materials, Appendix 2B.

Table 3 General linear model results on the relationship between solute storage metrics, weir-status (pre-installation tracer tests, tracer tests in presence of weirs) and stream discharge. See Appendix 2B for metrics derived for each sampling event.

Metric	Estimate	se	t-value	*p*-value
Long-term storage : weirs	-6.26	2.74	-2.29	0.040
Long-term storage : Q	-0.001	0.06	-0.02	0.985
Transient storage index : weirs	-192.21	174.28	-1.10	0.290
Transient storage index : Q	-8.83	2.00	-4.42	0.001
Modal velocity : weirs	-1.06	0.43	-2.48	0.028
Modal velocity : Q	0.02	0.00	3.91	0.002

4.3.1.2 Biologically-reactive tracers

The composition of biologically reactive tracer solutions was highly variable over the five biological tracer tests (n = 3 pre-installation, n = 2 post-weir installation; Table 4). For example, areas under curves for the upstream BTCs of all water quality parameters (i.e. upstream concentrations of ammonium, soluble reactive phosphorus, dissolved organic carbon, suspended solids) in September 2021 were markedly high than those in September 2022. There was 80 – 90% uptake of ammonium along the stretch in the two September 2021 tracer tests (Table 4). The reactive tracer test conducted in the presence of boulder weirs in April 2022 was under very similar stream discharges to the test conducted on 2 September 2021, but upstream concentrations and percentage uptake were substantially lower. Stream discharge was also quite variable among sampling events (Q = 4 – 82 L s^{-1} Table 4). It is difficult, therefore, to identify effects of the boulder weirs on nutrient uptake and suspended solid retention from the dataset. There was, however an indication that uptake of dissolved nutrients was higher prior to boulder weir installation and that suspended solids retention was increased following weir installation, but no significant effects were identified (Supplementary materials, appendix 1; Table S1).

*Table 4 Areas under curve (AUC) values of water quality parameters (ammonium, dissolved organic carbon (DOC), soluble reactive phosphorus (SRP) and suspended solids (SS); mg L^{-1}) from upstream and downstream reactive tracer breakthrough curves from biologically-reactive tracer tests conducted pre-intervention and post-weir installation in 2021 and 2022, respectively. AUC reduction (column 6) was calculated as the difference between upstream and downstream AUC values. Percentage (%) reduction was calculated as 100 * (AUC reduction / Upstream AUC). Discharge (Q) calculated from breakthrough curves of conservative tracer tests conducted 1 hour prior to biologically reactive tracer tests is shown in column 8 (L s^{-1}). AUC reduction (mg L^{-1} and %) are coloured along a green – yellow – red spectrum to signify degree of nutrient and SS reduction between upstream and downstream locations; Green: Strong reduction; Red Strong increase. Downstream breakthrough curves are available in Supplementary materials, Appendix 2B.*

Status	Date	Parameter	Upstream AUC (mg L^{-1})	Downstream AUC	AUC reduction (mg L^{-1})	% AUC reduction	Q (L s^{-1})
Pre-intervention	02-Sep-21	Ammonium	113.832	26.0875	87.74	77.08	4.3
	21-Sep-21		62.322	5.957	56.37	90.44	6.8
	17-Dec-21		0.36	1.117	-0.76	-210.28	82
	02-Sep-21	DOC	3892.98	924.075	2968.91	76.26	4.3
	21-Sep-21		2126.7	244.485	1882.22	88.5	6.8
	17-Dec-21		7.56	13.47	-5.91	-78.17	82
	02-Sep-21	SRP	51.15	13.191	37.96	74.21	4.3
	21-Sep-21		27.846	2.51	25.34	90.99	6.8
	17-Dec-21		0.288	0.5505	-0.26	-91.15	82
	02-Sep-21	SS	260.4	-3912.1	4172.5	1602.34	4.3
	21-Sep-21		428.4	259.3	169.1	39.47	6.8
	17-Dec-21		-201.6	-497.2	295.6	-146.63	82
Weirs	27-Apr-22	Ammonium	0.63	6.5	-5.87	-931.75	4
	29-Sep-22		-12.201	-29.285	17.08	-140.02	40
	27-Apr-22	DOC	17.15	74.75	-57.6	-335.86	4
	29-Sep-22		13.72	6.3	7.42	54.08	40
	27-Apr-22	SRP	1.225	-0.915	2.14	174.69	4
	29-Sep-22		2.303	0.6	1.7	73.95	40
	27-Apr-22	SS	301	705	-404	-134.22	4
	29-Sep-22		367.5	72.5	295	80.27	40

4.3.2 Leaky dams

Peak discharge values from high-flow events show that prior to leaky dam installation, peak discharges tended to increase along the section (Table 5).

Following the installation of leaky dams, the percentage difference between upstream and downstream peak discharge was reduced significantly (Table 5). Peak flow velocity attenuation during peak discharge was not found to be affected by leaky dams (Table 5). There was no apparent effect of leaky dams on flood peak peakiness in the analysis (Table 5).

During pre-intervention high-flow events peak discharges tended to increase between upstream and downstream locations, indicating a change to peak hydrograph shape along the reach, or addition of water to the system from ephemeral drains during high flow events (Table 5). As can be seen in Fig. 4, as upstream peak discharge increased, downstream peak discharge values increased ($p = 0.0367$; Table 5), and this effect was significantly stronger following the installation of leaky dams ($p = 0.0439$; Table 6 Fig. 4). Tables of leaky dam flood peak metrics for all events can be found in Appendix 2B, Table S2B4 and Table S2B5. Discharge hydrographs for all analyzed pre- and post-leaky dam installation high-flow events are shown in Appendix 2B, Fig. S2B3, S2B4.

Table 5 Mean pre-installation (n = 6) and post-leaky dam installation (n = 9) and standard error values for flood peak attenuation metrics (column 2, 3) as well as percentage differences (column 4) between pre-installation and weir tracer studies. Columns 4-7 show summary statistics from ANOVA tables. F-values are on 1 and 26 degrees of freedom. See Appendix 2B for metrics derived for each sampling event.

Analysis	Pre-intervention	Leaky dams	% Difference	Sum square	*f*-value $_{(1,13)}$	*p*-value
Peak Q change (Δ L s^{-1})	-35.6	-1.44	104	4199.8	4.36	0.0569
Peak Q change (%)	-39	-2.92	92.5	4700.2	5.22	0.0397
Peak velocity attenuation (Δ m s^{-1})	3.64	6.67	-58.78	33.06	0.37	0.5552
Peakiness (L s^{-2})	0.00212	0.00521	-84.31	0.00002541	0.41	0.5320

Table 6 Results from analysis on effect of upstream peak discharge on peak discharge attenuation during pre- and post-leaky dam installation high-flow events. df = 12; R^2 = 0.4018; $F_{(2, 12)}$ = 5.702. See Appendix 2B for event data.

	Estimate	SE	t-value	*p* - value
Peak Q reduction pre-intervention (Δ L s^{-1})	0.69	0.2845		
Peak Q reduction : Leaky dams(Δ L s^{-1})	31.78	14.12	2.25	0.0439

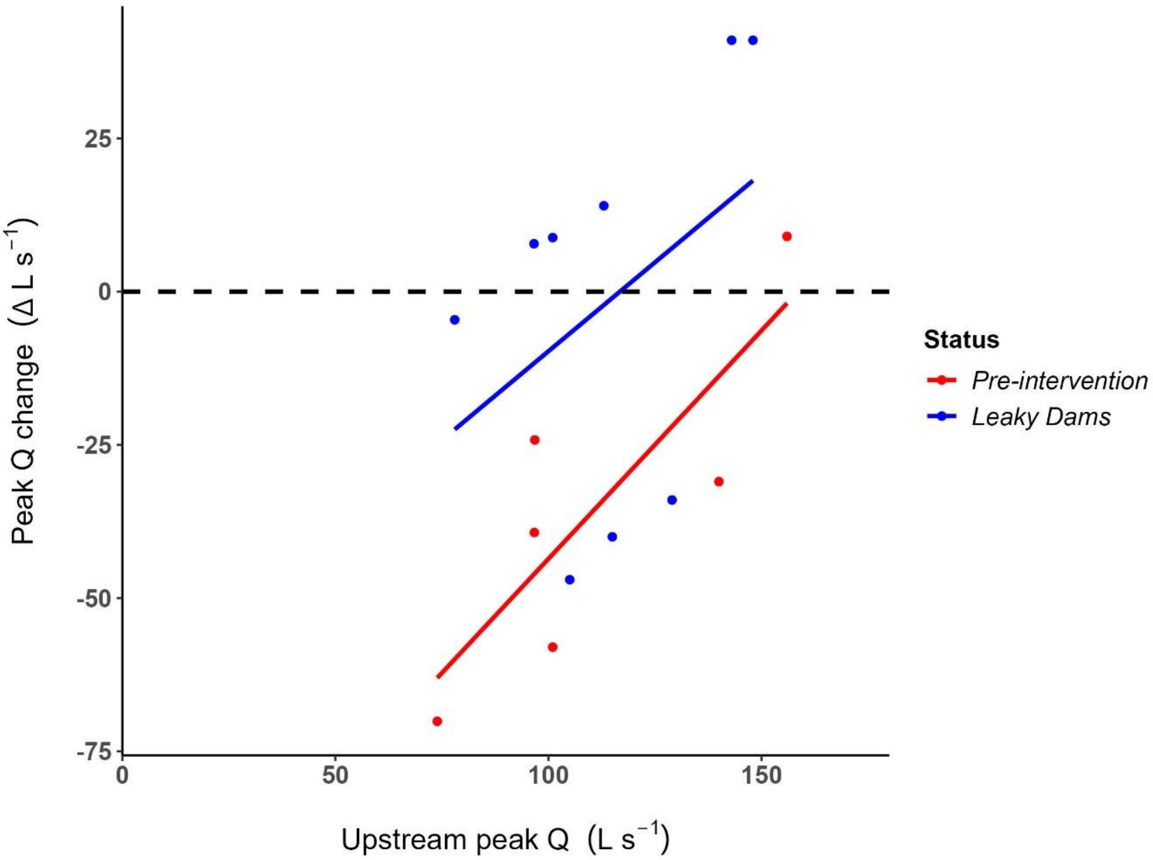

Figure 4 Change in peak discharge (Q) between upstream and downstream monitoring points of leaky dam section as a function of upstream peak discharge pre-intervention (No leaky dams; red line) and post-intervention (Leaky dams; blue). Positive y values (Peak Q change) indicate that peak discharge is reduced between upstream and downstream locations; negative values indicate higher peak discharge at downstream location.

4.4 Discussion

4.4.1 Effects of weirs on geomorphology and hydraulic retention

The significantly lower long-term storage and TSI values following weir installation, as well as lower variability of those metrics among events (lower post-weir installation standard error values), indicate that conservative tracer solutions travelled along the study section in a shorter and more confined pulse in the presence of weirs, and therefore spent less time interacting with the streambed surface or hyporheic zone than was the case prior to weir installation (Mason et al., 2012). Prior to weir installation, water depth and velocity were observed to be relatively uniform across the channel and along the length of the reach. During low discharges, the pattern of flow was consistently turbulent over the shallow, stony surface of the streambed. Following weir installation however, the reach was characterised by deeper, slower velocity backwater zones extending approx. 3m upstream of each weir, and faster-velocity zones extending approx. 2m downstream of each weir (Fig 1b). In effect, the boulder weirs appeared to reduce the extent of shallow turbulent flow over the length of stream section in which they were installed. In a study investigating the changes to transient storage resulting from the re-alignment of a stream channel to its historic route, Mason et al. (2012) found that tracer tests conducted in restored channels had lower tailing effects relative to pre-restoration tests, indicating a reduction in transient storage in restored channels. They attributed stronger pre-intervention tailing behaviour, and therefore greater transient storage, to the greater presence of channel roughness elements, relative to depth, in the shallow pre-restoration channels.

Stream discharge had a pronounced effect on solute storage metrics (Fig. 3). It is clear from the long-term storage and transient storage index metrics (Fig. 3 a, b) that as discharge increased, transient storage reduced. Schmadel et al., (2016) observed that stream discharge had a stronger influence over the shape of tracer breakthrough curves than geomorphic properties of study reaches, to the extent that variance in discharge may mask the effects of geomorphic structures on transient storage. It is noteworthy from Fig. 3a that at low discharges there was retention of conservative tracer (positive long-term storage values) during pre-intervention tracer tests, while there was an increase in solute concentration (negative long-term storage values) in the presence of weirs. This indicates that prior to weir installation, solute retention was higher along the reach during low flows. In the presence of weirs, however, areas under curve values of BTCs appears to increase between upstream and downstream monitoring points. One reason for this may be that streambed material containing organic matter was being eroded from the high-flow zones downstream of each weir and caused elevated conductivity (Fig. 1b).

Weirs were found to reduce modal velocities of BTCs (Table 2) and this effect was consistent at increasing velocities (Table 3; Fig. 3c, d). This suggests that, despite apparently reducing transient and long-term storage, the weirs reduced flow velocities and mediated the effect of increasing discharge. A similar observation was made by Mason et al. (2012) in which modal velocity was significantly lower following restoration of a modified channel back to its natural course. As was concluded by Mason et al. (2012), higher pre-intervention modal velocities in the current study may have been related to the low height of channel roughness elements (streambed gravels and stones) relative to stream height. At low flows transient storage may have been greater prior to weir installation due to consistent, shallow, rippling flow over streambed gravels. In this manner, weirs may be viewed more as high-flow attenuation structures than structures which may enhance long-term or transient storage. This finding may have important implications for NbS practitioners aiming to improve nutrient uptake in agricultural streams using features like those studied here.

Rana et al. (2017) observed that weirs reduced hydrodynamically-driven hyporheic exchange and lower uptake velocities of ammonium and SRP. This was attributed to a combination of a reduction in the volume of gravels sections downstream of weirs, due to scour, and to short hydraulic retention time in the fast flowing zones immediately downstream of weirs. Their study also found, however, that the backwater zones upstream of weirs facilitated greater hydrostatic transient storage, due to vertical pressure to the hyporheic zone from the overlaying water in the backwater zone, which may have facilitated slower nutrient transformation processes such as denitrification. Overall, Rana et al. (2017) found that weirs decreased the reach-scale nutrient uptake and hydraulic retention and suggested that for weirs to benefit water quality, the increases in hydrostatically-driven transient storage upstream of weirs must compensate for the loss of hydrodynamically-driven transient storage from the shallow gravel sections of amended reaches. Conversely, Cunha et al. (2018) observed that increases in cross-sectional area of the backwaters upstream of weirs increased the net transient storage and capacity for the stream to remove or transform nutrients. Results from the current study do not indicate that weirs contributed to greater transient storage and, but instead may have impaired transient storage along the reach through a combination of reducing the extent of transient storage areas through scour, and by reducing the duration of contact between solutes from the water column and gravels on and beneath the streambed.

Agriculture is known to increase the risk of clogging of streambeds through the emission of fine sediments from field surfaces and trackways (Kasahara et al., 2006; Melland et al., 2018). The study conducted by Cunha et al. (2018) was performed in a catchment with low-background nutrient levels and they, and others (e.g., Covino et al., 2010; Weigelhofer et al., 2018a) have noted that changes in transient storage and nutrient uptake in streams are strongly influenced by catchment practices such as agriculture, and associated effects on nutrient and sediment flux. Weigelhofer et al., (2018a) further found that high loadings of fine sediments and organic matter in agricultural catchments were associated with reduced hyporheic exchange. In their study, nutrient uptake from the water column to the hyporheic zone was shown to have been impaired by the layer of P-rich sediment at the streambed surface which limited further P-adsorption from the water column to the streambed. In the current study, deposition of sediment became evident soon after weir installation on the upstream side of the boulder weirs where flow velocities were lower (Fig. 5). Sediment accumulations in these backwater zones reached approx. 50% the height of the boulder weirs within four months of weir construction. This deposited sediment may have hindered flow through streambed gravels and occluded epilithic nutrient uptake processes (Brunke, 1999), further reducing the extent of transient storage zones in the study section. In the current study, it is likely that the effects of factors such as discharge, the composition of the biologically reactive tracer and the background nutrient and sediment concentrations overwhelmed any effects the boulder weirs may have had on improving nutrient uptake.

It is apparent that the formation of backwater zones upstream of weirs may compound any negative effects of the loss of downstream transient storage zones if POM and sediment deposition hinder flow through the hyporheic zone (Fig. 5). Hydraulic conductivity is a vital attribute of hyporheic exchange and the issue of siltation and colmation in weir backwaters has been considered in designs such as BEST (Biohydrochemical Enhancement Structures for Streamwater Treatment) structures, designed to enhance hyporheic exchange and improve nutrient uptake and pathogen removal (Herzog et al., 2016). Herzog et al. (2016) observed that the risk of upstream colmation was reduced as the BEST structures did not dramatically reduce upstream stream velocities via impoundment of waters behind weirs. Instead, contiguous longitudinal pressure gradients through the hyporheic zone ensured flow of water from stream through hyporheic gravels. This improved hydraulic conductivity was contingent on the re-engineering of the hyporheic gravels (Boulton, 2007; Herzog et al., 2018).

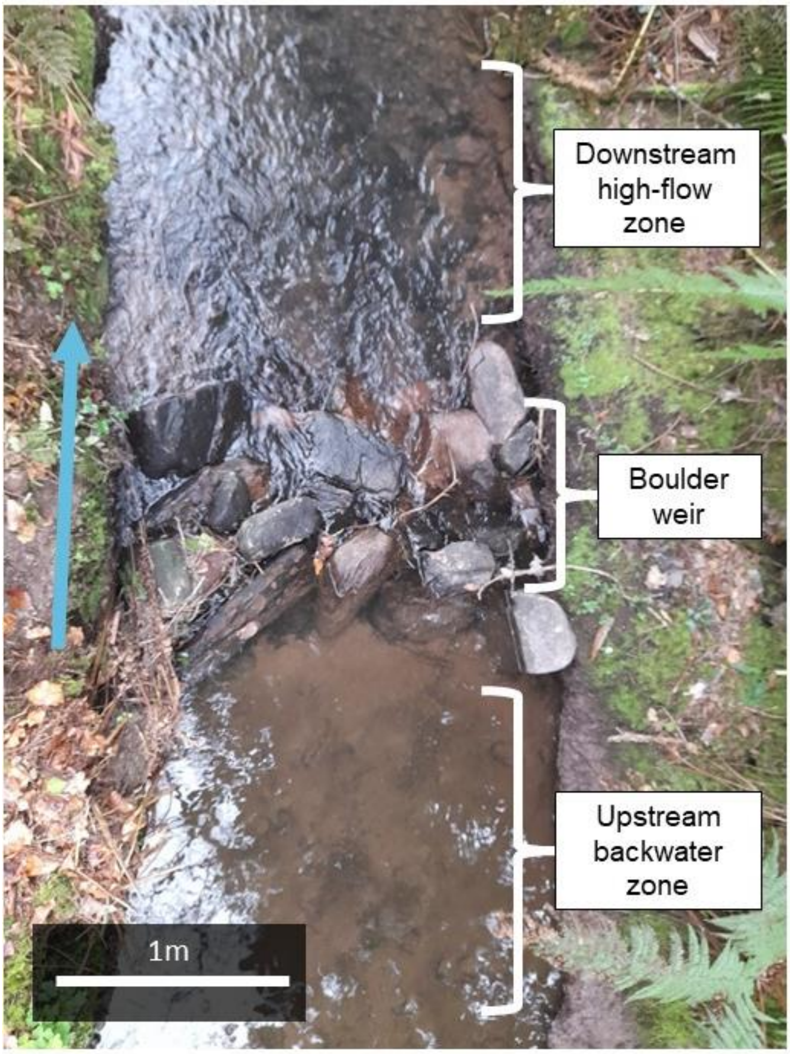

Figure 5 Boulder weir 3 months after construction with sediment deposition evident in the upstream back water zone. The streambed downstream of the boulder weir is relatively clear of sediment due to high flow derived from the hydraulic gradient from upstream to downstream of the boulder weir. Blue arrow indicates direction of stream flow. Scale of 1m is shown at bottom left.

While designs such as BEST have been shown to achieve substantial improvements in water quality, it has been noted by numerous authors that discharge variability and consequent variability in sediment flux and scour-deposition processes under different flow conditions may confound the effectiveness of in-stream measures for hydraulic retention and hyporheic exchange over longer spatial and temporal scales (Herzog et al., 2018; Hester and Doyle, 2008; Magliozzi et al., 2018). Additionally, enhancing transient storage and nutrient uptake through hyporheic rehabilitation may require levels of intervention beyond the capabilities or intention of most NbS or stream restoration projects.

Pander et al. (2015) noted that the use of any hard structure, such as boulder weirs, will inevitably induce localised scour and consequent mobilisation and downstream deposition of fine sediment. Given the high SS and POM loadings present in agricultural catchments (Graeber et al., 2012; Weigelhofer et al., 2018a) the potential for boulder weirs to illicit appreciable benefits to water quality may be limited if they contribute further to localised deposition of fine sediments. In the current study fine sediment was deposited upstream of all weirs, including the most upstream weir, suggesting that much of the sediment was derived from upstream of the study reach. Given the high load of suspended solids in the study catchment, it is likely that boulder weirs may have reduced hydraulic conductivity in the hyporheic zone by inducing deposition of fine sediments in backwater zones.

In a study by Salant et al. (2012) in-stream grade-control structures which were installed to improve conditions for native Redband Trout and other aquatic fauna reduced overall channel hydro-morphological diversity by creating backwater zones and scour pools devoid of gravels. They concluded that efforts to enhance or restore hydrologically or ecologically impaired stream-systems with simple modifications are likely to encounter unintended consequences due to a combination of continued inputs of stresses from upstream, and the complexity of geomorphic and biological conditions which affect stream communities. Hester et al. (2009) noted that while weirs may induce ecologically significant changes to streambed surfaces, their role on influencing the hyporheic zone is contingent on the presence of coarse streambed gravels through which water can flow. Additionally, local groundwater hydrostatic gradients and channel slope are known to exert strong influence over the degree of hyporheic exchange (Covino et al., 2010; Zarnetske et al., 2007) Through being recently modified from their natural course, streams in agricultural catchments may lack the necessary hydro-geomorphological conditions necessary to facilitate hyporheic exchange. In the absence of meaningful flow through the hyporheic zone it may be surmised that much of the transient storage that occurred in our study reach prior to weir construction was occurring at the streambed surface, and that processes of siltation and scour induced by the weirs reduced the extent of transient storage zones and nutrient processing potential in the reach. The negative effects of the reduction in hydraulic retention in fast-flowing zones downstream of the weirs are likely to have been compounded by the reduction in gravels in these zones due to scour – further reducing the potential for transient storage and microbial uptake of nutrients. Results from this study and those of Rana et al. (2017) and Weigelhofer et al. (2018b) indicated that the degree of channel modification and high nutrient and sediment loading in common agricultural channels may preclude any benefits from simple geomorphic alterations to channels, such as the installation of boulder weirs.

4.4.2 Leaky dams

While analyses of peak discharge metrics during pre- and post weir installation high-flow events showed that peak discharges were lower in the presence of leaky dams (Table 4), discharge hydrographs from these events illustrate the substantial variation the shape of hydrographs from high flow events (Fig. 6). Some high flow events occurred with a sudden increase in discharge (e.g., the peak on 7th September 2022, Fig. 6c), while others occurred within multi-peak events when inter-peak discharges were already high (e.g., 30th December 2021; Fig. 6b). The observation that peak discharges were attenuated by leaky dams in the current study is promising, but examination of hydrographs indicates that high-flow events are typified by more than just peak discharge values. As can be seen in Fig. 6c and Fig. 6d, there does not appear to be any change to the trajectory of the rising limb of flood peaks as discharge passes the threshold at which leaky dams were found to impede high flows.

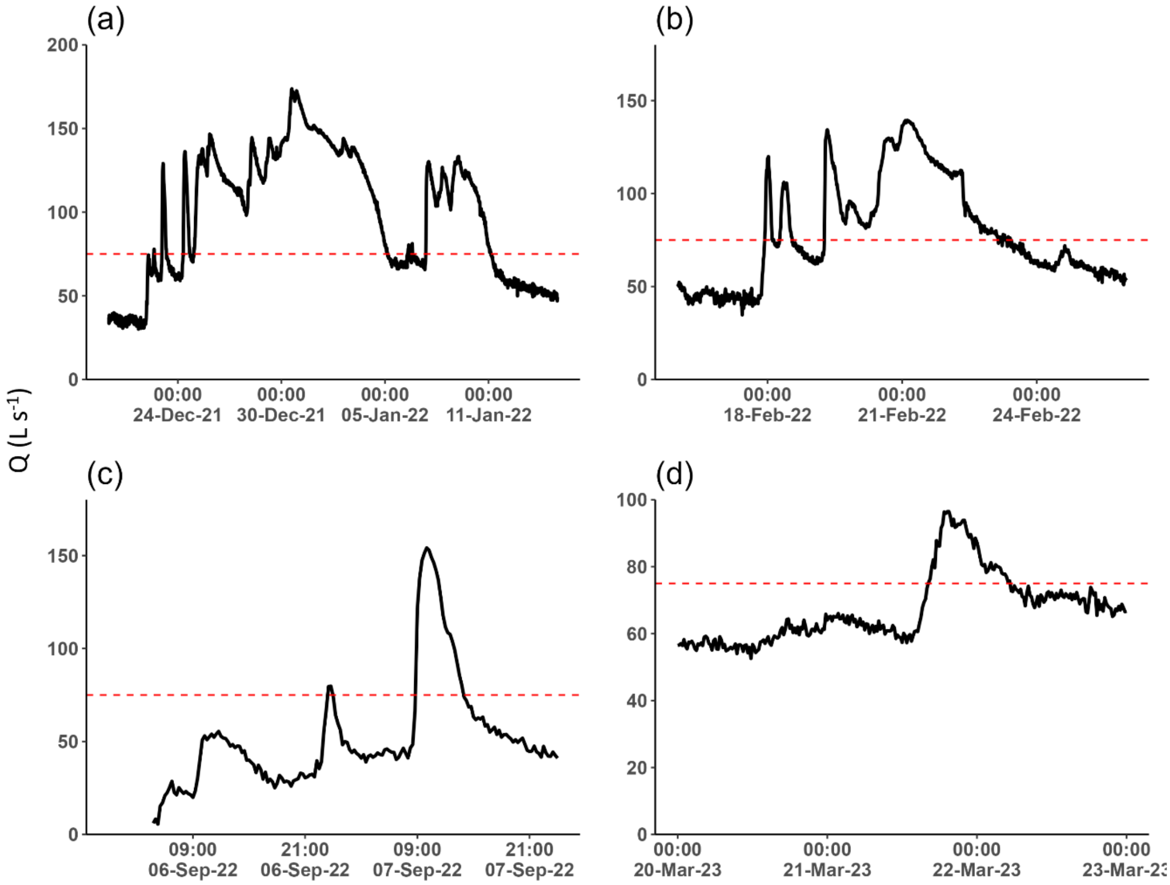

Figure 6 Hydrographs of high flow events pre-intervention (a-b) and in the presence of leaky dams (c-d). Discharge Q (y – axis) is given in litres per second (L s^{-1}) and time and date are shown on the x-axis of each hydrograph. The red dotted line indicates the discharge threshold (approx. 75 L s^{-1}) at which stream flow begins to be intercepted by leaky dams.

Van Leeuwen et al. (2024) showed that leaky dams brought about peak attenuation by a mean of 10% in flood events with a recurrence interval of < 1-in-1 year. Floods of higher magnitude, however were less affected by leaky dams. This was attributed to the fact that available storage volume upstream of leaky dams is depleted during the rising limb of large storms, such that leaky dams have no effect on peak discharges. Leaky dams in the study by Van Leeuwen et al. (2024) were shown to have greater potential for peak attenuation during single peak events, or in the initial peak of multi-peak events, than during multi-peak events. These findings are significant as large multi-peak events are those which are most likely to cause downstream flooding (Gordon et al., 2013; Morris and Brewin, 2014). Due to the lower sample size of the current study, it was not feasible to identify peak attenuation differences between single and multi-peak events before and after leaky dams installation, but in a parallel study, some multi-peak flood events dramatically limited the effectiveness of NFM features (Chapter 2). Indeed, the high-flow event which overwhelmed the flood detention basin in that study was not the event with the highest peak discharge over the study period, but was a flood peak following prolonged rainfall and high inter-peak discharges. As was observed by van Leeuwen et al. (2024), flood attenuation features will have limited effects on flood peak attenuation when space for storing more water has been filled, be it within the channel or within offline features such as flood detention basins, and this is likely to occur in large and multi-peak events.

Some studies have illustrated that leaky dams may attenuate floods by enhancing connection to floodplains during high-flow events either by connecting directly to floodplains or by helping to raise water-levels over larger scales and enhancing the potential for passive over-flow from channels to floodplains (Abbe et al., 2019; Barnes et al., 2023; Keys et al., 2018). While the use of leaky dams in this manner may allow attenuation of higher-magnitude flood peaks, it necessitates substantially higher land-take than would be the case if leaky dams are used simply for in-channel storage. It has been argued that the appeal of leaky dams as natural flood management (NFM) measures is the lower land-take and simplicity of design compared to other NFM measure such as flood-detention basins (Calder, Reid, 2003; Forbes et al., 2015; Grabowski et al., 2019). A major barrier to NFM, generally, is the concern that appreciable attenuation of floods that may impact downstream towns and cities would require NFM to operate across large scales – precluding, or altering agricultural practices in upper parts of catchments (Barnes et al., 2023; Grabowski et al., 2019).

While modelling studies can suggest the effects that structures like leaky dams may have across large spatial scales and high-flow conditions, they are inherently simplified and cannot fully predict how these measures would function in the real world (Addy and Wilkinson, 2019). The hydrographs of events examined in the current study and that of van Leeuwen et al. (2024) were highly variable in shape and peak discharge compared to those illustrated in modelling or less *natural* studies (Thomas and Nisbet, 2012; Wenzel et al., 2014). Further empirical evidence on the impacts of leaky dams on flood events is warranted, given the variable nature of flood events and the fact that storm events which impose social or economic harm on downstream settlements are typified by high inter-peak discharges, as well as by high peak discharges (Gordon et al., 2004).

Modelling and empirical studies such as those by Black et al. (2021) and Wenzel et al. (2014) respectively, showed that leaky dams may attenuate flood peaks by delaying the onset of downstream flood peaks. This may be an important aspect of flood mitigation in steeper areas of catchments where offline volumetric storage, such as on floodplains, is limited. Delaying flood peaks may help to desynchronise the flood flux in neighbouring tributaries, to the effect that the flood peak at lower elevations of the catchment is reduced (Metcalfe et al., 2017b). Peak desynchronisation has not been illustrated empirically, however, and there is also a risk that simultaneous delays to flood peaks across a catchment may be as likely to lead to synchronisation of flood peaks as de-synchronisation (Metcalfe et al., 2017a; Pattison et al., 2014). This study did not identify any effects of leaky dams on the onset of downstream flood peaks but the small spatial scale of the current study may have limited our ability to detect the changes observed in larger studies such as Wenzel et al. (2014).

Investigation into the effectiveness of leaky dams over large spatial scales is a major barrier quantifying their effects and advocating their use in the public realm. Numerous barriers to leaky dam implementation were highlighted by Grabowski et al. (2019). These included uncertainty around leaky dams' effects on geomorphology, the potential for slippage of LWD and consequent risk to downstream areas, and the effects that leaky dams may have on fish-passage and aquatic habitat. Changes to local- and reach-scale geomorphology are an inherent consequence of the increased resistance to flow following installation of in-stream structures (Hankin et al., 2020). Leaky dams may delay or reduce flood peaks by holding water back at the upstream side and this has two obvious consequences: decrease in water velocities upstream and increase in velocities through and downstream of leaky dams. Upstream accumulation of woody debris and sediment, and downstream scour and transport of gravels and sediment further natural consequences of in-channel LWD (Janes et al., 2017; Grabowski et al., 2019; Cooper et al., 2021). In the current study, streambed scour and upstream deposition of sediment occurred at all boulder weirs and leaky dams. Over a discharge threshold of approx. 80 L s^{-1}, most of the stream flow in the weir section passed over the boulder weirs, such that erosional processes around boulder weirs during high discharge events were likely to have diminished with increasing discharge. In the leaky dam section, however, flow began to be impeded by leaky dams above this threshold of 80 L s $^{-1}$ (i.e. the discharge at which the stream level reached the underside of a leaky dam) and continued to back up against the leaky dam until discharges increased to the point of flowing over the leaky dam (Q > 200 L s $^{-1}$). The erosional forces around the leaky dams were highest, therefore during this range of discharges (Q 80 – 200 L s^{-1}). This is the period of a flood peak when leaky dams are likely to be most effective at attenuating flow. Van Leeuwen et al. (2024) observed that leaky dams had an attenuating effect on peak flows at discharges of 400 – 500 L s^{-1}, but at increasing peak discharges their effect diminished, with evidence that at discharges of approx. 1500 L s^{-1}, peak discharges were attenuated more during pre-intervention high-flow events. In the current study, the observed peak discharges were lower than in the study by van Leeuwen et al. (2024) with maximum peak discharge being approx. 150 L s^{-1} (Fig. 4). Leaky dams may have had an attenuating effect on low to medium magnitude high-flow events such that they conferred maximum impediment to flow within a range of discharges, above and below which more stream flow passed under or over the leaky dams, respectively. The erosional forces around the leaky dams were highest, therefore during this range of discharges (Q 80 – 200 L s^{-1}). It was within this region of discharge that leaky dams were shown to bring about higher attenuation of peak flows (Fig. 4), suggesting that flood peak attenuation and increased erosion risk are coincidental. Certain design changes may be considered to mitigate the effects of erosional forces around leaky dams, such as the use of ‘living’ leaky dams, i.e. using living trees rooted in the stream banks to limit bank erosion (Wilkinson et al., 2014) or the incorporation of offline storage areas onto which water diverted by leaky dams from the channel may be stored (van Leeuwen et al., 2024).

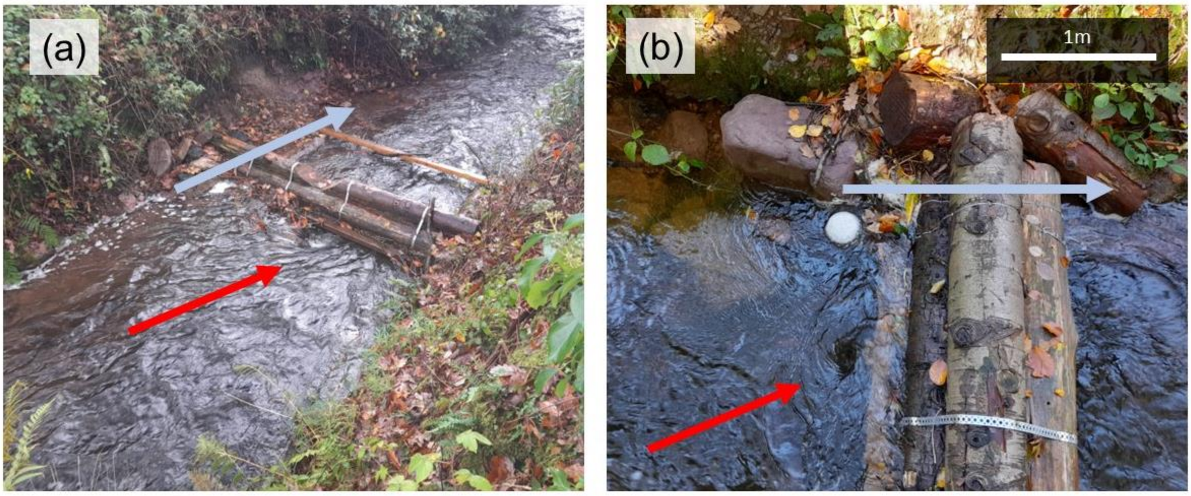

Figure 7 Photographs of leaky dams with red arrows indicating locations of streambed scour induced beneath leaky dams. Blue arrows indicate direction of stream flow. Partial blockage by woody debris of the most upstream leaky dam (Fig. 7a) causes downwelling and high flow velocities through the freeboard beneath the leaky dam. High flow conditions in Fig. 7b cause eddying of water on the upstream side of the leaky dam and consequent localised erosive forces on the streambed. 1m scale is shown at top right of Fig. 7b.

In a series of flume experiments investigating the flood peak attenuation potential of various leaky dam designs, Muhawenimana et al., (2021) found that leaky dams which more comprehensively occluded the stream channel brought about the greatest flood peak attenuation. Streambed erosion occurred at each of the four leaky dams. Substantial bank erosion occurred at the most upstream leaky dam (Fig. 7) and streambed erosion and high-flows during a storm event in October 2023 caused the most downstream leaky dam to be displaced 2m downstream (Fig. 8). The integrated 'sled' design and construction of the leaky dam prevented the structure from disintegrating and logs moving chaotically further downstream (Hankin et al., 2020). Unsurprisingly, all leaky dams were more effective at holding water back when woody debris collected at the upstream side (Fig. 7a), but this increased the erosive forces on the bank and the bed of the stream at each leaky dam. Additionally, strong vortices were seen at leaky dams during medium to high discharges when stream water was impounded by leaky dams but water levels were high enough to pass over the transverse logs (Fig. 7b).

Figure 8 View from downstream of leaky dam displaced approx. 2m downstream during storm event in October 2023

The erosion of channel banks in human-dominated landscapes can have severe consequences such as undermining of roads and buildings, and delivery of LWD sediment downstream – posing risk to culverts, bridges and buildings (Grabowski et al., 2019). Hankin et al. (2020) expressed concern over the introduction of leak dams in series in channels due to the risk of ‘cascade failure’ in which leaky dams installed within a contiguous channel section successively fail during a flood event. It is also presumed, however, that as the number of flood mitigation features in a catchment is increased, the greater their impact on peak discharges will be (Black et al., 2021; Forbes et al., 2015; Hankin et al., 2020). While conferring some flood peak attenuation, this study echoes the view taken by Hankin et al. (2020) in that the utmost care in the design and placement of leaky dams within the catchment should be taken to reduce the risks imposed by leaky dam failure to downstream communities.

4.4.3 The role of in-stream NbS measures

Nutrient transformation and hyporheic exchange are the products of multiple features of the hydro-morphological and biological make-up of the stream and its environs. Stream channels in agricultural catchments have lower geomorphological diversity and higher loadings of sediment, and particulate and dissolved nutrients than those in less human-dominated landscapes. It may be necessary to make numerous amendments simultaneously so that the conditions required for nutrient uptake can be established. Additionally, it is likely that weirs may reduce transient storage and nutrient uptake potential of agricultural channels through altering sediment scour and deposition processes. The case is similar for leaky dams: increases in sedimentation and scour due to localised changes in flow velocities around leaky dams may offset any benefits they have on peak flow attenuation. The less leaky the leaky dam, the more effective it can be at attenuating flood peaks, but decreased leakiness will confine flows and increase their erosive power (Muhawenimana et al., 2021), and in turn increase the risk of leaky dam failure (Hankin et al., 2020). The observation that both the boulder weirs and leaky dams in the current study helped to attenuate high flows is a promising result, but locating in-stream flood attenuation structure in incised channels where high-flow cannot flow over banks, will invariably cause localised erosion of channel banks and streambeds. Such geomorphological effects of in-stream structures are likely to increase as features age and gradually accumulate/liberate more sediment (Addy and Wilkinson, 2019; Wohl and Beckman, 2014). Whether these changes would make the features more effective at water quality or flood management is unclear, but it is likely that the accumulation of woody debris and erosion of streambed and banks during high flow events will put downstream structures at risk when leaky dams fail. Positioning such hydraulic retention structures in parts of catchments where high flows may be directed to offline storage areas may bring about appreciable flood mitigation, especially if combined with offline flood detention structures or afforestation (Barnes et al., 2023; Roberts et al., 2023).

4.5 Conclusions

This study identified some intriguing effects of in-stream features on hydraulic storage in a modified channel. Low-head boulder weirs may enhance transient storage and nutrient uptake velocities in certain situations but it is clear from this study that streambed substrate and discharge exert stronger effects than localised changes to hydraulic gradients over the streambed. Moreover, in modified channels in agricultural catchments, the presence of high background nutrient and sediment loadings may further limit hydraulic storage and hyporheic exchange. Both boulder weirs and leaky dams may help to reduce the flux of water at higher discharges and increases to hydraulic roughness, through the installation of channel-spanning features on a catchment scale, may bring about appreciable flood protection for downstream settlements. Given the inevitable scour and movement of woody debris and sediment that results from in installation channel-spanning features, however, such amendments may not be compatible with agricultural practices common to much of the upper catchments of Ireland and the UK.

4.6 Appendix 2A – Supplementary methods

Table S2A1 Data from flow discharge gauging sessions at the water level locations upstream of the leaky dams (LDs) and downstream of the LDs between 2020 and 2023. Discharge was derived from the sum of stream velocities per unit wetted area at 10 – 20cm intervals. Total wetted area and mean velocities for each sampling event are shown in columns 6 and 7. Wetted area and stream velocity values on certain dates were unavailable at all locations so discharges were based on nearby water level recorder locations.

Location	Date	Stream width (m)	Depth (m)	Discharge Q (L s^{-1})	Wetted area (m^{-2})	Mean velocity (m s^{-1})
Upstream of LDs	26-Nov-20	2	0.13	36.00	0.19	0.37
	16-Dec-20	2.2	0.16	78.64	0.27	0.56
	10-May-21	1.1	0.12	5.55	0.10	0.13
	21-May-21	1.6	0.17	24.02	0.19	0.20
	08-Jul-21	0.9	0.10	3.44	0.07	0.10
	02-Nov-21	2	0.24	54.07	0.31	0.28
	07-Jan-22	1.8	0.23	56.34	0.24	0.40
	08-Sep-22	1.1	0.16	18.85	0.13	0.26
	01-Nov-22	2.2	0.29	128.85	0.42	0.56
	28-Dec-23	NA	0.23	80.00	NA	NA
Downstream of LDs	26-Nov-20	2	0.07	37.09	0.18	0.41
	16-Dec-20	2	0.14	71.70	0.25	0.58
	10-May-21	1.8	0.05	9.71	0.07	0.27
	21-May-21	2.2	0.11	28.31	0.15	0.39
	08-Jul-21	1.6	0.05	4.45	0.05	0.15
	02-Nov-21	2.2	0.14	64.21	0.24	0.54
	08-Sep-22	2.2	0.07	21.04	0.12	0.36
	01-Nov-22	NA	0.18	135.58	NA	NA
	28-Dec-23	NA	0.14	80.00	NA	NA

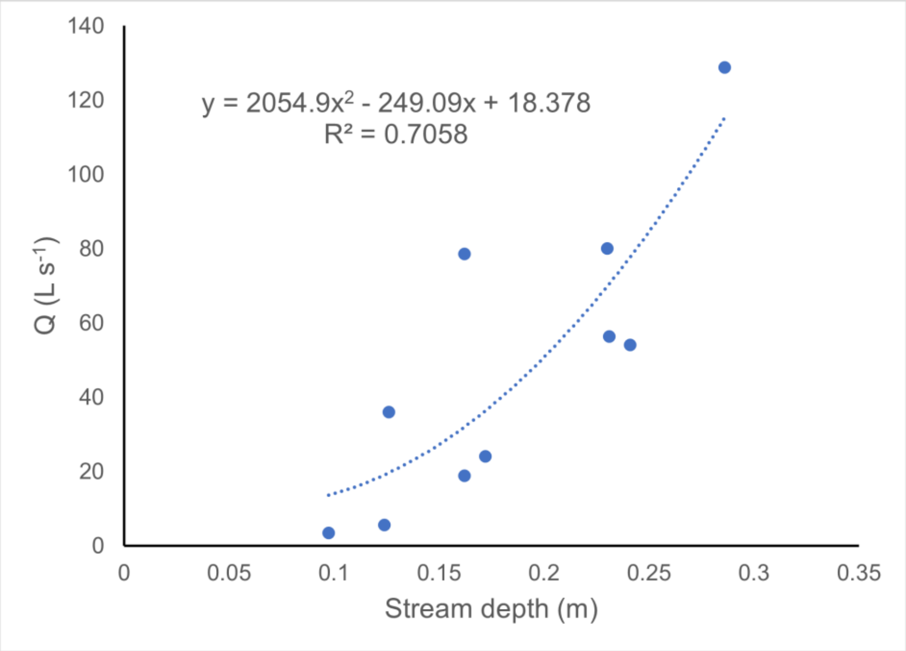

Figure S2A1 Flow rating curve for the water level recorder location upstream of the leaky dams, derived from stream discharge (Q; L s^{-1}; y-axis) and stream depth (m; x-axis) during ten instances between 2020 and 2023 (Table S2). Line of best fit equation and associated R^2 value are shown within the figure (derived in excel).

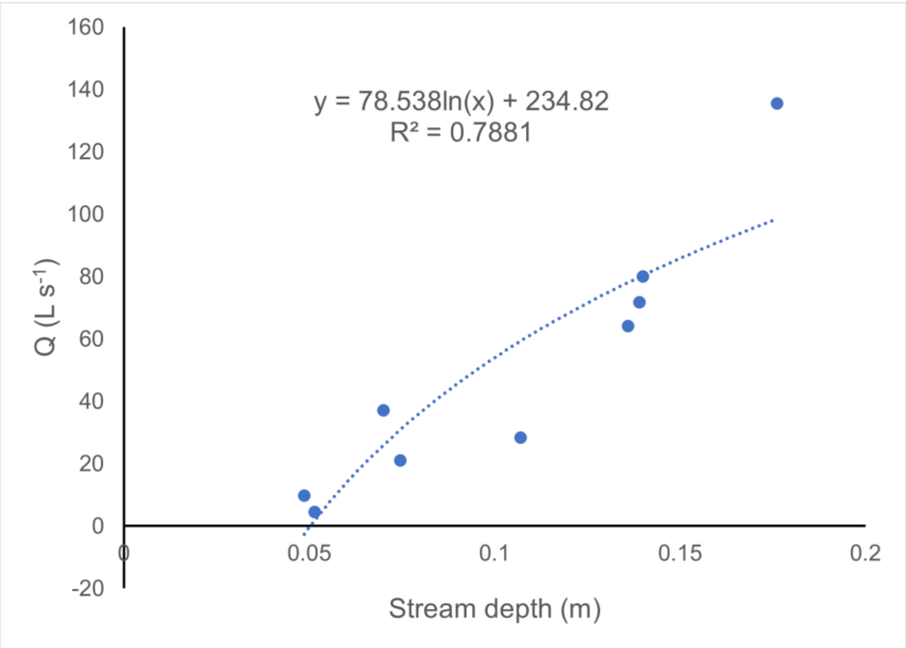

Figure S2A2 Flow rating curve for the water level recorder location downstream of the leaky dams, derived from stream discharge (Q; L s^{-1}; y-axis) and stream depth (m; x-axis) during ten instances between 2020 and 2023 (Table S2). Line of best fit equation and associated R^2 value are shown within the figure (derived in excel).

4.7 Appendix 2B - Supplementary results

Table S2B1 Area under curve values derived for upstream and downstream breakthrough curves in conservative tracer tests. AUC values are derived from the increase in stream conductivity following the application of 200g of NaCl. Conductivity increase above the baseline for each 2-second time interval was multiplied by 0.3656 to give concentration of NaCl. Curve was integrated to give area under curve of NaCl. Tracer loss (g NaCl and % AUC change) is referred to as long-term storage i.e. loss of conservative tracer to the streambed system beyond the detectable limits of the downstream breakthrough curve.

Status	Date	Upstream AUC (g NaCl)	Downstream AUC (g NaCl)	Tracer loss (g NaCl)	% AUC change
Pre-intervention	19/08/2021	80.77	69.97	10.79	13.36
	27/08/2021	68.59	61.64	6.94	10.12
	08/10/2021	4.55	2.76	1.79	39.27
	28/10/2021	3.34	1.51	1.83	54.84
	15/11/2021	5.51	3.02	2.50	45.28
	19/11/2021	5.15	4.37	0.78	15.11
	15/12/2021	4.34	2.11	2.23	51.33
Weirs	19/01/2022	4.23	2.87	1.36	32.05
	15/03/2022	2.09	1.43	0.65	31.30
	30/03/2022	8.50	6.80	1.70	19.99
	04/04/2022	9.03	7.70	1.34	14.81
	25/04/2022	11.22	7.87	3.35	29.87
	13/05/2022	11.88	17.33	-5.44	-45.77
	26/05/2022	24.01	32.05	-8.04	-33.50
	08/06/2022	23.44	36.48	-13.03	-55.60
	29/09/2022	8.52	8.17	0.35	4.10

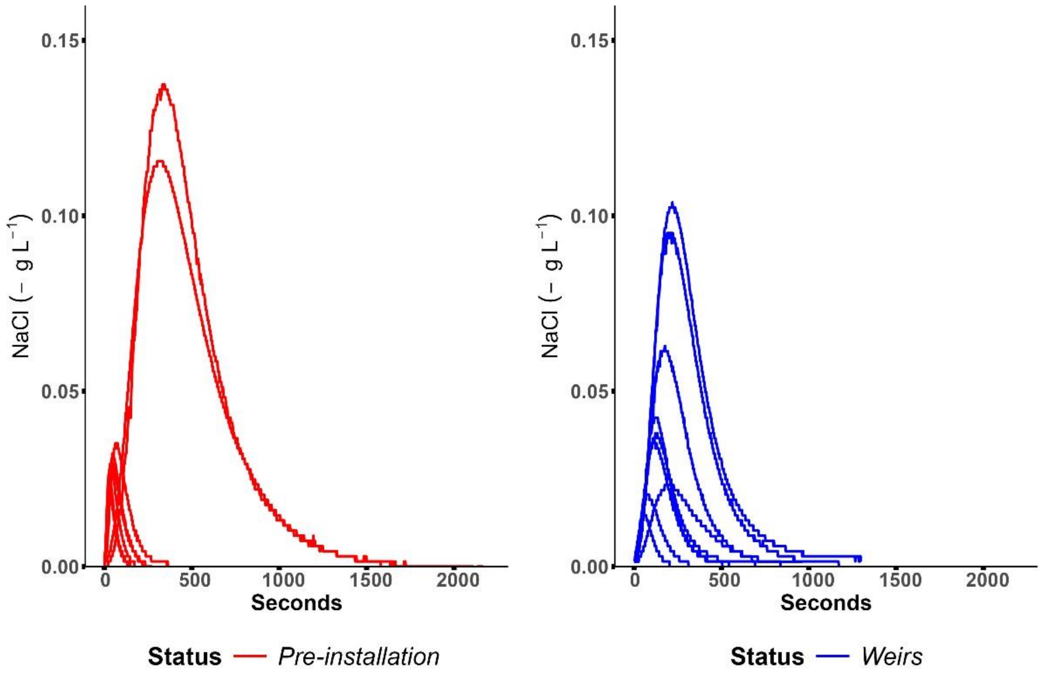

Figure S2B1 Breakthrough curves at the downstream location from conservative tracer tests.

Table S2B2 Time of upstream and downstream BTC peaks and the end of the downstream BTC curve ($t99_{D/S}$) used to calculate the modal velocity and transient storage index of BTCs in conservative tracer tests. Data are given for tests prior to weir installation (Pre-installation) and post weir-installation (weirs)

Date	Status	Peak us time	Peak ds time	$t99_{D/S}$	Time between peaks (s)	Discharge (L s^{-1})	Modal Velocity (m s^{-1})	TSI (s)
19/08/2021	Pre-installation	11:51:28	11:56:24	12:27:02	296	2.99	4.55	1838
27/08/2021		11:31:36	11:35:46	11:57:06	250	3.24	3.85	1280
08/10/2021		12:33:44	12:34:18	12:38:10	34	72.44	0.52	232
28/10/2021		15:29:38	15:29:56	15:32:00	18	132.65	0.28	124
15/11/2021		16:18:02	16:18:16	16:21:26	14	66.29	0.22	190
19/11/2021		13:28:06	13:28:56	13:33:58	50	45.75	0.77	302
15/12/2021		12:59:22	12:59:42	13:02:02	20	94.78	0.31	140
19/01/2022	Weirs	11:47:12	11:48:12	11:52:14	60	69.60	0.92	242
15/03/2022		13:14:32	13:15:10	13:17:46	38	139.41	0.58	156
30/03/2022		16:36:28	16:38:10	16:44:44	102	29.40	1.57	394
04/04/2022		13:40:16	13:41:56	13:49:12	100	25.99	1.54	436
25/04/2022		12:46:40	12:48:38	12:58:10	118	25.42	1.82	572
13/05/2022		11:13:28	11:16:16	11:27:20	168	11.54	2.58	664
26/05/2022		13:19:46	13:22:46	13:39:08	180	6.24	2.77	982
08/06/2022		14:30:16	14:33:46	14:51:44	210	5.48	3.23	1078
29/09/2022		11:38:34	11:41:16	11:54:28	162	24.49	2.49	792

Table S2B3 Background electrical conductivity-corrected uptake of water quality parameters over 65m study reach pre-installation and post-installation of boulder weirs. Uptake values in columns 2 and 3 describe difference between upstream and downstream AUC values: positive values imply uptake along the study section; negative values imply higher downstream concentrations.

Water quality parameter (mg L^{-1})	Pre-intervention mean uptake (mg L^{-1})	Weirs mean uptake (mg L^{-1})	% Difference	Mean uptake difference (mg L^{-1})	Sum square	F(1, 3)	p
Ammonia	6.91 (3.45)	-11.5 (5.85)	37.6	18.4	406.45	3.47	0.159
DOC	189 (116)	-1069 (471)	162	677	1898331	5.045	0.11
SRP	2.88 (1.31)	-6.89 (2.68)	29.5	9.78	114.75	5.767	0.0957
SS	-340 (187)	3475 (2563)	-10.9	3135	11794570	1.315	0.335

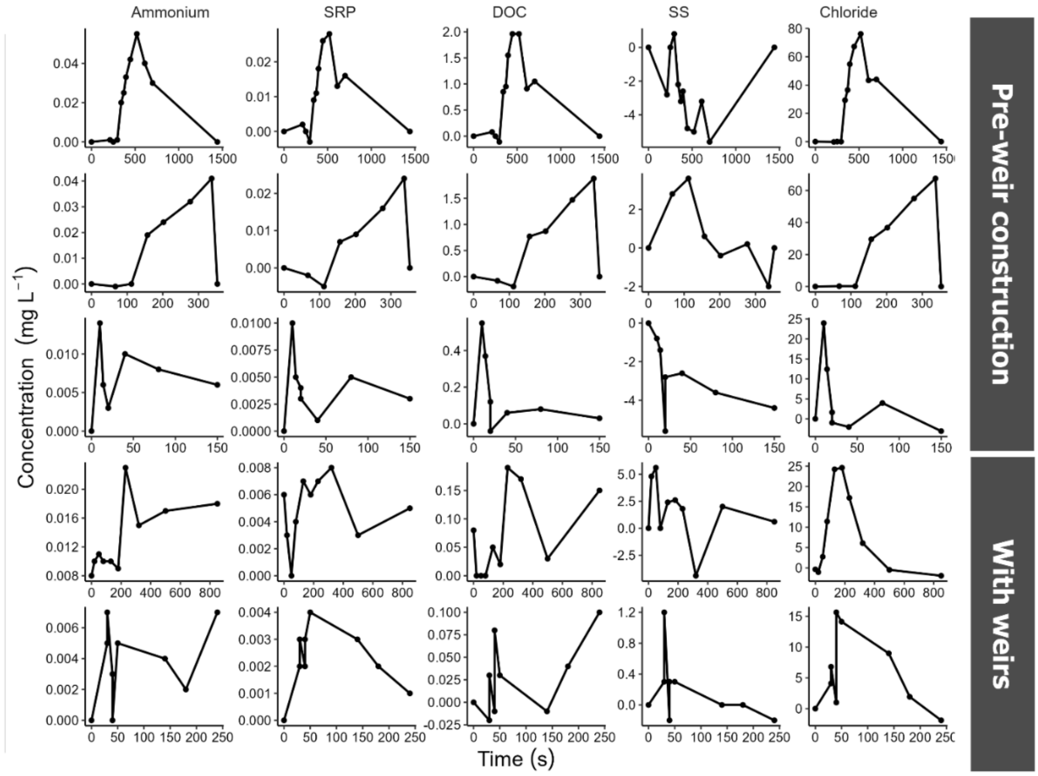

Figure S2B2 Bio-tracer breakthrough curves at the downstream location during the tracer tests with biologically active tracer pre-weir construction (2nd Sept 2021, 21st Sept 2021, 17th Dec 2021) and in the presence on boulder weirs (27th April 2022, 29th Sept 2022). Concentrations for quality parameters are given as Ammonium-N, soluble reactive phosphorus-P (SRP), dissolved organic carbon-C (DOC), suspended solids (SS), and chloride. Time since initial pulse of water quality parameter is shown on x-axes, concentration of each water quality parameter is given in mg L^{-1} on the y axes.

Table S2B4 Flood peak metrics from leaky dam (LD) section from flood events (high-flow events with peak discharges > 75 L s^{-1}) during the pre-leaky dam period and in the presence of leaky dams (LD status). Metrics of flood peaks are given for upstream (U-S) and downstream (D-S) locations. Discharge (Q) is presented in L s^{-1}. Leaky dam backup column shows observations made during high flow events at leaky dams which aided in identifying discharge at which water backed up against leaky dams.

Event date	LD status	U-S peak time	D-S peak time	Time difference (min)	U-S peak Q (L s^{-1})	D-S peak Q (L s^{-1})	Peak Q difference (L s^{-1})	Peak Q difference (%)	Water backup	Leaky dam backup
07/12/2021	Pre-leaky dam installation	06:25	06:20	-5	140	171	-31	-22.14	no	NA
30/12/2021		14:55	14:40	-15	156	147	9	5.77	no	NA
18/02/2022		00:30	00:30	0	96.8	121	-24.2	-25.00	no	NA
19/02/2022		07:45	08:00	15	96.7	136	-39.3	-40.64	no	NA
09/03/2022		10:40	11:10	30	101	159	-58	-57.43	no	NA
17/04/2022		11:10	11:25	15	73.9	144	-70.1	-94.86	no	NA
24/06/2022	Leaky dams	11:40	11:45	5	105	152	-47	-44.76	yes	LD 1 blocked, full
07/09/2022		10:25	10:05	-20	115	155	-40	-34.78	yes	LD 1, LD 3, LD 4 full to lip
11/09/2022		08:50	09:10	20	129	163	-34	-26.36	yes	LD 1-3 full to lip
02/11/2022		10:35	11:05	30	143	102	41	28.67	yes	LD 1, LD 3, LD 4 full to lip
10/01/2023		15:25	16:00	35	101	92.2	8.8	8.71	yes	LD 1, LD 3, LD 4 full to lip
13/03/2023		03:05	03:05	0	96.6	88.8	7.8	8.07	yes	not observed
21/03/2023		18:45	18:55	-170	113	99	14	12.39	yes	not observed
30/03/2023		23:50	00:20	30	148	107	41	27.70	yes	LD 3, LD 4 full to lip
12/04/2023		12:20	12:20	0	78	82.6	-4.6	-5.90	yes	not observed
		Mean no leaky dams		7			-35.60	-39.05		
		Mean leaky dams		-8			-1.44	27.26		
		Mean difference		14			-34.16	-66.31		

Table S2B5 Table of flood peak metrics from downstream of leaky dam section used to calculate flood peak 'peakiness' i.e., the degree to which flood peaks were flatted by leaky dams. Peakiness was calculated as the peak discharge above the interaction threshold (the discharge at which water backed up against leaky dams) divided by the duration of this period. Larger values imply a flatter flood peak.

Status	Peak date and time	Peak discharge ($L\ s^{-1}$)	Peak above 75 $L\ s^{-1}$ ($L\ s^{-1}$)	Peak duration over 75 $L\ s^{-1}$ (s)	Peakiness
No leaky dams	07/12/2021 06:20	170.80	95.80	22500	0.0043
	18/02/2022 00:30	120.97	45.97	16800	0.0027
	18/02/2022 09:00	107.72	32.72	24900	0.0013
	19/02/2022 08:00	135.58	60.58	41400	0.0015
	09/03/2022 11:10	159.12	84.12	80700	0.0010
	17/04/2022 11:25	144.27	69.27	36300	0.0019
Leaky dams	24/06/2022 11:45	151.84	76.84	2400	0.0320
	07/09/2022 10:05	155.16	80.16	18600	0.0043
	11/09/2022 09:10	162.72	87.72	15600	0.0056
	02/11/2022 11:05	101.71	26.71	86400	0.0003
	23/11/2022 01:00	173.55	98.55	280800	0.0004
	10/01/2023 16:00	92.21	17.21	57900	0.0003
	13/03/2023 03:05	88.84	13.84	6600	0.0021
	21/03/2023 18:55	99.00	24.00	47100	0.0005
	21/03/2023 18:55	99.00	24.00	47100	0.0005
	12/04/2023 12:20	82.63	7.63	6300	0.0012

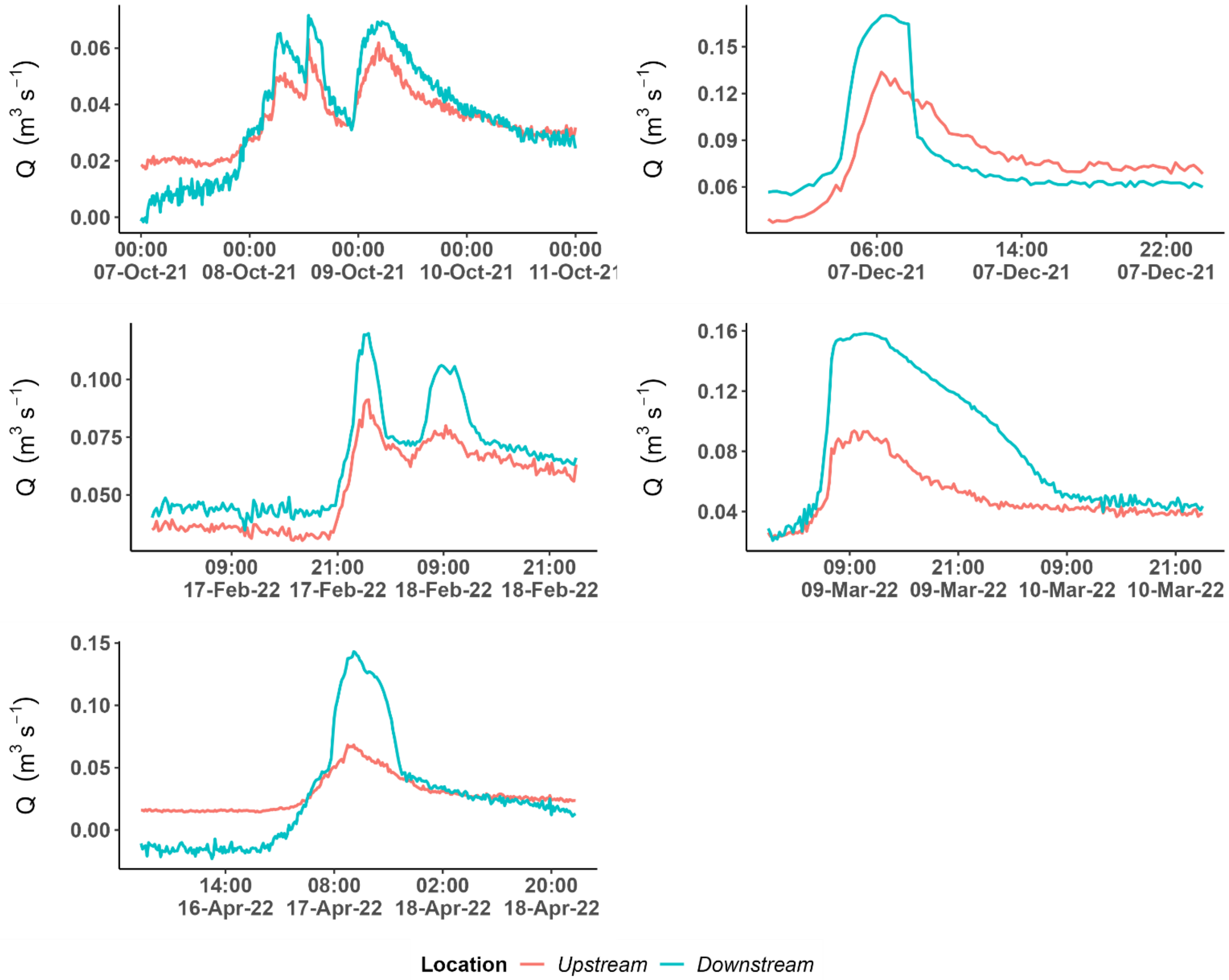

Figure S2B3 Hydrographs of discharge (Q m^3 s^{-1}) upstream (red) and downstream (blue) of the leaky dams section during peak flows (Discharge Q > 0.75 $m^3 s^{-1}$) between October 2021 and April 2022, prior to leaky dam installation. Hydrographs were derived from rating curves developed from water level data and manual stage-discharge measurements from the water level recorder locations upstream and downstream of the leaky dams section.

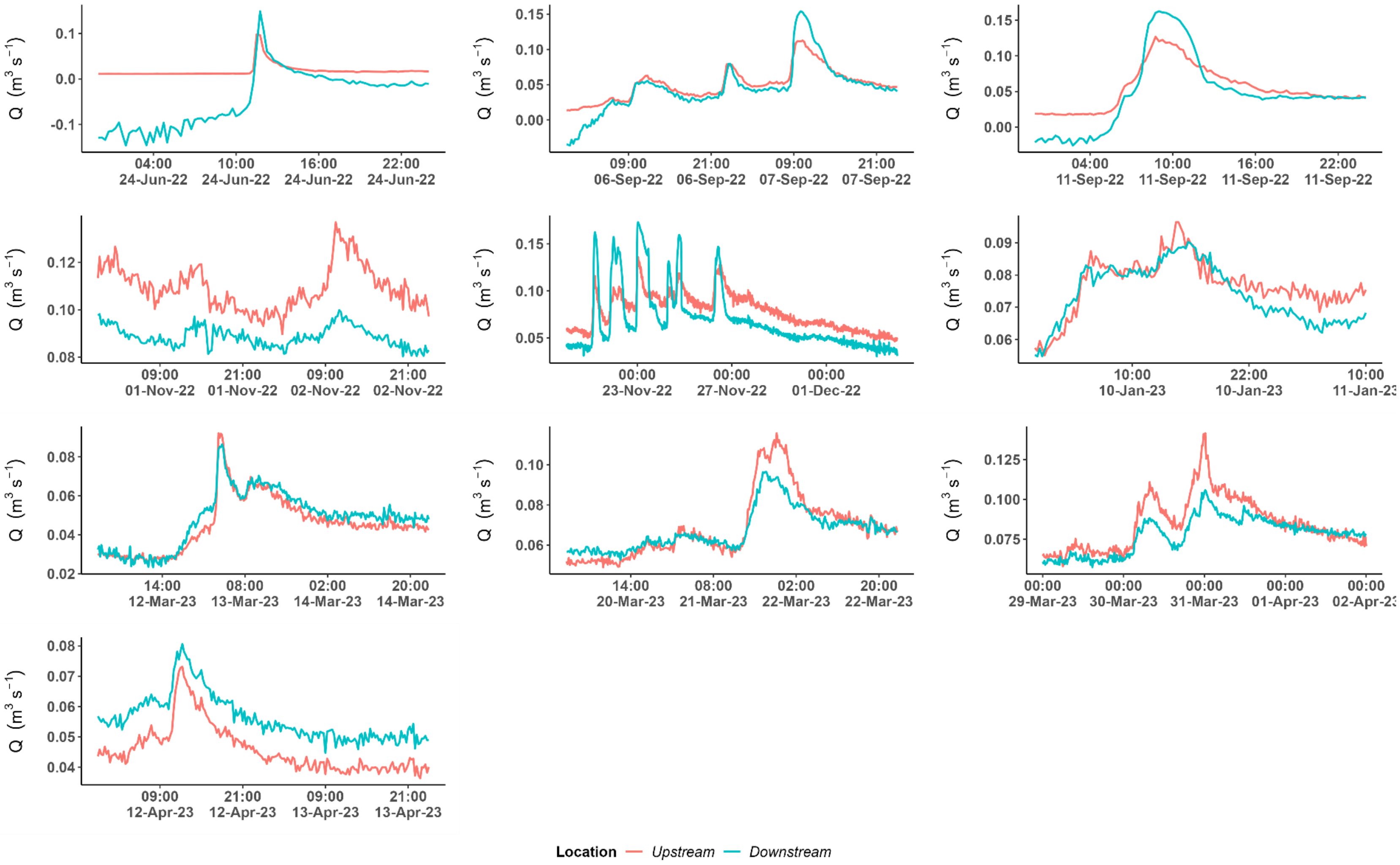

Figure S2B4 Hydrographs of discharge (Q m^3 s^{-1}) upstream (red) and downstream (blue) of the leaky dams section during peak flows (Discharge Q > 0.75 m^{3}s^{-1}) between June 2022 and April 2023, following the leaky dam of four leaky dams between the water level recorded locations. Hydrographs were derived from rating curves developed from water level data and manual stage-discharge measurements from the water level recorder locations upstream and downstream of the leaky dams section.

Chapter 5:

A modified woodland swale for the treatment of agricultural runoff

Abstract

Runoff from field surfaces, farmyards and trackways may deliver substantial loads of organic matter, sediment and dissolved nutrients to surface waters in agricultural catchments. There is a pressing need to design and implement measures to retain and treat agricultural runoff which are effective yet do not require substantial investment, land-take or maintenance. Nature-based Solutions can be installed at low cost and, through enhancing natural processes, provide somewhat self-sustaining conditions for the attenuation of anthropogenic pressures. Swales positioned adjacent to sources of agricultural pollution may retain particulate organic and mineral matter and provide substrate for geochemical and microbial attenuation of nutrients. This study showed that, by maximising the contact between nutrient-enriched water and a bare-soil soil and the overlaying atmosphere, pronounced changes in dissolved oxygen content and dissolved nutrient concentration may be induced. Importantly, changes in dissolved nutrient content were often strongly influenced by variability in influent nutrient concentration and discharge. Maximising the contact between the atmosphere and polluted water may be critical to heterotrophic metabolism of organic matter, but seasonal variability in nutrient loading and discharge should be accounted for in swale designs.

5.1 Introduction

Runoff from agricultural hard standings and trackways contaminated with bovine faecal and urine wastes, typically contains high concentrations of organic matter and mineralised dissolved nutrients such as soluble reactive phosphorus, nitrate, ammonium and dissolved organic carbon (Edwards and Hooda, 2008). Influx of labile organic matter and plant nutrients to surface waters can stimulate algal and microbial growth, so increasing biological oxygen demand and putting stress on in-stream fauna (Hooda et al., 2000; Edwards and Hooda, 2008; Friberg, 2014). Modifications to channels and transitional zones such as wetlands have been made in rural catchments for centuries to facilitate intensification and expansion of agriculture (Davidson, 2014). Wetlands have been widely drained and channels straightened and widened to promote downstream conveyance of peak flows and limit the risk of over-bank flooding to farmland (Seliger and Zeiringer, 2018). These hydrological modifications allow high loads of nutrients and sediment to be conveyed swiftly downstream during high-flow periods (Dodds, Walter, 2002; Webster et al., 2003). Streams in agricultural catchments are particularly vulnerable due to sources of high loadings of fine sediment, particulate organic matter and soluble nutrients (phosphorus, nitrate, ammonium, dissolved organic carbon) including surfaces of fields and farm road-ways and hard standings (Ockenden et al., 2014; Fenton et al., 2021, 2022).

The loss of riparian wetlands may limit the potential for nutrients and sediment to be stored and taken up into terrestrial bio-geochemical cycles such as the nitrogen cycle (Vymazal, 2007; Carstensen et al., 2020). Modified channels in agricultural catchments often lack geomorphic features, such as gravel riffles and debris dams, which can host microbial and macroinvertebrate communities and mediate the uptake, transformation and attenuation of nutrients (Weigelhofer et al., 2012; Seliger and Zeiringer, 2018). As a consequence of high nutrient loadings and impaired biological functioning of streambeds, the potential for low order streams in agricultural catchments to attenuate nutrients from the land has been diminished in recent decades (Weigelhofer, 2017). Member states of the European Union are obliged to implement policies and measures to limit further reductions in water quality under the water framework directive (CEC, 2000; Flávio et al., 2017).

A range of measures have been recently developed which are designed to treat diffuse- and point-source agricultural run-off such as field surfaces, farm trackways and livestock hard-standing areas, and limit the risk of pollution to surface waters. Constructed wetlands are a widely advocated measure for the treatment of agricultural runoff. These take the forms of Horizontal Flow and Vertical Flow wetlands, as well as hybrids and variants of these such as integrated constructed wetlands (Scholz et al., 2007; Vymazal, 2010). Contaminated surface waters flow over or through constructed wetland sediments where processes of physical trapping and biological nutrient processing or geochemical attenuation can occur. Attenuation or transformation of organic compounds and nutrients are driven by aerobic process at the more oxygenated upper portions of horizontal flow wetlands, or through anaerobic processes in the deeper sediments of vertical flow wetlands (Babatunde et al., 2008; Vymazal, 2010). In this manner, vertical hydraulic connectivity within the wetland can aid in more complete biochemical attenuation of nutrients (Cecchetti et al., 2020; Fleming-Singer and Horne, 2002). Constructed wetlands have been shown to be effective in removing phosphorus and reducing downstream biological oxygen demand (BOD) through allowing physical retention of particulate organic matter (POM) and sediment, and through uptake of dissolved nutrients into the soil biota and emergent macrophytes (Brix, 1994; Healy et al., 2007; Scholz et al., 2007). The breakdown of POM by soil and aquatic biota can be a slow process, especially under anaerobic conditions which may pervade within deeper wetland sediments (Tietz et al., 2008; Graeber et al., 2021). Attenuation of agricultural runoff, which can be rich in organic matter (OM), may be promoted by aerobic heterotrophic breakdown of organic forms of nutrients (phosphorus, nitrogen, carbon) so they may be amenable to microbial uptake and transformation (Kuypers et al., 2018; Graeber et al., 2021).

Constructed wetlands occupy relatively large areas to provide sufficient surface area and extended hydraulic residence times for effective removal of contaminants (Harrington et al., 2012). The substantial land-take recommended for effective functioning of constructed wetlands is considered to be major barrier to their adoption on agricultural land-holdings (Wilcock et al., 2012). Additionally, as vegetated constructed wetlands mature, hydraulic ‘short-circuiting’ may develop as preferential flow pathways form around vegetation roots, reducing the contact between water and the wetland substrate (Lightbody et al., 2008).

Unit-process shallow open-water wetlands have also been advocated as a simpler and less space-intensive alternative to constructed wetlands (Jasper et al., 2014). These are typically comprised of lined rectangular ponds, each occupying an area of up to 1ha (Jasper et al., 2014; Jones et al., 2018). Within the open-water wetland, water is retained to a depth of less than 0.5m, to maximise the penetration of light to the biomat that forms within the wetland, promoting photochemical breakdown of organic molecules (Jasper et al., 2014; Jasper and Sedlak, 2014), and the establishment of autotrophic biomats (Prasse et al., 2015; Jones et al., 2018). Compared to constructed wetlands open-water wetlands are less prone to hydraulic short-circuiting as they lack emergent macrophytes (Lightbody et al., 2008; Tietz et al., 2008) and, consequently, may promote more uniform delivery of nutrient-laden waters to soil surfaces and the biomat which develops at the water-soil interface (Fleming-Singer and Horne, 2002; Jasper et al., 2014). Open-water treatment wetlands have been shown to be effective in treating water contaminated with organic compounds and faecal indicator organisms from municipal sewerage, due to their capacity to provide large surface areas for ultraviolet irradiation, without occlusion by vegetation or U.V. absorbance by deep water above the soil surface (Jasper and Sedlak, 2014).

Athough simpler in design than constructed wetlands and therefore less costly, such open-water shallow treatment wetlands nonetheless require considerable land take and precise engineering design and construction. As such, they are unlikely to be widely adopted by many farmers in the EU, in the absence of suitable subsidy payments or policies.

Other methods of on-farm runoff treatment include more simple off-roadway features such as sediment traps and swales which may be installed at lower cost, occupy less space and may be formed without the level of investment and expertise required for constructed wetlands (Mackenzie et al., 2013; Duffy et al., 2016). Swales are spatially-discreet, low-gradient, land surface features that receive gravity-fed contaminated runoff and temporally store the polluted water as it moves slowly over the surface of the swale, partially or wholly treating it as it does so (Mackenzie and Mcilwraith C I, 2015). Sediment and particulate organic matter may be deposited on the surface of the swale and dissolved nutrients can be attenuated through chemical sorption to soil surfaces or assimilated through uptake of nutrients by plants and autotrophic and heterotrophic micro-organisms (Shaw Yu et al., 2001; Environmental Protection Agency, 2003). Retention and remediation of runoff within the swale may be enhanced with the inclusion of low-height check dams positioned perpendicular to flow, which can increase residence time of water within the treatment area and promote infiltration of water to soil (Shaw Yu et al., 2001; Fenton et al., 2021). Reports of the efficacy of swales in treating agricultural runoff, however, are mixed, with some studies showing substantial attenuation of suspended solids, total nitrogen and phosphorus (Shaw Yu et al., 2001) and others reporting negligible changes in runoff concentrations between swale inlets and outlets (Liljaniemi et al., 2003).

Both vegetated and open-water constructed wetlands have been shown to be more effective in treating runoff during summer months, due to the increase in microbial and autotrophic activity at higher temperatures (Dunne et al., 2005), but their efficacy during winter months, when runoff generation from agricultural land is generally higher (Deasy et al., 2009; Jordan et al., 2012), is relatively untested. Conveyance of high loadings of nutrients and sediment from the land to water bodies may also be of higher concern in winter due to the presence of exposed soils, high water tables and high densities of livestock and feed in yards (Edwards and Hooda, 2008; Fenton et al., 2021). While there is evidence that the impact of high-flow events on water quality is mediated by high dilution of nutrients and sediment in receiving waters (Vero et al., 2019), agricultural runoff is known to bring about substantial impairment to water quality during winter (Hooda et al., 2000; Boardman and Vandaele, 2023).

Open-water wetlands require constant supply of water to maintain the microbial biomats which aid in nutrient attenuation (Brady et al., 2021). While open-water and vegetated wetlands may provide more effective runoff attenuation than more simple features like swales, the intermittent nature of farm runoff from surfaces such as trackways, roofs and hard-standing areas may reduce the efficacy of wetlands in an agricultural context (Bulc and Klemenčič, 2011; Moloney et al., 2020). Viable options for on-site treatment of agricultural runoff should optimise nutrient processing yet minimise land-take, and construction and operational costs (Duffy et al., 2016; Melland et al., 2018; Fenton et al., 2021). Additionally, the planning requirements for the construction of constructed wetlands may be a disincentive to most land-owners (Fenton and Ó hUallacháin, 2012; Mackenzie et al., 2013). Due to the limited space available on agricultural land-holdings for non-profitable land-use, simple runoff attenuation features like swales which are designed to maximise nutrient metabolism and attenuation rates, while limiting the required land-take may be particularly attractive to land-owners (Liu et al., 2018; Ekka et al., 2021; Fenton et al., 2021). Such swales may also be more attractive to farmers if they can be sited in locations which neither hinder farm operations, nor reduce the potential productivity of a farmer's land-holding. Such locations include corners of fields that are difficult to exploit with large machinery, unexploited areas of scrub, or low conservation-value woodland plantation, all of course down-slope from areas generating contaminated water.

The current study investigated the potential of a 4m x 30m swale sited within a recent deciduous woodland plantation to treat contaminated agricultural runoff, from an area of hard-standing used for winter bovine housing and silage storage, and to promote dissolved oxygen recovery and infiltration. The study was conducted on a mixed-use farm in southern Ireland from 2021-2023. A small (20 cm deep and 40 cm wide) drainage channel flowed through the plantation, which intermittently received contaminated agricultural runoff during winter, was physically re-configured into a much wider and shallow (4m wide, 2-5 cm deep) bare-earth swale, with regular perpendicular check dams along its length. It was hypothesized that the contaminated runoff could be mitigated within the swale through the multiple processes of water oxygenation, increased exposure to sunlight, and through maximising the contact between soil and over-laying water, so facilitating the microbial action on dissolved and particulate contaminants. In turn, we hypothesised that the development of microbial biomats on the soil surface would lead to enhanced nutrient attenuation and transformation of the overlying waters, and that the differing morphology of the broad swale and narrow drain would bring about differing effects on water quality parameter concentrations as water flowed through the schemes.

5.2 Methods

5.2.1 Study site

The study site was located within a farm landholding, situated within the catchment of the Glashagariff river, a minor tributary of the impounded River Lee, SW Ireland (51°56'09 N 8°52'59W; 150.07 – 146.47m above sea level). The soil in the catchment consists primarily of fine loamy soil overlying Old Red Sandstone bedrock (Teagasc, 2023). The catchment is comprised of approximately 80% improved grassland, with the remaining land dominated by heathland and conifer plantations, with some small broadleaf plantations within the farm itself (Environmental Protection Agency, 2018). The area receives an average annual rainfall of 1305 mm (2000 – 2022; (met.ie, 2023).

Within the farm, a land drain outfall into an open channel from an area contaminated by runoff from hard standings, farm trackways and field surfaces, into a 4ha area of 15-year old (approx.) deciduous woodland plantation. Prior to construction of the woodland swale, the spring-fed drainage channel flowing through the plantation was approximately 0.2 m wide and x 0.4 m deep and extended for 50 m through the plantation before emptying into a first-order stream. In April 2022, the original channel in-filled and a new channel was formed in its place which as a much wider and shallower unvegetated swale, consisting of a series (n=20) of 2 m wide x 2 m long x 0.1 m deep shallow ‘cells’, bounded laterally by 10-20 cm diameter wooden logs and with similar sized logs placed laterally across the swale to form check dams between the cells (Fig. 1, wide swale). Water flowed into the swale during periods of high rainfall and soil saturation, when rainfall induced overland flow from adjacent fields and livestock hard-standing areas, such that contaminated water flowed into the spring feeding the swale (Edwards and Hooda, 2008).

In January 2022, a second narrower drainage channel was dug to run parallel to the wide swale and with dimensions similar to the original drainage channel (0.4m wide and 0.4m deep), but with wooden check dams situated at 2m intervals along its length (Fig. 1, narrow drain). This new channel received a similar flow of water from the same contaminated spring as the wider swale, via an inlet 2m upstream of the first broad swale cell (Fig. 1, narrow drain). The narrow drainage channel ran parallel to the broad swale for 30m, before emptying back into the broad swale, after cell 9. Construction of this second narrow channel, parallel to the wide swale and mimicking the original drainage channel that flowed through the woodland, enabled us to compare any changes in dissolved and particulate substances within the contaminated drainage water between the broad and narrow swale cell morphology. During sampling events, discharge in the narrow channel and broad swale was measured using an electromagnetic flow velocity meter (Valeport Electromagnetic Flow Meter; Model 801; Flat Type 0801001, UK) and measurement of the wetted perimeter at the flow-gauging site. Flow at the top of broad swale and narrow channel was adjusted on an incremental basis to allow similar discharge between the treatments. Following formation of the broad and narrow swales, water was allowed to flow through them for several months prior to water sampling, to allow the establishment of broadly comparable soil and microbial conditions in the two swales.

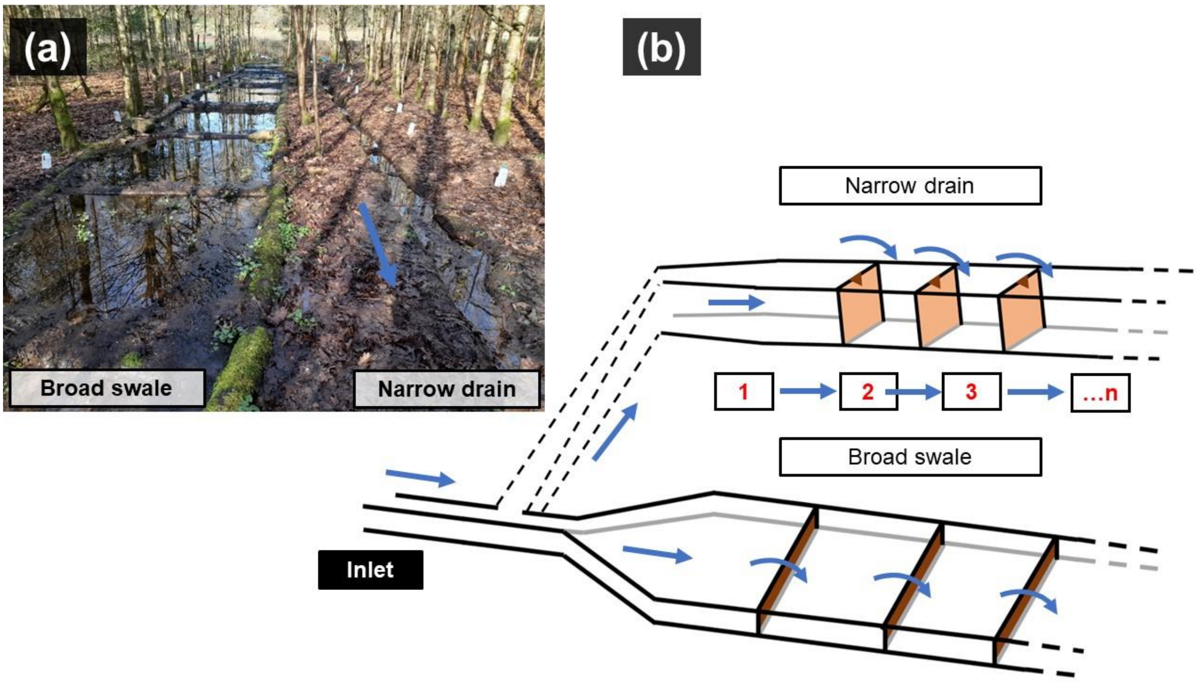

Figure 1 Photograph (Fig. 1a) and schematic (Fig. 1b) of the broad swale and narrow channel. Blue arrows in Fig. 1a and Fig. 1 indicate direction of flow through cells (Fig. 1b: cell 1 to 3…n), and over dividers between cells. Flow continued to cell 'n', i.e. until water infiltrated the soil. Both the narrow channel and broad swale were fed by a common inlet which divided upstream of cell one of the two schemes. See Appendix 3A for storage metrics for broad swale and narrow drain schemes.

5.2.2 Sampling protocol

Water within the two parallel schemes (broad swale and narrow channel) were sampled within the cells along their lengths on 11 occasions between Dec 2021 and Feb 2023, during periods when water was flowing along both schemes. On each sampling occasion, a single surface water sample was collected along with an *in-situ* reading of dissolved oxygen content at the downstream end of each cell (Fig. 1) to examine the cumulative effect of the swale cells on dissolved and particulate substances within the contaminated runoff. Dissolved oxygen (DO) measurements were made using a portable meter (WTW ProfiLine Cond 3110, Xylem Analytics, Germany; Oxygen and temperature: OxyGuard® Handy Polaris Hv. 3.15, EU, (https://www.oxyguard.dk, 2020). Surface water samples were collected in sterile 1L plastic bottles and stored in a cool-bag before being frozen at -80°C within 6 hours of collection. To avoid contamination of water samples, sampling was performed from downstream to upstream, terminating with water surface water sampling from the inlet to the two schemes. Water sampling was confined to the first 8 cells of the two schemes, after which water was only present intermittently due to infiltration into the soil, along the length of the broad swale and, to a lesser extent, the narrow drain. With the exception of flood events, when overland flow resulted in inundation of the two schemes, the narrow channel and broad swale were generally dry between the months of March and November.

5.2.3 Water quality analysis

Surface water samples were analysed for Nitrate (NO_3^- - N), Ammonium (NH_4^+- N), Soluble Reactive Phosphorus (SRP), Dissolved Organic Carbon (DOC) and Chloride. For determination of NH_4^+, samples were filtered through 0.45µm PVDF membrane filter and analysed by automated salicylate method using the Lachat Quikchem 8000 FIA (Zellweger Analytics, Inc. Milwaukee. USA. Method Code: QuikChem Method 10-107-06-3-D) (Method Detection Limit (MDL) = 0.002, Relative Standard Deviation (RSD) = 12%). SRP was determined by automated ascorbic acid method using the Lachat Quikchem 8000 FIA (Zellweger Analytics, Inc. (Milwaukee. USA. Method Code: QuikChem Method 10-115-01-1-B) (MDL = 0.001 mg P L^{-1}; RSD = 5%), following filtration through 0.45µm PVDF membrane filter. NO_3^- was analysed by automated FIA colorimetric method following filtration through 0.45µm PVDF membrane filter and reduction of nitrate to nitrite through copperised cadmium column (Method Code: 10-107-04-1-C) (MDL = 0.007 mg N L^{-1}; RSD = 3%). For DOC determination, samples were filtered through <0.45µm GF/C filter paper then measured by high-temperature combustion method using TOC-VCPH/CPN (SHIMADZU) (MDL = 0.12; RSD = 2.22%). For quality assurance, all laboratory analyses were carried out in accordance with Irish Environmental Protection Agency National Laboratory Proficiency Scheme, since 2010.

5.2.4 Statistical analysis

Statistical procedures were carried out in Rstudio v. 4.3.0 (Rstudio Team, Boston, MA, USA, 2016). Mixed effect linear models were performed on dissolved water quality parameter concentrations (dissolved oxygen, SRP, ammonium, nitrate, DOC) along the cells of the broad swale and narrow drain to test changes along the schemes' cells, and between the two different schemes (broad swale vs. narrow drain). Cell number (with the inlet to the scheme being Cell zero, and each consecutive section bounded by transverse logs being Cell 1 to Cell *n*; Fig. 1) was used as a discrete numeric explanatory variable against water quality parameter concentration as the dependent variable. Scheme type (broad swale vs. narrow inlet) was included as an additional dependent variable for events when both schemes were sampled. Sample date was included as a random effect to account for variance across sampling occasions in mixed effect models.

Removal efficiency (% RE) in the broad and narrow cells was calculated as the percentage difference in concentrations between the wetland inlet (C_{in}) and Cell no. 8 (C_{in}), which was the most consistent maximum extent of surface water within the scheme across sampling events (100 * ((Cin – C8)/ Cin), Carstensen et al., 2020;

Fleming-Singer and Horne, 2002). Linear models were used to estimate the effect of flow discharge and of inlet concentrations %RE.

All mixed effect linear model residuals were checked for normality and goodness-of-fit using the DHARMa package which provided Quantile-quantile estimates, residual vs. predicted estimates and associated statistical tests of normality (Hartig, 2022). Normality of model residuals from linear models was determined via inspection of normality plots produced by the autoplot function from the ggplot package in R (Wickham, 2016). Normality tests with $p < 0.05$ indicated significant deviance of model residuals from normality. A p-value of < 0.05 was used to reject the null-hypothesis in statistical models.

5.3 Results and Discussion

5.3.1 Nutrient concentration changes along broad swale and narrow drain

There was significant recovery of dissolved oxygen along the length of the broad swale throughout the study period (December 2021 – February 2023; Table 1, Fig. 2, Fig. 3). When the broad swale and narrow drain were sampled on the same dates (April 2022 – February 2023), DO recovery was found to be significantly higher in the broad swale than the narrow drain and this was consistent across sampling events (Table 2, Fig. 3).

Table 1 Water quality parameter summary results from the broad swale. Mean concentrations of water quality parameters (dissolved oxygen, ammonia, nitrate, soluble reactive phosphorus (SRP), dissolve organic carbon (DOC)) at the top (inlet) and bottom cell (Cell 8) of the broad cell swale are shown with mean percentage removal efficiency (%RE) over 11 sampling events 14th December 2021 and 15th February 2023. Mixed effect linear model summary results for change water quality parameter concentration are shown in columns 5-7. See Appendix 3B for metrics derived for each sampling event.

WQ Parameter	Inlet (mg l^{-1})	Cell 8 (mg l^{-1})	% RE	df	*t*-value	*p*-value
Dissolved oxygen	4.95	8.41	-69.90	89.00	16.68	< 0.0001
Ammonia	0.78	1.02	-31.44	97.33	1.93	0.0563
Nitrate	1.07	0.88	17.66	96.95	-4.07	< 0.001
SRP	0.229	0.343	-49.78	97.27	4.94	< 0.001
DOC	13.9	26.5	-90.65	97.33	3.35	0.0012

There was significant production of SRP and DOC within the broad swale over the study period (Table 1), but it is clear that the percentage change in concentration (% Removal efficiency; %RE) of SRP and DOC between the inlet and the final cell (Cell 8) of the broad swale varied substantially among sampling events (Fig. 4d and Fig. 4e). As there was no additional source of these nutrients downstream of the inlet, increases in concentrations were likely derived from two processes occurring within the broad swale itself – a) mineralisation of organic matter over the surface of the swale, or b) mobilisation of previously deposited mineral nutrients from the swale soil surface or c) a combination of the two (Shore et al., 2016; Vymazal, 2007). Heterotrophic breakdown of organic matter leads to mineralisation of organic nitrogen to soluble ammonium (ammonification), mineralisation of organic phosphorus to soluble reactive phosphorus (SRP) and the production of dissolved organic carbon (DOC) Kuzyakov et al., 2000; Heuck et al., 2015; Stutter et al., 2018). During certain sampling events (e.g., 14th December 2021, 23rd December 2021, 6th January 2022, Fig. 2; 18th January 2023, Fig. 3) there is evidence for linked or simultaneous production of soluble ammonium, SRP and DOC in the broad swale. This may have derived from mobilisation of nutrients from the surface of the swale or OM breakdown and mineralisation of organic forms of N, P and C from contaminated influent water (Harrison et al., 2019; Brady et al., 2021). Heterotrophic metabolism in waters polluted with OM induces high biological oxygen demand and it is apparent from comparisons of changes in nutrient concentrations along the broad swale and narrow drain (e.g., 18th Jan 2023), that the greater increase in DO in the broad swale than the narrow swale induced higher rates of OM mineralization in the broad swale (Fig. 3). Sampling on 18th Jan 2023 showed that ammonium, SRP and DOC concentrations increased coincidentally in a broadly linear trend along the broad swale, with little change in concentrations along the narrow drain (Fig. 3). Increases in SRP concentrations are often associated with desorption from Fe minerals from the soil under reducing conditions and high DOC concentrations (Stutter et al., 2018; Singh et al., 2020) so the observation that SRP concentrations increased with DO in the broad swale, but not in the narrow drain suggests that much of the SRP in the sampled water was derived from heterotrophic metabolism of OM, instead of through liberation of P stored in underlaying sediments (Graeber et al., 2021). The lack of change in DO or nutrient concentrations in the narrow drain on 18th January 2023 may also indicate that the polluted water passed through the drain with minimal microbiological transformation or attenuation of nutrients in the water before it infiltrated the soil.

Ammonium concentrations did not change significantly along the broad swale over the whole study period (Table 1), but concentrations were reduced between the inlet and the final cell of the broad swale on four out of eleven sampling events (Fig. 4). There was no significant effect of drain morphology (broad swale vs. narrow drain) on ammonium, DOC or SRP removal over the sampling period (Table 2), but it is clear that during sampling certain events changes in nutrient concentration along the broad swale and narrow drain differed substantially (Fig. 3), providing further evidence that the broad swale brought about greater breakdown of OM than the narrow drain.

Mineralization and immobilization of nutrients by soil microbial organisms may both be favoured under aerobic conditions, so it is likely that production and uptake of dissolved nutrients were occurring simultaneously within the broad swale and narrow drain (Kuzyakov et al., 2000; Revsbech et al., 2005; Wilcock et al., 2012). Relative rates of microbial mineralization and immobilization in soils are known to be affected by the stoichiometric balance among bioavailable N, P and C (Heuck et al., 2015; Stutter et al., 2018) and variability in water quality results among sampling dates in the current study may be influenced by the inherent variability in the constitution of agricultural runoff (Stutter et al., 2020). Additionally, processes such as adsorption and denitrification were likely to have been occurring alongside mineralization and immobilization processes: further complicating interpretation of the results (Heuck et al., 2015; Stutter et al., 2020). In this way, %RE represents the net change in nutrient concentrations following the multiple complex processes of mineralisation, immobilization and geochemical adsorption of dissolved nutrients occurring together in the intervening cells. Further research should focus on the relative contributions of the biofilm, which develops within the water columns of the feature and the underlaying soil, to the biological or geo-chemical processing, respectively, of agricultural runoff. This work may yield valuable insight into the designs of swale-type features to maximise agricultural runoff attenuation.

Over the whole study period, nitrate concentrations were significantly reduced along the length of the broad swale (Fig. 2, Fig. 3; Fig. 4c, Table 1) indicating consistent processes of denitrification or nitrate retention within the microbial biomat on the soil surface or below the soil surface (Wilcock et al., 2012). Denitrification is favoured under anaerobic conditions where there is an adequate supply of DOC, as nitrate is reduced instead of oxygen in the metabolism of DOC by denitrifying bacteria in these conditions (Leverenz et al., 2010; Zarnetske et al., 2011a). Interestingly, there was significantly higher nitrate attenuation in the broad cells than in the narrow cells (Fig. 3, Table 2) despite the higher DO concentrations in the former. DO concentrations however, have been found to decrease rapidly below the surface of wetland biomats. Jasper and Sedlak (2014) observed that DO concentrations dropped from 15 mg L^{-1} at the biomat surface to between 5 mg L^{-1} and 1 mg L^{-1} deeper than 1 cm below the biomat, promoting denitrification and anaerobic ammonium oxidation (ANAMMOX; Vymazal, 2007; Jasper et al., 2014a, 2014b). In the current study, the thickness of the biomat was dependent on the depth of standing water, and did not reach depths of 0.3m - 0.5m usually reported in open-water treatment wetlands (range of 2 cm - 10 cm in the broad swale; (Jasper et al., 2014a). Nonetheless, the observation that nitrate concentrations were reduced by the broad swale may be explained by the presence of anaerobic conditions below the surface of the swale biomat, despite its shallow depth and high DO in the upper 2 cm water column (Kröger et al., 2013; Stutter et al., 2018). SRP is known to be released from soils under anaerobic conditions. The increase in SRP and concurrent decrease in nitrate concentrations may be further evidence for the presence of reducing conditions within the biomat of the broad swale (Kröger et al., 2013). Wilcock et al. (2012) observed the attenuation of ammonium and production of nitrate in a swale-wetland, with only some of the observed nitrification ascribed to ammonium oxidation. They attributed low rates of denitrification to insufficient hydraulic residence within their swale. Jones et al. (2018) found that nitrate and ammonium attenuation improved in the biomat of an open-water wetland as the biomat matured and surmised that increasingly anaerobic conditions within the thickening biomat promoted denitrification and anammox activity by micro-organisms in the biomat. Jasper et al. (2014a) also noted that thick biomats facilitate a diverse range of nutrient attenuation processes resulting from the strong redox gradient between the oxic surface of the biomat and the anoxic regions at depth. Findings from the current study may suggest that, in addition to requiring the appropriate redox conditions for nutrient transformation, biofilm development and nutrient processing is also strongly influenced by the availability of substrate for microbial colonisation (Babatunde et al., 2008; Scholes et al., 2021).

In addition to providing more suitable redox conditions for N attenuation, the broad swale may also have enhanced nitrate concentration reduction by providing more surface area for bacterial colonisation and biomat formation. The total volume of the broad swale and narrow drain was similar (Broad swale volume = 2.3m^3; narrow drain volume = 2.42m^3; Supplementary methods, Appendix 3A, Table S3A1). The total wetted area (TWA), and therefore the area of substrate in contact with overlaying water, differed substantially however between the two treatments (broad swale TWA = 33.64 m^2; narrow drain TWA = 19.8 m^2; Supplementary methods, Appendix 3A, Table S3A1). The degree of contact between nutrients in the water column and underlaying substrates is known to strongly influence nutrient uptake in swales and constructed wetlands (Mustafa et al., 2009; Wilcock et al., 2012) and in natural streambeds (Hester and Doyle, 2008; Zarnetske et al., 2011b; Weigelhofer, 2017). Fleming-Singer and Horne (2002) observed increased nitrate removal in a shallow surface flow wetland following the inclusion of a loose epi-sediment layer owing to increased contact between biofilms on the sediment and nutrients in the water. Similarly, Scholes et al. (2021) observed that nitrate attenuation occurred in the top 2 cm of an open-water wetland and recommended that attenuation rates may be increased by providing additional surface area for biofilm formation.

The unit-process design of the woodland swale, with cells separated by wooden check dams, may promote these nutrient transformation and attenuation processes by maximizing the contact with the water column and soil surfaces, while providing sufficient gradient to allow flow of water through biofilms (Fleming-Singer and Horne, 2002; Mustafa et al., 2009; Shaw Yu et al., 2001). Furthermore, grassed swales have been reported to have poor performance in reducing nitrogen concentrations due to low settling rates of particulate organic nitrogen and low denitrification rates due to poor interaction with soil substrates (Ekka et al., 2021). The shade provided by the trees in the in this study likely to have reduced grass growth at the woodland floor, thereby increasing the surface area available for binding of solutes in the influent water to soil particles (Lightbody et al., 2008; Tietz et al., 2008). Neilen et al. (2017) reported that P losses from wooded riparian margins were lower than those from grassed ones owing to better availability of soil-binding sites under the tree canopy. SRP concentrations tended to increase along the broad swale and narrow drain in the current study, and P loss from swales and swale-wetlands has been reported in other studies (Deletic and Fletcher, 2006). The mechanisms which influence P-binding or release from soils are complex: being influenced by available binding sites to Fe, Al and Ca ions and due to processes of mineralization and immobilisation (Kröger et al., 2013). Several have recommended that the inclusion of media containing chemical compounds such as Al, Fe and Ca to swales to enhance SRP uptake (Ekka et al., 2021; Fenton et al., 2021). Given the simplicity of the design of the broad swale, addition of chemical media or fine clay to certain cells may be an easy and effective modification to the broad swale to enhance its attenuation performance (Ekka et al., 2021).

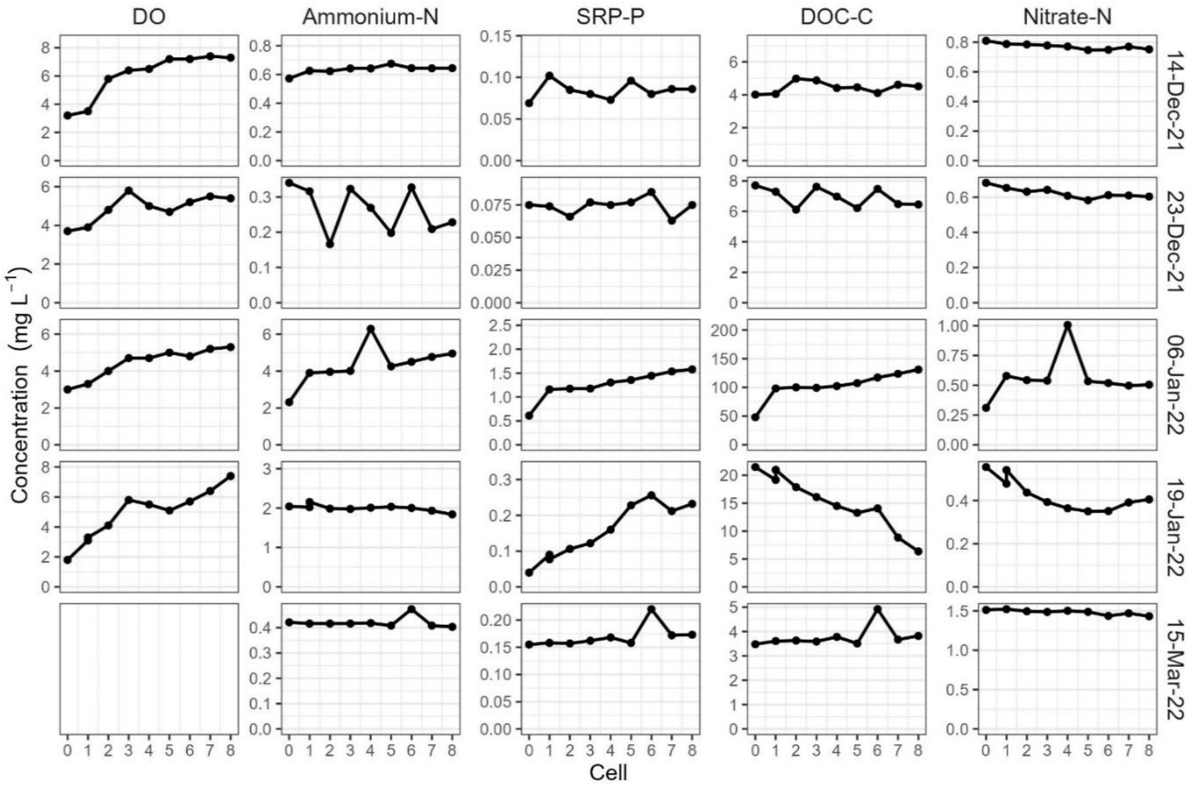

Figure 2 Concentrations of sampled water quality parameters at the between the inlet (Cell 0) and broad swale cell no. 8 on six sampling events between 14th December 2021 and 15th March 2022. Columns show concentration data for Dissolved oxygen (DO; mg O L $^{-1}$), ammonium (mg N L $^{-1}$), soluble reactive phosphorus (SRP; mg P L $^{-1}$), dissolved organic carbon (DOC; mg C L $^{-1}$) and nitrate (mg N L $^{-1}$). Flow discharge was measured at the inlet on 14th December (0.3 L s^{-1}), 23rd December 2021 (0.48 L s^{-1}) and 6th January 2022 (2.04 L s $^{-1}$). The discharge on 6th January 2022 was the highest of the study. See Appendix 3B for data for each sampling event.

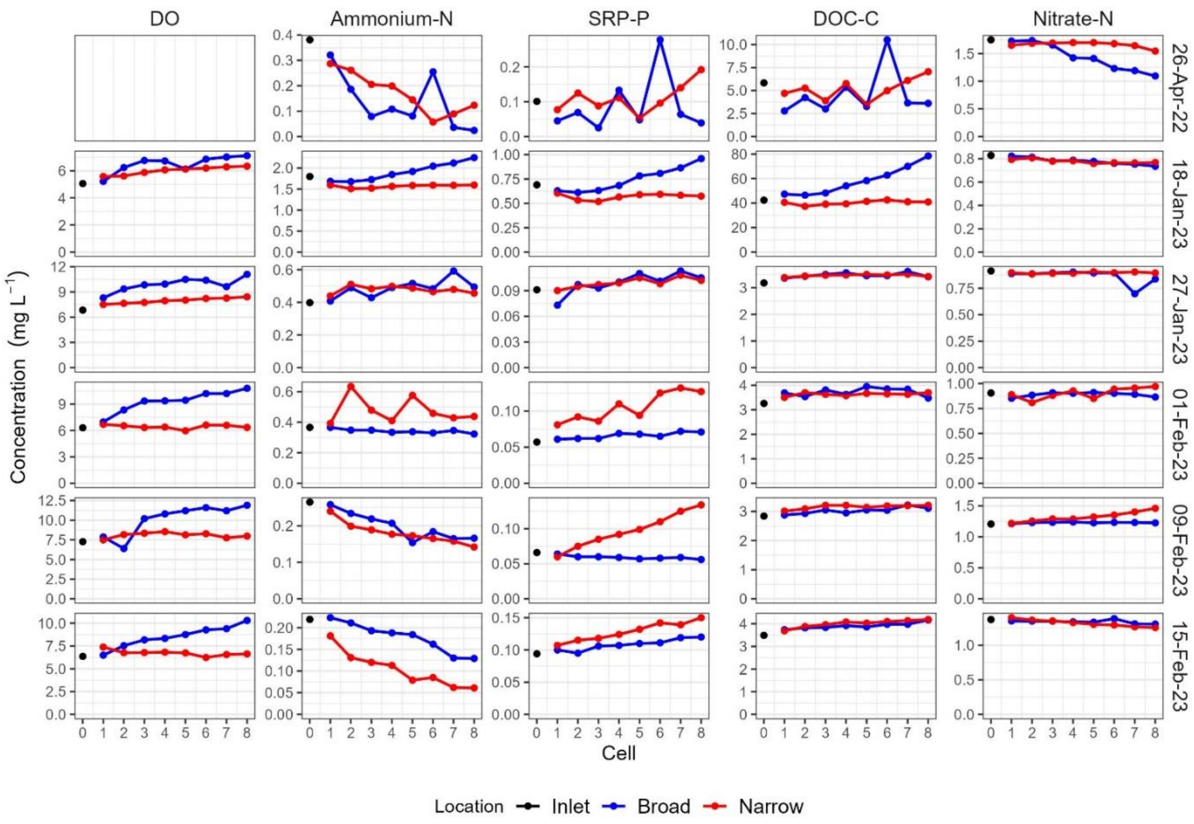

Figure 3 Water quality parameter concentrations in broad swale and narrow drain swale between the inlet (Cell 0) and the final cell of each treatment (Cell 8) between 26th April 2022 and 15th February 2023. Columns show concentration data for Dissolved oxygen (DO; mg O L $^{-1}$), ammonium (mg N L $^{-1}$), soluble reactive phosphorus (SRP; mg P L $^{-1}$), dissolved organic carbon (DOC; mg C L $^{-1}$) and nitrate (mg N L $^{-1}$). Discharges at cell 1 of broad swale and narrow drain range from 0.1L s^{-1} to 0.3L s^{1} (mean broad swale: 0.68 L s^{-1}; mean narrow drain: 0.14 L s^{-1}). See Appendix 3B for data for each sampling event.

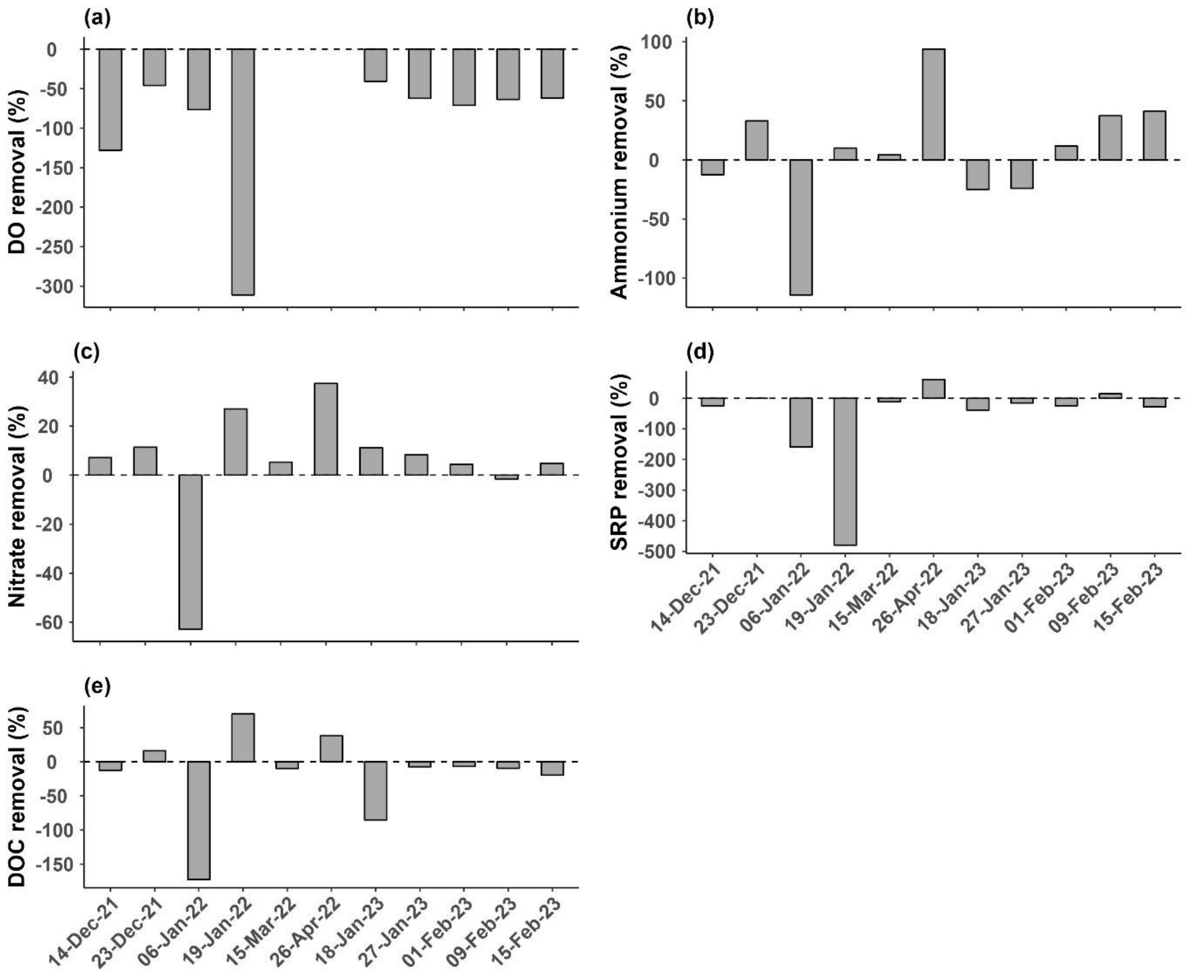

Figure 4 Percentage removal between broad swale inlet and swale end (cell 8) over 11 sampling events between 14th December 2021 and 15th February 2023. Positive values describe percentage removal of water quality parameters (i.e. relative decrease between inlet and outlet concentrations); negative values describe percentage increase between inlet and outlet. (a) Dissolved oxygen (mg O L $^{-1}$); (b) ammonium (mg N L $^{-1}$); (c) nitrate (mg N L $^{-1}$); (d) soluble reactive phosphorus (mg P L $^{-1}$); (e) dissolved organic carbon (mg C L $^{-1}$). Data on inlet and outlet concentrations, % RE are in Supplementary results, Appendix 3B, Table S3B1.

Table 2 Effect of swale morphology on nutrient attenuation along cells 1 – 8 of broad swale and narrow drain. Mixed effect model summary results nutrient concentrations (mg L $^{-1}$) from 6 sampling events between April 2022 and February 2023. See Appendix 3B for metrics derived for each sampling event.

Parameter	Independent variables	Estimate	Std. Error	df	*t* - value	*p* - value
DO	Intercept	7.002	0.56	5.652	12.495	<0.001 *
	Broad	0.417	0.047	72	8.919	<0.001 *
	Narrow	-0.076	0.334	72	-0.228	0.82
	Broad : Narrow	-0.39	0.066	72	-5.886	<0.001 *
Ammonium	Intercept	0.51	0.253	5.175	2.017	0.098 .
	Broad	0.007	0.007	87	1.014	0.313
	Narrow	0.03	0.049	87	0.605	0.547
	Broad : Narrow	-0.017	0.01	87	-1.704	0.092 .
Nitrate	Intercept	1.186	0.129	5.43	9.219	<0.001 *
	Broad	-0.022	0.005	87	-3.999	<0.001 *
	Narrow	-0.049	0.039	87	-1.263	0.21
	Broad : Narrow	0.024	0.008	87	3.099	0.003 *
SRP	Intercept	0.145	0.095	5.349	1.525	0.184
	Broad	0.011	0.004	87	2.993	0.004 *
	Narrow	0.011	0.026	87	0.408	0.685
	Broad : Narrow	-0.004	0.005	87	-0.856	0.395
DOC	Intercept	9.103	7.713	5.356	1.18	0.288
	Broad	0.826	0.297	87	2.783	0.007 *
	Narrow	0.286	2.119	87	0.135	0.893
	Broad : Narrow	-0.7	0.42	87	-1.668	0.099 .

5.3.2 Effects of inlet concentration and discharge on water quality at outlet

Discharge through the broad swale was shown to have a significant negative effect on %RE of ammonium, nitrate and SRP, i.e., ammonium, nitrate and SRP concentrations increased with increasing discharge (Table 3). RE's of DO and DOC were not affected by discharge. Sampling conducted on 6th January 2022 occurred during the highest discharge through the broad swale for the whole the study period (Q = 2.04 L s $^{-1}$; mean Q = 0.68 L s $_{-1}$; Appendix 3B, Table S4B3). The sampling event on this date showed a substantial increase in concentrations of all sampled parameters (Fig. 2). This date also saw the highest inlet and outlet (cell 8) concentrations of ammonium, SRP and DOC (Fig. 2), and the highest and second highest % increases in concentration of ammonium and SRP, respectively (Fig. 4).

Swales have been shown to be effective in attenuating particulate pollutants at higher discharges but attenuation of dissolved nutrients under high flow conditions tends to be limited (Shaw Yu et al., 2001). Amendments such as check dams, as used in the current study, may be effective in reducing the flow rate of water over the bed substrate (Davis et al., 2012), but nutrient attenuation rates through processes such as denitrification are effectively a function of hydraulic residence time, and there was little evidence for nitrate attenuation on dates with high discharge (Zarnetske et al., 2011b).

Table 3 Removal efficiency (%RE) of the broad swale on water quality parameters between cell 1 and cell 8 as a function of influent discharge (Q L s^{-1}) and starting concentration (inlet concentration mg L^{-1}). See Appendix 3B for metrics derived for each sampling event.

	Parameter	Estimate	F	df	R^2	*p*-value
% RE : Q	DO	-4.99	0.129	8	-0.107	0.729
	Ammonium	-68.11	12.71	9	0.539	0.006*
	Nitrate	-26.84	17.11	9	0.617	0.003*
	SRP	-46.82	7.628	9	0.399	0.022*
	DOC	-26.78	1.434	9	0.042	0.262
% RE : Inlet concentration	DO	23.14	5.011	9	0.286	0.052.
	Ammonium	-25.41	1.062	11	0.005	0.325
	Nitrate	-0.92	0.014	11	-0.09	0.909
	SRP	-32.51	0.029	11	-0.088	0.869
	DOC	-2.75	11.48	11	0.466	0.006*

The observed increases in nutrient concentrations through the broad swale and narrow drain during high-flow events may also represent mobilisation of previously stored unconsolidated material along the length of the features (Brady et al., 2021). The microbial biomat that developed within, or on, the soil bed substrate the broad swale may help to stabilise and retain nutrients under baseflow conditions (Mustafa et al., 2009), but degradation of the biomat during dry periods may lead to cell death and mineralisation of nutrients, increasing the risk of mobilisation (Brady et al., 2021). The substantial buffer zone formed by twelve additional cells downstream of the final sampled cell (cell 8) is likely to have provided additional area for nutrient and particulate sequestration, and further infiltration, during these infrequent high discharge events.

%RE of Do and DOC in the broad swale were significantly negatively correlated with inlet concentrations (Table 3). Swale morphology further affected these changes (Fig. 2, Fig.3). The sampling event on 18th January 2023 showed notable increases in concentrations of ammonium, SRP and DOC in the broad swale but not in the narrow drain. The inlet and outlet concentrations for these nutrients are similar to those observed on 6th January 2022, but the discharge through the broad swale on 18th January 2023 was substantially lower than the 6th January 2022 sampling event (6th January 2022: Broad swale Q = 2.04 L s^{-1}; 18th January 2023: Broad swale Q = 0.11 L s^{-1}, Narrow drain Q = 0.13 L s^{-1}; Supplementary results, Appendix 3B, Table S3B3). This suggests that inlet nutrient loading may have a stronger effect on nutrient processing than discharge and that nutrient processing at high concentrations differs between the broad swale and narrow drain.

Co-incidental increases in concentrations of dissolved ammonium, SRP and DOC over the length of the broad swale occurred during events when there were high (> 20 mg C L^{-1}) DOC concentrations (e.g., 6th January 2022 and 18th January 2023; Fig. 2, 3). The coincidental increase in DO content in the broad swale, and the relatively stable concentrations of DO and dissolved nutrients along the narrow drain on 18th January 2023, suggests that DO recovery promoted increases in concentrations of dissolved nutrients through mineralization of organic matter. Under lower OM concentrations, immobilization of nutrients may be a more dominant process than mineralization (e.g., decreases in ammonium concentration on 23rd December 2021, 26th April 2022, 9th and 15th February 2023; DOC < 5mg L^{-1}; Figs. 2, 3). On these dates, ammonium concentrations decreased along the length of the broad swale. Uptake or nitrification of ammonium is known to be favoured under aerobic conditions (Butturini et al., 2000; Harrison et al., 2019). Our results suggest that ammonium uptake predominates over organic-N mineralization with elevated DO concentrations but in the presence of lower nutrient loadings.

Higher rates of SRP concentration increase along the length of the narrow drain than the broad swale were observed during the final three sampling events (1st – 15th February 2023). Inlet nutrient concentrations on these dates were relatively low and it is possible that the weak DO recovery in the narrow drain compared to the broad swale facilitated the desorption of SRP from anoxic sediments (Stutter et al., 2018).

It is widely reported that the risk of nutrient export to downstream waters is greater during high-flow periods (Dalzell et al., 2005; Moloney et al., 2020; Vero et al., 2019). Biological uptake of nutrients is also known to be impaired under especially high nutrient loadings (Birgand et al., 2007; Knight et al., 2000; Vymazal and Kröpfelová, 2009). Results from this study indicate that the relative rates of nutrient removal, via immobilization or adsorption to sediments, and increases in nutrient concentrations, via mineralization and desorption, may also be impacted by nutrient loadings. The results suggest that recovery of DO in agricultural runoff lead may lead to increases in dissolved nutrient concentrations in the water column, by increasing OM metabolism rates. In effect the broad swale may make organically-bound nutrients more available to uptake by soil microorganisms by stimulating mineralization. This poses a challenge to the design of schemes for attenuation of agricultural runoff contaminated by nutrient-rich organic matter, such as faecal matter, urine and silage effluent. Aerobic treatment is a critical step in municipal wastewater treatment systems where recalcitrant organic matter is metabolised by aerobic bacteria and labile organic and mineral nutrients are produced which are amenable attenuation through plant uptake or through anaerobic processes such as denitrification (Chan et al., 2009; Vaiopoulou et al., 2007). High oxygen demand near influent waters at constructed wetlands has been implicated as an important cause of reduced nutrient attenuation efficiency of constructed wetlands, as organic matter is insufficiently metabolized as waters flow deeper into anoxic sediments (Nivala et al., 2013). Maximising the aeration of waters in the woodland swale by increasing the surface area in contact with the atmosphere may aid in promoting subsequent nutrient attenuation processes.

Jasper et al. (2014) found that the nutrient attenuation performance of an open-water wetland was higher during the warm, low flow conditions of summer. Both Brady et al. (2021) and Jasper et al. (2014) recommended that, given their promise for water quality remediation, operators should manage wetlands to account for seasonal variation in temperature and hydrology and maintain the integrity of wetland biomats. The results from the current study suggest that January may be a critical month for nutrient export (Fig.2, 3), potentially arising from high channel discharge and high degrees of connectivity between pollution sources and waterbodies (Moloney et al., 2020). Rates of microbial activity in wetlands may diminish during winter due to low temperatures (Birgand et al., 2007). While some studies have shown that constructed wetlands may be effective in attenuating nutrients during summer and winter (Brix and Arias, 2005; Mustafa et al., 2009), CWs that lack vegetation cover and deeper sediments, such as open-water wetlands may be less resilient against cold (Kadlec, 2009; Saeed and Sun, 2012). Scholes et al. (2021) observed reduced rates of nitrate attenuation in unit process open-water wetlands during winter. In the current study, the broad swale was shown to have a mean nitrate %RE of 17.66% (Table 1), and significantly higher rates of nitrate attenuation than the narrow cells (Table 3). It is notable also that water from the broad swale tended to fully infiltrate the soil within a few meters downstream of Cell 8 and water only reached the land-drain downstream during infrequent large flood events. This may have been a significant aspect of the pollution treatment potential of the swale, rather than just the biochemical processes occurring within the swale. Passive infiltration of agricultural runoff to farm soils has been cited as one of the most effective means of agricultural runoff treatment given the large surface area available for attenuation on farms, and the inherent geophysical and microbial conditions that may be present in farm soils which can favour nutrient attenuation (Fenton et al., 2021). By impounding water behind check dams in the broad swale, the area for Infiltration was increased relative to the narrow drain that preceded the intervention. Indeed, promoting soil infiltration over remediation of waters discharging to watercourses is likely to be much more desirable and practical to land-owners in dealing with runoff. Constructed wetlands which discharge to surface waters must ensure that effluent waters meet water quality standards and as such must be constructed and managed to a level which many landowners are unlikely to be able to achieve (Duffy et al., 2016; Easson et al., 2021). Swales which promote aeration and infiltration may be an appealing alternative.

5.3.3 Further sources of variability in runoff treatment

There was an indication that the percentage cover of autotrophic biomats increased between the start and end of February, and this was more pronounced in the broad cells than the narrow cells (Appendix 3B, Fig. S3B1; Table S3B4). While the sample size was small, the preliminary results are an encouraging sign that processes within the cells cumulatively contribute to meditating water quality, and that his effect appears to be stronger in the broad swale than the narrow drain. Heterotrophic micro-organism activity has been shown to be favoured in waters with high DOC concentration, with biomats transitioning to being dominated by autotrophs when a better stoichiometric balance among N, P and C has been established (Àvila et al., 2016; Graeber et al., 2021). Autotrophic biomats were much less apparent in the narrow cells suggesting that in the absence of appropriate substrate, DO and light incidence, autotrophic biofilms could not develop and continue nutrient transformation processes initiated in heterotrophic biofilms. Additionally, the highest %RE of ammonium in the broad swale cells occurred in April 2022 and February 2023, while there was strong autotrophic growth in the biomat. Ammonium is readily metabolised by photosynthetic organisms (Martí et al., 2020) and while inlet loadings of ammonium was lower in spring than during winter months, the observed attenuation of ammonium is an encouraging finding.

5.4 Conclusions

Although they are widely advocated as measures to tackle contaminated water from farm hard standings, there have been few empirical studies of the functioning of rural agricultural swales as described here (Shaw Yu et al., 2001; Mackenzie and Mcilwraith C I, 2015). By modifying the morphology of agricultural land drains to enhance water-soil contact and aeration area, the swale may bring about substantial improvements to dissolved oxygen content, biological oxygen demand and soil infiltration of water: mitigating the risk of pollution of downstream watercourses from incidental overland flow events. The self-colonising biomat at the surface of the swale may develop over a short time once the feature is inundated and may promote breakdown of aerobic breakdown of organic matter, immobilisation of dissolved nutrients and attenuation of nitrate. The potential for the swale to store and act as a source of SRP, POM and DOC is also noteworthy but it is conceivable that minor modifications to the feature may reduce the risk of mobilisation of biomats, especially during winter when nutrient concentrations and discharges may be higher. Outside of large flood events, all water from the scheme infiltrated the soil 20-30m upstream of the nearest water course. Despite increases in dissolved nutrients along the broad swale during some sampling events, therefore, the water that infiltrated the soil in the broad swale is likely to have had a higher DO and bioavailable nutrient content than the narrow drain. While the broad swale may not have facilitated complete nutrient uptake and attenuation of water quality parameters, it may have produced more labile forms of nutrients which could be further transformed within the soil of the woodland upon infiltration. In summation, simple modifications to typical agricultural land drains may be made at low cost and confer notable benefits to DO of overlaying waters, offering additional storage and space for nutrient attenuation during winter.

5.5 Appendix 3A – Supplementary methods

Table S3A1 Comparisons of surface area available for biomat colonisation and aeration of broad swale and narrow drain cells.

	Broad cells			Narrow Cells		
Cell	Volume (m^3)	Wetted area (m^2)	Aeration area (m^2)	Volume (m^3)	Wetted area (m^2)	Aeration area (m^2)
1	0.25	2.84	2.5	0.18	3	1.8
2	0.65	7.24	6.5	0.5	5.4	2.6
3	1.05	11.64	10.5	0.82	7.8	3.4
4	1.3	16.04	14.5	1.14	10.2	4.2
5	1.55	20.44	18.5	1.46	12.6	5
6	1.8	24.84	22.5	1.78	15	5.8
7	2.05	29.24	26.5	2.1	17.4	6.6
8	2.3	33.64	30.5	2.42	19.8	7.4

5.6 Appendix 3B – Supplementary results

Table S3B1 Inlet and Cell 8 concentrations, difference and removal efficiency for water quality parameters (dissolved oxygen (DO); ammonia; nitrate, soluble reactive phosphorus (SRP), dissolved organic carbon (DOC)) over 11 sampling events between December 2021 and February 2023.

Sample Date	WQ Parameter	Inlet (mg L^{-1})	Broad Cell 8 (mg L^{-1})	Difference (mg L^{-1})	% Removal efficiency
14/12/2021	DO	3.20	7.30	-4.10	-128.12
	Ammonia	0.57	0.64	-0.07	-12.59
	Nitrate	0.81	0.75	0.06	7.16
	SRP	0.07	0.09	-0.02	-24.64
	DOC	4.01	4.51	-0.50	-12.47
23/12/2021	DO	3.70	5.40	-1.70	-45.95
	Ammonia	0.34	0.23	0.11	32.94
	Nitrate	0.68	0.60	0.08	11.44
	SRP	0.08	0.08	0.00	0.00
	DOC	7.70	6.45	1.25	16.23
06/01/2022	DO	3.00	5.30	-2.30	-76.67
	Ammonia	2.31	4.95	-2.64	-114.28
	Nitrate	0.31	0.51	-0.20	-62.90
	SRP	0.61	1.58	-0.97	-159.11
	DOC	48.10	131.10	-83.00	-172.56
19/01/2022	DO	1.80	7.40	-5.60	-311.11
	Ammonia	2.04	1.84	0.20	9.94
	Nitrate	0.56	0.41	0.15	27.03
	SRP	0.04	0.23	-0.19	-480.00
	DOC	21.49	6.37	15.12	70.36
15/03/2022	Ammonia	0.42	0.40	0.02	4.28
	Nitrate	1.51	1.43	0.08	5.29
	SRP	0.16	0.17	-0.02	-11.61
	DOC	3.48	3.82	-0.34	-9.77
26/04/2022	Ammonia	0.38	0.02	0.36	93.70
	Nitrate	1.75	1.10	0.66	37.43
	SRP	0.10	0.04	0.06	61.39
	DOC	5.83	3.61	2.22	38.08
18/01/2023	DO	5.06	7.12	-2.06	-40.71
	Ammonia	1.80	2.25	-0.45	-25.03
	Nitrate	0.83	0.74	0.09	11.22
	SRP	0.69	0.96	-0.27	-38.99
	DOC	42.39	78.51	-36.12	-85.21

27/01/2023	DO	6.84	11.10	-4.26	-62.28
	Ammonia	0.40	0.49	-0.10	-24.12
	Nitrate	0.91	0.84	0.08	8.32
	SRP	0.09	0.11	-0.01	-15.38
	DOC	3.18	3.41	-0.23	-7.23
01/02/2023	DO	6.31	10.80	-4.49	-71.16
	Ammonia	0.37	0.32	0.04	11.75
	Nitrate	0.91	0.87	0.04	4.42
	SRP	0.06	0.07	-0.01	-24.56
	DOC	3.26	3.48	-0.22	-6.75
09/02/2023	DO	7.27	11.90	-4.63	-63.69
	Ammonia	0.27	0.17	0.10	37.36
	Nitrate	1.21	1.23	-0.02	-1.58
	SRP	0.07	0.06	0.01	15.15
	DOC	2.84	3.11	-0.27	-9.51
15/02/2023	DO	6.36	10.30	-3.94	-61.95
	Ammonia	0.22	0.13	0.09	41.10
	Nitrate	1.37	1.31	0.07	4.81
	SRP	0.09	0.12	-0.03	-27.66
	DOC	3.49	4.17	-0.68	-19.48

Table S3B2 Inlet and Cell 8 concentrations, difference and % removal efficiency for water quality parameters (dissolved oxygen (DO); ammonia; nitrate, soluble reactive phosphorus (SRP), dissolved organic carbon (DOC)) from simultaneous sampling of broad swale and narrow drain between April 2023 and February 2023.

Date	Parameter	Inlet (mg L^{-1})	Broad swale			Narrow drain		
			Cell 8 (mg L^{-1})	Difference (mg L^{-1})	% RE	Cell 8 (mg L^{-1})	Difference (mg L^{-1})	% RE
26 Apr 2022	Ammonia	0.38	0.02	0.36	93.7	0.12	0.26	67.72
	Nitrate	1.75	1.1	0.66	37.43	1.55	0.2	11.66
	SRP	0.1	0.04	0.06	61.39	0.19	-0.09	-90.1
	DOC	5.83	3.61	2.22	38.08	7.05	-1.22	-20.93
18 Jan 2023	DO	5.06	7.12	-2.06	-40.71	6.34	-1.28	-25.3
	Ammonia	1.8	2.25	-0.45	-25.03	1.6	0.2	11.23
	Nitrate	0.83	0.74	0.09	11.22	0.77	0.06	7.36
	SRP	0.69	0.96	-0.27	-38.99	0.57	0.12	16.81
	DOC	42.39	78.51	-36.12	-85.21	40.91	1.48	3.49
27 Jan 2023	DO	6.84	11.1	-4.26	-62.28	8.42	-1.58	-23.1
	Ammonia	0.4	0.49	-0.1	-24.12	0.46	-0.06	-14.57
	Nitrate	0.91	0.84	0.08	8.32	0.89	0.02	2.08
	SRP	0.09	0.11	-0.01	-15.38	0.1	-0.01	-12.09
	DOC	3.18	3.41	-0.23	-7.23	3.42	-0.24	-7.55
1 Feb 2023	DO	6.31	10.8	-4.49	-71.16	6.35	-0.04	-0.63
	Ammonia	0.37	0.32	0.04	11.75	0.44	-0.07	-19.67
	Nitrate	0.91	0.87	0.04	4.42	0.97	-0.06	-7.18
	SRP	0.06	0.07	-0.01	-24.56	0.13	-0.07	-122.81
	DOC	3.26	3.48	-0.22	-6.75	3.7	-0.44	-13.5
9 Feb 2023	DO	7.27	11.9	-4.63	-63.69	7.98	-0.71	-9.77
	Ammonia	0.27	0.17	0.1	37.36	0.14	0.12	46.42
	Nitrate	1.21	1.23	-0.02	-1.58	1.46	-0.25	-20.98
	SRP	0.07	0.06	0.01	15.15	0.13	-0.07	-103.03
	DOC	2.84	3.11	-0.27	-9.51	3.21	-0.37	-13.03
15 Feb 2023	DO	6.36	10.3	-3.94	-61.95	6.63	-0.27	-4.25
	Ammonia	0.22	0.13	0.09	41.1	0.06	0.16	72.15
	Nitrate	1.37	1.31	0.07	4.81	1.26	0.12	8.45
	SRP	0.09	0.12	-0.03	-27.66	0.15	-0.06	-59.57
	DOC	3.49	4.17	-0.68	-19.48	4.19	-0.7	-20.06

Table S3B3 Discharge (Q L s $^{-1}$) measurements in the broad swale and narrow drain treatments during 9 sampling events between 14th December 2021 and 15th February 2023, and between 18th January 2023 and 15th February 2023 in the narrow drain treatment. Discharge gauging was performed in the first cell of each treatment

Date	treatment	
	Broad Q (L s^{-1})	Narrow Q (L s^{-1})
14 Dec 2021	0.30	NA
23 Dec 2021	0.48	NA
06 Jan 2022	2.04	NA
26 Apr 2022	0.22	0.06
18 Jan 2023	0.11	0.13
27 Jan 2023	0.10	0.09
01 Feb 2023	0.12	0.30
09 Feb 2023	0.17	0.06
15 Feb 2023	0.31	0.22
Mean	0.68	0.14
Max	2.12	0.30
Min	0.10	0.06

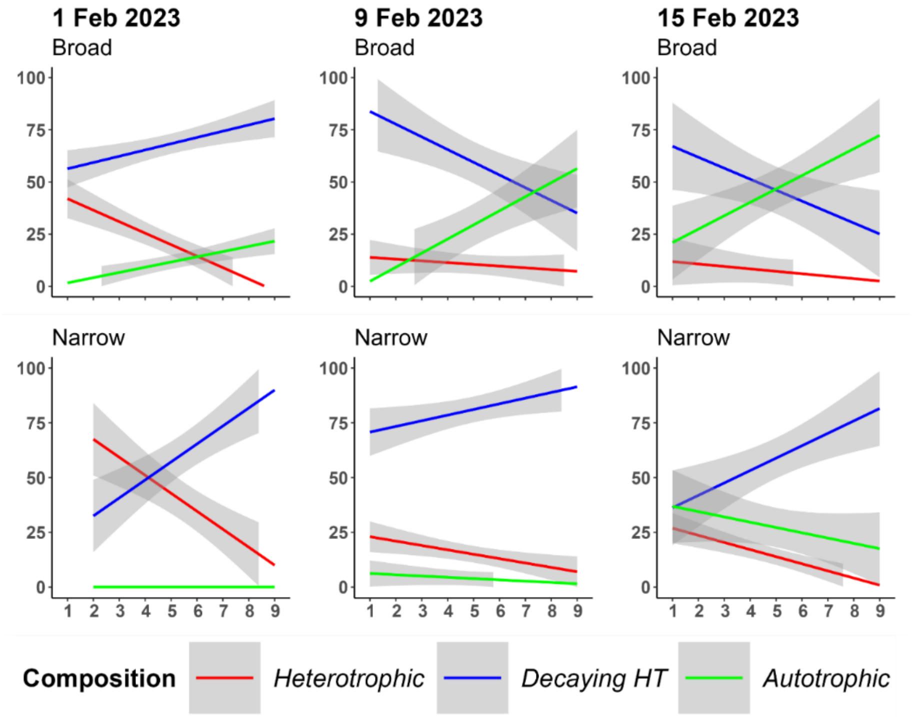

Figure S3B5 Estimates of percentage cover of heterotrophic and autotrophic biomats in the Broad swale and narrow drain during sampling events in February 2023. Lines represent best-fit of the data to linear models; standard error is indicated by grey zones around lines. One sample was collected for each cell.

The composition of biomats in broad and narrow cells of the SOWW was inspected during three sampling events in February 2023. The biomat composition water surface was similar in both treatments but became dominated by autotrophic growth over succeeding cells. Preliminary results from GLMs did not indicate a difference in cover between the two treatments but did show that autotrophic and decaying HT cover tended to increase along the broad cells, while heterotrophic cover decreased along the broad cells. There was also an indication that the percentage cover of autotrophic biomats increased between the start and end of February. Again, this was more pronounced in the broad cells than the narrow cells. While the sample size was small, the preliminary results are an encouraging sign than processes within the cells cumulatively contribute to meditating water quality. This effect appears to be stronger in the broad cells. Heterotrophic micro-organism activity has been shown to be favoured in waters with high DOC concentration, with biomats transitioning to being dominated by autotrophs when a better stoichiometric balance among N, P and C has been established (Àvila et al., 2016b; Graeber et al., 2021). While there was no indication of DOC attenuation in the biomat of the broad cells, the greater development of autotrophic biomats in the broad cells may suggest more effective organic matter breakdown and nutrient cycling. The highest %RE of ammonium in the broad cells occurred in April 2022 and February 2023, while there was strong autotrophic growth in the biomat. Ammonium is readily metabolised by photosynthetic organisms (Martí et al., 2020) and while inlet loadings of ammonium was lower in spring than during winter months, the observed attenuation of ammonium is an encouraging finding. No microbial analysis was performed to more accurately determine the make-up of the biomats formed within the broad and narrow drains, but the data suggested intriguing differences in the capacity for the two drain-morphologies to support microbial communities, which merit further investigation.

Table S3B4 Parameter estimates and general linear model summary results on percentage cover of heterotrophic (HT), decaying HT, and autotrophic biomat composition along all cells (broad swale and narrow drain: no significant difference identified between treatments) over three sampling events in February 2023

Parameter	Estimate	Std. Error	*t* value	*p* value
HT	32.29	5.62	5.74	< 0.001
Cell	-2.98	0.99	-3.01	0.003
Decaying HT	25.32	7.95	3.18	0.002
Autotrophic	-22.13	7.95	-2.78	0.006
Cell : Decaying HT	3.95	1.40	2.82	0.005
Cell : autotrophic	4.95	1.40	3.54	0.001

Chapter 6: General Discussion

6.1 Key observations

This thesis examined the potential for farm-scale nature-based solutions (NbS) to attenuate peak flows and water quality issues at the farm scale. The four experimental NbS features installed at the field site - the flood detention basin, low head boulder weirs, leaky dams, and woodland swale - all displayed some degree of benefit to high-flow management or water quality. Results from the flood detention basin study described in Chapters 2 and 3 suggest that, with proper management, they may be utilized to reduce downstream peak discharges and the flux of sediment, and may do so without impairing pasture productivity. The in-stream features (Chapter 4) also helped to reduce the conveyance of high flows. The woodland swale (Chapter 5) brought about marked dissolved oxygen recovery following modest, yet targeted modifications to a typical farm drain. Importantly, however, all NbS features studied had co-occurring positive and negative impacts on the environment. In the case of the in-stream features, the very process of restricting the flux of water through the channel had the consequence of inducing scour to adjacent streambed and channel banks. The flood detention basin may have promoted soil-surface anaerobic conditions for nitrate attenuation but these same conditions may have promoted the desorption of phosphorus from the soil. The broad swale aided in dissolved oxygen recovery in nutrient enriched water, but it also appeared to promote the production or liberation of dissolved nutrients to the water column. The success of each feature may need to be assessed through careful weighing up of these costs and benefits. Moreover, the effects of a given NbS feature are highly likely to vary between locations due to variability in hydro-morphology, upstream water quality pressures, and other localized variability in abiotic factors which affect nutrient processing, such as the availability of substrate for biofilm colonization and geochemical adsorption of dissolved nutrients (Harvey et al., 2013; Fenton et al., 2021). Given the extent of hydrological modification and nutrient surpluses in Irish agricultural catchments, building features which can restore the broad scope of natural hydrological and nutrient transformation processes that have been lost is a substantial challenge.

The mechanisms which govern biological and geochemical transformations of nutrients in the soil and streambeds are complex and the risk of ‘pollution swapping’ has been highlighted in previous studies in which a feature designed for the mitigation of one water quality parameter may bring about increases in another (Kröger et al., 2013; Stutter et al., 2018). Agricultural runoff can impair water quality in complex ways arising from variability in the composition and pathways taken by the runoff from terrestrial sources to waterways. Streams may be affected by high nitrate loadings in catchments where organic and mineral nitrogen applied to the land as slurry or mineral fertilizer may move through free-draining soils and reach surface waters via groundwater recharge and tile-drains (Jaynes and Isenhart, 2014; Melland et al., 2018). Conversely, heavier soils and hard farm infrastructure such as trackways, yards and hard-standings are likely to impose greater phosphorus burdens to adjacent waters as overland flow mobilizes particulate organic and mineral phosphorus. In the case of the latter, streams may co-incidentally be impacted by high loadings of particulate organic matter and mineral solids which can clog streambeds, affecting hyporheic exchange, nutrient processing, and biological oxygen demand (Fenton et al., 2021; Friberg et al., 2010; Weigelhofer et al., 2018a).

It is likely that in most farms in Ireland, any or all of these elements of pollution may be happening at once. By installing NbS features on the land which may attenuate one water quality pressure, while exacerbating another, we may be forced to weigh up the impacts of the various elements of agricultural runoff at a given location, and implement those features accordingly. Additionally, connecting a channel to a field may provide hydraulic retention similar to a natural floodplain (Nicholson et al., 2020), but this will not necessarily restore the biological and geochemical processing properties of natural floodplains or wetlands. Instead, the legacy of agricultural activities may affect the nutrient processing potential of the field (Acreman et al., 2003; Noe et al., 2019). In many Irish rural catchments, substantial phosphorus loss is likely to occur in a field that is connected to a stream channel due to the presence of phosphorus-saturated soils (Environmental Protection Agency, 2022; Hogan et al., 2023).

A central goal of this research was to install NbS features which brought about attenuation of a given pressure without limiting ongoing agricultural practices or profitability of the land hosting the NbS feature. The detention basin successfully and safely mitigated flood peaks over a two-year period and did not reduce the summer grazing potential of the field it was constructed on. An extended flooding period in October 2022 may have impaired grass growth in the ponding zone, as grass growth continued into early November in the non-ponding zone. This finding suggests that the use of the flood attenuation for peak flow attenuation should be prioritized for winter storms so that effects on farm productivity are minimized, and emphasizes the importance of fine-scale monitoring and adjustment of NbS features in order to maximize their effectiveness while minimizing their negative effects. Fine-scale monitoring and adjustment may be a critical aspect of NbS performance, generally. The necessity for adequate management of such NbS features may preclude broader uptake of similar NbS features, and goes against the notion of NbS features working passively and with nature as is often cited as an asset of NbS features (e.g. Keesstra et al., 2018, Wild et al., 2020).

Investigation into the performance of in-stream features in Chapter 4 gave further evidence for the complex effects of agriculture on water quality and hydrology. The low-head boulder weirs were installed with the expectation that they would improve transient storage and nutrient uptake along the stream section by inducing greater flow through the hyporheic zone beneath each boulder weir. Instead, the boulder weirs induced the formation of upstream backwater zones, which promoted settling of particulate organic and mineral material, and high-flow zones downstream of each boulder weir in which streambed gravels were scoured. The results suggest that these processes reduced the transient storage provided by the surface of the streambed, without improving hyporheic transient storage. The study was conducted in a straightened channel, recently (within the past 200 years) modified from its natural course, and subject to high loadings of agricultural runoff throughout the year. Nutrient processing in streams is known to be strongly affected by agriculture due to stoichiometric effects on microbial biofilm communities (Weigelhofer et al., 2018b) and due to the overwhelming influence of organic matter deposition on nutrient exchange between the streambed and water column (Weigelhofer et al., 2018a). The boulder weirs may have exposed water quality issues faced by the stream more than they mitigated them.

Both the boulder weirs and the leaky dams demonstrated that in-stream structures can, to some extent, attenuate higher flows. Stream velocities at higher discharges were lower in the presence boulder weirs, and peak discharges during storm events were reduced somewhat following leaky dam construction. Stream velocity is influenced by the friction imposed by instream elements (e.g., stones, vegetation, boulders), and the effects that these elements have on stream-flow is dependent on the proportion of channel flow that is in contact with roughness elements (Mason et al., 2012; Zarnetske et al., 2007). By increasing the presence of larger roughness elements that affected higher flows, the weir and leaky dam sections appear to have had an attenuating effect. Importantly, while evidently attenuating peak flows, the scour induced on streambeds and channel-banks around the leaky dams highlighted the very different nature of natural stream channels – which change over time due to dynamic erosion and deposition processes – and anthropogenic channels which should not change due risks of undermining adjacent roads or blocking downstream culverts or pipes (Grabowski et al., 2019).

The swale that was explored in Chapter 5 illustrated the acute and essentially anthropogenic nature of agricultural runoff. Under higher nutrient loadings, increases in the output concentrations of dissolved nutrients (likely via organic matter mineralization within the swale) appeared to dominate over nutrient uptake by soil biota or the soil substrate, while under lower nutrient loadings the swale induced better reduction in dissolved nutrient concentrations along its length. The nutrient loading of waters during some sampling events was markedly higher than those that would occur in streams which are unaffected by human activities (Cunha et al., 2020; Friberg et al., 2010; Graeber et al., 2012). Nonetheless, simple modification, via widening and shallowing of the channel, of a typical farm drain brought about substantial recovery of dissolved oxygen, which is central to efficient processing of organic matter. Through its simplicity further amendments to the swale may facilitate even greater nutrient processing and attenuation.

6.2 The promise of NbS

In a review of NbS, Keesstra et al. (2018) highlighted that for NbS features to be successful, they must be designed and managed with "*a deep understanding of nature's functioning and processes.*" Understanding and accounting for the myriad of hydrological and nutrient transformation processes that may occur within a stream or on the land is a substantial undertaking. It is unlikely that any single NbS feature can be constructed to simultaneously mediate all natural or anthropogenic nutrient or hydrological processes in the agricultural landscape, especially if the expectation is that the feature will operate and be managed at the farm scale. The promise of NbS is that by allowing natural processes to occur, emergent properties of the features may help to address additional or unforeseen challenges (Collier and Bourke, 2020; Heneghan et al., 2021). In agricultural catchments, the legacy and ongoing threat of surplus nutrient inputs and hydrological modification is substantial. The need for addressing the impacts of agriculture on aquatic and human communities is great, and mitigating its effects is a substantial undertaking. This research, and that done by others, has shown that simple modifications to the land such as forging connections between channels and offline retention areas (Acreman et al., 2003; Nicholson et al., 2020) or introducing in-stream impediments to flow (van Leeuwen et al., 2024; Wenzel et al., 2014) can help to reduce peak downstream discharges. Instream and offline NbS features for water quality management have been shown to attenuate targeted water quality pressures (Cunha et al., 2018; Robotham et al., 2021; Shaw Yu et al., 2001). Importantly, however, this research and that presented by others highlights that the functioning of these features may be impaired or even exacerbate target pressures under conditions such as multi-flood peak events (van Leeuwen et al., 2024) or high background nutrient concentrations (Noe et al., 2019; Weigelhofer et al., 2018a). These conditions are unavoidable in the real world and NbS features must not only be constructed to account for these more extreme conditions, but should be situated within the landscape where they do not cause harm to downstream communities if they should fail (e.g. through dislodging of in-stream debris, causing excessive erosion or releasing nutrient pulses downstream).

The success of NbS features, therefore, may be as much to do with appropriate design, as the locations and scale at which they operate within a catchment. NbS features may have to exist within a set, or ‘treatment train’, in which each feature deals with a restricted number of issues (e.g. offline flood peak attenuation) and is closely positioned to or associated with features which can deal with negative consequences of an upstream feature (e.g. phosphorus mitigation in a flood detention basin; Herzog et al., 2019; Lien and Magner, 2017; Stutter et al., 2012). Implementing these sets may be practically difficult within rural catchments due to the need for greater land-take and maintenance, as well as questions around who pays for and is responsible for the NbS features (Lien and Magner, 2017). Nonetheless, the ‘treatment-train’ approach may allow features to work on a scale whereby they confer appreciable benefit to targeted pressures, and whereby the risk of failure is built into the treatment train.

6.3 Limitations

This thesis endeavored to capture a broad range of hydrological, water quality and plant-health processes to gain a holistic understanding of the applicability of NbS at the farm scale. In-doing so, the observations made in the study are inherently bound to the specific land-use, soil type and agricultural history of the study site. The NbS features examined in this thesis produced interesting and frequently unexpected results. Whether these features would confer similar effects on water quality and hydrology in other catchments or in other types of farms should be investigated. This would aid in better targeting of specific features to address specific challenges.

Hydrological data on the effects of the offline and in-stream NbS structures on flood peak mitigation was collected for flood events of less than a 1-in-3-year recurrence interval. Longer-term datasets would yield useful information on how the features may attenuate floods of higher magnitude which pose a greater risk to downstream settlements. The limited timescale of data collection (2021-2023) is arguably a limitation to the interpretation of and broad applicability of all the studies' results.

Results from the swale study gave some insight into the highly variable natures of both the composition of agricultural runoff and of the nutrient transformation processes over the study period. It was clear that enhancing the surface area available for contact with the soil beneath and/or the atmosphere above the water within the swale affected the types and rates of nutrient processing that occurred. Further research may examine how these processes vary vertically within the swale biomat and within the soil (Jones et al., 2018) and how changes in the composition of the microbial community within the emergent biofilm occur over time or in response to changing influent nutrient concentrations (Brady et al., 2021; Jones et al., 2018).

6.4 Broken water

"*The streams from the mountain, the pools from the lea, all run from my faucet and down to the sea*." – Malvina Reynolds, The Faucets Are Dripping, 1959.

Much of Ireland's landscape has been modified either to facilitate flow through areas where flooding is undesirable, or to restrict flow and form reservoirs for municipal water supply or hydro-electricity production. The nutrient content of water and the capacity for stream and terrestrial ecosystems to mediate the flux of those nutrients has been pervasively altered by agriculture and industrial practices. Into the future, the demand for food production in Ireland is likely to intensify as population growth and the global effects of climate change impact food availability. In Ireland, it is predicted that more severe winters will cause livestock to be over-wintered in animal housing for longer periods, and may also reduce the length of the summer grazing period (White et al., 2021; Wreford and Topp, 2020). Longer housing of livestock will increase the need for winter fodder, and space for the storage and spreading of animal slurry, which will pose obvious risks to adjacent streams. In the absence of substantial financial and legal support these constraints may further limit the likelihood that individual landowners will devote their farmland to NbS features.

Supports for agri-environmental measures do exist and projects such as the Duhallow European Innovation Partnership (EIP) and the Pearl Mussel Project have been illustrating the growing appetite for NbS features on farmland, and are yielding encouraging results (Heneghan et al., 2021; McLoughlin et al., 2020). Although the effects on water quality were mixed, this study has empirically demonstrated that the use of pasture fields for flood peak attenuation need not lead to reduction in the health or productivity of the pasture sward. As awareness grows of our impacts on water quality and hydro-morphology, and the positive and negative effects of NbS are quantified and documented, NbS may be put to proper use. However, repairing the damage done and reducing the ongoing harm to aquatic ecosystems may be the vital initial steps.

6.5 Conclusions

This thesis set out to assess five main aspects of the functioning of NbS features in agricultural catchments, i.e. the potential for NbS features to mitigate downstream flood peaks and improve water quality; permit ongoing grazing of agricultural pasture, while providing a flood or water quality management role; to function effectively and in a sustained fashion in seasonally variable conditions; and to be constructed and managed simply and at farm scale yet provide a benefit to flood management and/or water quality. The research may be summarized thus:

1. By increasing the availability of offline or in-stream storage, NbS features can reduce peak flows of a recurrence of at least < 1-in-3 years.
2. Flooding of pasture farmland for peak-flow mitigation (i.e. approx. 150% the duration of a flood peak) during winter may be compatible with summer growth and livestock grazing.
3. In-stream structures will increase stream roughness at reach-scale and help to impede the flux of water, but localized changes to flow around in-stream structures will induce deposition and scour which may be undesirable.
4. Nutrient loadings in agricultural runoff can exert substantial biological oxygen demand. Simple modifications to drains receiving agricultural runoff may enhance processing through dissolved oxygen recovery and improving transient storage.
5. Process-led approach to design of NbS features may facilitate adaptation to local pressures: context and conversation with land-owners is essential.

The study has shown that while relatively simple, farm-scale features may bring about substantial flood peak attenuation – particularly in the case of the detention basin – their effectiveness may be limited to small-scale flood peaks yet be ineffective in mitigating the scale of flood event that brings about economic harm to downstream communities. Importantly, creating features which may operate at a sufficient scale to mitigate such storm events is likely to be beyond the capabilities or indemnity of individual landowners. In-stream flood management features may be more easily installed than offline features and may, in the short-term, permit landowners to incur lower risk to farmland than offline detention basins. These features are less effective for flood mitigation and, in the longer term, may bring about substantial damage to urban and rural infrastructure through bank and streambed erosion and blocking of downstream bridges and culverts.

The study showed that simple NbS features may bring about considerable changes to water quality during storm events and during periods of overland flow and mobilization of agricultural pollutants. Importantly, these changes were highly variable in scale and direction of change and are likely to require diligent and costly investigation and analyses so they can be designed and installed to bring about targeted benefits to water quality.

Future steps in this field should be made to identify locations where these features can be installed in scales at which they may operate to bring about attenuation of damaging flood peaks. Future work may also consider amendments that may be made to flood and water quality mitigation NbS features so that water quality may be improved in a directed and measurable manner. This must be done with acute cognizance of the timing and composition of agricultural runoff when river bodies are at most risk of pollution. Again, this is a task beyond individual landowners and will necessitate substantial engagement from regulatory and scientific stakeholders, as well as buy-in from landowners.

References

Abbe, T.B., Dickerson-Lange, S.E., Kane, M., Cruickshank, P., Kaputa, M., Soden, J., 2019. Can wood placement in degraded channel networks result in large-scale water retention? Federal Interagency Sedimentation and Hydrologic Modelling Conference 20.

Acreman, M., Holden, J., 2013. How wetlands affect floods. Wetlands 33, 773–786. https://doi.org/10.1007/s13157-013-0473-2

Acreman, M.C., Riddington, R., Booker, D.J., 2003. Hydrological impacts of floodplain restoration: A case study of the River Cherwell, UK. Hydrol Earth Syst Sci 7, 75–85. https://doi.org/10.5194/hess-7-75-2003

Addy, S., Wilkinson, M.E., 2019a. Representing natural and artificial in-channel large wood in numerical hydraulic and hydrological models. Wiley Interdisciplinary Reviews: Water. https://doi.org/10.1002/WAT2.1389

Addy, S., Wilkinson, M.E., 2019b. Geomorphic and retention responses following the restoration of a sand-gravel bed stream. Ecol Eng 130, 131–146. https://doi.org/10.1016/j.ecoleng.2019.01.013

Andrews, M., Scholefield, D., Abberton, M.T., McKenzie, B.A., Hodge, S., Raven, J.A., 2007. Use of white clover as an alternative to nitrogen fertiliser for dairy pastures in nitrate vulnerable zones in the UK: Productivity, environmental impact and economic considerations. Annals of Applied Biology 151, 11–23. https://doi.org/10.1111/j.1744-7348.2007.00137.x

Babatunde, A.O., Zhao, Y.Q., O'Neill, M., O'Sullivan, B., 2008. Constructed wetlands for environmental pollution control: A review of developments, research and practice in Ireland. Environ Int 34, 116–126. https://doi.org/10.1016/j.envint.2007.06.013

Bailey-Serres, J., Voesenek, L.A.C.J., 2008. Flooding Stress: Acclimations and Genetic Diversity. Annu Rev Plant Biol 59, 313–339. https://doi.org/10.1146/annurev.arplant.59.032607.092752

Baker, S., Lynch, M.B., Godwin, F., Boland, T.M., Kelly, A.K., Evans, A.C.O., Murphy, P.N.C., Sheridan, H., 2023. Multispecies swards outperform perennial ryegrass under intensive beef grazing. Agric Ecosyst Environ 345. https://doi.org/10.1016/j.agee.2022.108335

Ball, D.F., 1964. Loss-on-ignition as an estimate of organic matter and organic carbon in non-calcareous soils. Journal of Soil Science 15, 84–92.

Banach, K., Banach, A.M., Lamers, L.P.M., De Kroon, H., Bennicelli, R.P., Smits, A.J.M., Visser, E.J.W., 2009. Differences in flooding tolerance between species from two wetland habitats with contrasting hydrology: Implications for vegetation development in future floodwater retention areas. Ann Bot 103, 341–351. https://doi.org/10.1093/aob/mcn183

Barber, N., 2013. Sediment, nutrient and runoff management and mitigation in rural catchments. Newcastle University.

Barber, N.J., Quinn, P.F., 2012. Mitigating diffuse water pollution from agriculture using soft-engineered runoff attenuation features. Area 44, 454–462. https://doi.org/10.1111/j.1475-4762.2012.01118.x

Barickman, T.C., Simpson, C.R., Sams, C.E., 2019. Waterlogging causes early modification in the physiological performance carotenoids, cholorphylls, proline, and soluble sugars of sucumber plants. Plants 160, 1–15.

Barnes, M.S., Bathurst, J.C., Lewis, E., Quinn, P.F., 2023. Leaky dams augment afforestation to mitigate catchment scale flooding. Hydrol Process 37, 1–19. https://doi.org/10.1002/hyp.14920

Battin, T.J., Kaplan, L.A., Newbold, J.D., Hansen, C.M.E., 2003. Contributions of microbial biofilms to ecosystem processes in stream mesocosms. Nature 426, 439–442. https://doi.org/10.1038/nature02152

Beloni, T., Pezzopane, C.G., Rovadoscki, G.A., Fávero, A.P., Dias-Filho, M.B., Santos, P.M., 2017. Morphological and physiological responses and the recovery ability of Paspalum accessions to water deficit and waterlogging. Grass and Forage Science 72, 840–850. https://doi.org/10.1111/gfs.12281

Beltman, B., Willems, J.H., Güsewell, S., 2007. Flood events overrule fertiliser effects on biomass production and species richness in riverine grasslands. Journal of Vegetation Science 18, 625. https://doi.org/10.1658/1100-9233(2007)18[625:feofeo]2.0.co;2

Bencala, K.E., Walters, R.A., 1983. Simulation of solute transport in a mountain pool-riffle stream: a transient storage model. Water Resour Res 19, 718–724.

Bernard-Jannin, L., Sun, X., Teissier, S., Sauvage, S., Sánchez-Pérez, J.M., 2017. Spatio-temporal analysis of factors controlling nitrate dynamics and potential denitrification hot spots and hot moments in groundwater of an alluvial floodplain. Ecol Eng 103, 372–384. https://doi.org/10.1016/j.ecoleng.2015.12.031

Bhattarai, K.P., O’Connor, K.M., 2004. The effects over time of an arterial drainage scheme on the rainfall-runoff transformation in the Brosna catchment. Physics and Chemistry of the Earth 29, 787–794. https://doi.org/10.1016/j.pce.2004.05.006

Birgand, F., Skaggs, R.W., Chescheir, G.M., Gilliam, J.W., 2007. Nitrogen removal in streams of agricultural catchments - A literature review. Crit Rev Environ Sci Technol 37, 381–487. https://doi.org/10.1080/10643380600966426

Black, A., Peskett, L., Macdonald, A., Young, A., Spray, C., Ball, T., Thomas, H., Werritty, A., 2021a. Natural flood management, lag time and catchment scale : Results from an empirical nested catchment study. J Flood Risk Manag 1–16. https://doi.org/10.1111/jfr3.12717

Black, A., Peskett, L., Macdonald, A., Young, A., Spray, C., Ball, T., Thomas, H., Werritty, A., 2021b. Natural flood management, lag time and catchment scale : Results from an empirical nested catchment study. J Flood Risk Manag 1–16. https://doi.org/10.1111/jfr3.12717

Blaen, P.J., Kurz, M.J., Drummond, J.D., Knapp, J.L.A., Mendoza-Lera, C., Schmadel, N.M., Klaar, M.J., Jager, A., Folegot, S., Lee-Cullin, J., Ward, A.S., Zarnetske, J.P., Datry, T., Milner, A.M., Lewandowski, J., Hannah, D.M., Krause, S., 2018. Woody debris is related to reach - scale hotspots of lowland stream ecosystem respiration under baseflow conditions. Ecohydrology 1–9. https://doi.org/10.1002/eco.1952

Boardman, J., Vandaele, K., 2023. Soil erosion and runoff: The need to rethink mitigation strategies for sustainable agricultural landscapes in western Europe. Soil Use Manag 39, 673–685. https://doi.org/10.1111/sum.12898

Boulton, A.J., 2007. Hyporheic rehabilitation in rivers: Restoring vertical connectivity. Freshw Biol 52, 632–650. https://doi.org/10.1111/j.1365-2427.2006.01710.x

Brady, A.R., Vega, M.A., Riddle, K.N., Peel, H.F., Lundeen, E.J., Siegmund, J.G., Sharp, J.O., 2021. Biomat resilience to desiccation and flooding within a shallow, unit process open water engineered Wetland. Water (Switzerland) 13, 1–18. https://doi.org/10.3390/w13060815

Brasil, J., Macedo, M., Lago, C., Oliveira, Thalita, Júnior, M., Oliveira, Tassiana, Mendiondo, E., 2021. Nature-based solutions and real-time control: Challenges and opportunities. Water (Switzerland). https://doi.org/10.3390/w13050651

Brix, H., 1994. Functions of macrophytes in constructed wetlands. Water Science and Technology 29, 71–78. https://doi.org/10.2166/wst.1994.0160

Brix, H., Arias, C.A., 2005. The use of vertical flow constructed wetlands for on-site treatment of domestic wastewater: New Danish guidelines. Ecol Eng 25, 491–500. https://doi.org/10.1016/j.ecoleng.2005.07.009

Brotherton, S.J., Joyce, C.B., 2015. Extreme climate events and wet grasslands: plant traits for ecological resilience. Hydrobiologia 750, 229–243. https://doi.org/10.1007/s10750-014-2129-5

Brown, A.G., Lespez, L., Sear, D.A., Macaire, J., Houben, P., Klimek, K., Brazier, R.E., Oost, K. Van, Pears, B., 2018. Earth-Science Reviews Natural vs anthropogenic streams in Europe : History , ecology and implications for restoration , river-rewilding and riverine ecosystem services. Earth Sci Rev 180, 185–205. https://doi.org/10.1016/j.earscirev.2018.02.001

Brunke, M., 1999. Colmation and depth filtration within streambeds: Retention of particles in hyporheic interstices. Int Rev Hydrobiol 84, 99–117. https://doi.org/10.1002/iroh.199900014

Brunke, M., Gonser, T., 1997. The ecological significance of exchange processes between rivers and groundwater. Freshw Biol 37, 1–33. https://doi.org/10.1046/j.1365-2427.1997.00143.x

Bulc, T.G., Klemenčič, A.K., 2011. Run-off treatment of highly fluctuating waters with subsurface vegetated drainage ditch and river bed with meanders. Fresenius Environ Bull 20, 836–846.

Burek, P., Mubareka, S., Rojas, R., Roo, D., Bianchi, A., Baranzelli, C., Lavalle, C., Vandecasteele, I., 2012. Evaluation of the effectiveness of Natural Water Retention Measures Support to the EU Blueprint to Safeguard Europe’s. https://doi.org/10.2788/5528

Butturini, A., Battin, T.J., Sabater, F., 2000. Nitrification in stream sediment biofilms: The role of ammonium concentration and DOC quality. Water Res 34, 629–639. https://doi.org/10.1016/S0043-1354(99)00171-2

Calder, Reid, N. and G., 2003. Natural Flood Management Measures: A Practical Guide for Farmers.

Carballeira, T., Ruiz, I., Soto, M., 2017. Methanogenic activity of accumulated solids and gas emissions from planted and unplanted shallow horizontal subsurface flow constructed wetlands. Ecol Eng 98, 297–306. https://doi.org/10.1016/j.ecoleng.2016.10.079

Carstensen, M.V., Hashemi, F., Hoffmann, C.C., Zak, D., Audet, J., Kronvang, B., 2020a. Efficiency of mitigation measures targeting nutrient losses from agricultural drainage systems : A review. Ambio 49, 1820–1837. https://doi.org/10.1007/s13280-020-01345-5

Carstensen, M.V., Hashemi, F., Hoffmann, C.C., Zak, D., Audet, J., Kronvang, B., 2020b. Efficiency of mitigation measures targeting nutrient losses from agricultural drainage systems : A review. Ambio 49, 1820–1837. https://doi.org/10.1007/s13280-020-01345-5

CEC, 2000. Directive 2000/60/EC of the European Parliament and of the Council establishing a framework for Community action in the field of water policy.

Cecchetti, A.R., Stiegler, A.N., Graham, K.E., Sedlak, D.L., 2020. The horizontal levee: a multi-benefit nature-based treatment system that improves water quality and protects coastal levees from the effects of sea level rise. Water Res X 7, 100052. https://doi.org/10.1016/j.wroa.2020.100052

Chan, Y.J., Chong, M.F., Law, C.L., Hassell, D.G., 2009. A review on anaerobic-aerobic treatment of industrial and municipal wastewater. Chemical Engineering Journal. https://doi.org/10.1016/j.cej.2009.06.041

Clarke, D., 2013. The performance of Detainment Bunds (DBs) for attenuating phosphorus and sediment loss from pastoral farmland. University of Waiato.

Cole, L.J., Stockan, J., Helliwell, R., 2020. Managing riparian buffer strips to optimise ecosystem services: A review. Agric Ecosyst Environ 296, 106891. https://doi.org/10.1016/j.agee.2020.106891

Collentine, D., Futter, M.N., 2018. Realising the potential of natural water retention measures in catchment flood management: trade-offs and matching interests. J Flood Risk Manag 11, 76–84. https://doi.org/10.1111/jfr3.12269

Collier, M.J., Bourke, M., 2020. The case for mainstreaming nature-based solutions into integrated catchment management in Ireland. Biology and Environment 120B, 107–113. https://doi.org/10.3318/BIOE.2020.08

Colmer T.D., Voesenek L. (2009) Flooding tolerance: suites of plant traits in variable environments. *Functional Plant Biology*, **36**, 665–681. https://doi.org/10.1071/FP09144

Cook, H., Stearne, K., Williamson, T., 2003. The origins of water meadows in England. Agricultural History Review 51, 155–162.

Cooper, M.M.D., Patil, S.D., Nisbet, T.R., Thomas, H., Smith, A.R., McDonald, M.A., 2021. Role of forested land for natural flood management in the UK: A review. Wiley Interdisciplinary Reviews: Water 8, 1–16. https://doi.org/10.1002/wat2.1541

Council Directive 92/43/EEC, 1992. Council Directive 92/43/EEC of 21 May 1992 on the conservation of natural habitats and of wild fauna and flora.

Covino, T., McGlynn, B., Baker, M., 2010. Separating physical and biological nutrient retention and quantifying uptake kinetics from ambient to saturation in successive mountain stream reaches. J Geophys Res Biogeosci 115. https://doi.org/10.1029/2009JG001263

Crawford, S.E., Brinkmann, M., Ouellet, J.D., Lehmkuhl, F., Reicherter, K., Schwarzbauer, J., Bellanova, P., Letmathe, P., Blank, L.M., Weber, R., Brack, W., van Dongen, J.T., Menzel, L., Hecker, M., Schüttrumpf, H., Hollert, H., 2022. Remobilization of pollutants during extreme flood events poses severe risks to human and environmental health. J Hazard Mater 421, 126691. https://doi.org/10.1016/j.jhazmat.2021.126691

Cunha, D.G.F., Finkler, N.R., Calijuri, M. do C., Covino, T.P., Tromboni, F., Dodds, W.K., 2018. Nutrient uptake in a simplified stream channel: Experimental manipulation of hydraulic residence time and transient storage. Ecohydrology 11, 1–10. https://doi.org/10.1002/eco.2012

Cunha, D.G.F., Finkler, N.R., Gómez, N., Cochero, J., Donadelli, J.L., Saltarelli, W.A., Calijuri, M. do C., Miwa, A.C.P., Tromboni, F., Dodds, W.K., Boëchat, I.G., Gücker, B., Thomas, S.A., 2020. Agriculture influences ammonium and soluble reactive phosphorus retention in South American headwater streams. Ecohydrology 13, 1–14. https://doi.org/10.1002/eco.2184

Dadson, S.J., Hall, J.W., Murgatroyd, A., Acreman, M., Bates, P., Beven, K., Heathwaite, L., Holden, J., Holman, I.P., Lane, S.N., O’Connell, E., Penning-Rowsell, E., Reynard, N., Sear, D., Thorne, C., Wilby, R., 2017. A restatement of the natural science evidence concerning catchment-based “natural” flood management in the UK. Proceedings of the Royal Society A: Mathematical, Physical and Engineering Sciences 473. https://doi.org/10.1098/rspa.2016.0706

DAFM (Department of Agriculture, F. and the M., 2017. Protecting and enhancing water for sustainable agriculture. Water-related measures for the agri-food, forestry and marine sectors.

Dalal, V.K., Tripathy, B.C., 2018. Water-stress induced downsizing of light-harvesting antenna complex protects developing rice seedlings from photo-oxidative damage. Sci Rep 8, 10–16. https://doi.org/10.1038/s41598-017-14419-4

Daly, K., 2005. Environmental aspects of soil phosphorus testing. Irish Journal of Agricultural and Food Research 44, 261–279.

Dalzell, B.J., Filley, T.R., Harbor, J.M., 2005. Flood pulse influences on terrestrial organic matter export from an agricultural watershed. J Geophys Res Biogeosci 110, n/a-n/a. https://doi.org/10.1029/2005jg000043

Davidson, N.C., 2014. How much wetland has the world lost? Long-term and recent trends in global wetland area. Mar Freshw Res 65, 934–941. https://doi.org/10.1071/MF14173

Davis, A.P., Stagge, J.H., Jamil, E., Kim, H., 2012. Hydraulic performance of grass swales for managing highway runoff. Water Res 46, 6775–6786. https://doi.org/10.1016/j.watres.2011.10.017

Deasy, C., Quinton, J.N., Silgram, M., Bailey, A.P., Jackson, B., Stevens, C.J., 2009a. Mitigation Options for Sediment and Phosphorus Loss from Winter-sown Arable Crops. J Environ Qual 38, 2121–2130. https://doi.org/10.2134/jeq2009.0028

Deasy, C., Quinton, J.N., Silgram, M., Bailey, A.P., Jackson, B., Stevens, C.J., 2009b. Mitigation Options for Sediment and Phosphorus Loss from Winter-sown Arable Crops. J Environ Qual 38, 2121–2130. https://doi.org/10.2134/jeq2009.0028

Deletic, A., Fletcher, T.D., 2006. Performance of grass filters used for stormwater treatment - A field and modelling study. J Hydrol (Amst) 317, 261–275. https://doi.org/10.1016/j.jhydrol.2005.05.021

Department of Housing Local Government and Heritage, 2022. Third Cycle Draft River Basin Management Plan 2022-2027 - Consultation Report.

Dodds, Walter, K., 2002. Freshwater Ecology - Concepts and Environmental Applications. Academic Press.

Dodds, W.K., Martí, E., Tank, J.L., Pontius, J., Hamilton, S.K., Grimm, N.B., Bowden, W.B., McDowell, W.H., Peterson, B.J., Valett, H.M., Webster, J.R., Gregory, S., 2004. Carbon and nitrogen stoichiometry and nitrogen cycling rates in streams. Oecologia 140, 458–467. https://doi.org/10.1007/s00442-004-1599-y

Doody, D., Cross, P., Wither, P., Cassidy, R., Augustenborg, C., Pullin, A., Carton, O., Crosse, S., 2016. AgImpact Project: A systematic and participatory review of research on the impact of agriculture on aquatic ecosystems in Ireland.

Doody, D.G., Archbold, M., Foy, R.H., Flynn, R., 2012a. Approaches to the implementation of the Water Framework Directive: Targeting mitigation measures at critical source areas of diffuse phosphorus in Irish catchments. J Environ Manage 93, 225–234. https://doi.org/10.1016/j.jenvman.2011.09.002

Doody, D.G., Archbold, M., Foy, R.H., Flynn, R., 2012b. Approaches to the implementation of the Water Framework Directive: Targeting mitigation measures at critical source areas of diffuse phosphorus in Irish catchments. J Environ Manage 93, 225–234. https://doi.org/10.1016/j.jenvman.2011.09.002

Duan, S., Newcomer-Johnson, T., Mayer, P., Kaushal, S., 2016. Phosphorus retention in stormwater control structures across streamflow in urban and suburban watersheds. Water (Switzerland) 8, 1–17. https://doi.org/10.3390/w8090390

Duffy, A., Moir, S., Berwick, N., Shabashow, J., D'arcy, B., Wade, R., 2016. Rural Sustainable Drainage Systems A Practical Design and Build Guide for Scotland's Farmers and Landowners Helping to protect Scotland's most valuable resource.

Dunne, E.J., Culleton, N., O'Donovan, G., Harrington, R., Olsen, A.E., 2005. An integrated constructed wetland to treat contaminants and nutrients from dairy farmyard dirty water. Ecol Eng 24, 219–232. https://doi.org/10.1016/j.ecoleng.2004.11.010

Durand, P., Breuer, L., Johnes, P.J., Billen, G., Butturini, A., Pinay, G., van Grinsven, H., Garnier, J., Rivett, M., Reay, D.S., Curtis, C., Siemens, J., Maberly, S., Kaste, Ø., Humborg, C., Loeb, R., de Klein, J., Hejzlar, J., Skoulikidis, N., Kortelainen, P., Lepistö, A., Wright, R., 2011. Nitrogen processes in aquatic ecosystems. The European Nitrogen Assessment 126–146. https://doi.org/10.1017/cbo9780511976988.010

Easson, L., Keys, A., McAdam, J., 2021. Water Innovation Network EIP initial feasibility study.

Ebrahimiyan, M., Majidi, M.M., Mirlohi, A., Noroozi, A., 2013. Physiological traits related to drought tolerance in tall fescue. Euphytica 190, 401–414. https://doi.org/10.1007/s10681-012-0808-8

EC, 2015. Towards an EU research and innovation policy agenda for nature-based solutions and re-naturing cities. Final report of the Horizon 2020 Expert Group on nature-based solutions and re-naturing cities. Directorate-General for Research and Innovation 2015 Climate Action, Environment, Resource Efficiency and Raw Material. Luxembourg.

Edwards, A.C., Hooda, P.S., 2008. Farmyard point discharges and their influence on nutrient and labile carbon dynamics in a second order stream draining through a dairy unit. J Environ Manage 87, 591–599. https://doi.org/10.1016/j.jenvman.2007.02.013

Edwards, A.C., Kay, D., McDonald, A.T., Francis, C., Watkins, J., Wilkinson, J.R., Wyer, M.D., 2008. Farmyards, an overlooked source for highly contaminated runoff. J Environ Manage 87, 551–559. https://doi.org/10.1016/j.jenvman.2006.06.027

Edwards, A.C., Watson, H.A., Cook, Y.E.M., 2012. Source strengths, transport pathways and delivery mechanisms of nutrients, suspended solids and coliforms within a small agricultural headwater catchment. Science of the Total Environment 434, 123–129. https://doi.org/10.1016/j.scitotenv.2011.10.055

Ekka, S.A., Rujner, H., Leonhardt, G., Blecken, G.T., Viklander, M., Hunt, W.F., 2021. Next generation swale design for stormwater runoff treatment: A comprehensive approach. J Environ Manage. https://doi.org/10.1016/j.jenvman.2020.111756

Ellis, N., Anderson, K., Brazier, R., 2021. Mainstreaming natural flood management: A proposed research framework derived from a critical evaluation of current knowledge. Prog Phys Geogr 45, 819–841. https://doi.org/10.1177/0309133321997299

Enders, E.C., Scruton, D, C., Clarke, K, D., 2009. The “natural flow paradigm” and Atlantic Salmon - Moving from concept to practice. River Res Appl 25, 2–15. https://doi.org/10.1002/rra

Environmental Protection Agency, 2022. Water Quality in Ireland 2016-2021.

Environmental Protection Agency, 2018. Corine Landcover [WWW Document]. Corine Landcover 2018. https://doi.org/https://data.gov.ie/dataset/corine-landcover-2018

Environmental Protection Agency, 2003. Guidance on the construction of swales for water quality improvement and flow attenuation of lightly contaminated runoff from poultry farms.

European Union, 2007. Directive 2007/60/EC of the European Counil and European Parliment of 23 October 2007 on the assessment and management of flood risks. Official Journal of the European Union 27–34.

Fenton, O., Ó hUallacháin, D., 2012. Agricultural nutrient surpluses as potential input sources to grow third generation biomass (microalgae): A review. Algal Res 1, 49–56. https://doi.org/10.1016/j.algal.2012.03.003

Fenton, O., Rice, P., Murnane, J.G., Tuohy, P., Daly, K., 2022. Dairy farm roadway surface materials as a P-source within the nutrient transfer continuum framework. Front Environ Sci 10. https://doi.org/10.3389/fenvs.2022.878166

Fenton, O., Tuohy, P., Daly, K., Moloney, T., Rice, P., Murnane, J.G., 2021. A Review of On-farm Roadway Runoff Characterisation and Potential Management Options for Ireland. Water Air Soil Pollut 232. https://doi.org/10.1007/s11270-021-05027-0

Fiener, P., Auerswald, K., Weigand, S., 2005. Managing erosion and water quality in agricultural watersheds by small detention ponds. Agric Ecosyst Environ 110, 132–142. https://doi.org/10.1016/j.agee.2005.03.012

Fischer, H., Kloep, F., Wilzcek, S., Pusch, M.T., 2005. A river's liver - Microbial processes within the hyporheic zone of a large lowland river. Biogeochemistry 76, 349–371. https://doi.org/10.1007/s10533-005-6896-y

Flávio, H.M., Ferreira, P., Formigo, N., Svendsen, J.C., 2017. Reconciling agriculture and stream restoration in Europe: A review relating to the EU Water Framework Directive. Science of the Total Environment 596–597, 378–395. https://doi.org/10.1016/j.scitotenv.2017.04.057

Fleming-Singer, M.S., Horne, A.J., 2002. Enhanced nitrate removal efficiency in wetland microcosms using an episediment layer for denitrification. Environ Sci Technol 36, 1231–1237. https://doi.org/10.1021/es010967i

Forbes, H., Ball, K., McLay, F., 2015. Natural Flood Management Handbook. Scottish Environment Protection Agency.

Forshay, K.J., Stanley, E.H., 2005. Rapid nitrate loss and denitrification in a temperate river floodplain. Biogeochemistry 75, 43–64. https://doi.org/10.1007/s10533-004-6016-4

Fossitt, J.A., 2000. A guide to habitats in Ireland. Heritage Council. NPWS 115.

Friberg, N., 2014. Impacts and indicators of change in lotic ecosystems. Wiley Interdisciplinary Reviews: Water 1, 513–531. https://doi.org/10.1002/wat2.1040

Friberg, N., Skriver, J., Larsen, S.E., Pedersen, M.L., Buffagni, A., 2010. Stream macroinvertebrate occurrence along gradients in organic pollution and eutrophication. Freshw Biol 55, 1405–1419. https://doi.org/10.1111/j.1365-2427.2008.02164.x

Ganche, E., O'Donovan, M., Delaby, L., Boland, T.M., Kennedy, E., 2015. Does post-grazing sward height influence sward characteristics, seasonal herbage dry-matter production and herbage quality? Grass and Forage Science 70, 130–143. https://doi.org/10.1111/gfs.12113

Gattringer, J.P., Ludewig, K., Harvolk-Schöning, S., Donath, T.W., Otte, A., 2018. Interaction between depth and duration matters: flooding tolerance of 12 floodplain meadow species. Plant Ecol 219, 973–984. https://doi.org/10.1007/s11258-018-0850-2

Gooseff, M.N., Hall, R.O., Tank, J.L., 2007. Relating transient storage to channel complexity in streams of varying land use in Jackson Hole, Wyoming. Water Resour Res 43, 1–10. https://doi.org/10.1029/2005WR004626

Gooseff, M.N., McKnight, D.M., Runkel, R.L., Duff, J.H., 2004. Denitrification and hydrologic transient storage in a glacial meltwater stream, McMurdo Dry Valleys, Antarctica. Limnol Oceanogr 49, 1884–1895. https://doi.org/10.4319/lo.2004.49.5.1884

Gordon, N.D., McMahon, T.A., L.Finlayson, B., Gippel, C.J., Nathan, R.J., 2004a. Stream Hydrology: An Introduction for Ecologists, 2nd ed. Wiley.

Gordon, R.P., Lautz, L.K., Daniluk, T.L., 2013. Spatial patterns of hyporheic exchange and biogeochemical cycling around cross-vane restoration structures: Implications for stream restoration design. Water Resour Res 49, 2040–2055. https://doi.org/10.1002/wrcr.20185

Government of Ireland and Tailte Eire, 2023a. Geohive [WWW Document]. URL https://webapps.geohive.ie/mapviewer/index.html (accessed 12.15.23).

Government Publications Office, 1945. Arterial Drainage Act.

Grabowski, R.C., Gurnell, A.M., Burgess-Gamble, L., England, J., Holland, D., Klaar, M.J., Morrissey, I., Uttley, C., Wharton, G., 2019. The current state of the use of large wood in river restoration and management. Water and Environment Journal 33, 366–377. https://doi.org/10.1111/wej.12465

Graeber, D., Gelbrecht, J., Pusch, M.T., Anlanger, C., von Schiller, D., 2012. Agriculture has changed the amount and composition of dissolved organic matter in Central European headwater streams. Science of the Total Environment 438, 435–446. https://doi.org/10.1016/j.scitotenv.2012.08.087

Graeber, D., Tenzin, Y., Stutter, M., Weigelhofer, G., Shatwell, T., von Tümpling, W., Tittel, J., Wachholz, A., Borchardt, D., 2021. Bioavailable DOC: reactive nutrient ratios control heterotrophic nutrient assimilation—An experimental proof of the macronutrient-access hypothesis. Biogeochemistry 155, 1–20. https://doi.org/10.1007/s10533-021-00809-4

Grimaldi, C., Fossey, M., Thomas, Z., Fauvel, Y., Merot, P., 2012. Nitrate attenuation in soil and shallow groundwater under a bottomland hedgerow in a European farming landscape. Hydrol Process 26, 3570–3578. https://doi.org/10.1002/hyp.8441

Gulap, S., Gitika, T., 2019. Flood frequency analysis using Gumbel’s distribution method: a lower downstream of Lohit River (Dangori River), Assam (India). International Journal of Civil Engineering and Technology 10, 229–234.

Guthrie, S., Dunkerley, F., Tabaqchali, H., Harshfield, A., Ioppolo, B., Manville, C., 2018. Impact of ammonia emissions from agriculture on biodiversity: An evidence synthesis, Impact of ammonia emissions from agriculture on biodiversity: An evidence synthesis. https://doi.org/10.7249/rr2695

Hall, R.J.O., Bernhardt, E.S., Likens, G.E., 2002. Relating nutrient uptake with transient storage in forested mountain streams. Limnol Oceanogr 47, 255–265. https://doi.org/10.4319/lo.2002.47.1.0255

Hankin, B., Hewitt, I., Sander, G., Danieli, F., Formetta, G., Kamilova, A., Kretzschmar, A., Kiradjiev, K., Wong, C., Pegler, S., Lamb, R., 2020. A risk-based network analysis of distributed in-stream leaky barriers for flood risk management. Natural Hazards and Earth System Sciences 20, 2567–2584. https://doi.org/10.5194/nhess-20-2567-2020

Harrington, C., Scholz, M., Culleton, N., Lawlor, P.G., 2012. The use of integrated constructed wetlands (ICW) for the treatment of separated swine wastewaters. Wetland Services & Management 111–119. https://doi.org/10.1007/s10750-011-0945-4

Harrison, S., McAree, C., Mulville, W., Sullivan, T., 2019. The problem of agricultural 'diffuse' pollution: Getting to the point. Science of the Total Environment 677, 700–717. https://doi.org/10.1016/j.scitotenv.2019.04.169

Hartig, F., 2022. DHARMa: Residual Diagnostics for Hierarchical (Multi-Level / Mixed) Regression Models. R package version 0.4.6.

Harvey, J.W., Bencala, K.E., 1993. The effect of streambed topography on surface-subsurface water exchange in mountain channels. Water Resour Res 29, 89–98.

Harvey, J.W., Böhlke, J.K., Voytek, M.A., Scott, D., Tobias, C.R., 2013. Hyporheic zone denitrification: Controls on effective reaction depth and contribution to whole-stream mass balance. Water Resour Res 49, 6298–6316. https://doi.org/10.1002/wrcr.20492

Hauer, F.R., Lamberti, G.A., 2017. Methods in Stream Ecology, Methods in Stream Ecology: Third Edition. https://doi.org/10.2307/2266075

Healy, M.G., Rodgers, M., Mulqueen, J., 2007. Treatment of dairy wastewater using constructed wetlands and intermittent sand filters. Bioresour Technol 98, 2268–2281. https://doi.org/10.1016/j.biortech.2006.07.036

Heneghan, E., Collier, M., Kelly-Quinn, M., 2021. An evaluation of the potential applications of nature-based solutions for water quality protection: Ireland as a case study. Biology and Environment 121B, 147–162. https://doi.org/10.3318/BIOE.2021.14

Herzog, S.P., Eisenstein, W.A., Halpin, B.N., Potmann, A.C., Fitzgerald, Nicole, J.M., Ward, A.S., Higgins, C.P., Mccray, J.E., 2019. Co-design of engineered hyporheic zones to improve in-stream stormwater treatment and facilitate regulatory approval. Water (Basel) 11, 1–18.

Herzog, S.P., Galloway, J., Banks, E.W., Posselt, M., Jaeger, A., Portmann, A., Sahm, R., Kusebauch, B., Lewandowski, J., Ward, A.S., 2023. Combined Surface-Subsurface Stream Restoration Structures Can Optimize Hyporheic Attenuation of Stream Water Contaminants. Environ Sci Technol 57, 4153–4166. https://doi.org/10.1021/acs.est.2c05967

Herzog, S.P., Higgins, C.P., McCray, J.E., 2016. Engineered streambeds for induced hyporheic flow: Enhanced removal of nutrients, pathogens, and metals from urban streams. Journal of Environmental Engineering (United States) 142, 1–10. https://doi.org/10.1061/(ASCE)EE.1943-7870.0001012

Herzog, S.P., Higgins, C.P., Singha, K., McCray, J.E., 2018. Performance of Engineered Streambeds for Inducing Hyporheic Transient Storage and Attenuation of Resazurin. Environ Sci Technol 52, 10627–10636. https://doi.org/10.1021/acs.est.8b01145

Hester, E.T., Doyle, M.W., 2008. In-stream geomorphic structures as drivers of hyporheic exchange. Water Resour Res 44, 1–17. https://doi.org/10.1029/2006WR005810

Hester, E.T., Doyle, M.W., Poole, G.C., 2009. The influence of in-stream structures on summer water temperatures via induced hyporheic exchange. Limnol Oceanogr 54, 355–367.

Hester, E.T., Gooseff, M.N., 2010. Moving beyond the banks: Hyporheic restoration is fundamental to restoring ecological services and functions of streams. Environ Sci Technol 44, 1521–1525. https://doi.org/10.1021/es902988n

Heuck, C., Weig, A., Spohn, M., 2015. Soil microbial biomass C: N: P stoichiometry and microbial use of organic phosphorus. Soil Biol Biochem 85, 119–129. https://doi.org/10.1016/j.soilbio.2015.02.029

Hogan, S.C., O'Sullivan, J.J., Bruen, M., Jarvie, H.P., Cox, E.J., Bowes, M.J., Kelly-Quinn, M., 2023. A review of the nature and source of nutrient impairment in small streams: a desk based characterisation for targeted mitigation measures. Hydrobiologia. https://doi.org/10.1007/s10750-022-05114-1

Hooda, P.S., Moynagh, M., Svoboda, I.F., Miller, A., 2000. Macroinvertebrates as bioindicators of water pollution in streams draining dairy farming catchments. Chemistry and Ecology 17, 17–30. https://doi.org/10.1080/02757540008037658

https://www.oxyguard.dk, 2020. Oxyguard [WWW Document]. URL https://www.oxyguard.dk/media/iyykmbrn/h02a2-handy-atmosphere-brochure-gb-2020-01.pdf

Hurtado-Uria, C., Hennessy, D., Shalloo, L., O'Connor, D., Delaby, L., 2013. Relationships between meteorological data and grass growth over time in the south of Ireland. Irish Geography 46, 175–201. https://doi.org/10.1080/00750778.2013.865364

Insausti, P., Grimoldi, A.A., Chaneton, E.J., Vasellati, V., 2001. Flooding induces a suite of adaptive plastic responses in the grass Paspalum dilatatum. New Phytologist 152, 291–299. https://doi.org/10.1111/j.0028-646X.2001.257_1.x

Janes, V.J., Grabowski, R.C., Mant, J., Allen, D., Morse, J.L., Haynes, H., 2017. The impacts of natural flood management approaches on in-channel sediment quality. River Res Appl 33, 89–101. https://doi.org/10.1002/rra.3068

Jaramillo, D.M., Sheridan, H., Soder, K., Dubeux, J.C.B., 2021. Enhancing the sustainability of temperate pasture systems through more diverse swards. Agronomy. https://doi.org/10.3390/agronomy11101912

Jarvie, H.P., Sharpley, A.N., Scott, J.T., Haggard, B.E., Bowes, M.J., Massey, L.B., 2012. Within-river phosphorus retention: Accounting for a missing piece in the watershed phosphorus puzzle. Environ Sci Technol 46, 13284–13292. https://doi.org/10.1021/es303562y

Jasper, J.T., Jones, Z.L., Sharp, J.O., Sedlak, D.L., 2014a. Biotransformation of trace organic contaminants in open-water unit process treatment wetlands. Environ Sci Technol 48, 5136–5144. https://doi.org/10.1021/es500351e

Jasper, J.T., Jones, Z.L., Sharp, J.O., Sedlak, D.L., 2014b. Nitrate removal in shallow, Open-water treatment wetlands. Environ Sci Technol 48, 11512–11520. https://doi.org/10.1021/es502785t

Jasper, J.T., Sedlak, D.L., 2014. Phototransformation of Wastewater-Derived Trace Organic Contaminants in Open-Water Unit Process Treatment Wetlands. Environ Sci Technol 47, 10781–10790. https://doi.org//10.1021/es304334w

Jaynes, D.B., Isenhart, T.M., 2014. Reconnecting Tile Drainage to Riparian Buffer Hydrology for Enhanced Nitrate Removal. J Environ Qual 43, 631–638. https://doi.org/10.2134/jeq2013.08.0331

Jones, C.N., Scott, D.T., Guth, C., Hester, E.T., Hession, W.C., 2015. Seasonal Variation in Floodplain Biogeochemical Processing in a Restored Headwater Stream. Environ Sci Technol 49, 13190–13198. https://doi.org/10.1021/acs.est.5b02426

Jones, Z.L., Mikkelson, K.M., Nygren, S., Sedlak, D.L., Sharp, J.O., 2018. Establishment and convergence of photosynthetic microbial biomats in shallow unit process open-water wetlands. Water Res 133, 132–141. https://doi.org/10.1016/j.watres.2018.01.021

Jordan, P., Melland, A.R., Mellander, P.E., Shortle, G., Wall, D., 2012. The seasonality of phosphorus transfers from land to water: Implications for trophic impacts and policy evaluation. Science of the Total Environment 434, 101–109. https://doi.org/10.1016/j.scitotenv.2011.12.070

Jordan, P., Menary, W., Daly, K., Kiely, G., Morgan, G., Byrne, P., Moles, R., 2005. Patterns and processes of phosphorus transfer from Irish grassland soils to rivers — integration of laboratory and catchment studies. J Hydrol (Amst) 304, 20–34. https://doi.org/10.1016/j.jhydrol.2004.07.021

Joyce, C.B., Simpson, M., Casanova, M., 2016. Future wet grasslands: ecological implications of climate change. Ecosystem Health and Sustainability 2, 1–15. https://doi.org/10.1002/ehs2.1240

Jung, V., Hoffmann, L., Muller, S., 2009. Ecophysiological responses of nine floodplain meadow species to changing hydrological conditions. Plant Ecol 201, 589–598. https://doi.org/10.1007/s11258-008-9508-9

Kadlec, R.H., 2009. Comparison of free water and horizontal subsurface treatment wetlands. Ecol Eng 35, 159–174. https://doi.org/10.1016/j.ecoleng.2008.04.008

Kail, J., Hering, D., 2005. Using large wood to restore streams in Central Europe: Potential use and likely effects. Landsc Ecol 20, 755–772. https://doi.org/10.1007/s10980-005-1437-6

Kasahara, T., Hill, A.R., Kasahara, T., Hill, A.R., 2006. Effects of riffle-step restoration on hyporheic zone chemistry in N-rich lowland streams. Canadian Journal of Fisheries and Aquatic Sciences 63, 120–133. https://doi.org/10.1139/f05-199

Keesstra, S., Nunes, J., Novara, A., Finger, D., Avelar, D., Kalantari, Z., Cerdà, A., 2018. The superior effect of nature based solutions in land management for enhancing ecosystem services. Science of the Total Environment 610–611, 997–1009. https://doi.org/10.1016/j.scitotenv.2017.08.077

Keesstra, S., Sannigrahi, S., López-Vicente, M., Pulido, M., Novara, A., Visser, S., Kalantari, Z., 2021. The role of soils in regulation and provision of blue and green water. Philosophical Transactions of the Royal Society B: Biological Sciences 376. https://doi.org/10.1098/rstb.2020.0175

Keys, T.A., Govenor, H., Jones, C.N., Hession, W.C., Hester, E.T., Scott, D.T., 2018. Effects of large wood on floodplain connectivity in a headwater Mid-Atlantic stream. Ecol Eng 118, 134–142. https://doi.org/10.1016/j.ecoleng.2018.05.007

Kianpoor Kalkhajeh, Y., Jabbarian Amiri, B., Huang, B., Henareh Khalyani, A., Hu, W., Gao, H., Thompson, M.L., 2019. Methods for Sample Collection, Storage, and Analysis of Freshwater Phosphorus. Water (Basel) 11, 1889. https://doi.org/10.3390/w11091889

Kilpatrick, F.A., Cobb, E.D., 1985. Measurement of discharge using tracers, in: Unitied States Geological Survey.

Kitanović, V., Greet, J., McKendrick, S.A., Jones, C.S., 2023. Riparian and terrestrial grasses display unexpected tolerance to cool-season inundation. Wetl Ecol Manag 31, 551–564. https://doi.org/10.1007/s11273-023-09934-3

Kløve, B., 2000. Retention of suspended solids and sediment bound nutrients from peat harvesting sites with peak runoff control, constructed floodplains and sedimentation ponds. Boreal Environment Research 5, 81–94.

Knight, R.L., Payne, V.W.E., Borer, R.E., Clarke, R.A., Pries, J.H., 2000. Constructed Wetlands for Wastewater Management. Ecol Eng 15, 41–55.

Krause, S., Klaar, M.J., Hannah, D.M., Mant, J., Bridgeman, J., Trimmer, M., Manning-Jones, S., 2014. The potential of large woody debris to alter biogeochemical processes and ecosystem services in lowland rivers. Wiley Interdisciplinary Reviews: Water 1, 263–275. https://doi.org/10.1002/wat2.1019

Kröger, R., Dunne, E.J., Novak, J., King, K.W., McLellan, E., Smith, D.R., Strock, J., Boomer, K., Tomer, M., Noe, G.B., 2013. Downstream approaches to phosphorus management in agricultural landscapes: Regional applicability and use. Science of the Total Environment 442, 263–274. https://doi.org/10.1016/j.scitotenv.2012.10.038

Kuypers, M.M.M., Marchant, H.K., Kartal, B., 2018. The microbial nitrogen-cycling network. Nat Rev Microbiol 16, 263–276. https://doi.org/10.1038/nrmicro.2018.9

Kuzyakov, Y., Friedel, J.K., Stahr, K., 2000. Review of mechanisms and quantification of priming effects. Soil Biol Biochem 32, 1485–1498. https://doi.org/10.1016/S0038-0717(00)00084-5

Lappalainen, H. K.; Kerminen, V. M.; Petajä , T.; Kurten, T.;¨Baklanov, A.; Shvidenko, A.; Back, J.; Vihma, T.; Alekseychik, P.;¨Andreae, M. O.; Arnold, S. R.; Arshinov, M.; Asmi, E.; Belan, B.; Bobylev, L.; Chalov, S.; Cheng, Y.; Chubarova, N.; de Leeuw, G.; Ding, A.; Dobrolyubov, S.; Dubtsov, S.; Dyukarev, E.; Elansky, N.; Eleftheriadis, K.; Esau, I.; Filatov, N.; Flint, M.; Fu, C.; Glezer, O.; Gliko, A.; Heimann, M.; Holtslag, A. A. M.; Hõrrak, U.; Janhunen, J.; Juhola, S.; Jarvi, L.; Ja¨rvinen, H.; Kanukhina, A.; Konstantinov, P.;¨Kotlyakov, V.; Kieloaho, A. J.; Komarov, A. S.; Kujansuu, J.; Kukkonen, I.; Duplissy, E. M.; Laaksonen, A.; Laurila, T.; Lihavainen, H.; Lisitzin, A.; Mahura, A.; Makshtas, A.; Mareev, E.; Mazon, S.; Matishov, D.; Melnikov, V.; Mikhailov, E.; Moisseev, D.; Nigmatulin, R.; Noe, S. M.; Ojala, A.; Pihlatie, M.; Popovicheva, O.; Pumpanen, J.; Regerand, T.; Repina, I.; Shcherbinin, A.; Shevchenko, V.; Sipila, M.; Skorokhod, A.;¨Spracklen, D. V.; Su, H.; Subetto, D. A.; Sun, J.; Terzhevik, A. Y.; Timofeyev, Y.; Troitskaya, Y.; Tynkkynen, V. P.; Kharuk, V. I.; Zaytseva, N.; Zhang, J.; Viisanen, Y.; Vesala, T.; Hari, P.; Hansson, H. C.; Matvienko, G. G.; Kasimov, N. S.; Guo, H.; Bondur, V.; Zilitinkevich, S.; Kulmala, M. Pan-Eurasian Experiment (PEEX): towards a holistic understanding of the feedbacks and interactions in the land−atmosphere−ocean−society continuum in the northern Eurasian region. Atmos. Chem. Phys. 2016, 16, 14421−14461.

Lane, S.N., 2017. Natural flood management. Wiley Interdisciplinary Reviews: Water 4, 1–14. https://doi.org/10.1002/wat2.1211

Laughlin, G.P., Ranatunga, K., Brinkley, T.R., Johnson, I.R., Hutchinson, M.F., 2007. GROWEST PLUS: A tool for rapid assessment of seasonal growth for environmental planning and assessment. Environmental Modelling and Software 22, 1196–1207. https://doi.org/10.1016/j.envsoft.2006.06.014

Lehmann, J., Bossio, D.A., Kögel-Knabner, I., Rillig, M.C., 2020. The concept and future prospects of soil health. Nat Rev Earth Environ 1, 544–553. https://doi.org/10.1038/s43017-020-0080-8

Leverenz, H.L., Haunschild, K., Hopes, G., Tchobanoglous, G., Darby, J.L., 2010. Anoxic treatment wetlands for denitrification. Ecol Eng 36, 1544–1551. https://doi.org/10.1016/j.ecoleng.2010.03.014

Levine, B., Horne, D., Burkitt, L., Tanner, C., Sukias, J., Condron, L., Paterson, J., 2021. The ability of detainment bunds to decrease surface runoff leaving pastoral catchments: Investigating a novel approach to agricultural stormwater management. Agric Water Manag 243, 106423. https://doi.org/10.1016/j.agwat.2020.106423

Lewis, C., Rafique, R., Foley, N., Leahy, P., Morgan, G., Albertson, J., Kumar, S., Kiely, G., 2013. Seasonal exports of phosphorus from intensively fertilised nested grassland catchments. J Environ Sci (China) 25, 1847–1857. https://doi.org/10.1016/S1001-0742(12)60255-1

Lichtenthaler, H.K., Buschmann, C., 2001. Chlorophylls and Carotenoids Measurement and UV-VIS characterization. Current Protocols in Food Analytical Chemistry F4.3.1-F4., 1–8.

Lien, E., Magner, J., 2017. Engineered biosystem treatment trains: A review of agricultural nutrient sequestration. International Journal of Latest Technology in Engineering & Management 1, 5–10.

Lightbody, A.F., Avener, M.E., Nepf, H.M., 2008. Observations of short-circuiting flow paths within a free-surface wetland in Augusta, Georgia, U.S.A. Limnol Oceanogr 53, 1040–1053. https://doi.org/10.4319/lo.2008.53.3.1040

Liljaniemi, P., Vuori, K.M., Tossavainen, T., Kotanen, J., Haapanen, M., Lepistö, A., Kenttämies, K., 2003. Effectiveness of Constructed Overland Flow Areas in Decreasing Diffuse Pollution from Forest Drainages. Environ Manage. https://doi.org/10.1007/s00267-003-2927-4

Liu, C., Li, R., Fu, Y., 2022. Nutrient retention in agricultural headwater stream: artificial manipulation of main-channel morphology and hydrologic condition. Environmental Science and Pollution Research 29, 83004–83019. https://doi.org/10.1007/s11356-022-21660-6

Liu, M., Jiang, Y., 2015. Genotypic variation in growth and metabolic responses of perennial ryegrass exposed to short-term waterlogging and submergence stress. Plant Physiology and Biochemistry 95, 57–64. https://doi.org/10.1016/j.plaphy.2015.07.008

Liu, T., Bruins, R.J.F., Heberling, M.T., 2018. Factors influencing farmers' adoption of best management practices: A review and synthesis. Sustainability (Switzerland). https://doi.org/10.3390/su10020432

Lloyd, C.E.M., Johnes, P.J., Freer, J.E., Carswell, A.M., Jones, J.I., Stirling, M.W., Hodgkinson, R.A., Richmond, C., Collins, A.L., 2019. Determining the sources of nutrient flux to water in headwater catchments: Examining the speciation balance to inform the targeting of mitigation measures. Science of the Total Environment 648, 1179–1200. https://doi.org/10.1016/j.scitotenv.2018.08.190

Lockwood, T., 2022. Quantifying the efficacy of Natural Flood Management in agricultural headwater catchments.

Lockwood, T., Freer, J., Michaelides, K., Brazier, R.E., Coxon, G., 2022. Assessing the efficacy of offline water storage ponds for natural flood management. Hydrol Process 36, 1–17. https://doi.org/10.1002/hyp.14618

Loka, D., Harper, J., Humphreys, M., Gasior, D., Wootton-Beard, P., Gwynn-Jones, D., Scullion, J., Doonan, J., Kingston-Smith, A., Dodd, R., Wang, J., Chadwick, D., Hill, P., Jones, D., Mills, G., Hayes, F., Robinson, D., 2019. Impacts of abiotic stresses on the physiology and metabolism of cool-season grasses: A review. Food Energy Secur 8, 1–29. https://doi.org/10.1002/fes3.152

Lowe, B.J., Watts, R.J., Roberts, J., Robertson, A., 2010. The effect of experimental inundation and sediment deposition on the survival and growth of two herbaceous riverbank plant species. Plant Ecol 209, 57–69. https://doi.org/10.1007/s11258-010-9721-1

Ludwig, A., Hession, W.C., Scott, D., Gallagher, D., 2016. Simulated flood of a small constructed floodplain wetland in Virginia: Event-scale pollutant attenuation. Trans ASABE 59, 1321–1331. https://doi.org/10.13031/trans.59.11622

Ma, T., Rolett, B. V., Zheng, Z., Zong, Y., 2020. Holocene coastal evolution preceded the expansion of paddy field rice farming. Proc Natl Acad Sci U S A 117, 24138–24143. https://doi.org/10.1073/pnas.1919217117

Mackenzie, S.M., Mcilwraith C I, 2015. Constructed Farm Wetlands Treating agricultural water pollution and enhancing biodiversity.

Mackenzie, S.M., Mcilwraith, C.I., Mansfield, P., Mackenzie, S., Mcilwraith, C., 2013. Constructed farm wetlands-treating agricultural water pollution and enhancing biodiversity Produced by Wildfowl and Wetlands Trust with Natural England Catchment Sensitive Farming Contacts for this publication.

Magette, W.L., Hallissey, R., Hughes, K., Cosgrave, E., 2007. Eutrophication from Agricultural Sources : Field- and Catchment-Scale Risk Assessment, Environmental Protection Agency.

Magliozzi, C., Grabowski, R.C., Packman, A.I., Krause, S., 2018. Toward a conceptual framework of hyporheic exchange across spatial scales. Hydrol Earth Syst Sci 22, 6163–6185. https://doi.org/10.5194/hess-22-6163-2018

Mancuso, G., Bencresciuto, G.F., Lavrnić, S., Toscano, A., 2021. Diffuse water pollution from agriculture: A review of nature-based solutions for nitrogen removal and recovery. Water (Switzerland) 13, 1–22. https://doi.org/10.3390/w13141893

Martí, E., Feijoó, C., Vilches, C., Ferreiro, N., Gantes, P., Ranieri, C., Torremorell, A., Castro, M.C.R., Gultemiriam, M.L., Giorgi, A., Sabater, F., 2020. Diel variation of nutrient retention is associated with metabolism for ammonium but not phosphorus in a lowland stream. Freshwater Science 39, 268–280. https://doi.org/10.1086/708933

Martin, J.R., O'Neill, F.H., Daly, O.H., 2018. The monitoring and assessment of three EU Habitats Directive Annex I grassland habitats. Irish Wildlife Manuals, No. 102.

Mason, S.J.K., McGlynn, B.L., Poole, G.C., 2012. Hydrologic response to channel reconfiguration on Silver Bow Creek, Montana. J Hydrol (Amst) 438–439, 125–136. https://doi.org/10.1016/j.jhydrol.2012.03.010

McClain, M.E., Boyer, E.W., Dent, C.L., Gergel, S.E., Grimm, N.B., Groffman, P.M., Hart, S.C., Harvey, J.W., Johnston, C.A., Mayorga, E., McDowell, W.H., Pinay, G., 2003. Biogeochemical hot spots and hot moments at the interface of terrestrial and aquatic ecosystems. Ecosystems 6, 301–312. https://doi.org/10.1007/s10021-003-0161-9

McFarlane, N.M., Ciavarella, T.A., Smith, K.F., 2003. The effects of waterlogging on growth, photosynthesis and biomass allocation in perennial ryegrass (Lolium perenne L.) genotypes with contrasting root development. Journal of Agricultural Science 141, 241–248. https://doi.org/10.1017/S0021859603003502

McLoughlin, D., Browne, A., Sullivan, C.A., 2020. The delivery of ecosystem services through results-based agri-environment payment schemes (RBPS): three Irish case studies. Biology and Environment: Proceedings of the Royal Irish Academy 120B, 91–106. https://doi.org/10.1353/bae.2020.0018

Melland, A.R., Fenton, O., Jordan, P., 2018. Effects of agricultural land management changes on surface water quality: A review of meso-scale catchment research. Environ Sci Policy 84, 19–25. https://doi.org/10.1016/j.envsci.2018.02.011

Mendoza-Lera, C., Ribot, M., Foulquier, A., Martí, E., Bonnineau, C., Breil, P., Datry, T., 2019. Exploring the role of hydraulic conductivity on the contribution of the hyporheic zone to in-stream nitrogen uptake. Ecohydrology 12. https://doi.org/10.1002/eco.2139

Metcalfe, P., Beven, K., Hankin, B., Lamb, R., 2017a. A modelling framework for evaluation of the hydrological impacts of nature-based approaches to flood risk management, with application to in-channel interventions across a 29-km2 scale catchment in the United Kingdom. Hydrol Process 31, 1734–1748. https://doi.org/10.1002/hyp.11140

Metcalfe, P., Beven, K., Hankin, B., Lamb, R., 2017b. Simplified representation of runoff attenuation features within analysis of the hydrological performance of a natural flood management scheme. Hydrology and Earth System Sciences Discussions 1–33.

met.ie, 2023. Met Eireann [WWW Document]. URL https://www.met.ie/climate/available-data/historical-data (accessed 12.15.23).

Misstear, B.D.R., Brown, L., Daly, D., 2009. A methodology for making initial estimates of groundwater recharge from groundwater vulnerability mapping. Hydrogeol J 17, 275–285. https://doi.org/10.1007/s10040-008-0342-x

Moloney, T., Fenton, O., Daly, K., 2020. Ranking connectivity risk for phosphorus loss along agricultural drainage ditches. Science of the Total Environment 703, 134556. https://doi.org/10.1016/j.scitotenv.2019.134556

Moreno, S., Bedada, G., Yousef, R., Ingvarsson, P.K., Westerbergh, A., Lundquist, P.-O., 2023. Response to Waterlogging Stress in Wild and Domesticated Accessions of

Timothy (Phleum pratense) and Its Relatives P. alpinum and P. nodosum. Plants 12. https://doi.org/https:// doi.org/10.3390/plants12234033

Morris, J., Brewin, P., 2014. The impact of seasonal flooding on agriculture: The spring 2012 floods in Somerset, England. J Flood Risk Manag 7, 128–140. https://doi.org/10.1111/jfr3.12041

Muhawenimana, V., Wilson, C.A.M.E., Nefjodova, J., Cable, J., 2021. Flood attenuation hydraulics of channel-spanning leaky barriers. J Hydrol (Amst) 596, 125731. https://doi.org/10.1016/j.jhydrol.2020.125731

Murphy, D., Weatherill, J., Bourke, M., Quishi, X., Harrison, S., 2024. The hydrological and water quality performance of an agricultural flood detention basin: A case study - In review. Agric Ecosyst Environ.

Murphy, J., Riley, J.P., 1962. A modified single solution method for the determination of phosphate in natural waters. Anal Chim Acta 27, 31–36. https://doi.org/https://doi.org/10.1016/S0003-2670(00)88444-5.

Mustafa, A., Scholz, M., Harrington, R., Carroll, P., 2009. Long-term performance of a representative integrated constructed wetland treating farmyard runoff. Ecol Eng 35, 779–790. https://doi.org/10.1016/j.ecoleng.2008.12.008

Neilen, A.D., Chen, C.R., Parker, B.M., Faggotter, S.J., Burford, M.A., 2017. Differences in nitrate and phosphorus export between wooded and grassed riparian zones from farmland to receiving waterways under varying rainfall conditions. Science of the Total Environment 598, 188–197. https://doi.org/10.1016/j.scitotenv.2017.04.075

Newcomer Johnson, T.A., Kaushal, S.S., Mayer, P.M., Smith, R.M., Sivirichi, G.M., 2016. Nutrient retention in restored streams and rivers: A global review and synthesis. Water (Switzerland) 8, 1–28. https://doi.org/10.3390/w8040116

Nicholson, A.R., O'Donnell, G.M., Wilkinson, M.E., Quinn, P.F., 2020. The potential of runoff attenuation features as a Natural Flood Management approach. J Flood Risk Manag 13, 1–14. https://doi.org/10.1111/jfr3.12565

Nicholson, A.R., Wilkinson, M.E., O'Donnell, G.M., Quinn, P.F., 2012. Runoff attenuation features: A sustainable flood mitigation strategy in the Belford catchment, UK. Area 44, 463–469. https://doi.org/10.1111/j.1475-4762.2012.01099.x

Nivala, J., Wallace, S., Headley, T., Kassa, K., Brix, H., van Afferden, M., Müller, R., 2013. Oxygen transfer and consumption in subsurface flow treatment wetlands. Ecol Eng 61, 544–554. https://doi.org/10.1016/j.ecoleng.2012.08.028

Noe, G.B., Boomer, K., Gillespie, J.L., Hupp, C.R., Martin-Alciati, M., Floro, K., Schenk, E.R., Jacobs, A., Strano, S., 2019. The effects of restored hydrologic connectivity on floodplain trapping vs. release of phosphorus, nitrogen, and sediment along the Pocomoke River, Maryland USA. Ecol Eng 138, 334–352. https://doi.org/10.1016/j.ecoleng.2019.08.002

Ockenden, M.C., Deasy, C., Quinton, J.N., Surridge, B., Stoate, C., 2014. Keeping agricultural soil out of rivers: Evidence of sediment and nutrient accumulation within field wetlands in the UK. J Environ Manage 135, 54–62. https://doi.org/10.1016/j.jenvman.2014.01.015

O’Connell, E., Ewen, J., O’Donnell, G., Quinn, P., 2007. Is there a link between agricultural land-use management and flooding? Hydrol Earth Syst Sci 11, 96–107. https://doi.org/10.5194/hess-11-96-2007

Olorunwa, O.J., Adhikari, B., Brazel, S., Popescu, S.C., Popescu, G. V., Barickman, T.C., 2022. Short waterlogging events differently affect morphology and photosynthesis of two cucumber (Cucumis sativus L.) cultivars. Front Plant Sci 13, 1–16. https://doi.org/10.3389/fpls.2022.896244

Oram, N.J., Sun, Y., Abalos, D., van Groenigen, J.W., Hartley, S., De Deyn, G.B., 2021. Plant traits of grass and legume species for flood resilience and N2O mitigation. Funct Ecol 35, 2205–2218. https://doi.org/10.1111/1365-2435.13873

O’Rourke, E.; Finn, J.A., 2020. Farming for Nature: The Role of Results-based Payments, Farming for Nature: The Role of Results-based Payments.

O’Sullivan, J.J., Ahilan, S., Bruen, M., 2012. A modified Muskingum routing approach for floodplain flows: Theory and practice. J Hydrol (Amst) 470–471, 239–254. https://doi.org/10.1016/j.jhydrol.2012.09.007

Oviedo-Vargas, D., Royer, T. V., Johnson, L.T., 2013. Dissolved organic carbon manipulation reveals coupled cycling of carbon, nitrogen, and phosphorus in a nitrogen-rich stream. Limnol Oceanogr 58, 1196–1206. https://doi.org/10.4319/lo.2013.58.4.1196

Pan, J., Sharif, R., Xu, X., Chen, X., 2021. Mechanisms of Waterlogging Tolerance in Plants: Research Progress and Prospects. Front Plant Sci 11. https://doi.org/10.3389/fpls.2020.627331

Parris, K., 2011. Impact of agriculture on water pollution in OECD countries: Recent trends and future prospects. Int J Water Resour Dev 27, 33–52. https://doi.org/10.1080/07900627.2010.531898

Pattison, I., Lane, S., Hardy, R., Reaney, S., 2014. The role of tributary relative timing & sequencing in controlling large floods. American Geophysical Union 50, 5444–5458. https://doi.org/10.1002/2013WR014067

Pattison, I., Lane, S.N., 2012. The link between land-use management and fluvial flood risk: A chaotic conception? Prog Phys Geogr 36, 72–92. https://doi.org/10.1177/0309133311425398

Pearson, C., 2016. Modelling the potential impact of spatially targeted natural flood management at the landscape scale for a rural UK catchment. Durham University.

Pierce, S.C., Kröger, R., Pezeshki, R., 2012. Managing artificially drained low-gradient agricultural headwaters for enhanced ecosystem functions. Biology (Basel) 1, 794–856. https://doi.org/10.3390/biology1030794

Piper, L.R., Cross, W.F., McGlynn, B.L., 2017. Colimitation and the coupling of N and P uptake kinetics in oligotrophic mountain streams. Biogeochemistry 132, 165–184. https://doi.org/10.1007/s10533-017-0294-0

Poff, N.L., Allan, J.D., Bain, M.B., Karr, J.R., Prestegaard, K.L., Brian, D., Sparks, R.E., Stromberg, J.C., Richter, B.D., 1997. The Natural Flow Regime. Bioscience 47, 769–784.

Prasse, C., Wenk, J., Jasper, J.T., Ternes, T.A., Sedlak, D.L., 2015. Co-occurrence of Photochemical and Microbiological Transformation Processes in Open-Water Unit

Process Wetlands. Environ Sci Technol 49, 14136–14145. https://doi.org/10.1021/acs.est.5b03783

Pronk, G.J., Heister, K., Vogel, C., Babin, D., Bachmann, J., Ding, G.C., Ditterich, F., Gerzabek, M.H., Giebler, J., Hemkemeyer, M., Kandeler, E., Kunhi Mouvenchery, Y., Miltner, A., Poll, C., Schaumann, G.E., Smalla, K., Steinbach, A., Tanuwidjaja, I., Tebbe, C.C., Wick, L.Y., Woche, S.K., Totsche, K.U., Schloter, M., Kögel-Knabner, I., 2017. Interaction of minerals, organic matter, and microorganisms during biogeochemical interface formation as shown by a series of artificial soil experiments. Biol Fertil Soils 53, 9–22. https://doi.org/10.1007/s00374-016-1161-1

Puijalon, S., Lena, J.P., Bornette, G., 2007. Interactive effects of nutrient and mechanical stresses on plant morphology. Ann Bot 100, 1297–1305. https://doi.org/10.1093/aob/mcm226

Quinn, P., O'Donnell, G., Nicholson, A., Wilkinson, M., Owen, G., Jonczyk, J., Barber, N., Hardwick, M., Davies, G., 2013. Potential use of runoff attenuation features in small rural catchments for flood mitigation. NFM RAF Report.

Quinn, P.F., Hewett, C.J.M., Wilkinson, M.E., Adams, R., 2022. The Role of Runoff Attenuation Features (RAFs) in Natural Flood Management. Water (Basel) 14. https://doi.org/https://doi.org/10.3390/w14233807 Academic Editors: David Proverbs and Bingunath Ingirige Received:

R Core Team, 2023. R: A Language and Environment for Statistical Computing.

Rana, S.M.M., Scott, D.T., Hester, E.T., 2017. Effects of in-stream structures and channel flow rate variation on transient storage. J Hydrol (Amst) 548, 157–169. https://doi.org/10.1016/j.jhydrol.2017.02.049

Raymond, P.A., Saiers, J.E., Sobczak, W. V, 2016. Hydrological and biogeochemical controls on watershed dissolved organic matter transport: pulse-shunt concept. Ecology 97, 5–16.

Regan, J.T., Rodgers, M., Healy, M.G., Kirwan, L., Fenton, O., 2010. Determining Phosphorus and Sediment Release Rates from Five Irish Tillage Soils. J Environ Qual 39, 185–192. https://doi.org/10.2134/jeq2008.0514

Revsbech, N.P., Jacobsen, J.P., Nielsen, L.P., 2005. Nitrogen transformations in microenvironments of river beds and riparian zones. Ecol Eng 24, 447–455. https://doi.org/10.1016/j.ecoleng.2005.02.002

Riley, W.D., Potter, E.C.E., Biggs, J., Collins, A.L., Jarvie, H.P., Jones, J.I., Kelly-quinn, M., Ormerod, S.J., Sear, D.A., Wilby, R.L., Broadmeadow, S., Brown, C.D., Chanin, P., Copp, G.H., Cowx, I.G., Grogan, A., Hornby, D.D., Huggett, D., Kelly, M.G., Naura, M., Newman, J.R., Siriwardena, G.M., 2018. Small water bodies in great Britain and Ireland : Ecosystem function, human-generated degradation, and options for restorative action. Science of the Total Environment 645, 1598–1616. https://doi.org/10.1016/j.scitotenv.2018.07.243

Roberts, M.T., Geris, J., Hallett, P.D., Wilkinson, M.E., 2023. Mitigating floods and attenuating surface runoff with temporary storage areas in headwaters. Wiley Interdisciplinary Reviews: Water 10, 1–18. https://doi.org/10.1002/wat2.1634

Roberts, W.M., Gonzalez-Jimenez, J.L., Doody, D.G., Jordan, P., Daly, K., 2017. Assessing the risk of phosphorus transfer to high ecological status rivers: Integration of nutrient management with soil geochemical and hydrological conditions. Science of the Total Environment 589, 25–35. https://doi.org/10.1016/j.scitotenv.2017.02.201

Roberts, W.M., Stutter, M.I., Haygarth, P.M., 2012. Phosphorus Retention and Remobilization in Vegetated Buffer Strips: A Review. J Environ Qual 41, 389–399. https://doi.org/10.2134/jeq2010.0543

Robertson, A.L., Wood, P.J., 2010. Ecology of the hyporheic zone: Origins, current knowledge and future directions. Fundamental and Applied Limnology 176, 279–289. https://doi.org/10.1127/1863-9135/2010/0176-0279

Robotham, J., Old, G., Rameshwaran, P., Sear, D., Gasca-Tucker, D., Bishop, J., Old, J., McKnight, D., 2021. Sediment and nutrient retention in ponds on an agricultural stream: Evaluating effectiveness for diffuse pollution mitigation. Water (Switzerland) 13. https://doi.org/10.3390/w13121640

Robotham, J., Old, G., Rameshwaran, P., Sear, D., Trill, E., Bishop, J., Gasca-Tucker, D., Old, J., McKnight, D., 2022. Nature-based solutions enhance sediment and nutrient storage in an agricultural lowland catchment. Earth Surf Process Landf 243–258. https://doi.org/10.1002/esp.5483

Rogger, M., Aglonetti, M., Alaoui, A., Bathhurst, J.C., Bodner, G., Borga, M., Chaplot, V., Gallart, F., Glatzel, G., Hall, J., Holden, J., Holka, L., Horn, R., Kiss, A., Kognova, S., Leitinger, G., Lennartz, B., Parajka, J., Peth, S., Plavcova, L., Quinton, J.N., Robinson, M., Salinas, J.L., Santor, A., Szolgay, J., Tron, S., van den Akker, J.J.H., Viflione, A., Blosh, G., 2017a. Land use change impacts on floods at the catchment scale: Challenges and opportunities for furture research. Water Resour Res 53, 5209–5219. https://doi.org/10.1002/2017WR020723

Rogger, M., Aglonetti, M., Alaoui, A., Bathhurst, J.C., Bodner, G., Borga, M., Chaplot, V., Gallart, F., Glatzel, G., Hall, J., Holden, J., Holka, L., Horn, R., Kiss, A., Kognova, S., Leitinger, G., Lennartz, B., Parajka, J., Peth, S., Plavcova, L., Quinton, J.N., Robinson, M., Salinas, J.L., Santor, A., Szolgay, J., Tron, S., van den Akker, J.J.H., Viflione, A., Blosh, G., 2017b. Land use change impacts on floods at the catchment scale: Challenges and opportunities for furture research. Water Resour Res 53, 5209–5219. https://doi.org/10.1002/2017WR020723

Romani, A.M., Huasch, H., Balaguer, M.D., 2016. Aquatic Biofilms: Ecology, Water Quality & Wastewater Treatment, Aquatic Biofilms: Ecology, Water Quality and Wastewater Treatment. https://doi.org/10.21775/9781910190173.11

S∅vik, A.K., Augustin, J., Heikkinen, K., Huttunen, J.T., Necki, J.M., Karjalainen, S.M., Kl∅ve, B., Liikanen, A., Mander, Ü., Puustinen, M., Teiter, S., Wachniew, P., 2006. Emission of the Greenhouse Gases Nitrous Oxide and Methane from Constructed Wetlands in Europe. J Environ Qual 35, 2360–2373. https://doi.org/10.2134/jeq2006.0038

Saeed, T., Sun, G., 2012. A review on nitrogen and organics removal mechanisms in subsurface flow constructed wetlands: Dependency on environmental parameters, operating conditions and supporting media. J Environ Manage 112, 429–448. https://doi.org/10.1016/j.jenvman.2012.08.011

Salant, N.L., Schmidt, J.C., Budy, P., Wilcock, P.R., 2012. Unintended consequences of restoration: Loss of riffles and gravel substrates following weir installation. J Environ Manage 109, 154–163. https://doi.org/10.1016/j.jenvman.2012.05.013

Schmadel, N.M., Ward, A.S., Kurz, M.J., Fleckenstein, J.H., Zarnetske, J.P., Knapp, J.L.A., Klaar, M.J., Romeijn, P., Datry, T., Keller, T., Folegot, S., 2016. Stream solute tracer timescales changing with discharge and reach length confound process interpretation. Water Resour Res 3227–3245. https://doi.org/10.1002/2015WR018062.Received

Scholes, R.C., Vega, M.A., Sharp, J.O., Sedlak, D.L., 2021. Nitrate removal from reverse osmosis concentrate in pilot-scale open-water unit process wetlands. Environ Sci (Camb) 7, 650–661. https://doi.org/10.1039/d0ew00911c

Scholz, M., Harrington, R., Carroll, P., Mustafa, A., 2007. The integrated constructed wetlands (ICW) concept. Wetlands 27, 337–354. https://doi.org/10.1672/0277-5212(2007)27[337:TICWIC]2.0.CO;2

Seliger, C., Zeiringer, B., 2018. River Connectivity, Habitat Fragmentation and Related Restoration Measures, Riverine Ecosystem Management. https://doi.org/10.1007/978-3-319-73250-3_9

Shaw Yu, B.L., Kuo, J.-T., Fassman, E.A., Pan, H., 2001. Field test of grassed-swale performance in removing runoff pollution. J Water Resour Plan Manag 168–171.

Shore, M., Jordan, P., Mellander, P.E., Kelly-Quinn, M., Daly, K., Sims, J.T., Wall, D.P., Melland, A.R., 2016. Characterisation of agricultural drainage ditch sediments along the phosphorus transfer continuum in two contrasting headwater catchments. J Soils Sediments 16, 1643–1654. https://doi.org/10.1007/s11368-015-1330-0

Short, C., Clarke, L., Carnelli, F., Uttley, C., Smith, B., 2019. Capturing the multiple benefits associated with nature-based solutions: Lessons from a natural flood management project in the Cotswolds, UK. Land Degrad Dev 30, 241–252. https://doi.org/10.1002/ldr.3205

Singh, G., Kaur, G., Williard, K., Schoonover, J., Nelson, K.A., 2020. Managing phosphorus loss from agroecosystems of the midwestern United States: A review. Agronomy 10, 1–64. https://doi.org/10.3390/agronomy10040561

Smith, P., Adams, J., Beerling, D.J., Beringer, T., Calvin, K. V., Fuss, S., Griscom, B., Hagemann, N., Kammann, C., Kraxner, F., Minx, J.C., Popp, A., Renforth, P., Vicente Vicente, J.L., Keesstra, S., 2019. Land-Management Options for Greenhouse Gas Removal and Their Impacts on Ecosystem Services and the Sustainable Development Goals. Annu Rev Environ Resour 44, 255–286. https://doi.org/10.1146/annurev-environ-101718-033129

Sommer, L., Klinger, Y.P., Donath, T.W., Kleinebecker, T., Harvolk-Schöning, S., 2023. Long-term success of floodplain meadow restoration on species-poor grassland. Front Ecol Evol 10, 1–15. https://doi.org/10.3389/fevo.2022.1061484

Son, K., Oh, M.-M., 2015. Growth, photosynthetic and antioxidant parameters of two lettuce cultivars as affected by red, green, and blue light-emitting diodes. Hortic Environ Biotechnol 56, 639–653. https://doi.org/10.1007/s13580-015-1064-3

Spundova, M., Popelkova, H., Ilik, P., Skotnica, J., Novotny, R., Naus, J., 2003. Ultra-structural and functional changes in the chloroplasts of detached barley leaves senescing under dark and light conditions. J Plant Physiol 160, 1051–1058.

Stoffers, T., Altermatt, F., Baldan, D., Bilous, O., Borgwardt, F., Buijse, A. D., Bondar-Kunze, E., Cid, N., Erős, T., Ferreira, M. T., Funk, A., Haidvogl, G., Hohensinner, S., Kowal, J., Nagelkerke, L. A. J., Neuburg, J., Peller, T., Schmutz, S., Singer, G. A., … Hein, T. (2024). Reviving Europe's rivers: Seven challenges in the implementation of the nature restoration law to restore free-flowing rivers. WIREs Water, e1717. https://doi.org/10.1002/wat2.1717

Striker, G.G., Colmer, T.D., 2017. Flooding tolerance of forage legumes. J Exp Bot 68, 1851–1872. https://doi.org/10.1093/jxb/erw239

Stutter, M., Graeber, D., Weigelhofer, G., 2020. Available Dissolved Organic Carbon alters uptake and recycling of phosphorus and nitrogen from river sediments. Water (Basel) 12, 3321. https://doi.org/10.3390/w12123321

Stutter, M., Kronvang, B., Ó hUallacháin, D., Rozemeijer, J., 2019. Current Insights into the Effectiveness of Riparian Management, Attainment of Multiple Benefits, and Potential Technical Enhancements. J Environ Qual 48, 236–247. https://doi.org/10.2134/jeq2019.01.0020

Stutter, M.I., Chardon, W.J., Kronvang, B., 2012. Riparian Buffer Strips as a Multifunctional Management Tool in Agricultural Landscapes: Introduction. J Environ Qual 41, 297–303. https://doi.org/10.2134/jeq2011.0439

Stutter, M.I., Graeber, D., Evans, C.D., Wade, A.J., Withers, P.J.A., 2018. Balancing macronutrient stoichiometry to alleviate eutrophication. Science of the Total Environment 634, 439–447. https://doi.org/10.1016/j.scitotenv.2018.03.298

Stutter, M.I., Langan, S.J., Cooper, R.J., 2008. Spatial and temporal dynamics of stream water particulate and dissolved N, P and C forms along a catchment transect, NE Scotland. J Hydrol (Amst) 350, 187–202. https://doi.org/10.1016/j.jhydrol.2007.10.048

Stutter, M.I., Langan, S.J., Lumsdon, D.G., 2009. Vegetated buffer strips can lead to increased release of phosphorus to waters: A biogeochemical assessment of the mechanisms. Environ Sci Technol 43, 1858–1863. https://doi.org/10.1021/es8030193

Suttles, K.M., Eagle, A.J., McLellan, E.L., 2021. Upstream solutions to downstream problems: Investing in rural natural infrastructure for water quality improvement and flood risk mitigation. Water (Switzerland) 13. https://doi.org/10.3390/w13243579

Sweka, J.A., Hartman, K.J., 2001. Effects of turbidity on prey consumption and growth in brook trout and implications for bioenergetics modeling. Canadian Journal of Fisheries and Aquatic Sciences 58, 386–393. https://doi.org/10.1139/cjfas-58-2-386

Tank, J.L., Rosi-Marshall, E.J., Baker, M.A., Hall, R.O., 2008. Are rivers just big streams? A pulse method to quantify nitrogen demand in a large river. Ecology 89, 2935–2945. https://doi.org/10.1890/07-1315.1

Tanou, G., Fotopoulos, V., Molassiotis, A., 2012. Priming against environmental challenges and proteomics in plants: Update and agricultural perspectives. Front Plant Sci 3, 1–5. https://doi.org/10.3389/fpls.2012.00216

Teagasc, 2023. Teagasc 2023 [WWW Document]. URL http://gis.teagasc.ie/soils/map.php (accessed 12.15.23).

Teagasc, 2017. Teagasc soil index system [WWW Document]. https://www.teagasc.ie/crops/soil--soil-fertility/soil-analysis/soil-index-system/. URL https://www.teagasc.ie/crops/soil--soil-fertility/soil-analysis/soil-index-system/

Thomas, H., Nisbet, T., 2012. Modelling the hydraulic impact of reintroducing large woody debris into watercourses. J Flood Risk Manag 5, 164–174. https://doi.org/10.1111/j.1753-318X.2012.01137.x

Tietz, A., Langergraber, G., Watzinger, A., Haberl, R., Kirschner, A.K.T., 2008. Bacterial carbon utilization in vertical subsurface flow constructed wetlands. Water Res 42, 1622–1634. https://doi.org/10.1016/j.watres.2007.10.011

Tockner, K., Pennetzdorfer, D., Reiner, N., Schiemer, F., Ward, J. V., 1999. Hydrological connectivity, and the exchange of organic matter and nutrients in a dynamic river-floodplain system (Danube, Austria). Freshw Biol 41, 521–535. https://doi.org/10.1046/j.1365-2427.1999.00399.x

Todorova, D., Aleksandrov, V., Anev, S., Sergiev, I., 2022. Photosynthesis alterations in wheat plants induced by herbicide, soil drought or flooding. Agronomy 12, 1–13. https://doi.org/10.3390/agronomy12020390

Trill, E., Robotham, J., Bishop, J., Old, G., Rameshwaran, P., Gasca, 2022. Littlestock Brook natural flood management pilot: hydrological and water quality monitoring and analysis report.

Vaiopoulou, E., Melidis, P., Aivasidis, A., 2007. An activated sludge treatment plant for integrated removal of carbon, nitrogen and phosphorus. Desalination 211, 192–199. https://doi.org/10.1016/j.desal.2006.02.092

Van Eck, W.H.J.M., Lenssen, J.P.M., Rengelink, R.H.J., Blom, C.W.P.M., De Kroon, H., 2005. Water temperature instead of acclimation stage and oxygen concentration determines responses to winter floods. Aquat Bot 81, 253–264. https://doi.org/10.1016/j.aquabot.2004.10.006

Van Eck, W.H.J.M., Lenssen, J.P.M., Van De Steeg, H.M., Blom, C.W.P.M., De Kroon, H., 2006. Seasonal dependent effects of flooding on plant species survival and zonation: A comparative study of 10 terrestrial grassland species. Hydrobiologia 565, 59–69. https://doi.org/10.1007/s10750-005-1905-7

van Leeuwen, Z.R., Klaar, M.J., Smith, M.W., Brown, L.E., 2024. Quantifying the natural flood management potential of leaky dams in upland catchments, Part II: Leaky dam impacts on flood peak magnitude. J Hydrol (Amst) 628, 130449. https://doi.org/10.1016/j.jhydrol.2023.130449

VanKempen-Fryling, R.J., Camper, A.K., 2017. Escherichia coli O157:H7 attachment and persistence within root biofilm of common treatment wetlands plants. Ecol Eng 98, 64–69. https://doi.org/10.1016/j.ecoleng.2016.10.018

Vero, S.E., Daly, K., McDonald, N.T., Leach, S., Sherriff, S.C., Mellander, P.E., 2019. Sources and mechanisms of low-flow river phosphorus elevations: A repeated synoptic survey approach. Water (Basel) 11. https://doi.org/10.3390/w11071497

Vero, S.E., Doody, D., Cassidy, R., Higgins, S., Nicholl, G., Campbell, J., Mellander, P.E., McDonald, N., Burgess, E., Daly, K., Sherry, E., 2022. Comparison of soil phosphorus index systems for grassland in the cross-border region of Ireland#. Journal of Plant Nutrition and Soil Science 185, 110–119. https://doi.org/10.1002/jpln.202100194

Vervuren, P.J.A., Blom, C.W.P.M., De Kroon, H., 2003. Extreme flooding events on the Rhine and the survival and distribution of riparian plant species. Journal of Ecology 91, 135–146. https://doi.org/10.1046/j.1365-2745.2003.00749.x

Vymazal, J., 2010. Constructed Wetlands for Wastewater Treatment. Water (Basel) 2, 530–549. https://doi.org/10.3390/w2030530

Vymazal, J., 2007. Removal of nutrients in various types of constructed wetlands. Science of the Total Environment 380, 48–65. https://doi.org/10.1016/j.scitotenv.2006.09.014

Vymazal, J., Kröpfelová, L., 2009. Removal of organics in constructed wetlands with horizontal sub-surface flow: A review of the field experience. Science of the Total Environment 407, 3911–3922. https://doi.org/10.1016/j.scitotenv.2008.08.032

Walter, J., Nagy, L., Hein, R., Rascher, U., Beierkuhnlein, C., Willner, E., Jentsch, A., 2011. Do plants remember drought? Hints towards a drought-memory in grasses. Environ Exp Bot 71, 34–40. https://doi.org/10.1016/j.envexpbot.2010.10.020

Walworth J. 2013. Nitrogen in soil and the environment. College of Agriculture and Life Sciences Cooperative Extension, The University of Arizona, Tucson, AZ

Wang, J.P., Bughrara, S.S., Nelson, C.J., 2008. Morpho-physiological responses of several fescue grasses to drought stress. HortScience 43, 776–783. https://doi.org/10.21273/hortsci.43.3.776

Wang, S., Callaway, R.M., Zhou, D.W., Weiner, J., 2017. Experience of inundation or drought alters the responses of plants to subsequent water conditions. Journal of Ecology 105, 176–187. https://doi.org/10.1111/1365-2745.12649

Wang, X., Li, M., Jannasch, A.H., Jiang, Y., 2020. Submergence stress alters fructan and hormone metabolism and gene expression in perennial ryegrass with contrasting growth habits. Environ Exp Bot 179, 104202. https://doi.org/10.1016/j.envexpbot.2020.104202

Ward, A.S., Gooseff, M.N., Voltz, T.J., Fitzgerald, M., Singha, K., Zarnetske, J.P., 2013. How does rapidly changing discharge during storm events affect transient storage and channel water balance in a headwater mountain stream? Water Resour Res 49, 5473–5486. https://doi.org/10.1002/wrcr.20434

Ward, N.D., Bianchi, T.S., Medeiros, P.M., Seidel, M., Richey, J.E., Keil, R.G., Sawakuchi, H.O., 2017. Where carbon goes when water flows: Carbon cycling across the aquatic Continuum. Front Mar Sci 4, 1–27. https://doi.org/10.3389/fmars.2017.00007

Watson, K.B., Ricketts, T., Galford, G., Polasky, S., O'Niel-Dunne, J., 2016. Quantifying flood mitigation services: The economic value of Otter Creek wetlands and floodplains to Middlebury, VT. Ecological Economics 130, 16–24. https://doi.org/10.1016/j.ecolecon.2016.05.015

Waylen, K.A., Wilkinson, M.E., Blackstock, K.L., Bourke M., 2024. Nature-based solutions and restoration are intertwined but not identical: highlighting implications for societies and ecosystems. Nature-Based Solutions, 5, 100116.

https://doi.org/10.1016/j. nbsj.2024.100116.

Weatherill, J.J., Krause, S., Ullah, S., Cassidy, N.J., Levy, A., Drijfhout, F.P., Rivett, M.O., 2019. Revealing chlorinated ethene transformation hotspots in a nitrate-impacted hyporheic zone. Water Res 161, 222–231. https://doi.org/10.1016/j.watres.2019.05.083

Webster, J.R., Mulholland, P.J., Tank, J.L., Valett, H.M., Dodds, W.K., Peterson, B.J., Bowden, W.B., Dahm, C.N., Findlay, S., Gregory, S. V., Grimm, N.B., Hamilton, S.K., Johnson, S.L., Martí, E., McDowell, W.H., Meyer, J.L., Morrall, D.D., Thomas, S.A., Wollheim, W.M., 2003. Factors affecting ammonium uptake in streams - An inter-biome perspective. Freshw Biol 48, 1329–1352. https://doi.org/10.1046/j.1365-2427.2003.01094.x

Weigelhofer, G., 2017. The potential of agricultural headwater streams to retain soluble reactive phosphorus. Hydrobiologia 793, 149–160. https://doi.org/10.1007/s10750-016-2789-4

Weigelhofer, G., Fuchsberger, J., Teufl, B., Welti, N., Hein, T., 2012. Effects of riparian forest buffers on in-stream nutrient retention in agricultural catchments. J Environ Qual 41, 373–379. https://doi.org/10.2134/jeq2010.0436

Weigelhofer, G., Ramião, J.P., Pitzl, B., Bondar-Kunze, E., O'Keeffe, J., 2018a. Decoupled water-sediment interactions restrict the phosphorus buffer mechanism in agricultural streams. Science of the Total Environment 628–629, 44–52. https://doi.org/10.1016/j.scitotenv.2018.02.030

Weigelhofer, G., Ramião, J.P., Puritscher, A., Hein, T., 2018b. How do chronic nutrient loading and the duration of nutrient pulses affect nutrient uptake in headwater streams? Biogeochemistry 141, 249–263. https://doi.org/10.1007/s10533-018-0518-y

Wenzel, R., Reinhardt-Imjela, C., Schulte, A., Bölscher, J., 2014. The potential of in-channel large woody debris in transforming discharge hydrographs in headwater areas (Ore Mountains, Southeastern Germany). Ecol Eng 71, 1–9. https://doi.org/10.1016/j.ecoleng.2014.07.004

White, H.J., Caplat, P., Emmerson, M.C., Yearsley, J.M., 2021. Predicting future stability of ecosystem functioning under climate change. Agric Ecosyst Environ 320. https://doi.org/10.1016/j.agee.2021.107600

Wickham, H., 2016. ggplot2: Elegant Graphics for Data Analysis. New York.

Wilcock, R.J., Müller, K., Van Assema, G.B., Bellingham, M.A., Ovenden, R., 2012. Attenuation of nitrogen, phosphorus and E. coli inputs from pasture runoff to surface waters by a farm wetland: The importance of wetland shape and residence time. Water Air Soil Pollut 223, 499–509. https://doi.org/10.1007/s11270-011-0876-8

Wild, T., Bulkeley, H., Naumann, S., Vojinovic, Z., Calfapietra, C., Whiteoak, K., 2020. Nature-based solutions: State of the art in EU-funded projects, Luxembourg: Publications Office of the European Union. https://doi.org/10.2777/236007

Wilkinson, M. E., Quinn, P. F., Barber, N. J., & Jonczyk, J. (2014). A framework for managing runoff and pollution in the rural landscape using a catchment systems engineering approach. Science of the Total Environment, 468, 1245–1254. https://doi.org/10.1016/j.scitotenv.

2013.07.055

Wilkinson, M.E., Addy, S., Quinn, P.F., Stutter, M., 2019. Natural flood management: small-scale progress and larger-scale challenges. Scottish Geographical Journal 135, 23–32. https://doi.org/10.1080/14702541.2019.1610571

Withers, P.J.A., Jarvie, H.P., 2008. Delivery and cycling of phosphorus in rivers: A review. Science of the Total Environment 400, 379–395. https://doi.org/10.1016/j.scitotenv.2008.08.002

Wohl, E., Beckman, N.D., 2014. Leaky rivers: Implications of the loss of longitudinal fluvial disconnectivity in headwater streams. Geomorphology 205, 27–35. https://doi.org/10.1016/j.geomorph.2011.10.022

Wreford, A., Topp, C.F.E., 2020. Impacts of climate change on livestock and possible adaptations: A case study of the United Kingdom. Agric Syst 178. https://doi.org/10.1016/j.agsy.2019.102737

Yorkshire Dales Rivers Trust, 2018. Naturally Resilient - Slowing the Movement of Water - Leaky Dams 2–4.

Zarnetske, J.P., Gooseff, M.N., Brosten, T.R., Bradford, J.H., McNamara, J.P., Bowden, W.B., 2007. Transient storage as a function of geomorphology, discharge, and permafrost active layer conditions in Arctic tundra streams. Water Resour Res 43, 1–13. https://doi.org/10.1029/2005WR004816

Zarnetske, J.P., Haggerty, R., Wondzell, S.M., Baker, M.A., 2011a. Labile dissolved organic carbon supply limits hyporheic denitrification. J Geophys Res Biogeosci 116. https://doi.org/10.1029/2011JG001730

Zarnetske, J.P., Haggerty, R., Wondzell, S.M., Baker, M.A., 2011b. Dynamics of nitrate production and removal as a function of residence time in the hyporheic zone. J Geophys Res Biogeosci 116, 1–12. https://doi.org/10.1029/2010JG001356

Zhang, L., Scholz, M., Mustafa, A., Harrington, R., 2008. Assessment of the nutrient removal performance in integrated constructed wetlands with the self-organizing map. Water Res 42, 3519–3527. https://doi.org/10.1016/j.watres.2008.04.027